THE PERCEPTION OF MOTION

Kenneth Scott Brown

A Thesis Submitted for the Degree of PhD
at the
University of St Andrews

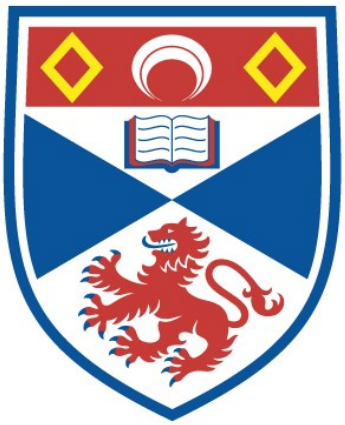

1996

The Perception Of Motion

KENNETH SCOTT BROWN

School of Psychology
University of St Andrews

Submitted for the Degree of PhD, February 1996.

ABSTRACT

Extracting a motion signal for a two-dimensional contour requires the human visual system to derive a velocity vector from the spatially limited receptive fields of motion sensitive cortical cells. An individual cell's response may not specify the contour's true velocity. Models of motion often combine the outputs of different classes of receptive fields to generate a reliable motion signal. Their efficacy was tested by comparing their predictions with human psychophysical performance.

The perceived speed of co-linear inclined line segments in horizontal translation was subject to a bias in favour of the local components of the contour. Single tilted lines were also subject to a bias in perceived speed. Experiments investigated the effects of grouping, co-linearity, eccentricity, terminator proximity and stimulus uncertainty on perceived speed and clearly showed that the perceived velocity of line segments is not obtained by a simple averaging process of local velocity signals and veridical velocity signals of line terminators. Variation of the spatial position of terminators was sufficient to abolish the bias in perceived speed of horizontally drifting inclined lines. Neither "vector-average" nor "winner-take-all" rules are sufficient to account for this.

The method of integration of one-dimensional components into two-dimensional plaid patterns was explored in two experiments recording thresholds for perceived rotation of drifting plaids. Type II plaids are not subject to the oblique effect found for rotation discrimination thresholds for type IS plaids. Plaid rotation induced by a speed change in one of the components showed that direction perception does not follow a strict interpretation of the "intersection of constraints rule".

As current models of motion integration fail to provide a full account of the perceived speed and direction of two-dimensional patterns; higher-order attentional processes should be incorporated into models of motion perception.

Declarations:

(i)

I, Kenneth Scott Brown, hereby certify that this thesis, which is approximately 42,134 words in length, has been written by me, that it is the record of work carried out by me and it has not been submitted in any previous application for a higher degree.

Date 10/6/96 Signature of Candidate

(ii)

I was admitted as a research student in October 1992 and as a candidate for the degree of PhD in October, 1992; the higher study for which this is a record was carried out in the University of St. Andrews between 1992 and 1995.

Date 10/6/96 Signature of Candidate

(iii)

I hereby certify that the candidate has fulfilled the conditions of the Resolution and Regulations appropriate for the degree of PhD in the University of St. Andrews and that the candidate is qualified to submit this thesis in application for that degree.

Date Signature of Supervisor

10/6/96

Thesis Copyright Declaration

Unrestricted

In submitting this thesis to the University of St. Andrews I understand that I am giving permission for it to be made available for use in accordance with the regulations of the University Library for the time being in force, subject to any copyright vested in the work not being affected thereby. I also understand that the title and abstract will be published, and that copy of the work may be made and supplied to any bona fide library or research worker.

Date 10/6/96 Signature of Candidate

Visual Motion Perception

TABLE OF CONTENTS

List of Illustrations

CHAPTER 5

CHAPTER 6

CHAPTER 7

CHAPTER 8

CHAPTER 9

List of Tables

Visual motion perception: psychophysical and physiological perspectives.

CHAPTER 1

Motion detection, the aperture problem and MT.

INTRODUCTION

Motion Processing Mechanisms:

The motion processing architecture of the primate visual system (within the geniculo-striate-extrastriate pathways) can be described neurophysiologically. Cells in the visual cortex possess response properties selective for movements in specific directions across the retinae (Hubel & Wiesel, 1968). For a single unit, motion in certain directions produced strong responses while motion in other directions produced weak responses. Fig. 1.1 shows the responses from a cell with a preferred motion of up and to the right (opposing directions are indicated by arrows). Cells from primary visual cortex (V1) are the first in the visual pathway to exhibit this property (Hubel & Wiesel, 1968; Schiller, Finlay & Volman, 1976), and these cells are the foundation of the larger anatomically distinct motion subsystem that extends through several layers of cortex (Livingstone & Hubel, 1988). Fig. 1.2 shows a schematic map of the pathways in the striate and extrastriate cortex of the primate, as reviewed by Livingstone and Hubel.

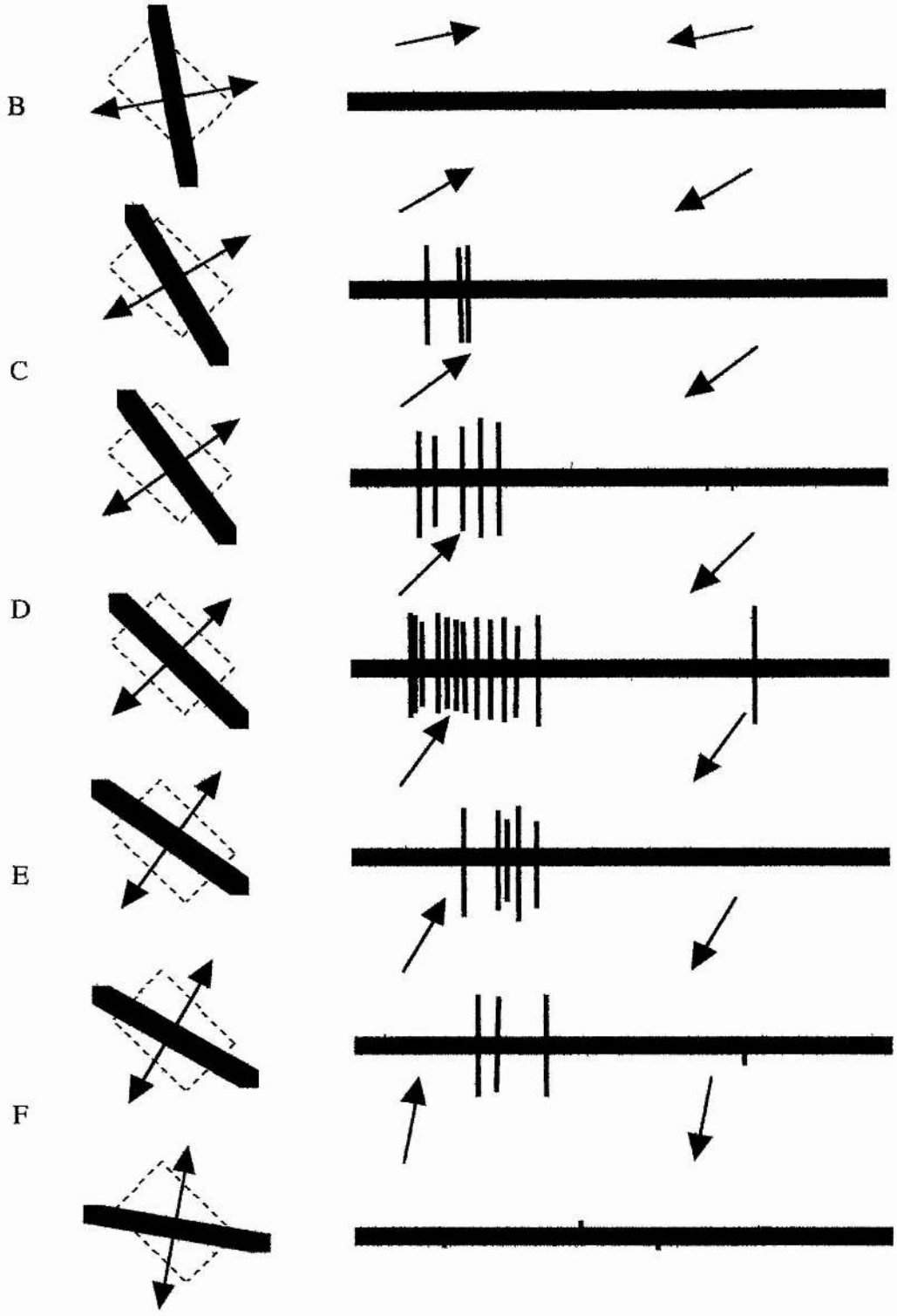

FIGURE 1.1 Neuronal directional selectivity, 14 different directions were tested and the response profiles drawn. Adapted from Hubel and Wiesel (1968).

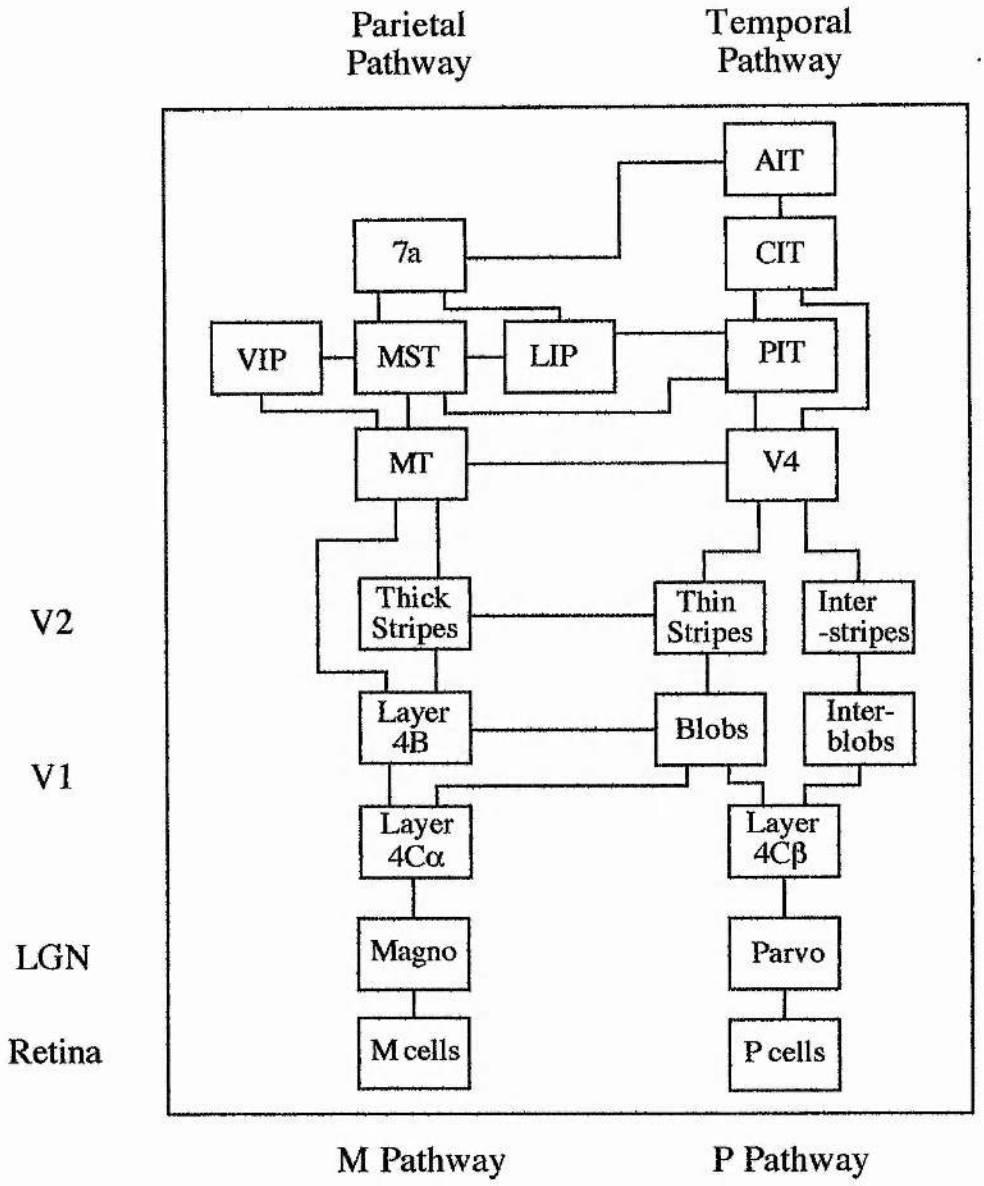

FIGURE 1.2 Schematic map of the anatomical connectivity of several regions of the extrastriate visual cortex (top) and earlier connections from retinal ganglion cells (bottom). The magnocellular channel is grouped on the left while the parvocellular channel components are grouped on the right. Note that nearly all the connections shown here are bi-directional. This implies that the system is not simply based on feed-forward processing but involves feedback processing or pre-processing. The implications of this will be discussed in more detail in chapter nine.

MT was first discovered by Dubner and Zeki (1971) in the macaque brain, situated along the posterior extent of the lower bank of the superior temporal sulcus. It is "visuotopically" organised (Zeki, 1974) and receives ascending projections from V1,

V2 and V3 (van Essen, Maunsell & Bixby, 1981; Ungerleider & Mishkin, 1979). "Visuotopic representation" means that the spatial relationships between items in visual space are preserved in neural representation. The relative strength of representations may vary but relationships regarding proximity are maintained. Another term for the V1 - MT pathway is the "magnocellular" ("M") stream. The "parvocellular" (or "P") stream is anatomically parallel and may well serve complementary functions (Livingstone & Hubel, 1988). Ganglion cells terminating in the M layers of the Lateral Geniculate Nucleus (LGN) have poor spatial resolution and are un-selective for colour. They possess high contrast sensitivity and transmit signals relatively quickly. Cells in the P layer of LGN have high spatial resolution and are colour-selective. They possess low contrast sensitivity and transmit signals relatively slowly. As the M-channel progresses through consecutive cortical areas it passes through the middle temporal area (MT or V5). Unlike the surrounding area of cortex 95 % of the neurones in MT show strong directional selectivity* of the basic form described by Hubel and Wiesel (1968), but a lack of selectivity for form or colour (Zeki, 1974; Maunsell & van Essen, 1983; Albright, 1984). On the basis of this evidence Zeki proposes that MT is one of the main elements of motion processing in the cortex. Macaque monkey MT cells appear to be selective both for direction and for speed. Direction tuning of cells remains constant over large changes in speed (Rodman & Albright, 1987). Ibotenic acid lesions to MT selectively impair motion sensitivity. Contrast thresholds remain unaffected by such lesions (Newsome & Paré, 1988). Rhesus monkeys were trained in motion detection experiments involving dynamic random dot displays. Variation of the percentage of correlated motion behind a masking motion noise signal allowed the derivation of motion thresholds. Contrast thresholds were obtained using an orientation discrimination task for static sinusoidal gratings. The absence of any impairment to contrast thresholds suggests that MT specifically processes motion rather than more general information.

It is suggested that, in humans, the homologous section to MT is the suprasylvian sulcus (Hess, Baker & Zihl, 1989; Zeki, Watson, Lueck, Friston, Kennard & Frackowiack, 1991; Regan, Giaschi, Sharpe & Hong, 1992). Neuropsychological investigations have revealed a patient with "cerebral akinetopsia" (motion-blindness); the patient was shown to have suffered bilateral lesions in the superior temporal region (Hess, Baker & Zihl, 1989).

Positron Emission Tomography (PET) has been used to explore the loci of motion and colour processing in the human brain. Area V4 was found to be maximally active for

---

* For motion along a linear path in the fronto-parallel plane.

colour tasks while V5 (MT in monkeys) was shown to exhibit maximum regional blood flow during visual motion tasks (Zeki *et al.* 1991). Patients with parietooccipital brain lesions to the area underlying Brodmann cortical areas 18, 19, 21, 22, 37 and 39 in the temporoparietal cortex have been shown to be unable to recognise letters defined by motion (Regan, Giaschi, Sharpe & Hong, 1992).

Microstimulation

Microstimulation experiments have provided more direct evidence of the key role that MT plays in motion perception. Low amplitude microstimulation pulses (10 μA, 200 Hz) to groups of MT neurones with similar preferred directions have been shown to bias monkeys' choices towards the neurone group's preferred direction in direction discrimination tasks (Salzman, Britten & Newsome, 1990; Salzman, Murasugi, Britten & Newsome, 1992).

Subsequent experiments investigated the sensitivity of the monkey to microstimulation variation around the normal levels of stimulation frequency (Murasugi, Salzman, & Newsome, 1993). Alert monkeys were given a direction discrimination task involving dynamic random-dot kinematogram stimuli. Amplitude of stimulating pulses was shown to influence the directional specificity of the microstimulation effect. Small stimulating currents affected thresholds in a specific direction, presumably because they operated within single columns. Large currents however gave a non-specific impairment in direction discrimination presumably because large currents activated a wider group of columns (which would encode many directions).

Functional significance of MT and associated neural hardware:

The work reported in this thesis investigates the methods by which the visual system accomplishes the retrieval and coding of an object's trajectory in a form that will permit behavioural responses to such motion. Uses for visual motion information in mammalian vision include time to contact decisions (Lee, 1980), image segmentation (Braddick, 1974), estimating direction of self motion (Koenderink, 1986), control of posture and balance (Gibson, 1950) and also recovering the three-dimensional (3-D) structure of a visual scene (Wallach & O'Connell, 1953).

Models of motion detection

Models to account for motion detector computations come in two basic forms: correlation models (eg. Reichardt, 1961) and energy-based models (eg. Adelson and Bergen, 1985; Watson and Ahumada, 1985).

More complete and detailed models of motion detection are reviewed later in this chapter. In the first instance, all that needs to be examined is the form of the two classes

since they suggest different neural implementations. The auto-correlation principle proposed by Reichardt was based on the visual system of the fly. Two luminance sensitive neurones that are adjacent on the retinal map will fire at different times as an image tracks across the retina. The product of the two outputs provides the motion signal.

A similar mechanism was proposed for motion detection in the rabbit retina, in the form of a spatio-temporal comparator (Barlow & Levick, 1965). This model relies on inhibition from one detector being delayed on its journey to a neighbouring receptor. Fig. 1.3 shows how the connections in neural circuitry would permit this correlation method of motion perception. Motion in the null direction results in parallel inhibition along the circuit. The receptor output is effectively nulled. Inhibition will be less or even zero for motion directions other than the null direction. In this way, the direction of motion of the stimulus dictates the level of neuronal activity (the subsystem is directionally selective).

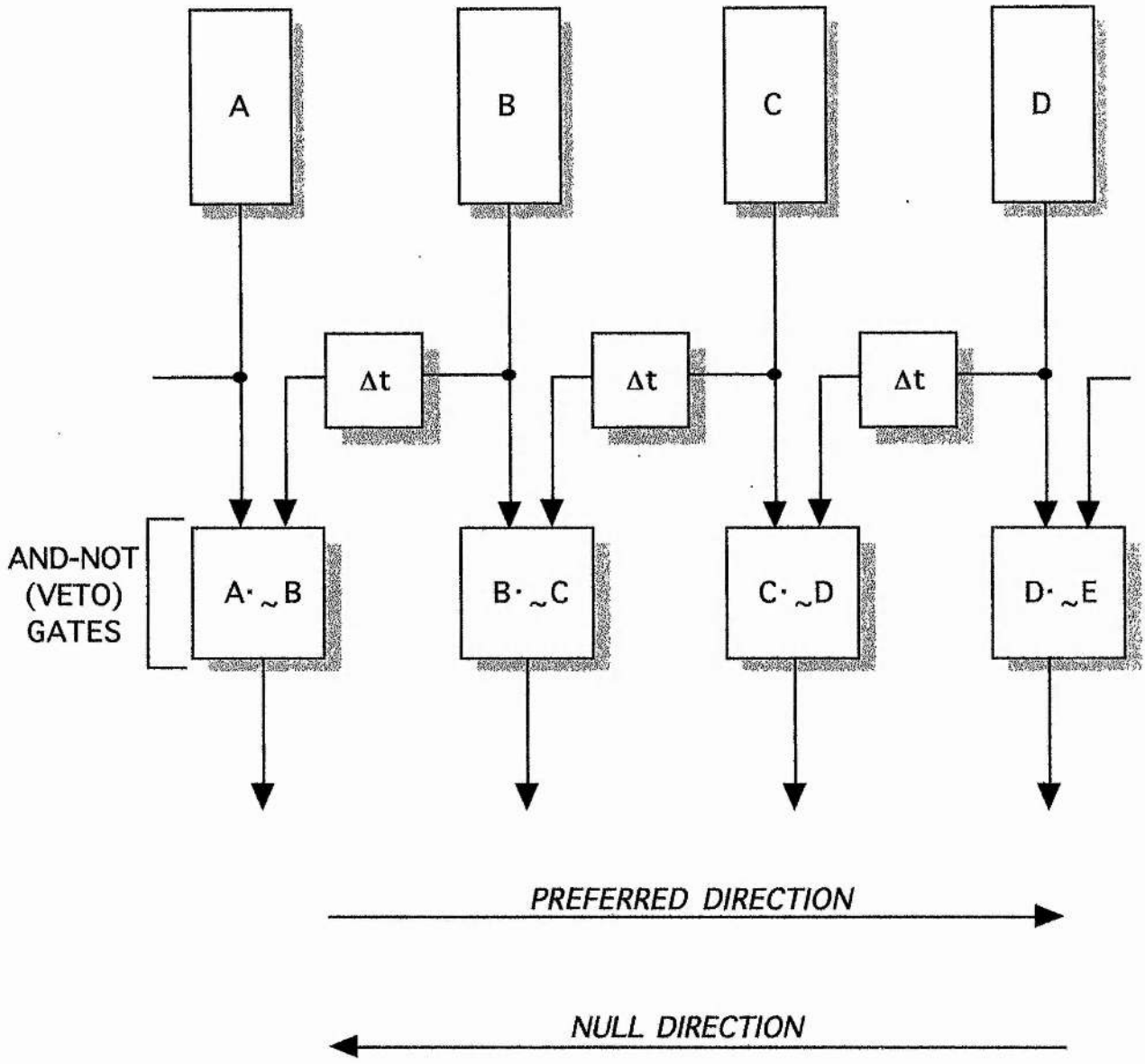

FIGURE 1.3 Direction of motion may be calculated by means of a spatio-temporal comparator: Reichardt (1961), Barlow and Levick (1965). The neural circuit consists of a sequence of "input" neurones A - D. Each input neurone possesses an excitatory connection (+) that extends directly and a time-delayed (Δt) inhibitory connection (-) that extends the next motion detection neurone. These motion sensitive neurones operate as AND-NOT gates. The time-delayed connection from one side makes the gate direction selective. Rightward motion (receptive field stimulation sequence A, B, C & D) sends a direct excitatory input to each motion detector in turn. The lateral inhibitory connections have no functional effect in this situation. Leftward motion, however, triggers an inhibitory signal that spreads laterally and in parallel with the displacement of input signals. The output of the system depends on the

direction of the input signals. Each gate responds more strongly to rightward motion than leftward motion.

Spatio-temporal filter

Another way of visualising a linear spatio-temporal filter is to represent motion in the dimensions of space and time (Fig. 1.4 A): The gradient of a line in this space represents the speed motion of the object. A receptive field oriented in space and time will preferentially signal motion at a certain speed (ie. gradient) as shown. Adelson and Bergen (1985) and Watson and Ahumada (1985) choose to describe motion in this way and propose "motion-energy" models. Calculation of motion in the spatio-temporal frequency domain in this way is formally equivalent to correlation methods (van Santen & Sperling, 1985) but has been supported by neurophysiological data from Emerson, Bergen and Adelson (1992).

Smooth motion indicates continuous motion, whilst sampled motion indicates successive positions of a stimulus in time and space. A movie is an example of sampled motion: stroboscopic presentation of static images at high frequency is sufficient to provide a perception of motion. The spatio-temporal filter is sensitive to either type of motion.

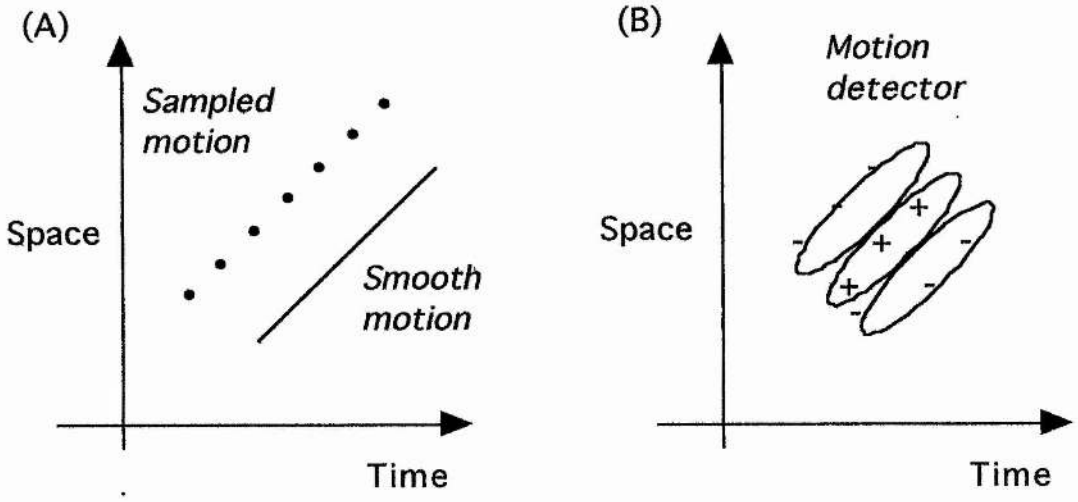

FIGURE 1.4 (A) Space-time representation of the trajectories of objects in smooth and sampled motion. (B) Diagrammatic representation of the spatio-temporal receptive field of a simple linear filter that would preferentially respond to targets moving with the direction and velocity of those shown in A. Targets moving at different velocities would not fit the positive zone of the receptive field of this filter (because they would have a different gradient). Reproduced from Movshon (1990).

Limitations of One-Dimensional (1-D) signals

The image projected onto the mammalian retina is Two-Dimensional (2-D) but the signals generated from the motion detectors discussed above are 1-D. In order to describe adequately the motion of a retinal image, a 2-D vector comprising a magnitude and a direction is needed. Because they are orientation selective, V1 neurones are only sensitive to gradients of image contrast in one direction. The contrast gradient of such a neurone is perpendicular to its preferred orientation, it is along this *and only this* axis that visual motion may be detected. The signal from such a directionally selective neurone is ambiguous and is insufficient to recover the true velocity of a 2-D object reliably. To extract the motion of complex objects, pooling over retinal space is required to integrate the 1-D signals and interpret the visual scene. Recently, investigators have become interested in the time-varying properties of receptive fields. Full characterisation of the receptive field requires a description of its behaviour both in the time domain as well as in the space domain. This extra time-varying dimension of

receptive field response properties may pose additional questions for the role of such units in motion perception (see DeAngelis, Ohzawa & Freeman, 1995 for a review).

Estimating speed from successive retinal images

Algorithms for the estimation of veridical speed and direction of an object have been proposed by Fennema and Thompson (1979), Limb and Murphy (1975) and Horn and Schunck (1981). The calculations involved are based on local computations, such as derivation of image velocity from the relationship between the temporal and spatial gradients of image intensity. In order for these models to work, however, assumptions about image motion are required. The assumptions constrain the infinite number of interpretations of retinal images. Fennema and Thompson's (1979) model derives a veridical velocity field from perpendicular components. The assumption is that image motion comes from rigid bodies moving in the fronto-parallel plane (ie. no rotation, deformation approach or retreat from the observer occurs). This assumption is based on the observation that image motion comes from solid objects and surfaces, which move coherently in relation to the observer. If this assumption is valid, all the parts of one object will move with the same velocity. Velocity will be constant over small areas of the image, but will change abruptly at occluding edges . The use of the rigidity assumption limits the usefulness of any model to instances of targets moving across a visual field. Many every-day occurrences of visual stimuli involve looming or rotating objects such as moving people and trees blowing in the wind. These types of motion are much more complex than simple translation relative to a static observer.

Assumptions

Algorithms with less strict constraints than those mentioned above have been devised, such as the assumption that velocity can vary over images of objects but it does so *smoothly*. This "smoothness assumption" is a reasonable assumption for the behaviour of natural scenes. Sudden changes in velocity should occur only at occluding edges. To account for certain types of motion, however, further assumptions are required: eg. velocity variation is minimised over areas of the image (Horn & Schunck, 1981; Hildreth, 1984). Fig. 1.5 illustrates the well-documented barber-pole illusion (Wallach, 1976). The pattern on the cylinder rotates horizontally but the appearance is of vertical motion of tilted bars.

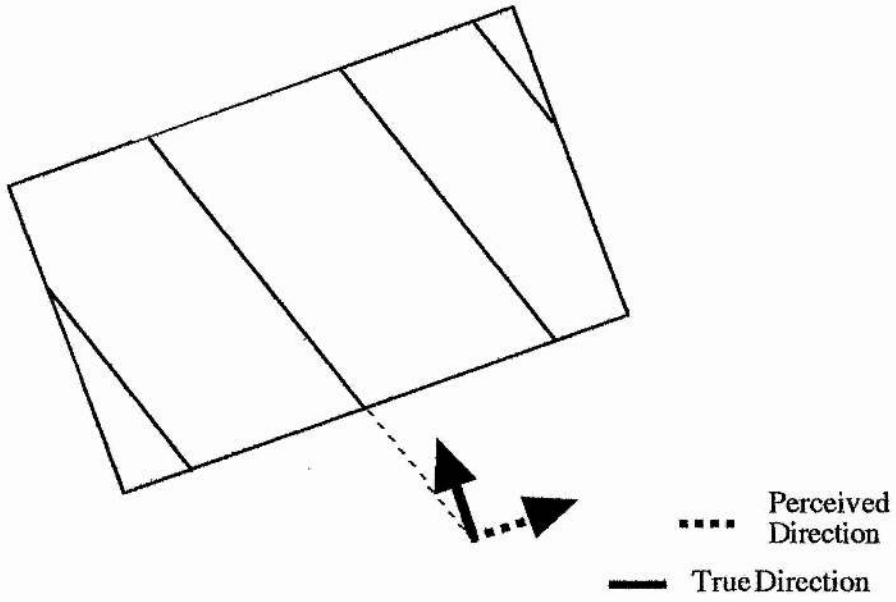

FIGURE 1.5. The barber-pole illusion. A 2-D view of a cylinder with a helix on its surface rotating around the vertical axis. The veridical and perceived direction of the motion of the bars is shown in legend.

Minimising variation in velocity along a contour yields correct velocities for objects with straight lines and yields errors that match human perception (e.g. the barber-pole in Fig. 1.6). In the barber-pole illusion a rotating cylinder with a helix on its surface is seen to move up or move down rather than around. The veridical velocity field in (b) contains horizontal components but the computed velocity field (d) with velocity minimisation contains vertical components.

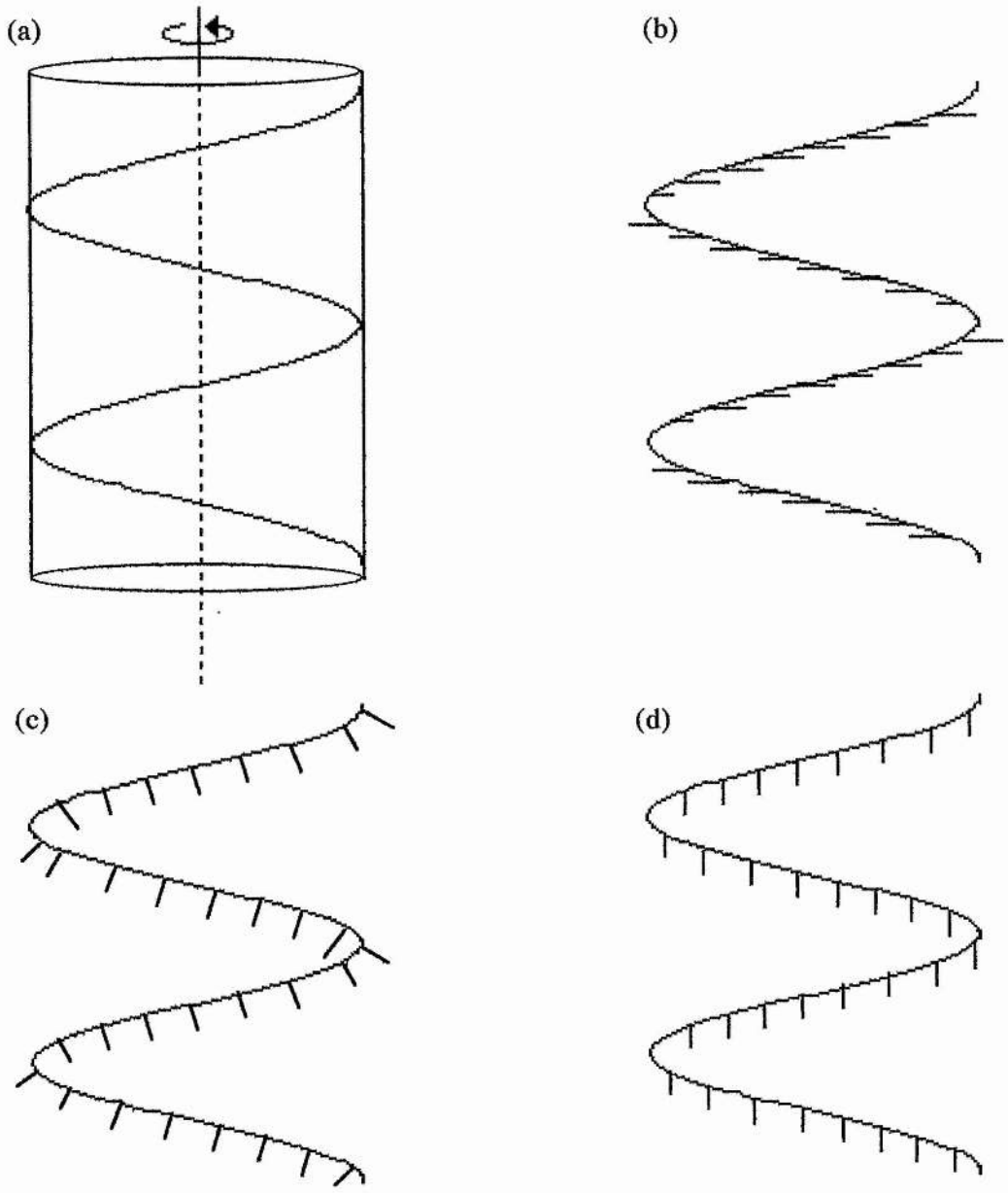

FIGURE 1.6. The barber-pole illusion. (a) A cylinder with a helix on its surface rotating around the vertical axis. (b) A two-dimensional projection of the helix surface with straight lines representing the point velocities of the surface. (c) Straight lines indicating perpendicular components of velocity. (d) Straight lines indicating velocity field that minimises variation in velocity along the edge. Reproduced from Hildreth (1984)

Similar to the gradient model above but originating in the domain of biological models is the Marr and Ullman (1981) scheme of spatio-temporal derivatives. Its limitation is that it only computes direction of motion and not speed.

Hildreth's (1984) model predicts deviations from veridical perception in human vision, providing evidence that minimisation of velocity variation is an organising principle in mammalian vision. The simplest assumption from the above models, however, is that local velocity measurements are measured and subsequently integrated in a two-stage process.

The Aperture Problem

The actual process of velocity estimation is complicated by the ambiguity of individual velocity estimates from motion detectors. The inability of local readings to yield veridical object velocity is known as the "aperture problem" (Horn & Schunck, 1981; Hildreth, 1984; Hildreth & Koch, 1987). This is illustrated in Fig. 1.7, below. The relatively small receptive field of a motion detector can only signal the component of motion perpendicular to the edge of the contour that extends beyond the receptive field's boundary.

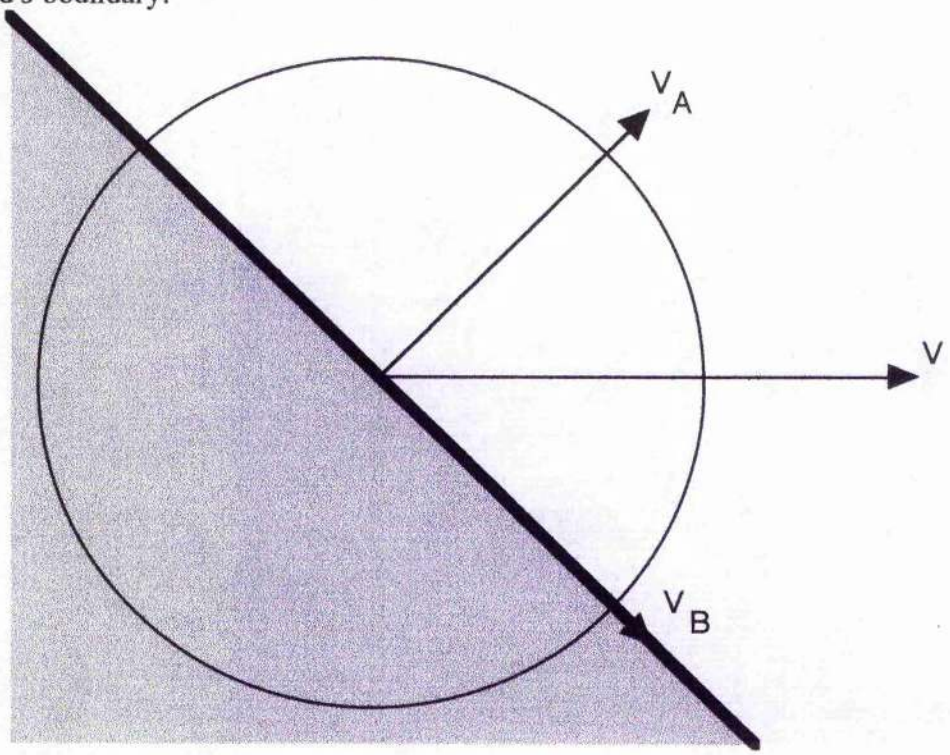

FIGURE 1.7. The aperture problem: the velocity V comprises two components V_A and V_B; only V_A can be sensed by the motion detector.

Morgan, Findlay & Watt (1982) discuss the broader issue of viewing whole objects behind apertures. It is possible to recognise an object from successive views of parts of the object. An example used in the paper is that of the spokes of a cart wheel moving behind a narrow aperture. Observers have no difficulty in perceiving the individual

spokes as belonging to the wheel of a cart. This demonstrates the ability of the visual system to integrate isolated aspects of the visual image and combine them into a meaningful percept.

Integration of Motion Measurements

In order to compute the velocity field of an object the visual system must be able to represent the components of the object's motion in 2 dimensions. Motion detection mechanisms of the type described by Barlow and Levick (1965) (discussed previously) deal only with motion along one axis. Fig. 1.8 shows an array of (1-D) motion detectors' receptive fields with an edge passing over them. Each of the individual detectors can only signal the component motion V_A as was shown in Fig. 1.7. The perpendicular components of velocity derived from motion detectors must be integrated in some way to provide the true velocity signal.

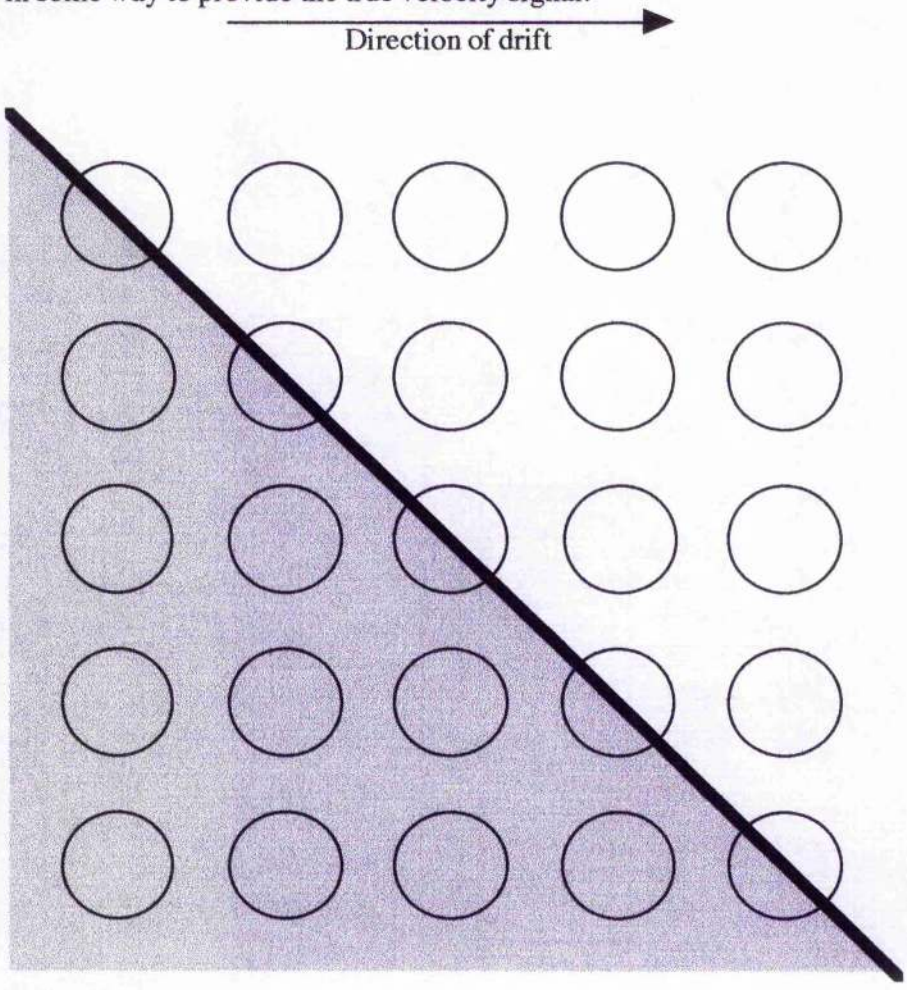

FIGURE 1.8 Array of receptive fields with an edge passing over them.

THE INTEGRATION OF MOTION MEASUREMENTS.

A number of models have been proposed to account for the combination of 1-D signals from motion detectors into a velocity field.

INTERSECTION OF CONSTRAINTS

The measurement of perpendicular components and their integration can be seen as two separate stages of visual processing. The Intersection of Constraints (IOC) model provides a solution to the perceptual ambiguities arising from the aperture problem and the problem of integration of motion signals across motion detectors. The IOC is supported by psychophysical studies (Adelson & Movshon, 1982; Welch, 1989; Ferrera & Wilson, 1987; Stone, Watson & Mulligan, 1990; Derrington & Suero, 1991; Smith & Edgar, 1991) and some physiological evidence (Movshon, Adelson, Gizzi & Newsome, 1985).

In addition to discoveries about the barber-pole illusion, Wallach (1976) also noticed that two, spatially overlapping, drifting stimuli may evoke a percept of motion in a different direction and a different speed from either of the components. This process is the subject of the combination model described by Adelson and Movshon (1982).

Consider the motion of a grating behind an aperture as depicted in Fig. 1.9. The bars generate a retinal image motion that is compatible with a whole family of velocities and directions. The ends of the velocity vectors of the bars in this instance could lie anywhere on the vertical line shown in the picture. This line is called the "constraint line" (Adelson & Movshon, 1982). However in the absence of other cues what observers always see is the perpendicular solution "P".

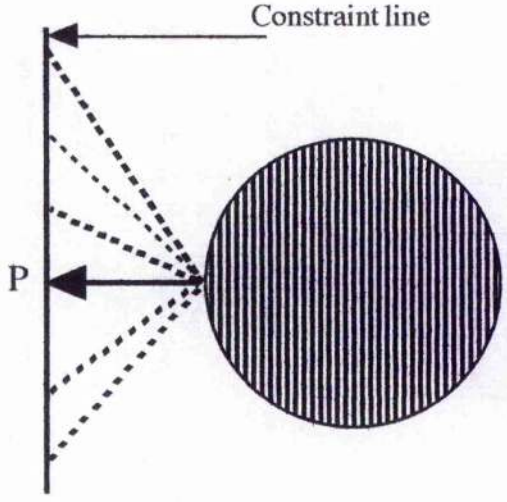

FIGURE 1.9. Constraint line. Family of possible motions for an edge moving behind an aperture defined by constraint line.

If two gratings drifting at similar speeds are superimposed behind an aperture, what is seen is very different from the single grating motion above. Fig. 1.10 shows the distinctive tartan "plaid" pattern formed by superimposed gratings. The ambiguity of motion is eliminated. Only when extreme differences in speed and size between the two gratings are introduced does the "component motion" appear (where two gratings move transparently over each other). The vector P represents the resultant perceived motion of the pattern which is very different from the motion of either component C1 or C2.

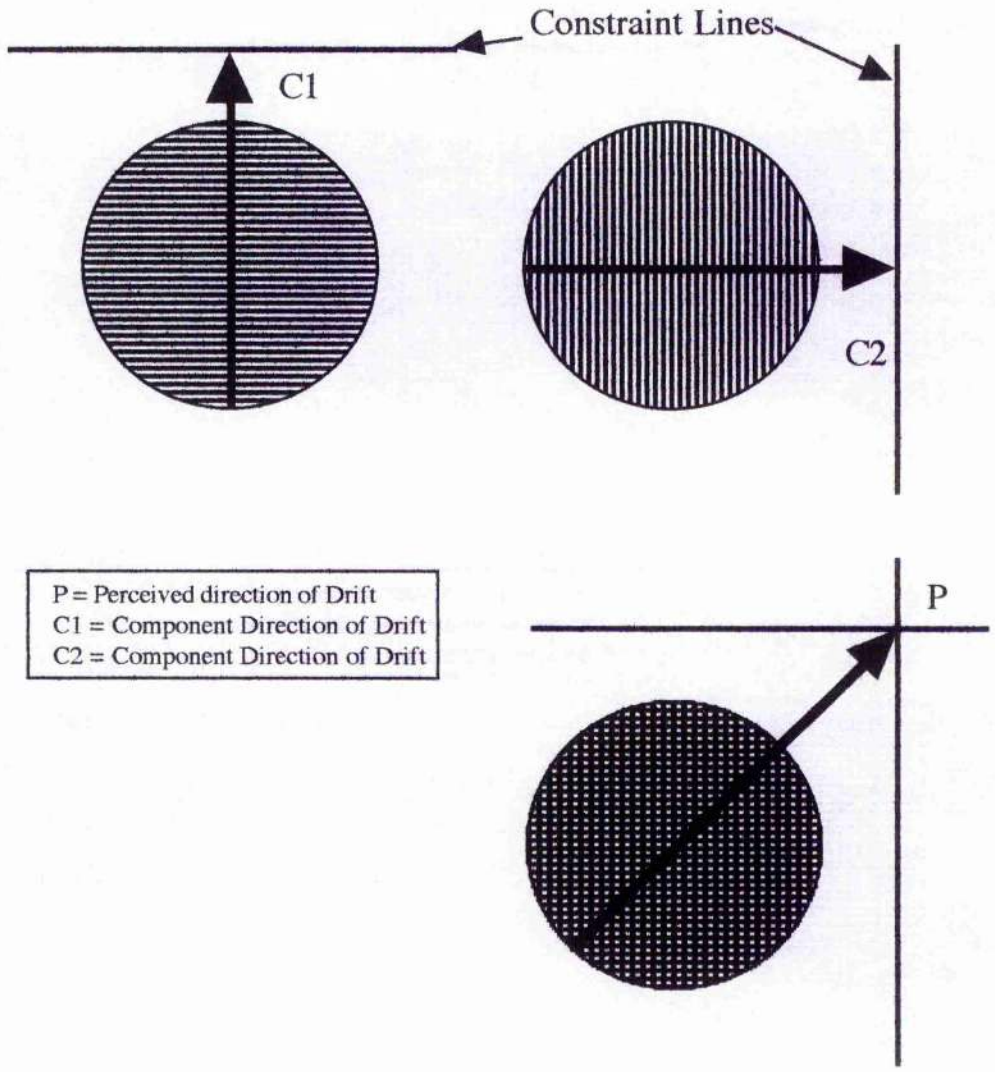

FIGURE 1.10. Superimposed gratings form a plaid pattern. The intersection of constraint lines determines the resultant motion. This means of representation is known as a vector-space diagram. The arrowed lines are "vectors" whose length indicates a magnitude (speed in this case) and whose orientation indicates a direction. This method of presentation is applied throughout this thesis.

The widely held explanation of this resultant percept is called the Intersection of Constraints Model (IOC). Adelson and Movshon (1982) proposed that the visual system generates "constraint lines" as depicted in Fig. 1.10, one for each set of gratings. The intersection (loci) of these two lines is calculated and this uniquely specifies the motion of the resultant two-dimensional pattern (see resultant P at intersection).

Psychophysical experiments involving speed perception (Welch, 1989) showed that the speed of the underlying components of a plaid determined the ability of observers to discriminate the speed of the whole plaid pattern. Intuitively one would expect the speed discrimination to be limited by the speed of the blobs of the pattern (ie. the intersections of the gratings) but this was not the case. This finding is consistent with the IOC model in that component speed is analysed first and resultant motion (speed) is then computed from the intersections of the constraint lines.

Vector Summation as a method of combination.

The resultant direction of plaid patterns could perhaps be computationally solved by a simple vector summation rule rather than an IOC rule. A vector summation rule applied to the vectors of the component gratings would yield the correct result most of the time. However Fig. 1.11 shows how under certain circumstances the summation rule yields particularly non-veridical results, the predicted perceived direction and speed differs radically from what observers actually perceive. Fig. 1.11(a) shows the IOC prediction for a combination of components. The vector P is the actual perceived direction. Fig. 1.11(b) shows the vector summation solution. The vector P' is the predicted vector but it is the wrong length (speed) and is pointing in the wrong direction. This means that simple vector summation can be discounted as a method of combination for veridical results.

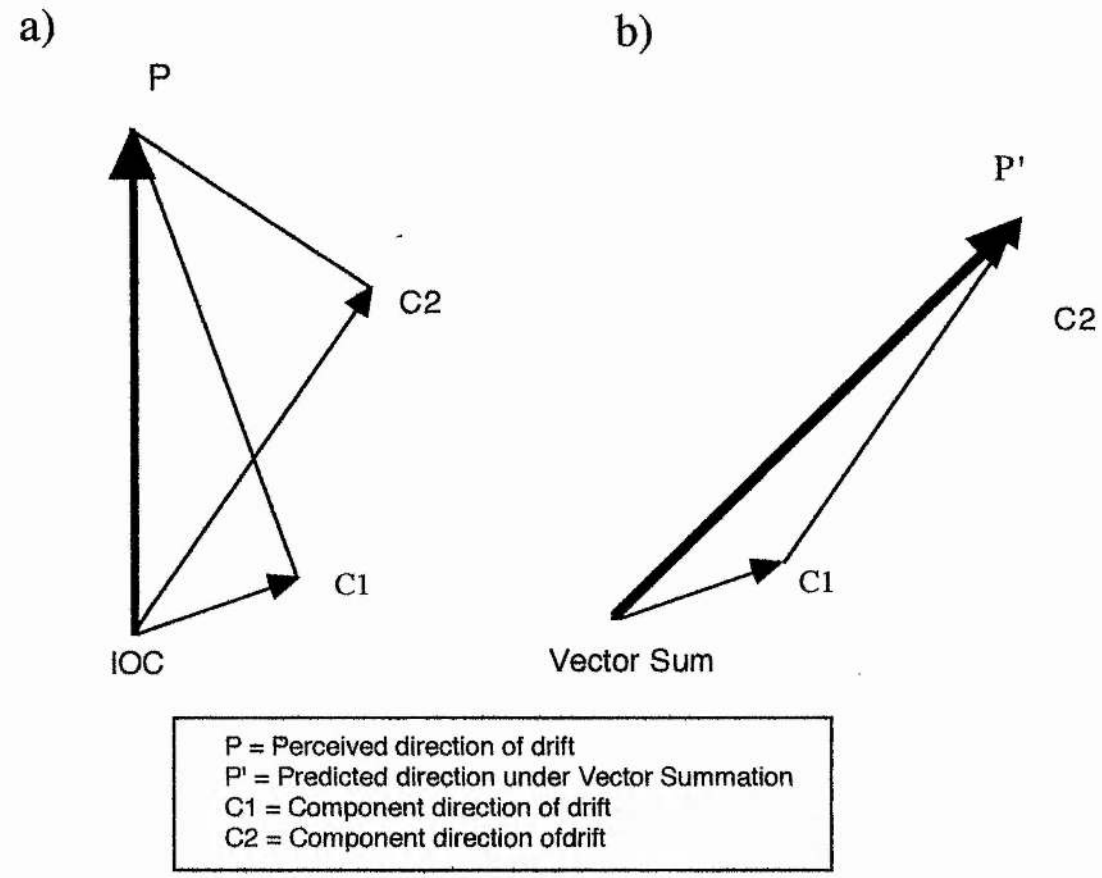

FIGURE 1.11. IOC versus vector summation. Vector summation yields non-veridical results.

Note that the phenomenon of motion transparency (Ramachandran, 1990; Stoner, Albright, & Ramachandran, 1990; Noest, & van den Berg, 1993), where the components of a plaid appear to drift over each other instead of forming a coherent pattern, means that the visual system must be able to compute perpendicular components but not integrate them. This perceptual dissociation is most likely to happen when the bars of the gratings are semi-transparent. The existence of such motion percepts argues against a fixed recombination of local motion signals into a plaid signal. Perrone(1990) and Wilson, Ferrera and Yo (1992) propose alternatives to the IOC stage as discussed later in this chapter. Fig. 1.12 illustrates the different perceived directions of coherent and transparent motion in such displays when they are formed by the superposition of independently drifting gratings.

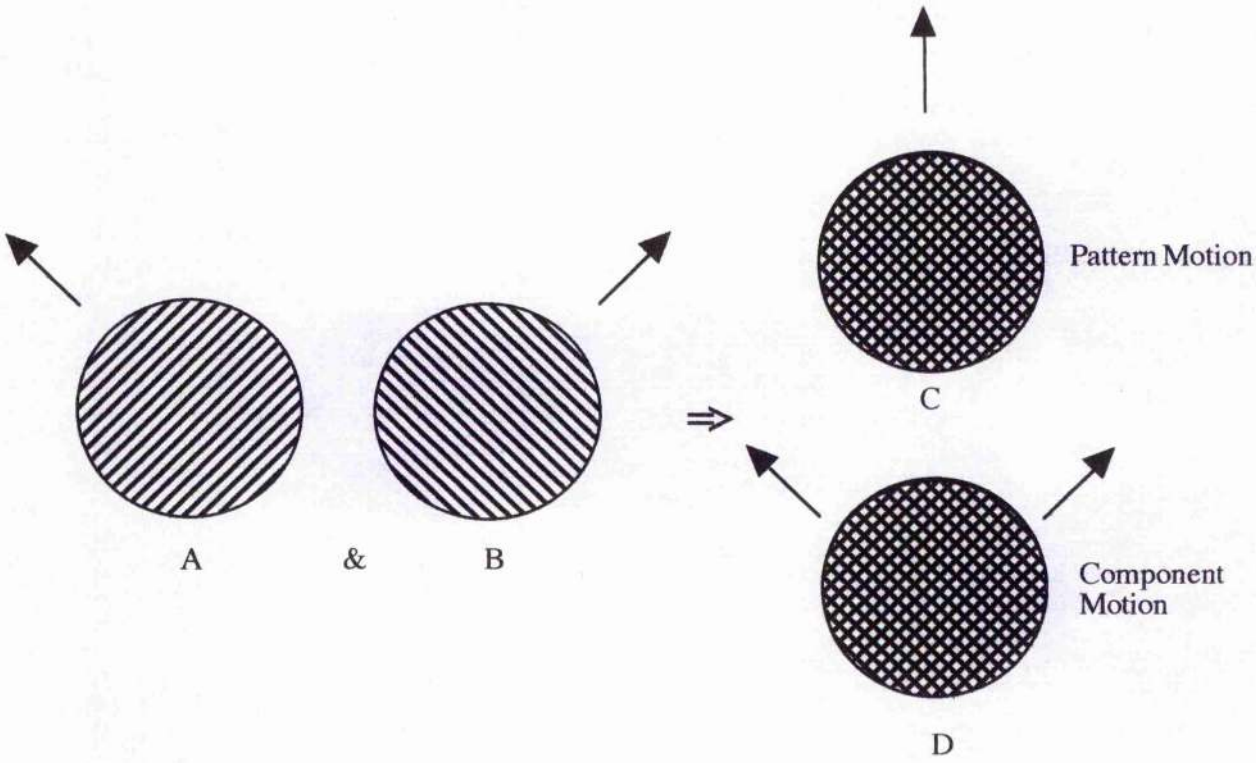

FIGURE 1.12. Two superimposed gratings (A & B) drifting orthogonally form either coherent (C) or transparent (D) percepts depending on the viewing conditions. Perceived direction of motion is indicated by the arrows. In case D where the component motion is seen, the individual gratings appear to slide over one another.

VECTOR AVERAGE

Three solutions to ambiguous motion

The three possible solutions to the inherent ambiguity of motion in an aperture are shown in Fig. 1.13. As well as the IOC solution, a *vector average* of the component directions normal to the contour orientations could recover the motion. Psychophysical performance for some visual displays has been interpreted as evidence supporting this method of combination (Ferrera & Wilson, 1987; Watson & Ahumada, 1985; Williams & Phillips, 1987). Displays comprising more than one contour contain features ("blobs") where the contours meet or cross over each other. By tracking the progress of such features across the aperture, the visual system can recover the veridical direction of motion of an object.

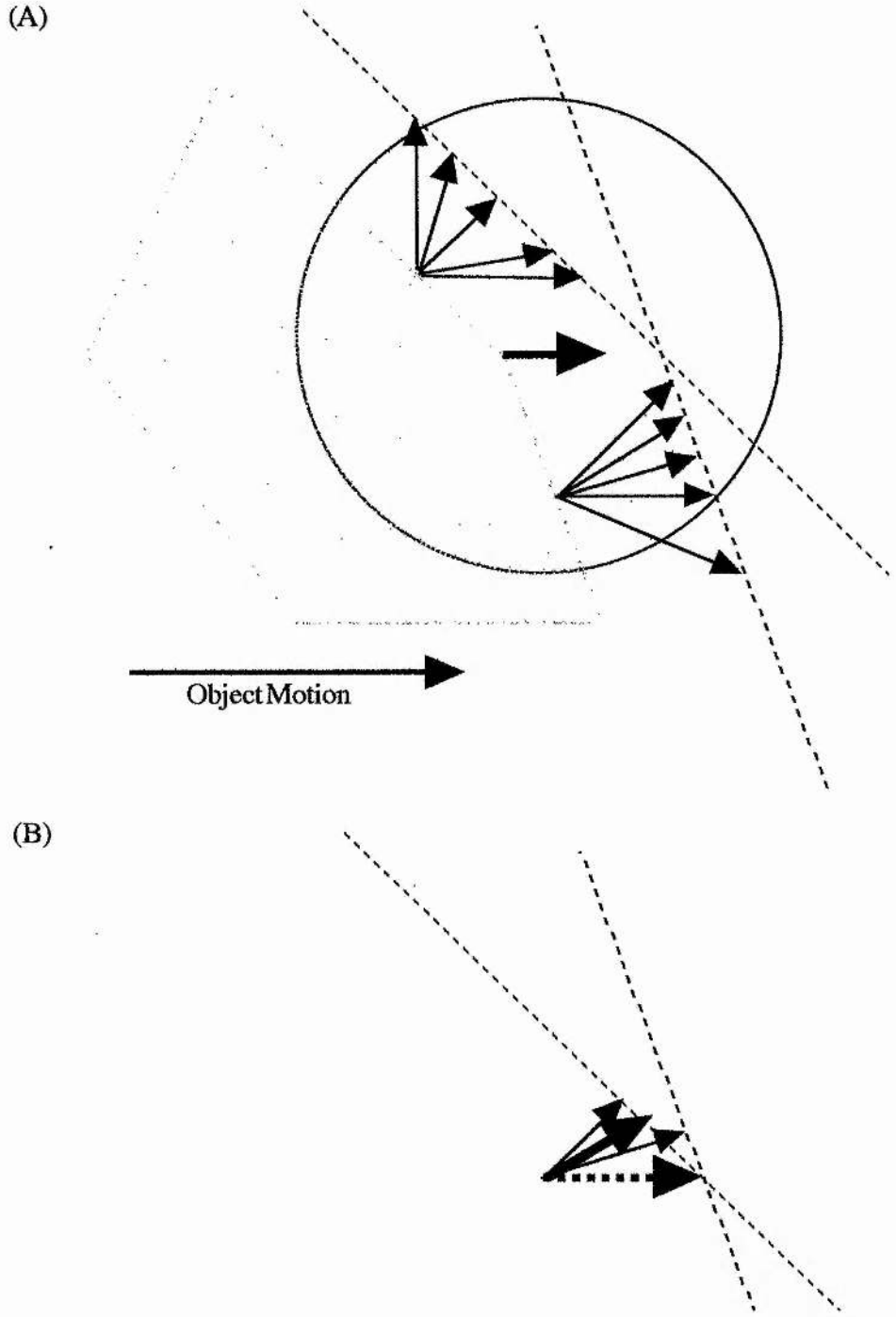

FIGURE 1.13. Object motion behind apertures. (A) An object with a corner moves horizontally behind a circular aperture. The thick arrow indicates the trajectory of the corner, while the thin arrows indicate some of the motions consistent with local information at straight edge segments. (B) The two thin arrows indicate the component motions for the diagram in (A); the thick arrow represents the average of two component vectors, and the dashed arrow represents the IOC solution in velocity space, which corresponds with the trajectory of the corner in (A). Reproduced from Mingolla, Todd and Norman (1992) p 1016.

Adelson and Movshon (1982) and Movshon *et al.* (1985) argue against vector average computational solutions and feature-tracking solutions. In a series of "coherence" detection experiments, the threshold for coherence was varied in the following fashion. Parallel strips of 1-D noise of varying widths were superimposed on plaid patterns. On some trials the orientation of the strips was parallel to one of the component gratings, while on other trials the strips were oriented perpendicularly relative to the plaid motion. Noise oriented within 20 deg. of the components was better at masking the resultant percept than was noise perpendicular to plaid direction.

Almost all the prior experiments that were used as evidence in favour of the IOC rule included a confounding factor. Apart from an experiment by Ferrera and Wilson (1991), all the relevant experiments featured plaid stimuli whose intersections (or "blobs") moved in the same direction as the resultant vector of the IOC. The exception was a speed matching experiment where the observers were found to produce reliable speed matches only when the plaid was compared with a grating drifting at the same speed and in the same direction as the intersections of the plaid (Ferrera & Wilson, 1991). Mingolla, Todd and Norman (1992) removed the identical solution for IOC and feature tracking to control for this and found evidence in favour of a vector average computation. The stimuli involved displays with no identifiable features, only oriented contours. They also compared the relative perceptual salience of velocity space (IOC) solutions with vector averaging solutions.

Despite this evidence in favour of vector averaging, it is important to note that not all motion perception involves vector averaging. If either the contrast or the speed of each component of a plaid is sufficiently different, it is possible for them to appear to move transparently over each other. This means that multiple velocity signals can exist in one point in space. A vector-averaging solution does not permit this percept. A strict application of vector averaging would force averaging across object boundaries which would also yield results inconsistent with the observed motion of "transparent" components.

THE BLOB TRACKER / FEATURE TRACKER THEORY
(One stage models)

Neurophysiological evidence does not directly distinguish the method of integration of motion signals. However, a one-stage feature-tracking model (Gorea & Lorenceau, 1991; Alais, Wenderoth & Burke, 1994) is a more parsimonious solution than the two-stage models of motion integration. Gorea and Lorenceau tested the prediction that the perceived direction of coherent plaids should be unaffected by the direction of one or other of their component gratings if the direction predicted by the intersection of the lines of constraint (or blobs) remains unchanged. This was achieved by the use of a

compound stimulus (plaid) with only one drifting component in a series of threshold and reaction time (RT) experiments. It was shown that perceived direction depended on the directional analysis of both Fourier components and higher contrast regions of complex drifting stimuli.

Derrington and Badcock (1992) suggest that the mechanism operates at a low level, while Burke and Wenderoth (1993) propose that it is monocular in nature. The mechanism is often referred to as a "blob-tracking" (BT) mechanism since it is presumed to operate by tracking the "blobs" evident in plaid patterns at the intersections.

In addition to the evidence cited in previous sections for two-stage mechanisms, Derrington and Suero (1991) and Stone, Watson and Mulligan (1990) support such processes. Thus it has been proposed that IOC and BT mechanisms coexist (Burke, Alais & Wenderoth, 1994). Furthermore it has been proposed that the linear interaction of component and plaid based mechanisms is more likely to involve parallel rather than serial processing (Gorea & Lorenceau, 1991).

SPATIO-TEMPORAL INTEGRATION SOLUTIONS: MODELS OF FOURIER AND NON-FOURIER MOTION

Representing motion in x-y-t space

Heeger (1987) and Grzywacz and Yuille (1991) have proposed models to account for motion perception using spatio-temporal mechanisms of the type described earlier in this chapter. A class of visual stimuli exists which gives a distinct impression of motion without providing a consistent signal for conventional low-level motion detectors such as these. Such motion stimuli are coded according to the information that they contain; related classification schemes distinguish between "Fourier" and "non-Fourier" motion (Chubb & Sperling, 1988) or between "first-order" and "second-order" motion (Cavanagh & Mather, 1989).

A single point is sufficient to define first-order stimuli (luminance or colour). However two points are required to define the local values of each attribute of second-order stimuli (differences in texture, depth or motion). Texture involves two points separated in space, binocular disparity involves two points separted by eye and motion involves two points separted in time.

Fourier-based motion detectors can extract a velocity signal from oriented intensity contours in a space-time plot (Chubb & Sperling, 1988). Fig. 1.14 shows how motion in the fronto-parallel plane can be represented in three dimensions, with time as the

third dimension. Orientation in the space-time domain (x-t) describes the motion of the stimulus when it subjected to Fourier analysis (Chubb & Sperling, 1989a).

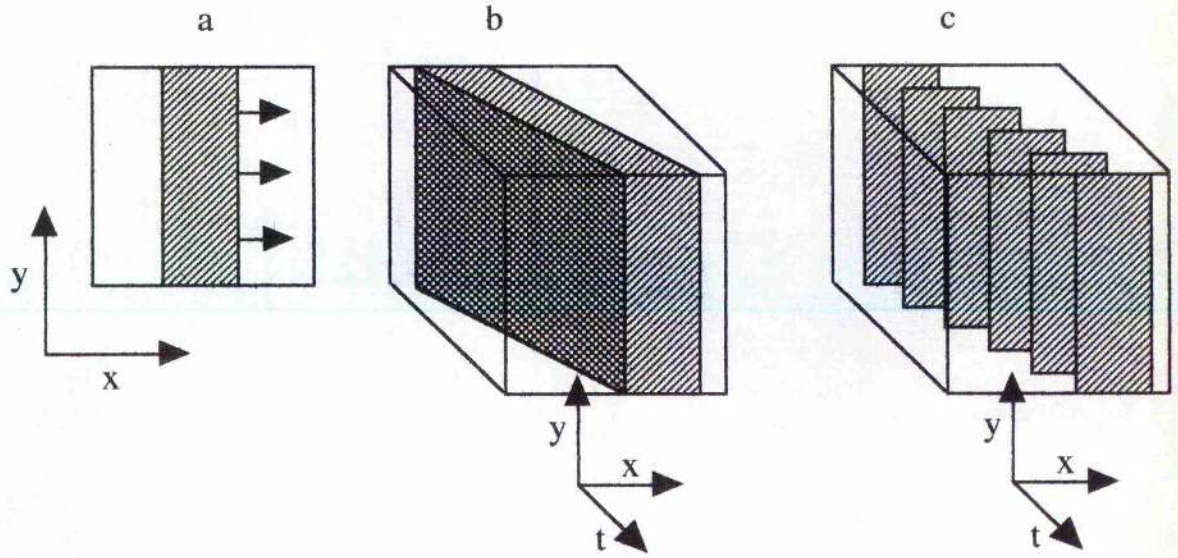

FIGURE 1.14 Motion in space and time. Section a is a picture of a rightward moving vertical bar. Section b, is a depiction of the stimulus motion in three dimensions, the normal x and y of space and t representing time. Section c is a spatio-temporal picture of sampled motion as found in a movie.

Non-Fourier and Fourier Stimuli

Adelson and Bergen (1985) give an example of a system of low-level motion processing which uses standard motion analysis. Other models of motion perception using standard motion analysis as input are Heeger (1987) and van Santen and Sperling (1985).

Non-Fourier stimuli, termed "drift-balanced", contain equal amounts of motion energy in opposite directions when subject to Fourier analysis. Such stimuli are invisible to conventional low-level motion detectors (Chubb & Sperling, 1988; 1989a). Such spatio-temporal Fourier energy can be interrupted, however, by removing the oriented energy. This can be done by altering the intensity of successive time slices through the space-time plot. An example of this would be contrast reversals over time.

First-order and second order motion

Cavanagh and Mather (1989) use the terms "first-order" motion and "second-order" motion to classify the information contained in patterns. Differences in colour or mean

intensity in image regions define first-order contours. Image regions that have the same mean intensity but different spatial, temporal or ocular distributions of luminance or colour define second-order contours. The range of stimuli described as "second-order" are characterised by the apparent motion of second-order contours.
Second-order stimuli necessarily lack local motion cues. For example by spatially modulating the contrast of a dynamic random dot field according to a moving sine function, a textured sinusoidal grating is produced. Despite the absence of coherent motion amongst the constituent dots, observers perceive the continuous motion of a contrast envelope. The second-order stimuli described by Cavanagh and Mather within this classification system coincide with a subset of Chubb and Sperling's (1989a) non-Fourier stimuli (ie. the stimuli that involve second-order contours).

Despite the *description* of second-order stimuli, no strong agreement exists for the *explanation* of the visual process responsible for supporting such motion perception. Three classes of explanation for the mechanism mediating second-order or non-Fourier motion perception have emerged in the literature:

a) a post-attentive object-tracking mechanism;
b) a low-level detection mechanism responsible for first-order motion which possesses non-linear properties affording it weak responses to second-order motion;
c) a mechanism separate from the first-order system but specialised for extracting the motion of second-order contours.

To summarise: explanation a) is essentially a feature mapping approach whilst b) and c) involve motion-energy detection by single and multiple mechanisms respectively. A feature mapping approach involves a high-level mechanism computing the temporal correspondence between features extracted from the image. A motion-energy approach involves a low-level mechanism operating on a non-linear, neural transformation of the luminance profile of the image.

Non-Fourier motion and Feature Mapping

Non-Fourier motion stimuli *appear* to embody features, and as such would be amenable to processing by a high-level feature-matching mechanism. Examples of such features are evident in the high and low contrast bars of a contrast-modulated noise field. Braddick (1980) proposed just such a mechanism, whilst Cavanagh ((1992) proposed a feature-tracking mechanism operating post-attentively. A feature-tracking mechanism is developed by Ullman (1979) in the so-called "minimal mapping theory". The account

includes algorithms to compute the most likely correspondences between the basic "elements" of figures. These elements consist of edges, lines, blobs, corners, etc.

Chubb and Sperling (1988) demonstrated that explicit encoding of global features is not necessary in many cases of second-order motion. Energy-based motion detection involving simple non-linear transformation of the image's luminance profile followed by spatial and temporal filtering can recover a motion signal. A recent development of the idea of a luminance non-linearity (in this case rectification) is reported by Wilson, Ferrera and Yo (1992).

Evidence in support of the use of feature-based strategies in the detection of second-order motion comes from Smith (1994a). Two experiments were presented involving contrast-modulated motion stimuli.

Using an inter-stimulus-interval (ISI) between the updates of the position of the stimulus in order to favour the use of a high-level, feature-based strategy, it was found that observers reported motion in the direction of the features. (Georgeson & Harris (1990) reported that an ISI greater than 40 msec was sufficient to favour feature-based strategies.) The imposition of second-order masks designed to decrease feature salience was shown to reduce direction identification performance.

The study by Smith (1994a) shows, however, that second-order motion is not exclusively detected by a high-level feature-based mechanism. When no ISI was used, direction judgements were consistent with the use of low-level motion-detecting strategies. This finding suggests that low-level detection may be more important in second-order motion processing.

Low-Level Motion Mechanisms.

The second and third explanations of second-order motion processing [(b) and (c) above] both come under the umbrella of low-level motion mechanisms. Such systems obviate the need to encode features and their relations. This class of explanation may be subdivided into two main types.

i) Separate mechanism models. Separate second-order detectors are used but they operate on qualitatively similar principles.

ii) Single mechanism models. Both first and second-order motion are detected by the same low-level mechanism.

Two Separate Mechanisms.

As indicated above, Chubb and Sperling (1988, 1989a) and Werkhoven, Sperling and Chubb (1993) suggest that motion energy is incorporated in neural representations of

the image by rectification of the image's luminance profile followed by conventional energy detection. Wilson and Mast (1993) provide evidence to support the instantiation of such a model (Wilson *et al.*, 1992) with the discovery that it can predict the perceived direction of type II plaids* and texture boundaries. Chubb and Sperling (1989b) used motion displays containing first and second-order motion in opposite directions to show that perceived direction reverses according to viewing distance. This also suggests that different mechanisms operate depending on the viewing conditions.

Harris and Smith (1992) observed that first-order motion stimuli elicited Optokinetic Nystagmus (OKN) whereas second-order motion stimuli did not. This result implies that two separate systems operate, with only one able to drive OKN.

Mather and West (1993) investigated direction discrimination performance for three kinds of two-frame random dot kinematogram (RDK). A pair of frames featured either intensity-defined random blocks, texture-defined random blocks or a mixture of the two. Where the texture differed from the background only in terms of contrast, RDKs had second-order properties. Second order properties are, as explained above, features of the stimuli that are invisible to standard Fourier (first-order) motion detection systems [such as those described by Barlow and Levick (1965) or Reichardt (1961)]. Luminance defined dots exhibited first-order properties. When the same properties (first or second order) were used in both the first and the second frame, observers were able to detect the direction of RDK displacement. In situations where the two frames had different properties, subjects' direction discrimination fell to chance. The implication was that observers could not integrate the two (mixed) frames of the RDK. Ledgeway and Smith (1994) conducted a conceptually similar study but used continuous motion as opposed to two-frame stimuli. In addition, periodic stimuli were used instead of random dot patterns. This allowed the formulation of precise predictions about perceived direction as a function of phase shift. Integration of first and second-order frames by the visual system would lead to an unambiguous percept of motion in a particular direction whereas separate analysis would lead to an ambiguous motion percept.

Single Mechanism.

The third interpretation claims that the same low-level mechanism detects both first and second-order motion stimuli. Two models of this type have been proposed recently.

---

* Type II plaids are a specific type of second-order 2-D stimulus and are discussed in detail in chapters seven and eight.

Grzywacz (1992) proposes motion detection by the same means as Chubb and Sperling (1988, 1989a) but without the separate linear mechanism. The second model from Johnston, McOwan and Buxton (1992) owes its inspiration to the spatio-temporal gradient scheme of Marr and Ullman (1981).

It is possible that conventional, low-level detectors may process second-order motion using an internally generated distortion product. A luminance non-linearity at an early level in the visual system could account for second-order motion perception. Distortion products at the retinal level (Burton, 1973; Macleod, Williams & Makous, 1992) as well as at the Lateral Geniculate Nucleus (LGN) (Derrington, 1987) have been implicated in the perception of second-order motion. The second-order stimuli in the studies were produced by summing two sinusoidal gratings of similar spatial frequency. The result is a perception of spatial and moving "beats".

CONCLUSION

Smith (1994b; Personal Communication) concludes that three motion detection mechanisms co-exist in human vision. Two are based directly on image intensity analysis and the third on feature tracking (see Fig. 1.15). This conclusion is based on the assimilation of the implications of the results of the experiments reported above (including his own). Experiments such as those of Derrington and Badcock (1985) argue against the simple explanation of contrast-modulation perception in terms of distortion products.

A single mechanism such as that proposed by Johnston *et al.* (1992) should be able to integrate successive frames of first and second-order contours. The experiments of Mather and West (1993) and Ledgeway and Smith (1994) show that such integration does not happen.

The finding of Harris and Smith (1992), that second-order patterns do not elicit OKN suggests that a second-order mechanism based on intensity is separate from the first-order intensity based system involved in driving OKN.

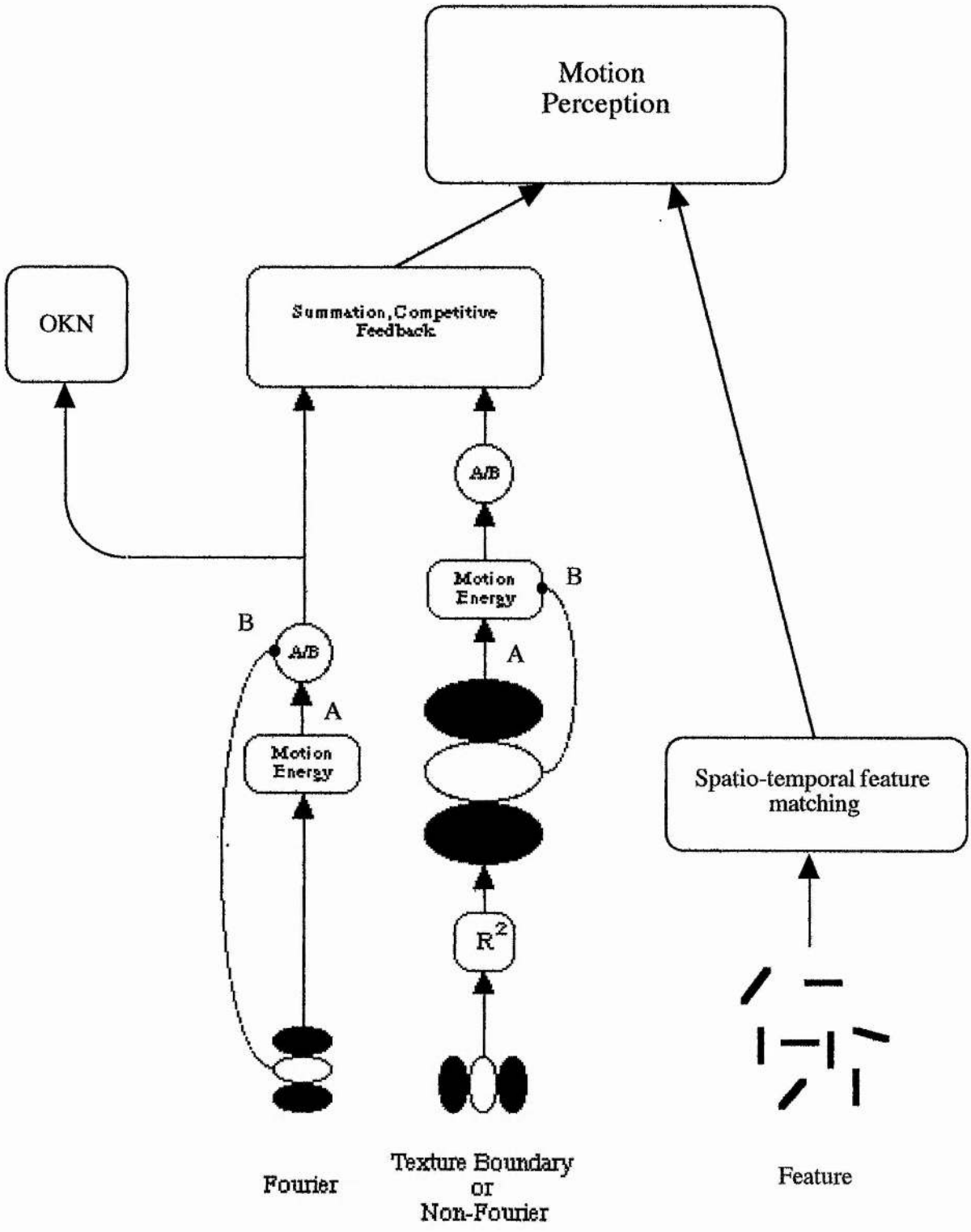

FIGURE 1.15. Smith and Ledgeway's (1994) version of the Wilson, Ferrera and Yo (1992) cosine weighted model: the additions are a separate path for feature mapping and a module to drive OKN from only first-order motion.

INTEGRATION SCHEMES LACKING CROSS-DIRECTIONAL INTERCONNECTIVITY

The balance of the literature at the moment favours Smith's interpretation, particularly since he is not committed to any particular instantiation of the three-track model. As will be discussed later however, models such as that of Wilson *et al.* (1992) require detailed scrutiny to ensure that the conclusions being drawn are correct. The Wilson *et al.* (1992) model involves cosine weighting of the Fourier and Non-Fourier channels to yield a vector-sum estimate of 2-D pattern motion. This particular model has been shown to map onto the known physiology of the geniculostriate pathways as shown in Fig. 1.16.

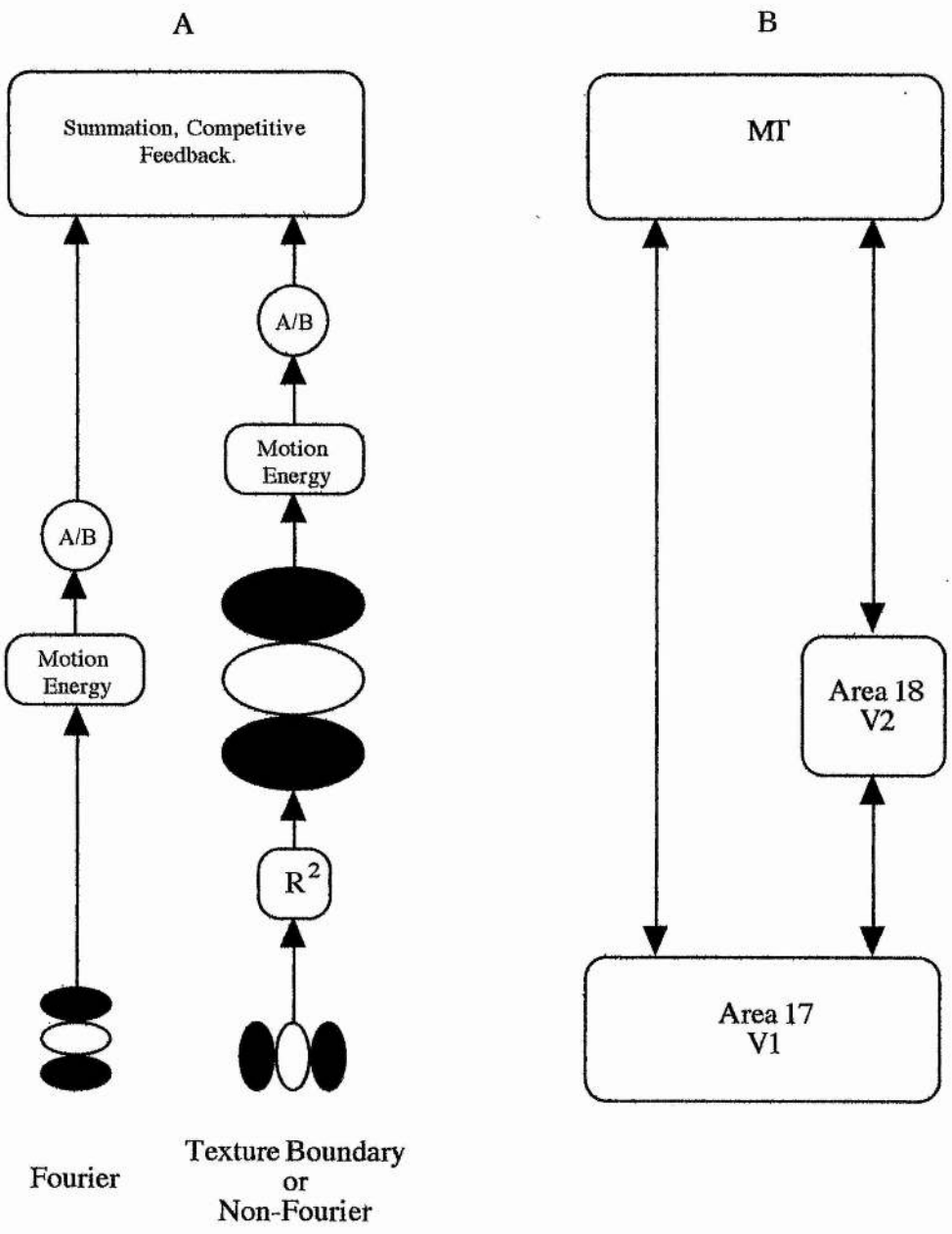

FIGURE 1.16. (A) Basic model of Wilson *et al.* (1992). (B) physiological correlates of the cosine-weighted model.

DISCUSSION

Image Segmentation Cues

It should be noted that all the above mechanisms are essentially low level. Recent evidence suggests that "higher level" influences (Kooi, de Valois, Switkes & Grosof, 1992) exert a critical influence on judgements of coherence and transparency in plaids.

Depth stratification cues exert especially strong cues on transparency (Stoner, Albright & Ramachandran 1990; Vallortigara & Bressan, 1991; Trueswell & Hayhoe, 1993). These results imply that coherence judgements may be modulated by signals from beyond the motion detection system. Until the origin of coherence and transparency judgements is known it will not be possible to ascertain whether coherence judgements originate two-stage or one-stage mechanisms.

Form-cue invariant perception

Form-cue invariant perception is the hypothesis that, at some level in the visual system, there should be neurones that signal the displacement of a feature, regardless of whether it is defined by colour, luminance or texture (Albright, 1992). The advantage of form-cue invariance is that the system is afforded more consistent sensitivity to motion from the wide range of cues in the visual environment. Form-cue invariance is found for luminance and chrominance defined stimuli (Cavanagh & Anstis, 1991; Dobkins & Albright, 1993) and for second-order stimuli (Chubb & Sperling, 1988 - texture; Julesz & Payne, 1968 - stereoscopic depth). Given that MT is sensitive to both first-order (Albright, 1984) and second-order motion (Dobkins & Albright, 1994) it becomes a strong candidate for the neuronal site of form-cue invariant processing.

A possible limitation of single-unit studies

A caveat should be noted about the results from single-cell studies. Whilst many research groups now practice environmental enrichment (Wolfensohn & Lloyd, 1994), other groups do not (or have not in the past). Un-enriched environments run the risk of depriving the subjects of valid or appropriate stimulation for the developing visual system. In addition such environments may promote undesirable adaptation effects in the visual system due to the limited focal distances involved in these circumstances. Whether such effects were occurring could be investigated in a straight forward manner. By measuring the resting vergence angle of monkeys over time and comparing them with those from monkeys from enriched environments, differences due to living arrangements could be observed*.

Blakemore and Cooper (1970) showed that kittens raised in environments containing vertical orientation had normal numbers of cells with a vertical preference but a reduction in the number of cells favouring other orientations. This experiment suggests

* There is evidence to suggest that aspects of the visual system such as resting vergence angle have "default" settings but that these may be subject to change in certain situations (Heeley, personal communication).

that at the very least any effects of environment on the normal lab monkey are relatively subtle since normal, lab raised, cats did not show the deficit. Thus whilst acknowledging that environment may affect the development or the adaptation of the visual system, a separate issue is whether any such differences would be of a sufficient magnitude to compromise the generalisability of a particular study. This may depend on the experimental task the animal is required to do and the visual abilities under scrutiny. This question is a small part of the much bigger issue of whether the primate visual system is hard wired from birth or whether it is subject to plasiticity. At present this is an area that lacks conclusive evidence (Hubel, 1988) and so merits further investigation.

FORMAL VERSUS NEURAL NETWORK SOLUTIONS:

Mechanisms such as a logical ANDing of inputs (Movshon *et al.* 1985) will accurately reproduce a formal solution to the IOC model by rigorously defining the speed and direction corresponding to the intersection of the two active projection fields.

In the same way a winner-take-all mechanism - which maximally activates neurones receiving the most input and which suppresses those receiving less input (Bultoff, Little & Poggio, 1989) can reproduce the formal IOC solution. However this assumes that units with non-maximal input will have no say on the effect of 2D motion computation, which seems unlikely.

This explains the attraction of a weighted-average over a population of active pattern neurones (Castet, Lorenceau, Shiffrar & Bonnet, 1993). This model of the integration of motion measurements is particularly appealing because of the small number of assumptions it makes. The model mimics the properties of endstopped and normal cell receptive fields to account for speed perception; the method of combination is a weighted-average. This mechanism avoids problems associated with a winner-take-all model by using the relative strengths of different signals in the integration process. No neural network solution is provided as yet but the algorithm does account for human observers' perceptions of the speed of lines of various lengths and inclinations. The experiments reported in chapters two, three, four and five test the predictions of the model in some detail.

Topological arrangement affects the perceived speed of tilted lines in horizontal translation

CHAPTER 2*

Co-linearity determines the perceived speed of inclined line segments in horizontal translation?

INTRODUCTION

Castet, Lorenceau, Shiffrar and Bonnet (1993) have reported that horizontally moving tilted lines appear to drift more slowly than vertical lines. Their experiments showed that the magnitude of the illusion increased with the angle of inclination of the line, with greater line lengths and when the contrast of the line was reduced. They proposed that the visual system uses two velocity signals to derive an estimate of the speed of a translating line. The model incorporates small, spatially limited, units as depicted in Fig. 2.1 (A). Consider the vertical line in the figure. As the contour moves it may be formally characterised by a velocity field in two-dimensions, where each point in the image is given a magnitude of velocity and a direction. The two end units signal the motion of the terminators (line ends). The other units signal the motion of the relevant section of contour. Now consider the motion of a tilted line as in Fig. 2.1 (B). The motion of the terminators over time provides the true direction of the line. The units signalling the middle sections of the line cannot recover the veridical direction of motion. They signal a direction perpendicular to the line and as a result the magnitude of the vector is also shorter. This means that these units underestimate the true speed of the line. This underestimation emerges as a result of the units experiencing the "aperture problem" (Wallach, 1976) as discussed in chapter one.

* These data were first presented at the 1995 ARVO meeting, Fort Lauderdale, Florida. Scott-Brown, K., and Heeley, D. W. (1995). *Investigative Ophthalmology and Visual Science*, **36**(4), 54.

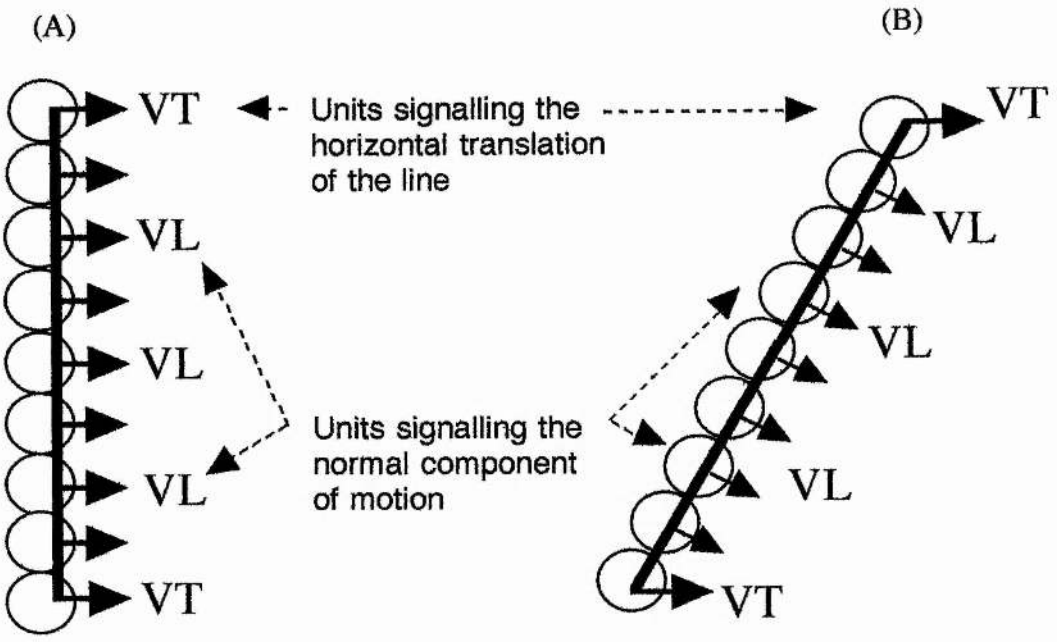

FIGURE 2.1. Schematic diagram of vertical and inclined contours traversing hypothetical spatially limited units.

The relative importance of V_T and V_L changes depending on the orientation and the length of the line. This is shown in Fig. 2.2 where the magnitude of the local velocity vectors V_L decreases as the angle of inclination is increased.

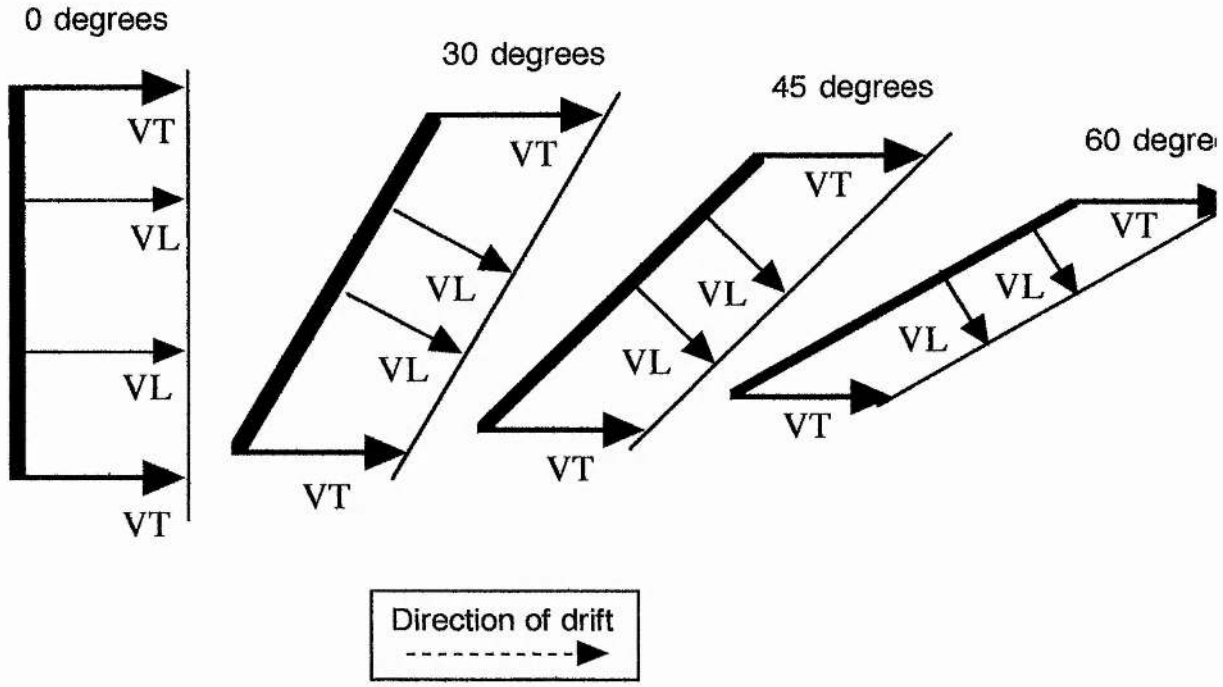

FIGURE 2.2. Magnitude of local velocity signals decreases with increasing tilt.

The model proposed by Castet *et al.* (1993), based on a weighted average process, is shown in Fig. 2.3. The strength of the two signals is allowed to vary according to the relative perceptual salience of each signal.

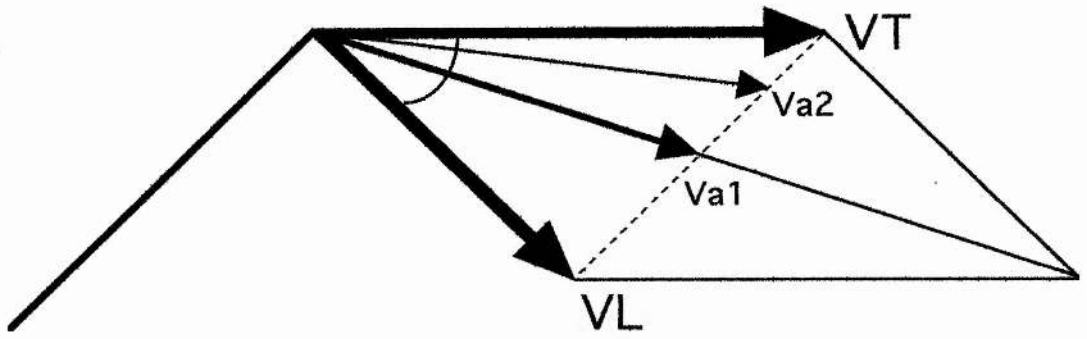

$$Va_i = \alpha * V_L + \beta * V_T$$

FIGURE 2.3. Upper part of a tilted moving line illustrating the weighted average calculus. The translation of the line is represented by the solid vector V_T attached to the upper line terminator. The components of motion perpendicular to the contour are represented by the vector V_L. The vector Va1, the half diagonal parallelogram constructed with V_L and V_T is an equally weighted average (the mean) of V_L and V_T. As the relative weight α assigned to V_L is reduced, the resultant average vector Va_i "slides" along the dashed line towards V_T ($Va_i = \alpha * V_L + \beta * V_T$ with $\alpha+\beta= 1$). Va2 corresponds to the weight α of 1/2. (Adapted from Castet *et al.* ,1993)

As the length of the line increases, V_L becomes larger and the α weight increases. If the contrast is reduced, then the terminators become less salient and the V_T weight is reduced. The full instantiation of the equation is as shown below. The derivation of this equation is reported in the paper by Castet *et al.* (1993), p 1931 and in Appendix 2.A

$$\mathbf{Va_i^2 / V_T} = \sqrt{(\beta^2 + (\alpha^2 + 2 * \alpha * \beta)\,(\mathbf{V_L / V_T})^2)} \qquad (1)$$

The experiment tested the predictions of the model by manipulating the number of terminators in the stimulus. Breaking up the line into six co-linear segments created ten more terminators (each of which carry a veridical velocity signal) and shorter line segments. According to the weighted averaging hypothesis, such stimuli should exhibit considerably less bias in perceived speed than continuous lines (Castet *et al.*, 1993). The presence of extra terminators in the stimulus dramatically increases the amount of veridical speed information in the stimulus due to the unambiguous motion of terminators. The segments were arranged either in a co-linear fashion or in a randomly scattered manner. The orientation of the segments in a particular trial was always constant. Scattering the segments serves a control function since it ensures that the co-

linear condition provides a test of the weighted average method of integration of motion signals. The model does not explicitly state whether a group of lines is treated separately or together. Segments could be grouped together before analysis or analysed separately. If the mechanism treats them separately, then the weighted average model predicts that the perceived speed for both scattered and co-linear segments should be the same. If a grouping mechanism operates first, however, observers should report different perceived speeds for scattered and co-linear conditions.

METHODS

Apparatus and Procedure

Stimuli were presented on the screen of a Sun *IPX* Sparc Station. A large dark board with a circular aperture was placed in front of the monitor. Viewing was binocular with natural pupils, from a distance of 57 cm, and was conducted in a dimmed experimental chamber. The subject's head position was unrestrained throughout. A fixation spot was displayed on the screen; the lines travelled horizontally on a path 1.5 degrees above this point. Subjects were instructed to maintain fixation throughout each trial. The width of the lines was two pixels. There were 32.9 pixels per degree of visual angle.

A two-alternative forced-choice (2AFC) staircase method was used to estimate the matching speed of a vertical line compared to an inclined line (Cornsweet, 1962; Wetherill & Levitt 1965). The speed of the tilted line (the *standard*) was held constant at 2 degrees per second, while the speed of the vertical line (the *comparison*) was adjusted by the subject's response. In a given trial the subject saw two stimulus intervals, one containing the tilted stimulus and the other containing the vertical stimulus; the order of presentation of the two stimuli was randomised. Each stimulus swept across the screen once in a randomly selected direction (left to right or right to left). The subject was required to indicate whether the second interval was travelling faster or slower than the first. If the subject indicated that the vertical one was travelling faster than the tilted one then in the next trial it was presented more slowly. (The size of the step in the staircase was 10% of the starting velocity.) This continued until the subject indicated that the tilted line was going faster than the vertical line. The speed of the vertical line was then increased again. The staircase continued until 6 reversals accrued. The average of these six points gives the matched speed of the vertical line. Two staircases were randomly interleaved to prevent subjects from anticipating the speed of lines from the previous trial. Five estimates were accumulated and averaged to give the matched velocity for a given stimulus condition. The order of conditions was randomised for each subject.
Subjects could use consistent duration or distance cues in fine velocity discrimination (McKee, 1981). Therefore to ensure that neither distance nor duration yielded a consistent cue to the discrimination of velocity, the starting point of a sweep was

subject to a 25% random variation. The actual length of a sweep could also vary independently by 25%. In this way the actual speed of the patterns had to be observed.

Stimuli

Stimuli were short lines (0.33 deg.) and long lines (2.0 deg.). The investigation of topological arrangement involved the following conditions: short lines, long lines, co-linear short lines and scattered short lines as shown in Fig. 2.4. Both co-linear and scattered conditions comprised six line segments thus giving a total line length of 2.0 deg. Estimates were obtained for seven angles of tilt ranging from 25 - 90 degrees. The separation of co-linear segments was 0.25 degrees of visual angle.

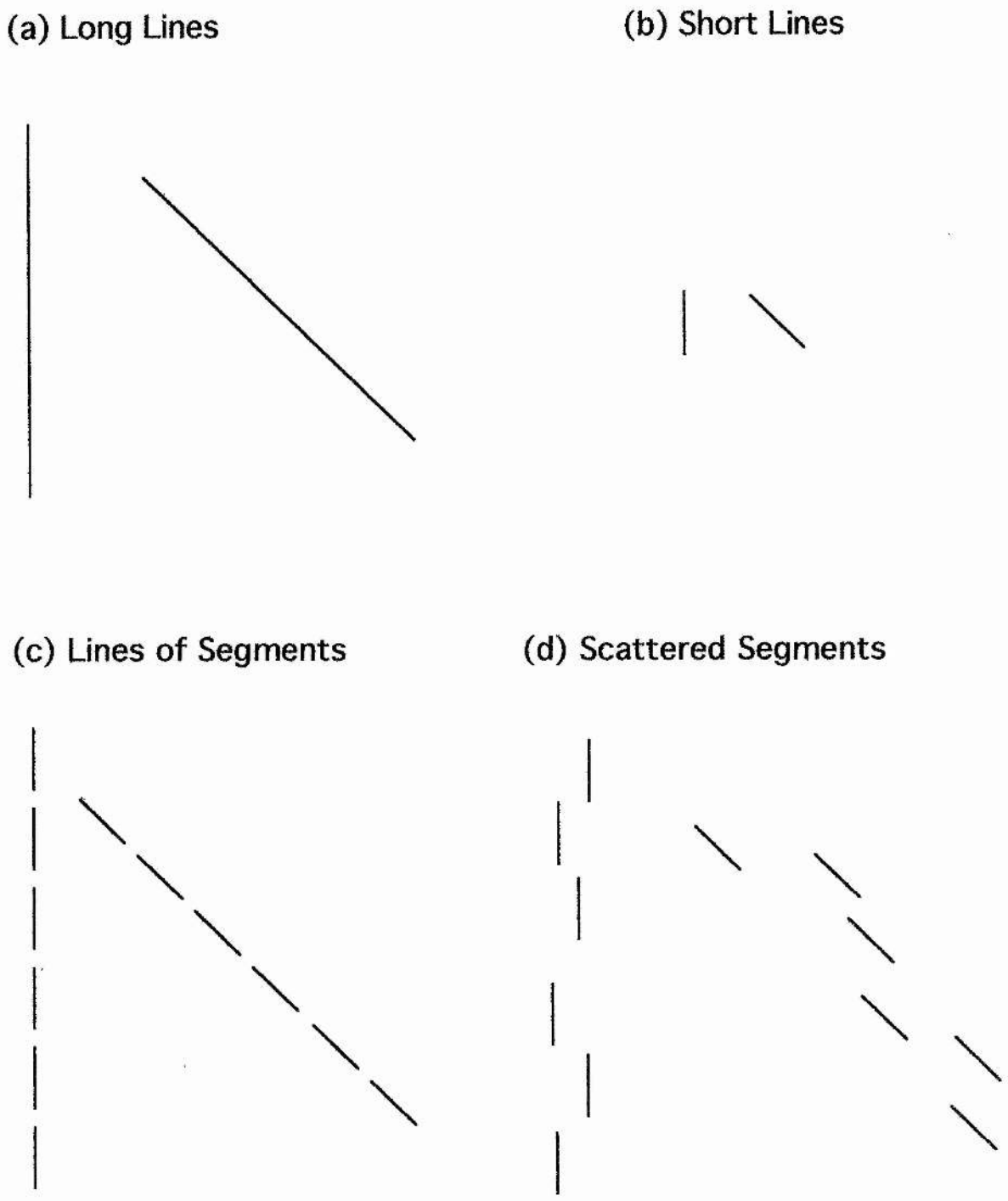

FIGURE 2.4. Diagram of stimulus conditions for experiment 1 (a & b) and experiment 2 (c & d). (Not to scale.) The length of line was chosen to be similar to the lines used by Castet *et al.* (1993).

The mean luminance of the display was 66cd/m^2. Contrast was defined as (L_{max} - L_{min})/(L_{min}), where L_{max} and L_{min} were the maximum and mean luminances in the pattern. Experiments one and two both used contrasts of 0.1, 0.05 and 0.025

Observers

Three of the four observers were unaware of the purposes of the experiment. All had normal or corrected to normal vision with no astigmatism greater than 0.25 dioptres. Subjects were exposed to extensive practice in the tasks to minimise learning effects during the experiment.

EXPERIMENT 1: THE EFFECT OF LINE LENGTH

Results

The individual subject data and the contrast data are shown in Appendix 2.A. The same pattern of data were observed at each level of contrast with the effect strongest at lower contrasts (0.05, 0.025). Analysis of covariance revealed that there was no significant effect of contrast for either the α parameters ($F(1,10) = 2.846$, $P = 0.1225$) or the β parameters ($F(1,10) = 3.828$, $P = 0.0879$). Thus the data are averaged over the three levels of contrast for the purposes of the comparisons. All the figures in the text depict the average of four subjects.

The results are presented in the same manner as Castet *et al.* (1993). VC/VS is the ratio of the comparison speed to the standard speed. A ratio of one means that veridical speed perception occured, but a VC/VS ratio of less than one means that observers perceived the tilted line as travelling more slowly than the vertical line. This measure of relative perceived speed is then plotted against V_L/V_T, which is the ratio of the speed of V_L (representing the orthogonal component) and V_T (representing the terminator speed). The ratio of V_L/V_T is used because the model proposed by Castet *et al.* (1993) uses a weighted average of the two signals V_L/V_T. The upper x-axis shows the angle of inclination (θ) of the standard stimulus at each value of V_L/V_T. ($\cos(\theta) = V_L/V_T$).

Effect of line length. Speed estimates for long lines (diamonds) were found to be substantially lower as the angle of inclination approached 90 degrees. Speed estimates were higher for short lines (squares). The smooth curves in Figs. 2.5 and 2.6 are the weighted average model fitted to the data with two free parameters, α and β (cf. Castet *et al.*, 1993). These parameters relate to V_L and V_T respectively, and they weight signals derived from local velocity estimates and signals from velocity estimates generated by the line terminators. Table 2.1 shows the derived values for α and β.

Parameter α is larger for long lines, reflecting the increased number of local signals in long lines. β should be identical in both conditions, since the number of terminators does not depend upon line length.

The parameters the tables 2.1 and 2.2 were derived from the average data for the four subjects and so have no error bars associated with them.

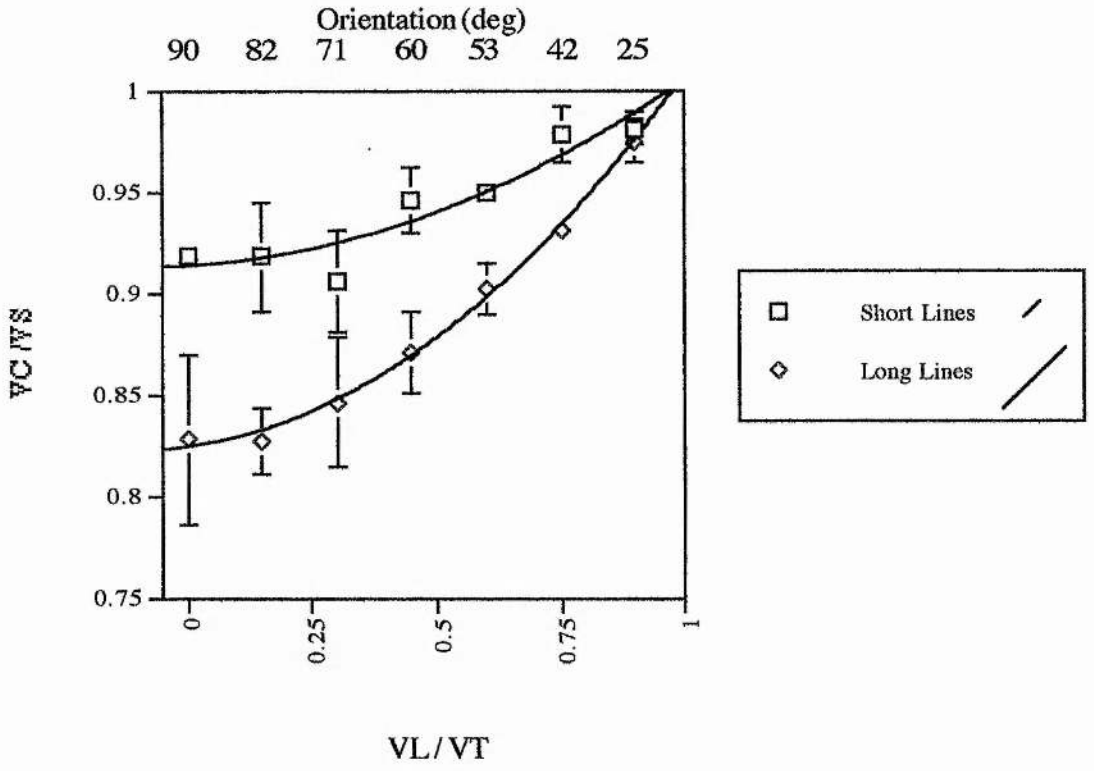

FIGURE 2.5. Relative perceived speed of short lines and long lines as a function of the ratio of the local speed to the translation speed (V_L/V_T). The upper axis shows the 7 angles (θ) of inclination of the standard stimulus from vertical. Continuous lines show the model of Castet *et al.* (1993) fitted to the data with two free parameters α and β from the model. Bars through the symbols show ± 1 SE (where no error bars are indicated, the error bars lie within the data symbol). Long lines were 2 deg. in length, short lines were 0.33 deg. in length. Speed of the standard was 2 deg./sec. Each data point is the perceived speed averaged across three levels of contrast and four observers (n=4).

Effect of line orientation. Speed estimates for long lines (diamond symbols) and short lines (square symbols) were found to be substantially lower as the angle of inclination approached 90 degrees. This finding is a replication of the results of Castet *et al.* (1993), which found that tilted lines appear to travel more slowly than vertical lines in horizontal translation.

LINE TYPE	WEIGHT	
	α	β
Short	0.09	0.92
Long	0.18	0.82

TABLE 2.1. Weights attached to V_L and V_T as derived from the data according to Castet *et al.'s* (1993) model, (n=4).

EXPERIMENT 2: THE EFFECT OF TOPOLOGICAL ARRANGEMENT

Results

Effect of stimulus type. Fig. 2.6 illustrates the strength of the illusion with the two stimulus arrangements. These have the same overall length of segments and the same number of terminators but yielded different misperceptions of velocity. (The length of a "long" line was equal to the product of the number of segments and the length of an individual segment.) The misperception is greater with the co-linear condition than with random scattering. This indicates that the model in its current state is too simple to make predictions about the effects of the numbers of terminators as it ignores their spatial arrangement. Note that the model predicts identical levels of misperception for the two conditions but the observed parameters for the two types of stimuli are very different. Table 2.2 shows the derived values for α and β. In this instance the α parameters representing the V_L components should be identical because the total amount of local component signals is the same in both stimuli (2 deg. of visual angle). The β components (representing V_T) should also be identical, reflecting the identical number of terminators in each condition (ten in each).

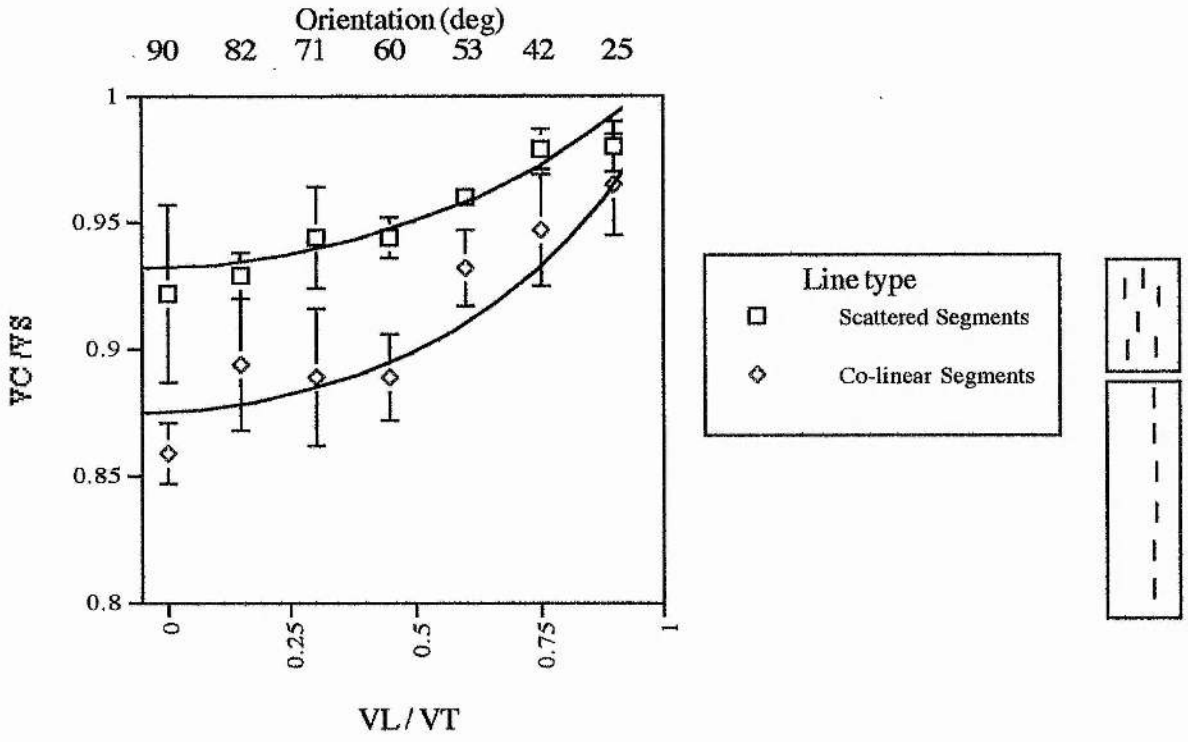

FIGURE 2.6. Relative perceived speed of scattered and co-linear segments as a function of the ratio of the local speed to the translation speed (V_L/V_T). The upper axis shows the 7 angles (θ) of inclination of the standard stimulus from vertical. Continuous lines show model of Castet *et al.* (1993) fitted to the data with two free parameters α and β. Bars through the symbols show ± 1 SE. Line segments were 0.33 deg. in length, the number of segments was 6. The speed of the standard was 2 deg./sec. Each data point is the perceived speed averaged across three levels of contrast and four observers. Because no difference was found between the three contrast levels used, the data for this experiment was averaged over the three levels (n=4).

(Notations are the same as in Fig 2.5.) Legends are not to scale.

LINE TYPE	WEIGHT	
	α	β
Scattered Segments	0.07	0.93
Co-linear Segments	0.11	0.87

TABLE 2.2. Weights attached to V_L and V_T as derived from the data according to Castet *et al.*'s (1993) model, (n=4).

Effect of number of terminators: Comparison of the graphs from experiments one and two reveals that the data for co-linear segments resemble the data for long lines, rather than short lines or scattered segments; as if the co-linear segments are processed in the same manner as a continuous line.

Is co-linearity the critical factor in determining the perceived speed of inclined line segments in horizontal translation?

Experiment 2 has shown that stimuli having the same overall segment length but with different numbers of terminators yielded different perceptions of velocity. It was found that contrary to the predictions of the model of Castet *et al.* (1993) the perceived speed of co-linear line segments was lower than the perceived speed of scattered segments at all angles of inclination. The magnitude of the gap between each of the co-linear segments remained constant throughout the experiment however.

It is possible that the motion of the co-linear stimuli is signalled by a low frequency mechanism that is insensitive to the gaps. To ensure that co-linearity is the determining factor, the experiment was repeated with differing sizes of gaps between the segments. Experiments 3, a and b explored the effects of systematically varying the size of the gaps between each co-linear segment. In this way, it was possible to confirm that the effect of co-linearity of segments on perceived speed was independent of segment separation.

A slightly different mechanism which could also account for the co-linear results is the proximity collator unit (Moulden, 1994). The mechanism for grouping in this instance is more active but the key factor is that proximity is very important. This experiment should be able to extend the gaps between the segments to beyond the scope of the receptive fields.

EXPERIMENT 3 (a): THE EFFECT OF GAP-SIZE ON THE PERCEIVED SPEED OF CO-LINEAR SEGMENTS IN HORIZONTAL TRANSLATION.

The perceived speed of inclined co-linear segments was compared with the perceived speed of similarly inclined continous lines with the same length equal to the product of the length of an individual segment and the number of segments. In addition to the original segment separation distance, three new separations were introduced (two, three and four times the original gap-size).

In addition to this experiment a control experiment was conducted with lines whose length matched the length of the co-linear segments. The results of this comparison are reported in section (b).

Methods

The apparatus and procedure is as described earlier in experiment 1. In this experiment however, the contrast ratio of line brightness to background brightness was held constant at 0.05 (this level ensured that the misperception was at it strongest).

Stimuli

Stimuli were short line segments (0.33 deg.) and continuous lines (2.0 deg.). The experiment involved the following conditions: long lines, co-linear short lines and scattered short lines. Both co-linear and scattered conditions comprised six line segments thus giving a total line length of 2.0 deg. Estimates were obtained for angles of tilt ranging from 0 - 90 degrees. Separation of co-linear segments was 0.25, 0.50, 0.75 or 1.0 degrees of visual angle. Fig. 2.8 depicts the stimuli used in experiment 3(a).

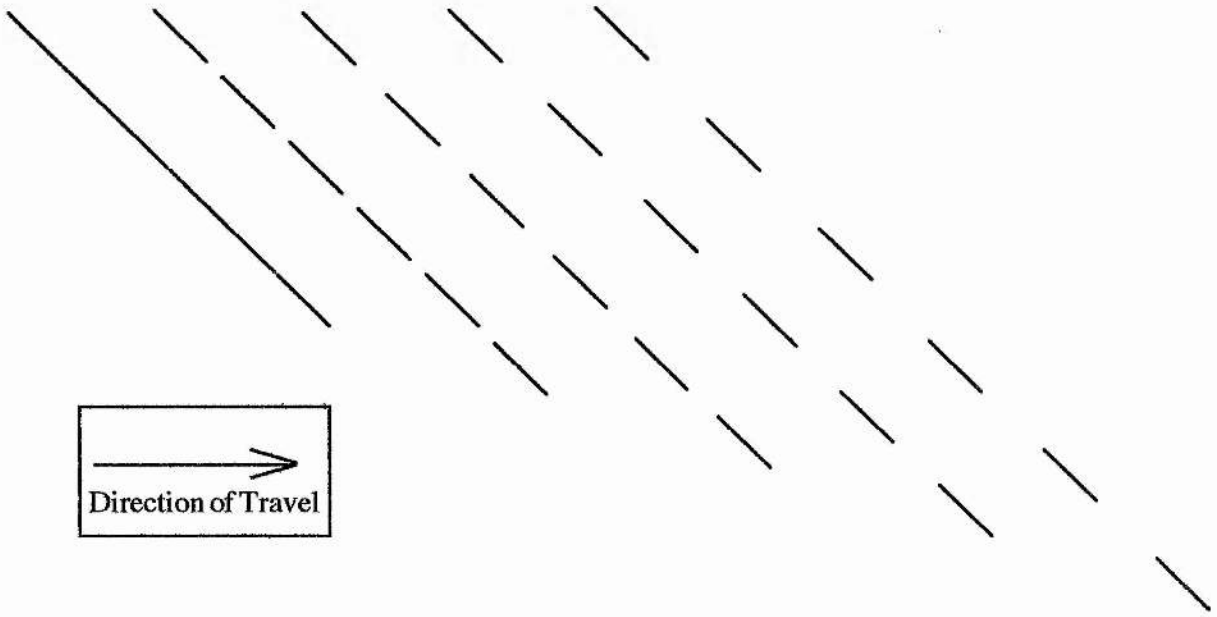

FIGURE 2.8 Spatial arrangement of line segments. The separation of the six co-linear segments was 0.25 deg., 0.50 deg., 0.75 deg. and 1.0 deg. of visual angle in different experiments. The length of the continuous line was 2 deg. of visual angle.

The height of trajectory of the tilted line stimuli was varied according to the length of the overall stimulus. The various vertical extents are shown in Table 2.3.

Gap Length	*Sum of Gaps*	*Overall Length*	*Vertical Offset*
.250	1.250	3.250	1.500
.500	2.500	4.500	2.750
.750	3.750	5.750	4.000
1.000	5.000	7.000	5.250

TABLE 2.3. Stimulus parameters for experiment 3(a). (Segment length = 0.33, Sum of segments = 2.0.)

Observers

The three observers were unaware of the purposes of the experiment. All had normal or corrected to normal vision with no astigmatism greater than 0.25 dioptres. Observers were experienced psychophysical observers and were paid for their time.

Results

Co-linear segments appeared to travel more slowly than scattered segments irrespective of segment separation. In addition the perceived speed of continuous lines was lower than both randomly scattered segments and co-linear segments.

Fig. 2.9 displays the data for increasing separation of the six co-linear segments, six scattered segments along with the data for continuous lines of length 2 deg. of visual angle.

Effect of line orientation. In each case as the angle of inclination increased, so did the bias in perceived speed for all three stimuli types. The two exceptions to this were in the co-linear segment conditions where at 90 deg. of inclination the perceived speed was almost as high as in the scattered condition for separations of 0.25 and 1.0 deg. of visual angle.

FIGURE 2.9. (Overleaf) Relative perceived speed as a function of the ratio of the local speed to the translation speed (V_I/V_T) for segment separations of 0.25, 0.5, 0.75 and 1.0 degrees of visual angle. Continuous lines show the model of Castet *et al.* (1993) fitted to the data with two free parameters α and β. Bars through the symbols show ± 1 SE. Continuous lines were 2.0 deg. in length, segments were 0.33 deg. in length and segment separations were 0.25, 0.5 deg 0.75 deg or 1 deg. of visual angle. The speed of the standard (vertical line) was 2 deg./sec. Each data point is the perceived speed averaged across three observers (n=3).

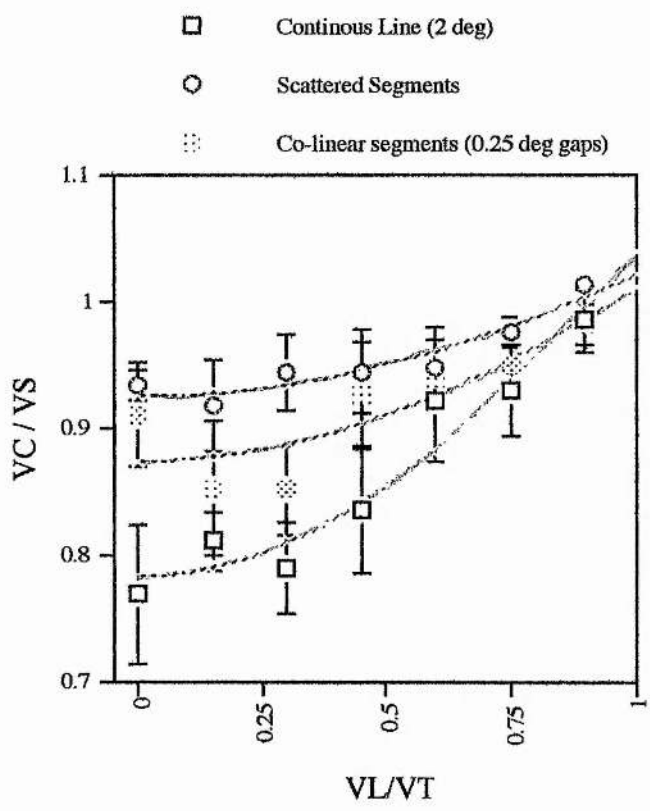
Continous Line (2 deg)
Scattered Segments
Co-linear segments (0.25 deg gaps)
VC / VS
VL/VT
1.1
1
0.9
0.8
0.7
0
0.25
0.5
0.75
1

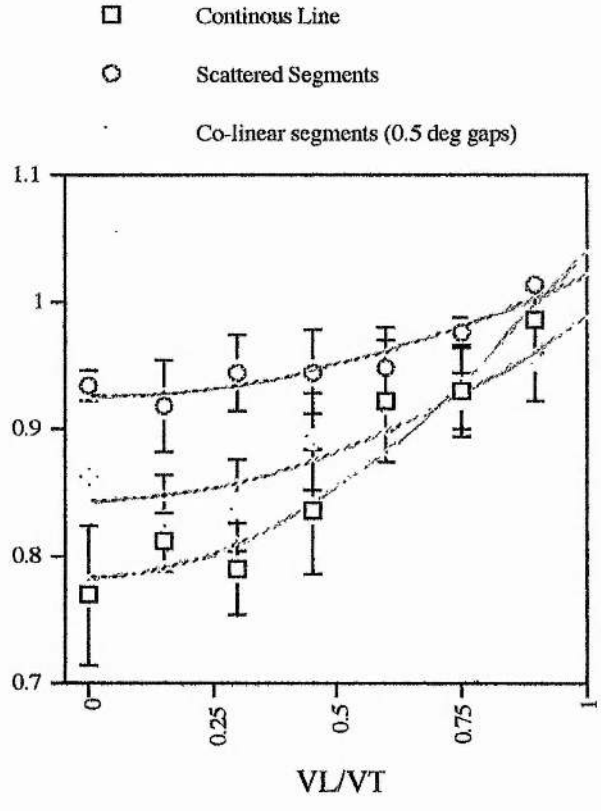
Continous Line
Scattered Segments
Co-linear segments (0.5 deg gaps)
VL/VT
1.1
1
0.9
0.8
0.7
0
0.25
0.5
0.75
1

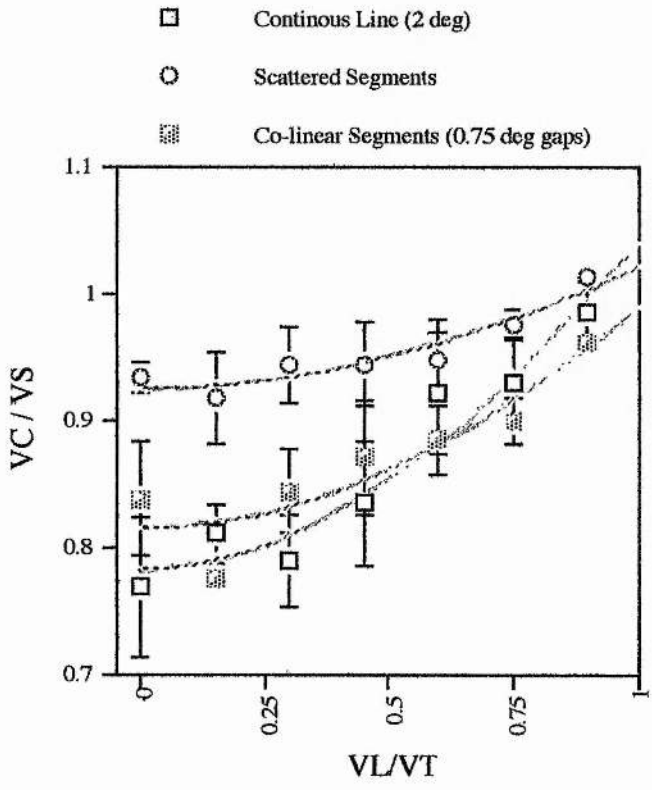
Continous Line (2 deg)
Scattered Segments
Co-linear Segments (0.75 deg gaps)
VC / VS
VL/VT
1.1
1
0.9
0.8
0.7
0
0.25
0.5
0.75
1

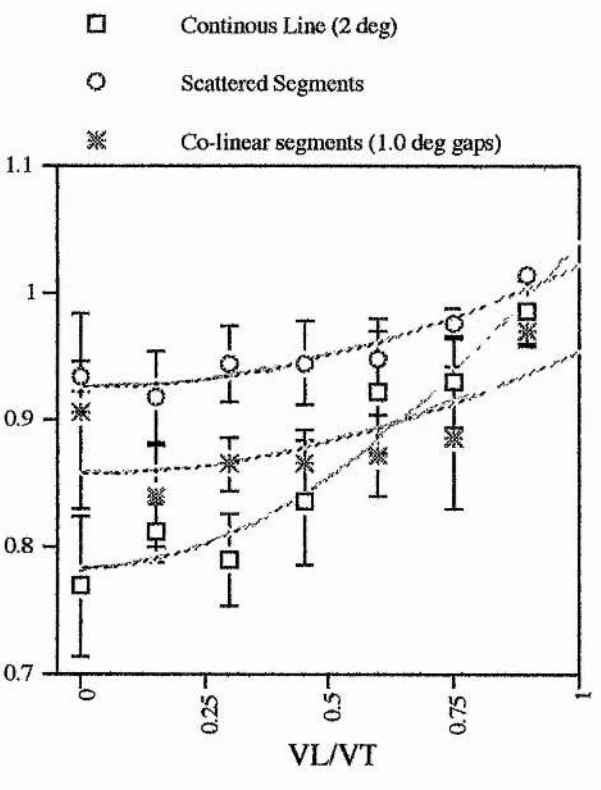
Continous Line (2 deg)
Scattered Segments
Co-linear segments (1.0 deg gaps)
VL/VT
1.1
1
0.9
0.8
0.7
0
0.25
0.5
0.75
1

Figs. 2.10 and 2.11 show the α and b parameters for each condition.

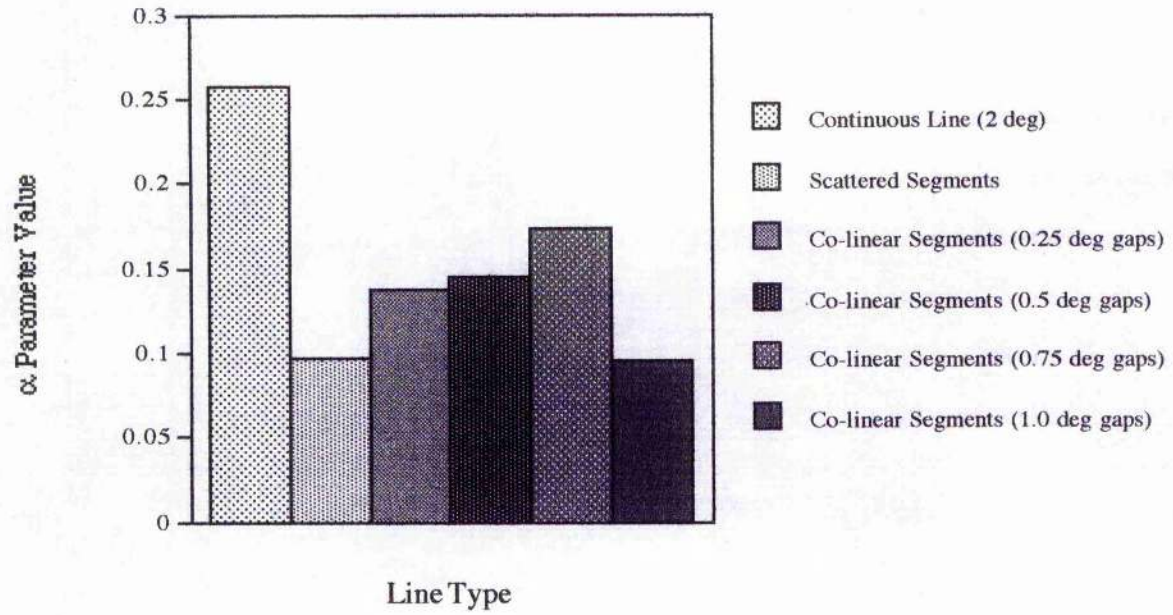

FIGURE 2.10. Magnitudes of α weights for each condition according to Castet *et al.'s* (1993) model, (n=3).

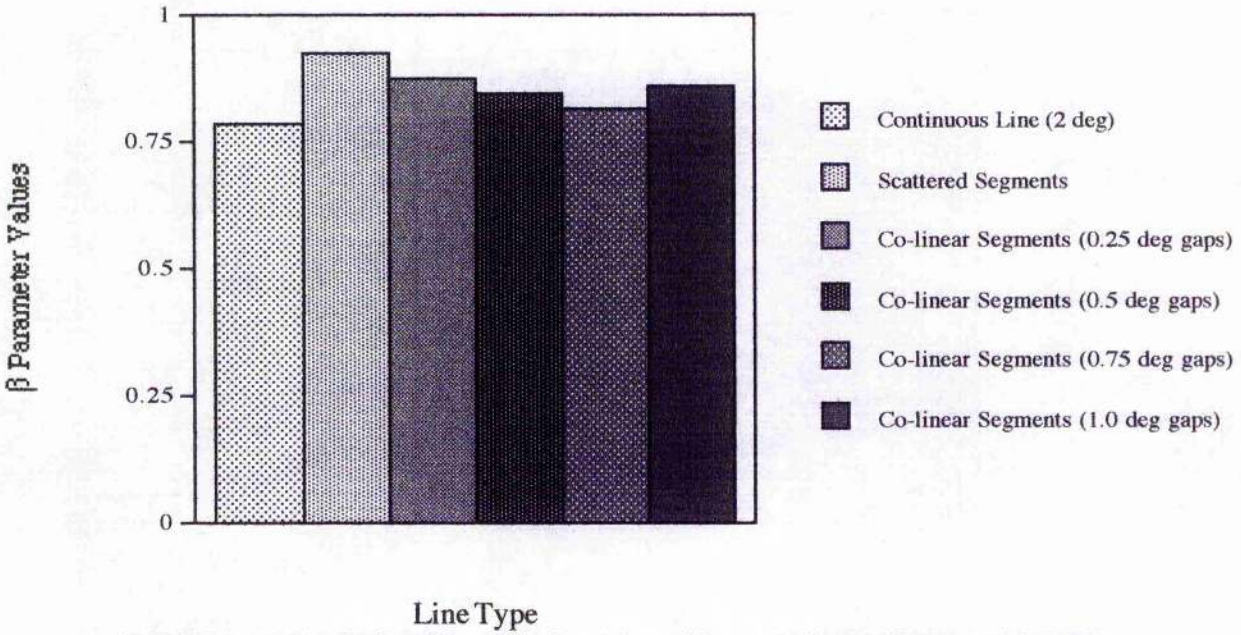

FIGURE 2.11. Magnitudes of β weights for each condition according to Castet *et al.'s* (1993) model, (n=3).

EXPERIMENT 3 (b): LENGTH MATCH CONTROL FOR CO-LINEAR STIMULI

In this experiment new data for continuous lines is compared with results from the previous experiment. The continuous lines were matched to the length of the entire co-linear segment stimuli.

Methods

The apparatus and procedure are described in experiment 1. In this experiment the contrast ratio of line brightness to background brightness was held constant at 0.05.

Stimuli

Stimuli were short line segments (0.33 deg.) and continuous lines (3.25, 4.5, 5.75 and 7.00 deg.). The following conditions were used: long lines, co-linear short lines and scattered short lines. Both co-linear and scattered conditions comprised six line segments thus giving a total line length of 2.0 deg. Estimates were obtained for angles of tilt ranging from 0 - 90 degrees. Separation of co-linear segments was 0.25, 0.50, 0.75 or 1.0 degrees of visual angle. Fig 2.12 depicts the continuous line stimuli next to their partner co-linear stimuli used.

The data were collected at the same time as data for experiment 3(a) and so the order of presentation of stimuli was randomised between all the conditions in the two experiments. The data for continuous lines of length 2 deg. is used in the analysis of both experiments.

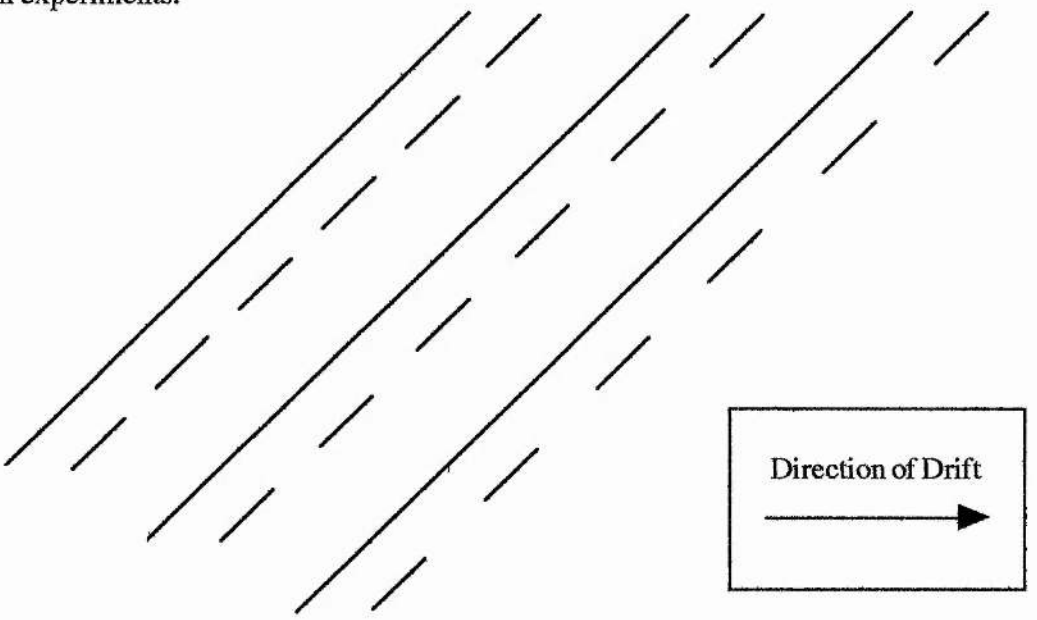

FIGURE 2.12 Spatial arrangement of line segments. The separation of the six co-linear segments was 0.50 deg., 0.75 deg. and 1.0 deg. of visual angle in different experiments. The length of the continuous line was 2 deg. of visual angle.

The height of the trajectory of the tilted line stimuli was varied according to the length of the overall stimulus. The various vertical extents are shown in Table 2.4.

Gap Length	*Sum of Gaps*	*Continuous Line Length*	*Vertical Offset for Continuous Line*
.500	2.500	4.500	2.750
.750	3.750	5.750	4.000
1.000	5.000	7.000	5.250

TABLE 2.4. Stimulus parameters for experiment 3(b). (Segment length = 0.33, Sum of segments = 2.0.)

Observers

The three observers were those who participated in experiment 1.

Results

Effect of line orientation.

The results for Experiment 3 (b) show the typical progressive bias in perceived speed for inclined line stimuli and co-linear line segments. Fig 2.13 shows three graphs with the data for co-linear segments and a line matched to the overall length of the stimulus. The three gap sizes are 0.5, 0.75 and 1.0 degrees of visual angle respectively and the matched line lengths are 4.5, 5.75 and 7.0 degrees of visual angle. The error bars touch or overlap for every orientation of line stimulus in the first two graphs. In the third graph, only the data for 71 and 90 degrees of inclination do not overlap. This suggests that there is little or no difference between the perceived speed of co-linear segments and continuous lines matched to the overall length of the segments.

Effect of stimulus configuration.

The continuous lines and the co-linear segments are behaving very similarly up to a gap size of .75 degrees. Even at 1.0 degrees of gap size there is a qualitative similarity in the data.

How does the model fit the data?

The co-linear stimuli inclined by 90 degrees to vertical seem to suffer slightly less bias than the other inclined stimuli. However, weighted-average model treats these stimuli identically since they contain veridical terminator information and no local component information at all. There should therefore be no appreciable bias in perceived speed for either co-linear or continuous lines since there is no local information present to bias the signal.

FIGURE 2.13 (Overleaf). Relative perceived speed as a function of the ratio of the local speed to the translation speed (V_L/V_T). Continuous lines show the model of Castet *et al.* (1993) fitted to the data with two free parameters α and β. Bars through the symbols show ± 1 SE. Continuous lines were 4.5, 5.75 or 7.0 deg. in length, segments were 0.33 deg. in length and segment separation 0.5 deg., 0.75 deg. or 1 deg. of visual angle as indicated in the legend. The speed of the standard (vertical line) was 2 deg./sec. Each data point is the perceived speed averaged across three observers (n=3).

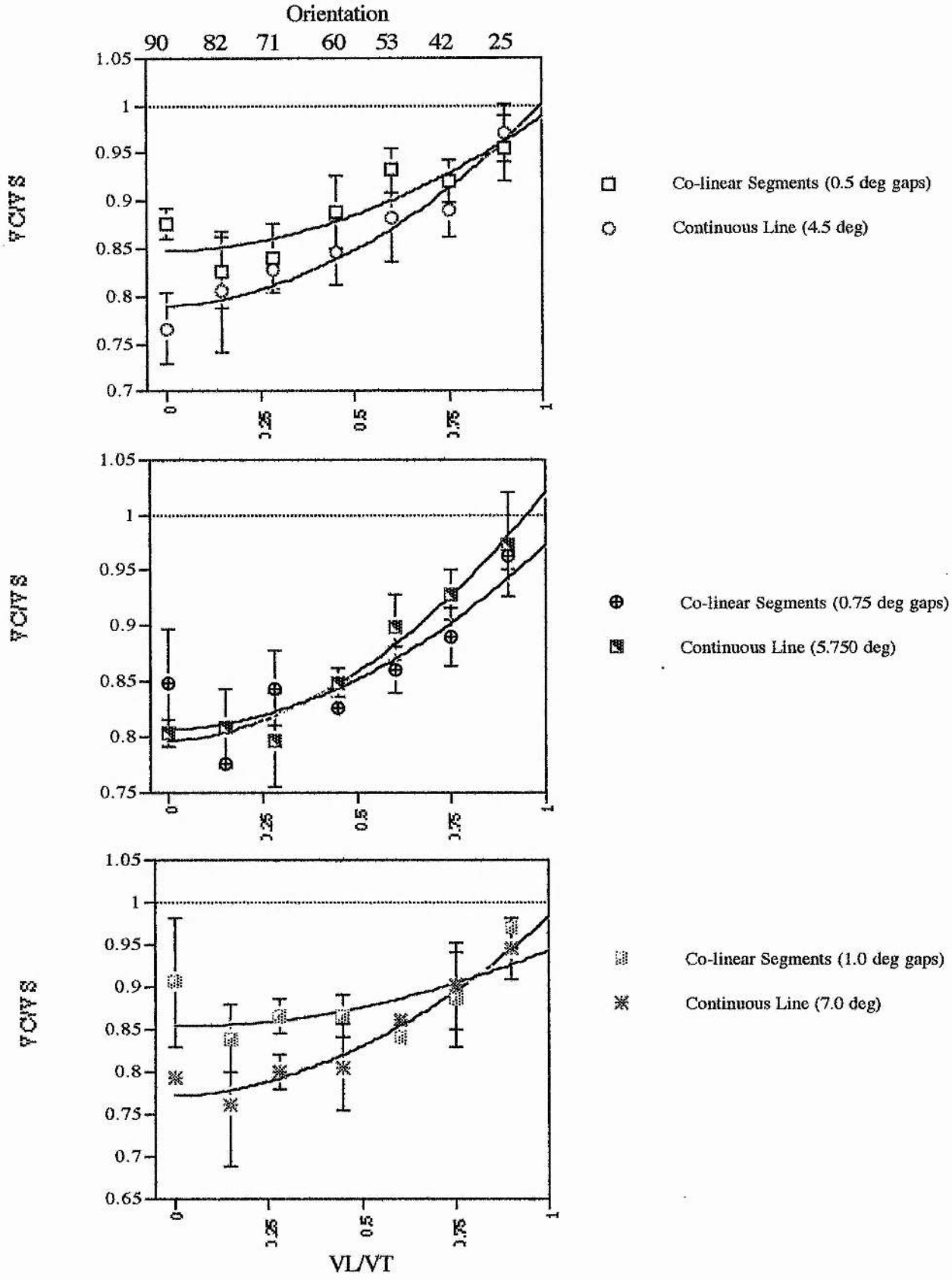
Orientation
90 82 71 60 53 42 25
VC/VS
VL/VT
Co-linear Segments (0.5 deg gaps)
Continuous Line (4.5 deg)
Co-linear Segments (0.75 deg gaps)
Continuous Line (5.750 deg)
Co-linear Segments (1.0 deg gaps)
Continuous Line (7.0 deg)

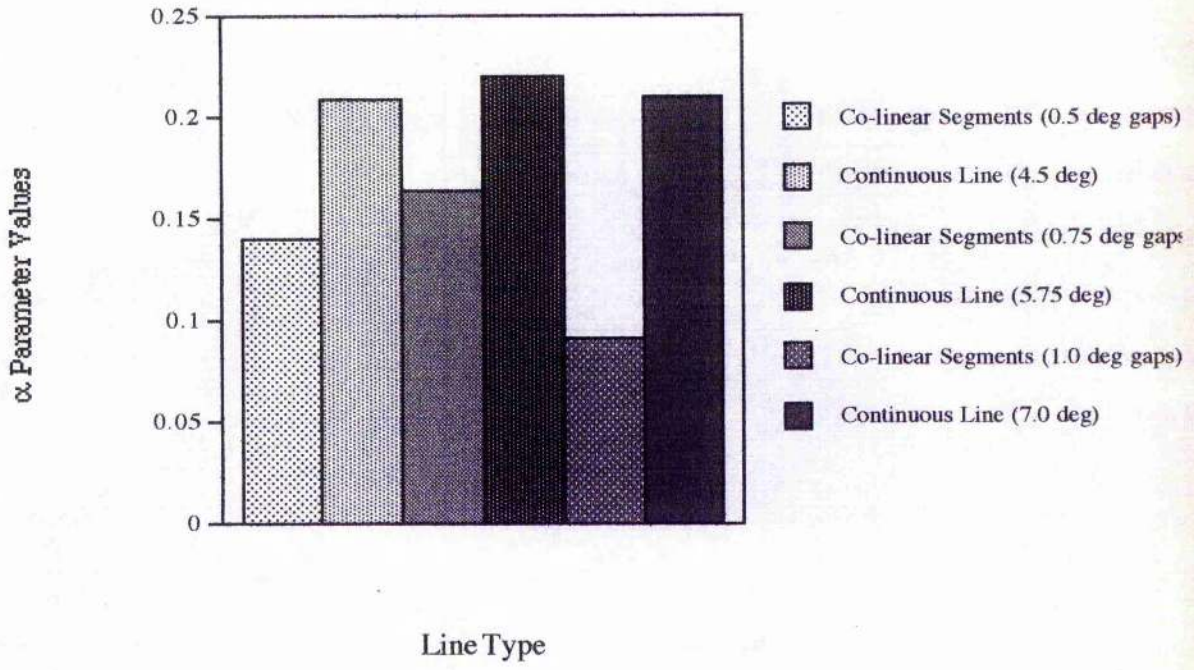

FIGURE 2.14. Magnitudes of weights α for each condition in Expt 3(a) according to Castet et al's (1993) model, (n=3).

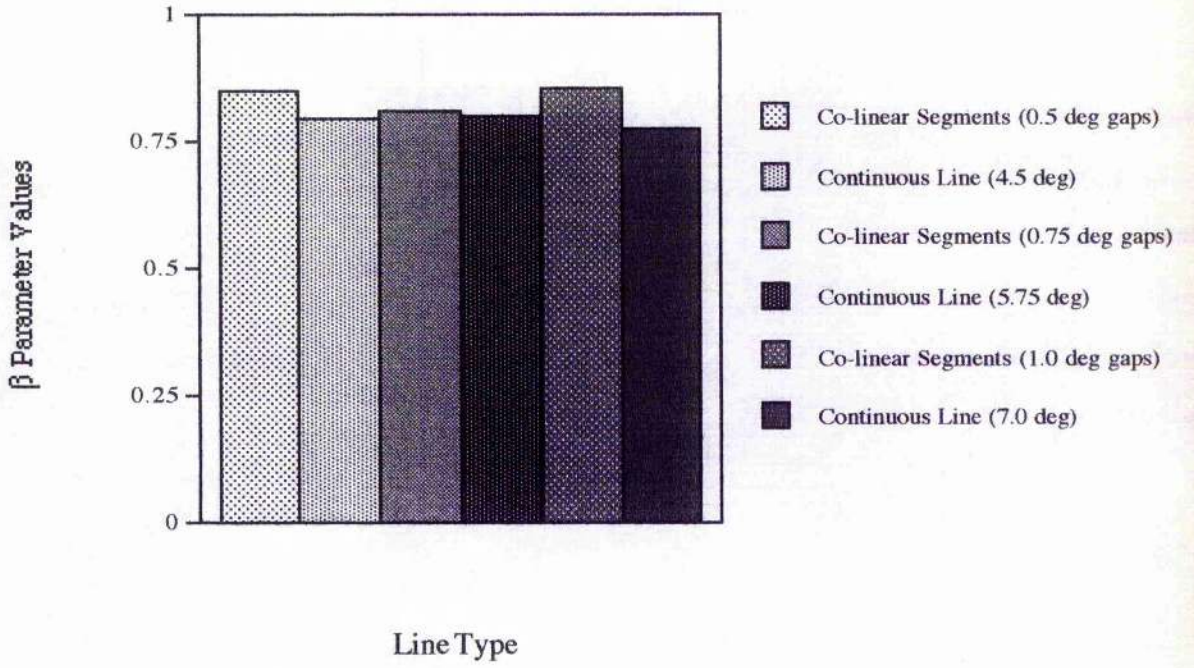

FIGURE 2.15. Magnitudes of weights β for each condition in experiment 3(b) according to Castet et al's (1993) model, (n=3).

DISCUSSION

The perceived speed of inclined co-linear line segments in horizontal translation is much lower than the perceived speed of similarly inclined scattered line segments. This finding is not predicted by the weighted-average model (it suggests that the two sets of data should effectively be superimposed). Thus the data from experiments 1 and 2 clearly show that the perceived velocity of line segments is not obtained by a simple averaging process of local velocity signals and veridical velocity signals of the line terminators as suggested by Castet *et al.* (1993).

Experiments 3 (a) and (b) extended the gaps between co-linear segments and compared the speed of co-linear segments with continuous lines matched to the overall length of the segments. Inclined co-linear segments appear to be subject to the same bias in perceived speed associated with continuous lines of similar orientations. According to the Castet *et al.* (1993) weighted-average model the addition of the ten extra terminators in the co-linear segments condition should substantially reduce the bias in perceived speed found for inclined lines. However, the data suggest that co-linear segments behave in qualitatively similar ways to continuous lines of the same overall length. In experiments 3(a) and 3(b), the model parameters α and β should be identical for each of the co-linear segment stimuli; as can be seen however, they are not. In addition the parameters for the scattered segments in experiment 2 should be the same as those for the co-linear segments, and this is not the case. This indicates that the model is too simple in its current state as it ignores the spatial arrangement of terminators. For the same reason, the model is unable to make accurate predictions about the effects of the number of terminators. As far as the motion processing system is concerned, the co-linear segment stimulus is not treated as the sum of its parts, nor is it treated as a whole stimulus of equivalent overall length.

The results of Castet *et al.* (1993) regarding line length and line orientation were replicated: speed misperception increases as a function of both of these factors. Pilot data collected in the laboratory at St Andrews corroborated the above findings with tilted line stimuli in a series of experiments with grating stimuli. The pattern of results for line length, line orientation and line contrast was replicated with sine-wave and square-wave gratings at two spatial frequencies.

If motion detection is preceded by a low pass filter (Morgan, 1992) then a high pass filter of the stimuli would show whether some low frequency component of the stimulus was contributing to the differences in perceived speed of co-linear segments and scattered segments. However the fact that direction perception can be distance invariant suggests that motion detection can in fact utilise high spatial frequencies (van de Grind, Koenderink and van Doorn, 1992). Smith, Snowden and Milne (1994) have confirmed that global motion perception for random-dot kinematogram stimuli (RDKs)

arises from the integration of local motion signals across space rather than from the operation of a low frequency mechanism. The perception of global motion in RDK stimuli was found to be unaffected by a high pass filter featuring a 12c/deg. cut off which effectively removed the low spatial frequency information.

Explanation at the systems level

Whilst the results as they stand cannot suggest the precise mechanism under operation, a number of mechanisms *could* account for the data, however. There could be pooling across the receptive fields to generate a "long line" percept for co-linear stimuli. "collator units" which act as second-stage orientational filters are a possible mechanism by which this may be achieved (Moulden, 1994). Experiments 3 (a) and (b) investigated the effects of increasing the gaps between segments and found very small differences in perceived speed of co-linear segments even when the gaps were four times the original size. This argues against the integration across receptive field hypothesis since it would require very large receptive fields to operate effectively.

An alternative mechanism is a high level, or gestalt, process with the co-linear association coming back down the system from higher levels to influence the speed. This explanation differs from most other proposed mechanisms since it is a top-down approach to the problem. It supposes that the source of the perceptual decision is relatively high up the hierarchy of visual processing: at the level of a symbolically mapped description of the objects in the image (Marr, 1982; Watt & Morgan 1985)

If perceived speed of co-linear segments varies as a function of duration, giving a duration effect such that short durations abolish the bias in perceived speed then it is possible that this is due to a delay in the perception of the higher order properties of the stimulus. Such an effect can also be accommodated by "bottom up" models of motion perception, however. It could be argued that a larger, "global", receptive field is involved in generating a motion signal. The "texture boundary motion" pathway of the model of Wilson, Ferrera and Yo (1992) possesses such a larger secondary receptive field by virtue of the initial filtering followed by response squaring before the extraction of motion energy. The bias in perceived direction of type II plaids at short durations is modelled by such a pathway because the extra processing involved requires more time than the "motion energy" pathway (Yo & Wilson, 1992).

Higher order influences in the bias in perceived speed - proposals for research.

It is possible that the co-linear stimuli, due to their salient arrangement, are being recognised by a high level system prior to motion analysis, whereas the scattered segments may be proceeding directly to motion energy analysis. A difference in the latency of judgements for each stimulus type would provide evidence for such a process occurring.

By putting each of the co-linear segments in a different depth plane (Fig. 2.16), to try and disrupt the grouping of the segments in the co-linear arrangement, it is possible discover whether the coherent co-linear percept remains in the form of a bias in perceived speed. In the uncrossed disparity condition line segments would appear further away and so may appear to travel more slowly while segments in front may appear to travel more quickly. If this happened it would be strong evidence that signals from outside the motion system (in this case surface segmentation cues) have a critical influence on motion perception. Trueswell and Hayhoe (1993) have shown that the grouping of local motion signals depends on whether the surface interpretation of a plaid (defined by stereoscopic depth) is consistent with pattern motion (grouped contours) or with component motion (segregated components).

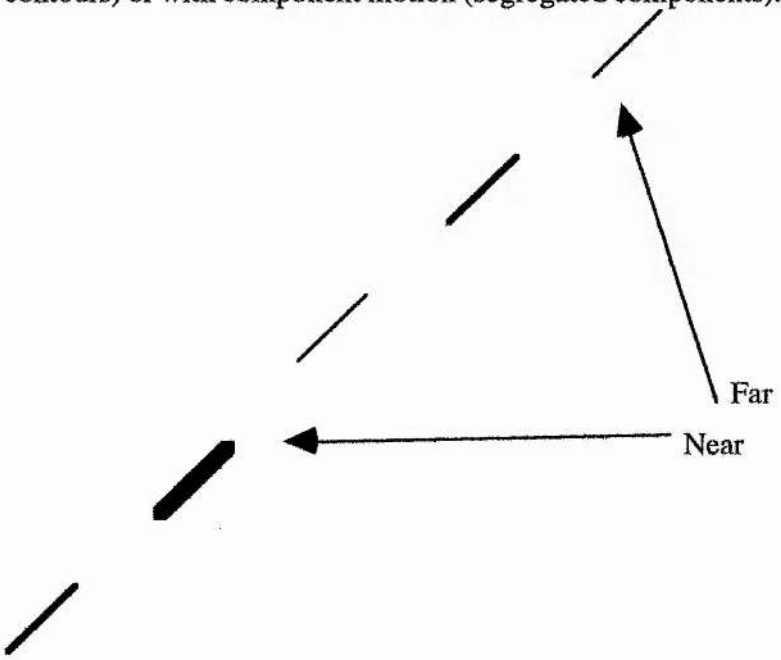

FIGURE 2.16 Segments arranged in co-linear fashion but in different depth planes.

By manipulating the global orientation of the stimulus independently of the orientation of the local line segments the role of shape and orientation in perceived speed may be investigated. This is shown diagrammatically in Fig. 2.17. The two stimulus types may help to distinguish between local and global processing of speed. A bias in the perceived speed of the right hand group of lines would suggest that global processing occurs prior to speed processing. A bias for the left hand group would suggest the reverse however.

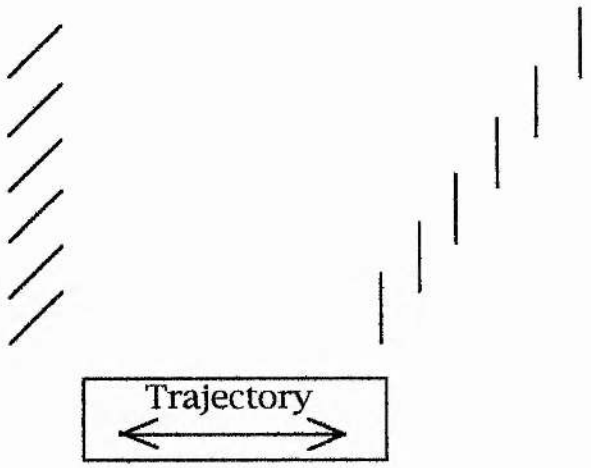

FIGURE 2.17. Manipulation of local orientation of line segments and global orientation of line segments.

In summary, the segment and scattered conditions are identical in terms of the local information and terminator information available in the stimulus. Thus it is possible that the model is working at a psychological level, where co-linearity dictates the interpretation of the stimulus with motion processing following on after this recognition stage. An alternative is that second-stage orientational filters could be integrating the line into a longer unified stimulus prior to motion analysis. This possibility was explored by extending the size of the gaps between co-linear stimuli beyond the scope of such receptive fields. The experiments reported in the next chapter investigate the effect of varying the number of terminators in the co-linear conditions and varying the length of the line segments themselves.

The effect of the number and size of line segments on perceived speed of tilted line segments in horizontal translation.

CHAPTER 3

Number of terminators affects perceived speed.

INTRODUCTION

Co-linear line segments in horizontal translation are subject to a bias in perceived speed (Scott-Brown & Heeley, 1995). In the previous chapter it has also been shown that this misperception is independent of the size of the gaps between the segments. To investigate the limits of the bias in perceived speed in more detail, the number and length of line segments were varied to provide a systematic variation of the number of terminators in the stimulus whilst maintaining overall line length. As shown in Fig. 3.1 the number of segments was either three, six or nine and each set could be arranged in either co-linear or scattered format.

METHODS

Apparatus and Procedure

The apparatus and procedure are described in chapter 2. In these experiments the contrast ratio of line brightness to background brightness was held constant at 0.05.

Observers

The three subjects were experienced psychophysical observers who were unaware of the hypothesis under investigation. All were professionally refracted and were found to have normal or corrected to normal vision with no astigmatism greater than 0.25 dioptres.

Experiment 4: *Terminators*

The co-linear segments of total length 2.0 deg. comprised either three, six or nine segments according to the condition. In each condition the gap size was 0.25 deg. Line segments were arranged in either co-linear or scattered fashion.

Stimuli

Stimuli were short lines (0.667, 0.33 or 0.074 deg.) and long lines (2.0 deg.) - (See Fig 3.1). Estimates were obtained for angles of inclination ranging from 0 to 90 degrees.

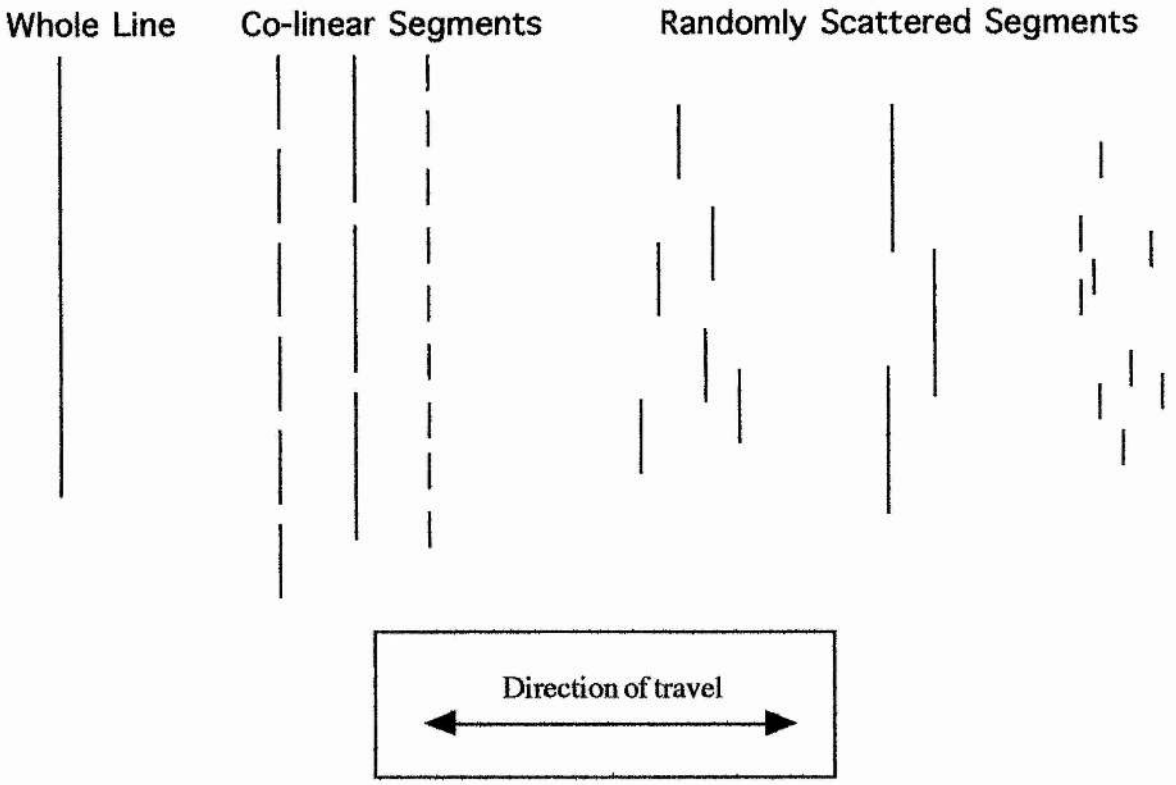

Fig. 3.1. Diagram of stimulus conditions for first experiment.

Experiment 5: *Dots*

The dot condition (Fig. 3.2) provides a stimulus with six terminators but no local contributions.

Stimuli

Stimuli were dots (0.0625 deg). The size of the gaps between the six co-linear dots was 0.327 deg. Estimates were obtained for angles of tilt ranging from 0 - 90 degrees.

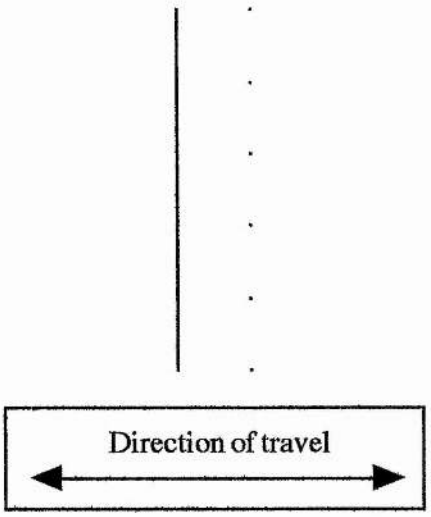

FIGURE 3.2. Diagram of stimulus conditions for second experiment. Long line 2.0 deg., six points span 2.0 deg. of visual angle.

RESULTS

Experiment 4.

The data for three co-linear and three randomly scattered line segments are shown in the first graph (Fig. 3.3). It can be seen that the data points for both stimuli follow a similar trend of increasing speed misperception as a function of angle of inclination. As in previous chapters, the smooth curves are the weighted average model fitted to the data with the two free parameters α and β. On this occasion the two curves are qualitatively similar. This is in marked contrast to the situation in chapter two where the curve for six co-linear segments differed from the curve for six randomly scattered segments. Table 3.1 shows that the α weight for the three co-linear segments condition is larger than the same parameter for the 6 segment co-linear condition, which is in turn larger than the α weight for the nine co-linear segments condition. (The α weight is attached to the V_L signals derived from local velocity estimates.)

The situation for six segments (Fig. 3.4) is very similar to the data reported in chapter two. On this occasion the trend of increasing bias in speed perception as a function of line inclination is reversed at 90 degrees of inclination (i.e. VL / VT = 0.0). This anomaly arises from an outlying data point from a single observer that has skewed the distribution. When the model is fitted to the data, the usual differences are evident with the α weight approximately double the size in the co-linear condition.

The perceived speed of nine co-linear segments (Fig. 3.5) is subject to a very small bias in perceived speed but this is again significantly larger than the bias in perceived speed for nine randomly scattered segments. It is also worth noting that, in contrast to the data for three and six segment co-linear stimuli, the trend of the data for the co-linear segments is non-linear. There are two components to the plot; perceived speed decreases as a function of inclination until 63.26 degrees (VL / VT < 0.5), thereafter the trend is for a slight increase in perceived speed again. The key finding is that there is a substantial difference in the perceived speed of nine co-linear segments compared to nine scattered segments. As in both the three and the six segment co-linear conditions, the α weight of the model is approximately double the size for the co-linear segments than the scattered segments.

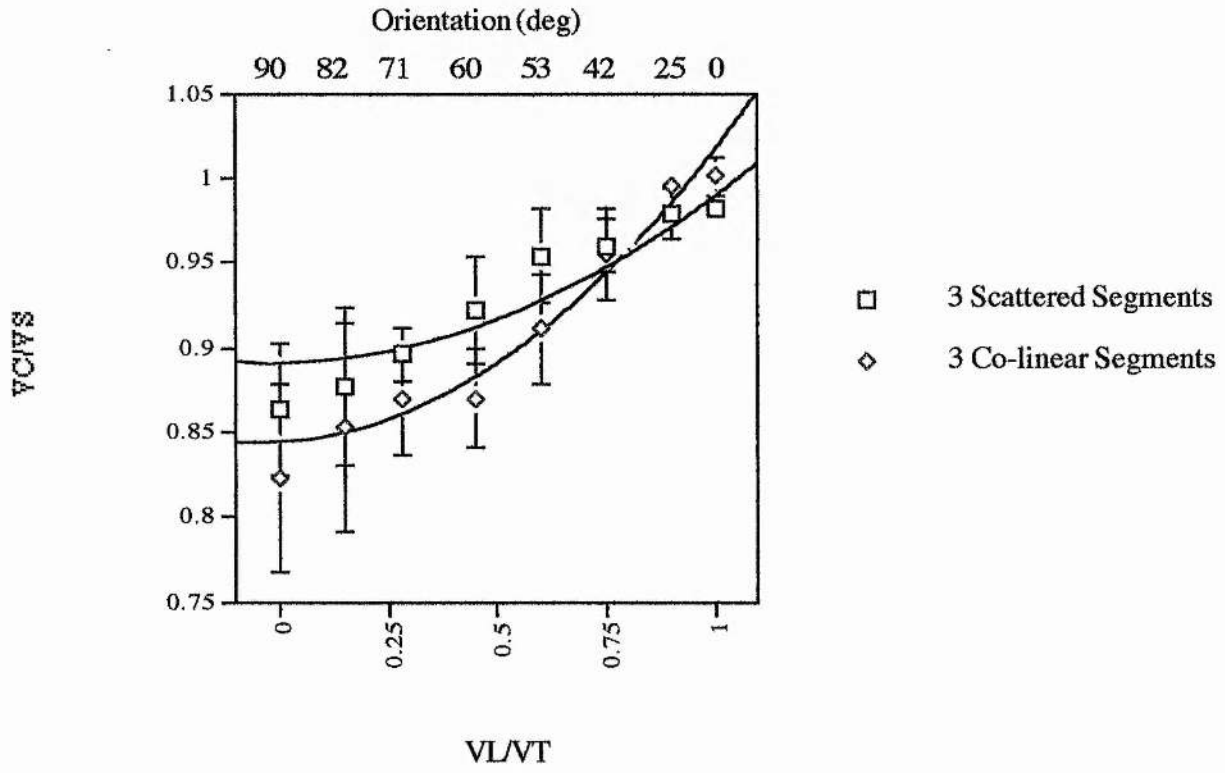

FIGURE 3.3

FIGURE 3.3- 3.6 Relative perceived speed as a function of the ratio of the local speed to the translation speed (V_L/V_T). Continuous lines show model of Castet *et al.* (1993) fitted to the data with two free parameters α and β. The bars through the symbols show ± 1 SE. The speed of the standard was 2 deg./sec. Legends beside the graphs depict the stimulus conditions in each instance. Stimuli described in detail in methods. Each data point is the perceived speed averaged across three observers (n=3).

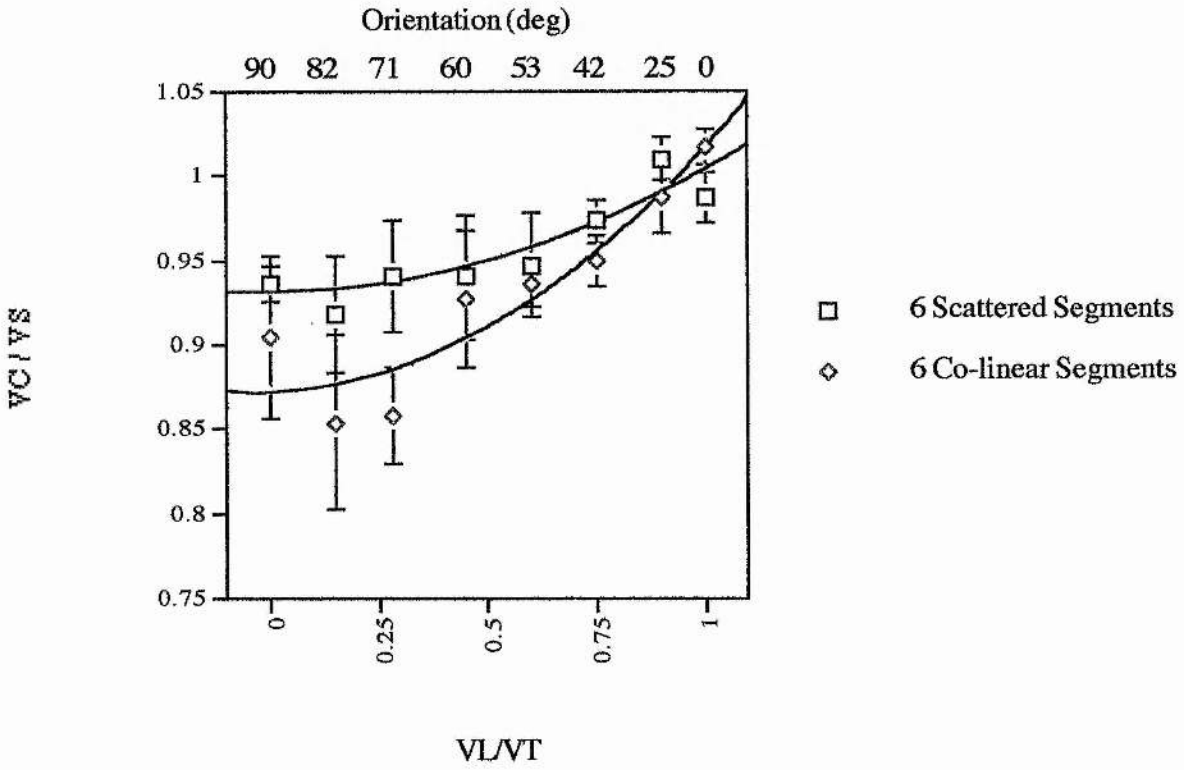
Orientation (deg)
90 82 71 60 53 42 25 0
1.05
1
0.95
0.9
0.85
0.8
0.75
VC / VS
0 0.25 0.5 0.75 1
VL/VT
6 Scattered Segments
6 Co-linear Segments

FIGURE 3.4

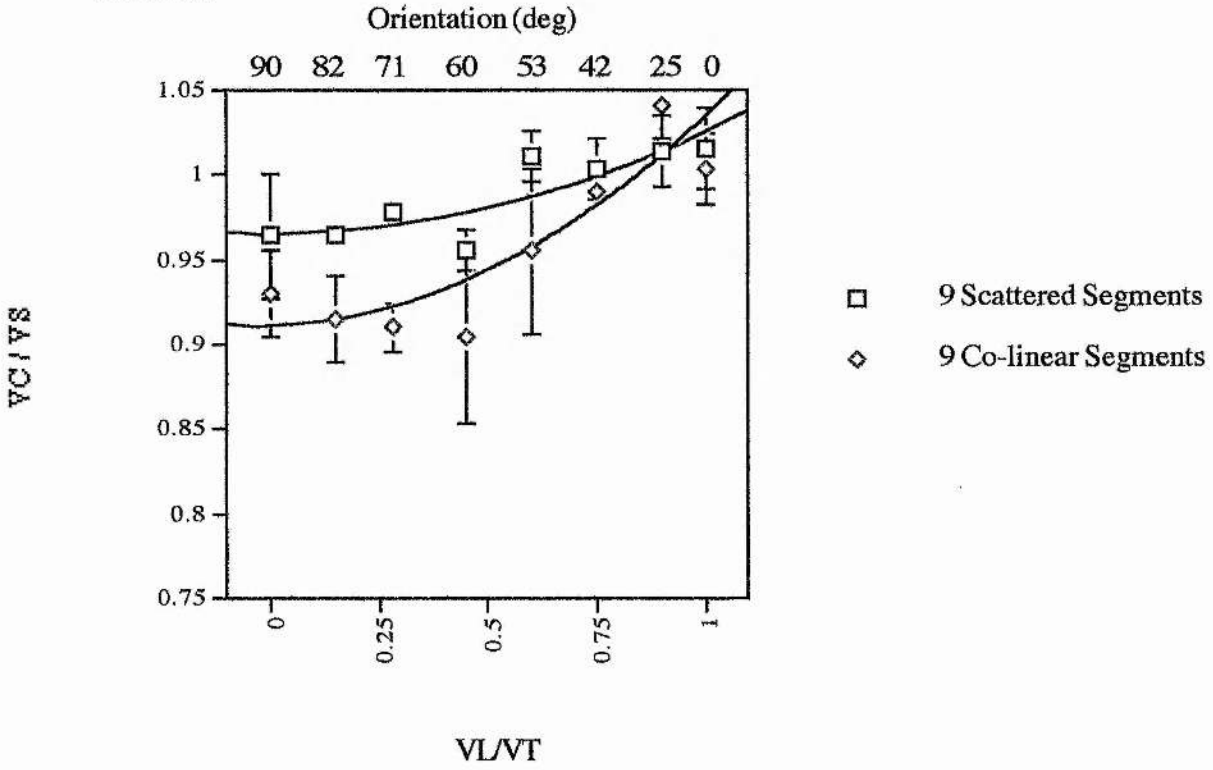
Orientation (deg)
90 82 71 60 53 42 25 0
1.05
1
0.95
0.9
0.85
0.8
0.75
VC / VS
0 0.25 0.5 0.75 1
VL/VT
9 Scattered Segments
9 Co-linear Segments

FIGURE 3.5

Effect of number of terminators: comparison of the data for three, six and nine co-linear segments with the curve for a continuous long line (Fig 3.6) reveals the effect of the number of terminators on the perceived speed of tilted stimuli in horizontal translation. It has been shown above that there is a systematic difference between the perceived speed of co-linear and scattered segments It is apparent, however, that as the number of line segments increases from six to nine - the bias in speed decreases.

Table 3.1 show the parameters α and β derived from the data according to the weighted average of Castet *et al.* (1993).

There is a general increase in the value of β for 3, 6 and 9 co-linear segments, however the differences are more subtle than the differences in α across conditions. The β weight should reflect differences in the importance of the terminators. This is evidence in support of the contention that the model does not take full account of the number and spatial position of the terminators.

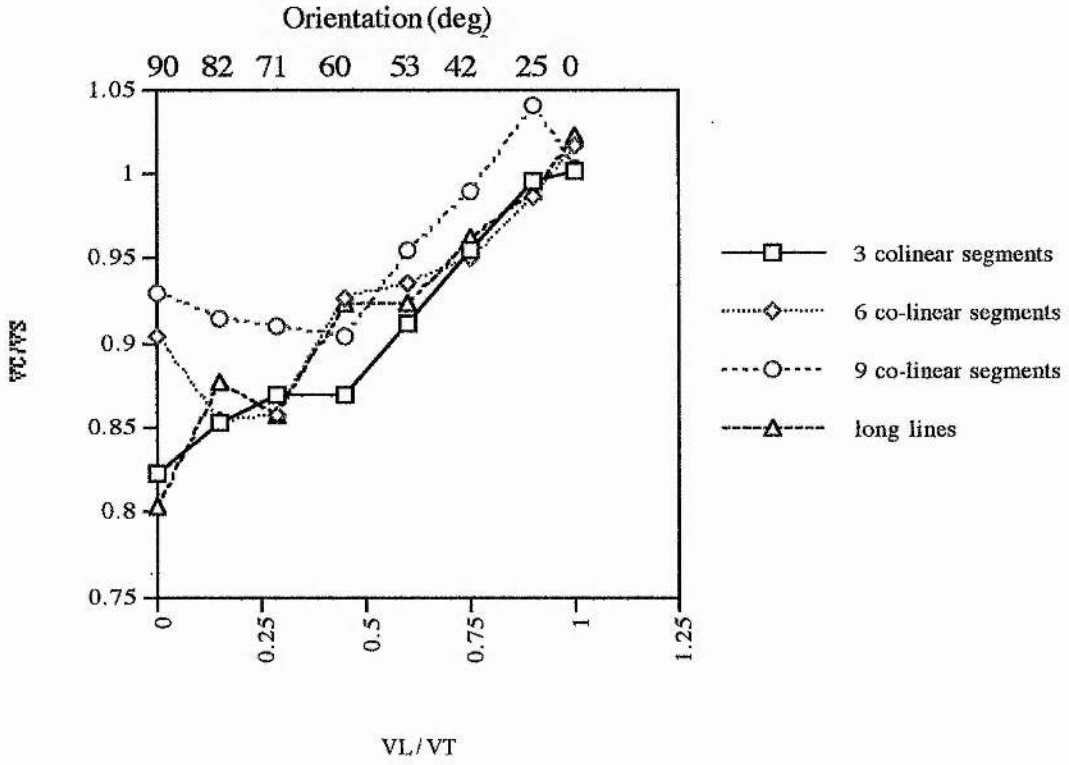

FIGURE 3.6 Mean perceived speed as a function of line inclination for four stimulus types as indicated in the legend. Data are averaged over three observers (n=3).

LINE TYPE	WEIGHT	
	α	β
3 scattered seg.	.097	.891
3 co-linear seg.	.170	.845
6 scattered seg.	.072	.931
6 co-linear seg.	.143	.873
9 scattered seg.	.060	.965
9 co-linear seg.	.122	.912

TABLE 3.1. Weights attached to V_L and V_T as derived from the data according to Castet *et al.'s* (1993) model.

Experiment 5.

The second experiment involved measuring the perceived speed of six co-linear dots in horizontal translation. As can be seen in Fig. 3.7, there is bias in the perceived speed of inclined co-linear dots but this is weak. The data resemble those for nine co-linear segments. Both of these stimuli contain very salient terminators and so this is to be expected. Table 3.2 shows the parameters for each condition as derived from the weighted average model of Castet *et al.* (1993). There is a considerable difference in the size of the α parameter for dots and whole lines: α is almost exactly double the size for long line stimuli.

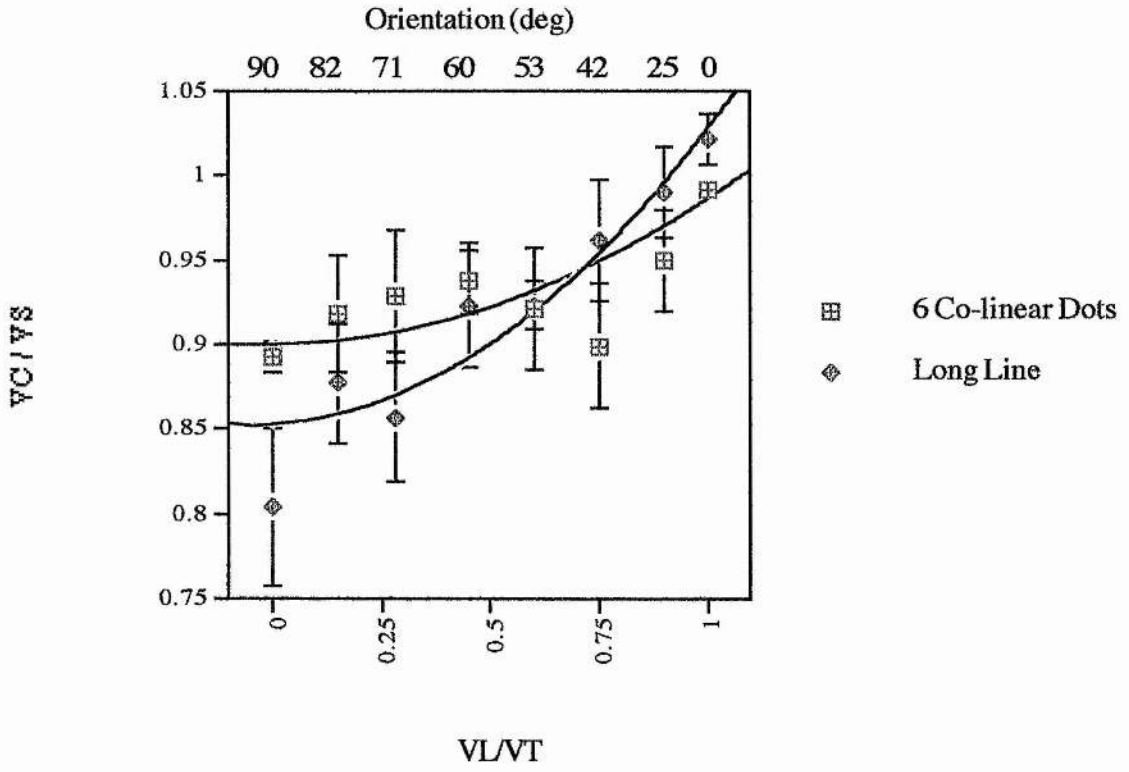

FIGURE 3.7 Relative perceived speed of co-linear dots and a long line as a function of the ratio of the local speed to the translation speed (V_L/V_T). Continuous lines show model of Castet *et al.* (1993) fitted to the data with two free parameters α and β. Bars through the symbols show ± 1 SE. The speed of standard was 2 deg./sec. Legends beside the graphs depict the stimulus conditions. Stimuli are described in detail in methods. Each data point is the perceived speed averaged across three observers, (n=3).

LINE TYPE	WEIGHT	
	α	β
long lines	.171	.854
co-linear dots	.085	.900

TABLE 3.2. Weights α and β attached to V_L and V_T as derived from the data according to Castet *et al.*'s (1993) model, (n=3).

DISCUSSION

Effect of orientation

For stimuli comprising 3 co-linear segments and 3 randomly scattered segments, it has been shown that as the angle of inclination of the standard stimulus increases its apparent speed decreases (Fig 3.3). The same trend is apparent for six segments (Fig 3.4) with the exception of one outlier as explained earlier. The picture for nine segments is somewhat different however, with a flat or even slightly u-shaped distribution of data across orientations as can be seen in Fig. 3.5.

In experiment five the level of misperception of co-linear dots decreases at first, then increases and subsequently decreases as a function of the angle of inclination of the stimulus. As we have seen, these data are not effectively modelled by the Castet *et al.* (1993) equation. What is required is something that takes more account of the motion of terminators in isolation because as seen in Fig. 3.7 there is a slight bias in perceived speed ($V_C/V_S = 0.9$) at certain orientations.

Effect of stimulus configuration:

In the experiment involving three segments, co-linear and scattered stimuli are seen to travel at very similar speeds. Nonetheless there is still a systematic difference between the two, with the co-linear segments appearing to travel more slowly than the scattered segments. There is a marked difference in the perceived speed of scattered segments compared to co-linear segments in both the six and nine segment conditions.

With only three segments there is much less variability in the three randomly scattered segment conditions than in the six or nine scattered segment conditions. In addition there are only six terminators in the three scattered segment stimuli and so one would anticipate more bias in the perceived speed of three inclined scattered segments than six. Nonetheless, with terminators proposed as particularly salient elements of the stimulus, providing veridical information, one ought to expect no bias at all.

Effect of number of terminators

Experiment 4: Fig. 3.6 plots data points for stimuli containing 2, 6, 12 and 18 terminators. Most notable is the difference between 12 and 18 terminators (ie. six and nine co-linear segments). The addition of six more terminators to the stimulus dramatically increased the perceived speed of the stimulus. This reduced bias for nine co-linear segments could be due either to the added number of terminators or because of the reduced length of the individual line length. Experiments from chapter one and Castet *et al.* (1993) suggest that shorter line length elicits a reduced bias in perceived speed as a function of orientation.

Experiment 5: Whilst co-linearity has been shown to be a critical factor in determining the perceived speed of inclined line segments in horizontal translation the results from the experiment involving six co-linear dots have shown that it is not the only factor. In the absence of line segments, the perceived speed of the co-linear stimulus was subject to only a very small bias. This shows that perceived speed is not simply governed by a "gestalt" grouping effect. Although co-linear segment stimuli elicit similar misperceptions to whole lines, some line elements are required to generate local motion components.

Applicability of models of motion.

Perrone's (1990) model incorporates a voting scheme for integration across space (which predicts Castet *et al.*'s (1993) line length effect) and so is a candidate model for accounting for the results reported here. It would have to be assumed that eight gaps were sufficient to disrupt the spatial pooling of the model. However Castet *et al.* (1993) report that the model is unable to account for the effects of luminance on perceived speed.

Smith and Edgar (1991) provide an account of integration of motion invoking the averaging of spatial scales. The co-linear segment stimuli used here appear very different at low and high spatial frequencies. At high spatial frequencies many terminators are visible but at low spatial frequencies only the two extreme terminators are evident, and they are not particularly salient. If the motion detectors have large receptive fields (van de Grind, Koenderink & van Doorn, 1986), then it is possible that the whole line could be processed as a blob. This would fit well with results of the experiments involving co-linear segments. The exception to this is the co-linear dot condition where the whole "blob" is still oriented but does not elicit a bias in perceived speed at large angles of inclination.

How well does the weighted average model account for the data?

In each of the co-linear segment versus scattered segment comparisons the smooth curves depicting the weighted-averaging model fitted to the data should lie on top of each other, and the derived parameters α and β should be the same. The best overlap is obtained in the three segments condition; both the six and the nine segments conditions exhibit significant differences in the parameters.

The individual curves should provide a good description of the data points for all orientations within one stimulus type. There is a reasonable fit for the six segments condition (taking account of the outlying data point) but the model does not fit the nine segments data very well. The data for the co-linear segments are much better described by a U shaped curve.

In experiment five the data for co-linear dots is actually best described by a third order polynomial equation - there are two turning points in the data.

Proposals for future research.

Whether randomly scattered dots would behave in the same way as scattered segments is at present unknown. Speed estimates from such an experiment could be compared with the perceived speed of co-linear dots in horizontal translation. In addition, twelve dots could be used to mimic the number of terminators in the six segments condition instead of the three segments condition as was used.

One hypothesis is that the misperception of inclined co-linear segments is governed by a very precise grouping factor. Slight changes in the spacing and length of the elements may be sufficient to abolish the bias in perceived speed (the limits of this could be ascertained empirically).

CONCLUSION

This chapter explored the limits of the effects of gap size in co-linear segments reported in the previous two chapters. The co-linearity effect was compromised by the presence of 18 terminators and also by the absence of line segments. Given that the overall line length is the same as in experiment four and that the overall stimulus length in experiment five is the same, it remains to be explained why the different stimuli appear to travel at different speeds (in contrast to the predictions of the Castet *et al.* (1993) weighted averaging model).

The results may be explained with reference to any or all of the following stimulus parameters: the number of terminators, the number of gaps or the eccentricity of the different stimulus types. The experiments manipulating the eccentricity of the standard stimulus, which are reported in the next chapter, rule out the hypothesis that the increased eccentricity of the nine segments stimulus may have reduced the system's ability to integrate across the whole contour. In addition the gap size experiment in

chapter three showed that with very long lines of co-linear segments a misperception of speed still occurs. The experiments manipulating terminator position (reported in chapter five) help to reveal the exact mechanisms responsible for encoding the speed of tilted lines.

The effect of eccentricity on the perceived speed of tilted lines in horizontal translation.

CHAPTER 4

Eccentricity of tilted lines in translation does not affect perceived speed.

INTRODUCTION

The perceived speed of lines inclined with respect to their direction of travel was estimated. The study investigated the effect of increasing the eccentricity of the tilted line from the fixation point. The purpose of this was to ensure that the effects on perceived speed of lines of co-linear segments (Scott-Brown & Heeley, 1995; chapter 2 experiments 2 and 3 (a)) could not be accounted for by the increased eccentricity of these stimuli compared to the eccentricity of the continuous lines used in the previous two experiments.

Variation of motion integration across visual field.

A difference between the capabilities of central and peripheral vision has been a common theme in vision research (Westheimer, 1982; McKee & Nakayama, 1984; Koenderink, van Doorn & van de Grind, 1985). Positional acuity has been found to be poorer in peripheral viewing conditions (Westheimer, 1982; Burbeck & Yap, 1990). The reduction in positional certainty may affect the perceived speed by increasing the influence of local component motion relative to terminator motion. If this is the case, the bias in perceived speed should increase.

Moving random checkerboard patterns have been used at different eccentricities to investigate the motion detector properties of the monocular visual field and permit the derivation of a structurally invariant scaling factor (van de Grind, Koenderink & van Doorn, 1986). Sensitivity to the motion of sinusoidal gratings displaced sinusoidally over time decreases as a function of retinal eccentricity (Wright, 1987). However a spatial scaling function was found to be sufficient to equalise performance over visual space. (Sensitivity was defined as the reciprocal of the threshold displacement amplitude.)

Receptive field size increases as a function of eccentricity (Rovamo & Virsu, 1979) and may be used as an explanation of the observed differences in peripheral and central perception of motion (McKee & Nakayama, 1984). This explanation, if true, bears directly on the experiments reported here. It is possible that increasing eccentricity and receptive field size increase could actually reduce the *effective* length of a line in the

periphery. This reduction in length, and associated reduction in misperception (Castet *et al.* (1993), could mask any increased bias in perceived speed arising from the reduced visibility of terminators in periphery.

This chapter explores the effects of peripheral viewing on the perceived speed of tilted lines in horizontal translation. It aims to determine whether results reported in previous chapters arose as a result of the differences in stimulus eccentricity across conditions. The difference in eccentricity of co-linear segments and continuous lines can be seen in Fig. 4.1.

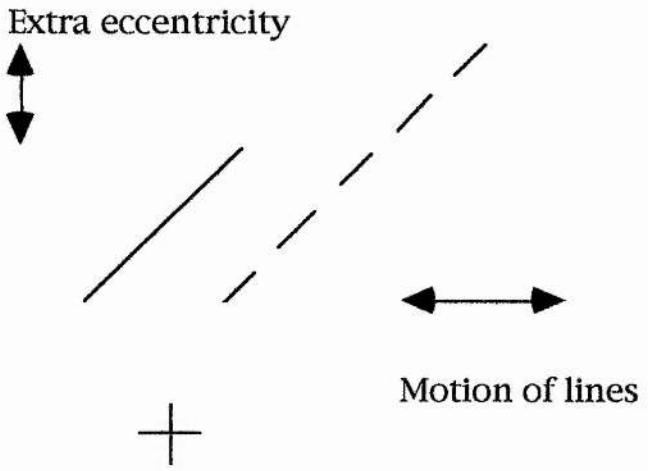

FIGURE 4.1 Stimulus configuration showing the increased eccentricity of co-linear segments compared to whole lines in the experiments in chapters 2 and 3. The cross indicates the fixation point.

METHODS

Apparatus and Procedure

The apparatus and procedure are described in chapter 2. In both experiments, the contrast ratio of line brightness to background brightness was held constant at 0.05.

The vertical line passed through the fixation point and the tilted line travelled on a horizontal trajectory either above or below the fixation point. The eccentricity of the line was either 0.0, 1.5, 2.75, 4.0 or 5.25 deg. of visual angle. Experiments included line translation both above and below the fixation point. These dimensions are the same as the overall length of the co-linear stimuli featured in chapter three.

Observers

Three observers were experienced psychophysical observers who were unaware of the purposes of the experiment. The fourth observer was the author. All were

professionally refracted and had normal or corrected to normal vision with no astigmatism greater than 0.25 dioptres.

Experiment 6

Stimuli were lines of 2.0 deg. visual angle. Speed estimates were obtained for angles of tilt ranging from 0 - 90 degrees. Fig. 4.2 shows the stimulus eccentricities used above the fixation point.

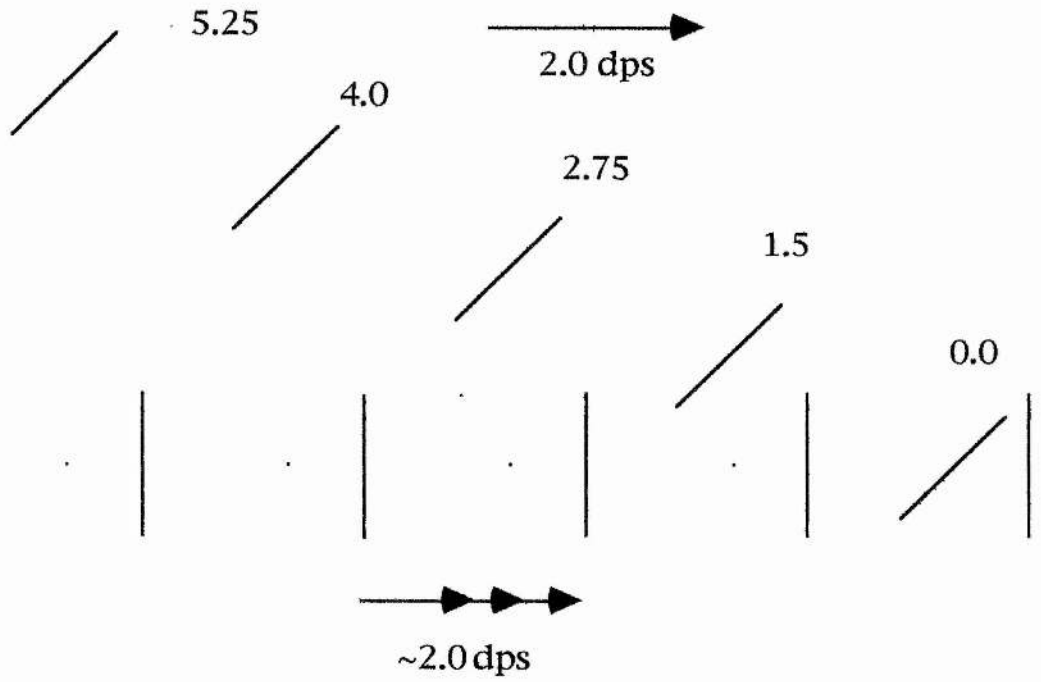

FIGURE 4.2 Diagram of stimulus arrangements. Eccentricity is indicated beside each standard (inclined) stimulus.

Experiment 7

Stimuli were lines of various lengths as indicated in Fig. 4.3. Speed estimates were obtained for vertical lines drifting horizontally. Fig. 4.3 shows the stimulus eccentricities used above the fixation point. The "test" stimulus in the staircase procedure travelled above the fixation point while the "standard" stimulus travelled through the fixation point.

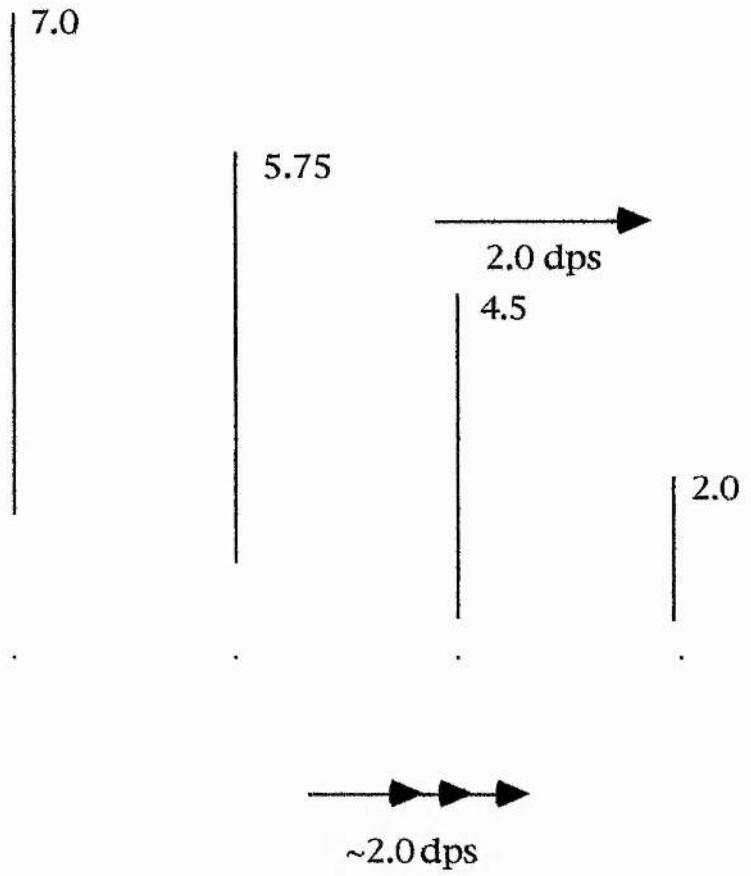

FIGURE 4.3 Stimulus arrangements for experiment 7. The lines of various lengths from 2.0 deg to 7.0 deg. are indicated. For each line length the comparison stimulus travelled through the fixation point.

RESULTS

As in previous chapters, the results are presented in the same manner as Castet *et al.* (1993). (V_C/V_S) is the ratio of the comparison speed to the standard speed. This measure of relative perceived speed is then plotted against V_L/V_T, which is the ratio of the speed of V_L (representing the orthogonal component) and V_T (representing the terminator speed). The ratio of V_L/V_T is used because the model proposed by Castet *et al.* (1993) uses a weighted-average of the two signals V_L/V_T.

Experiment 6

The data are presented as the average of four observers. The data for the individual observers is shown in Appendix 4.A.

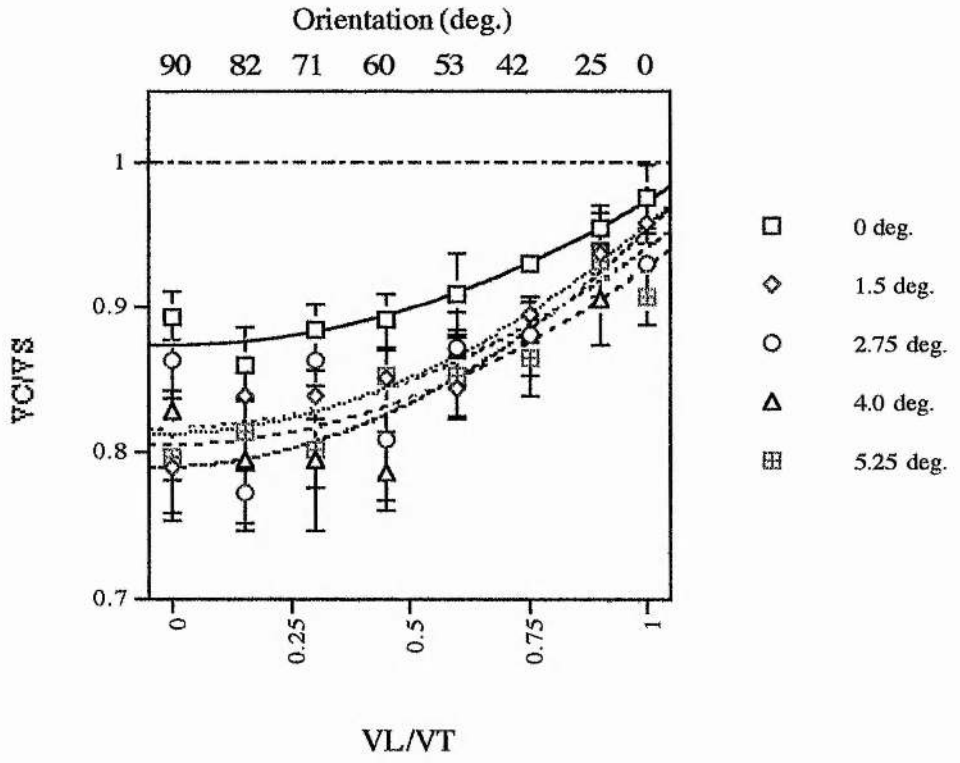

FIGURES. 4.4-4.5 Relative perceived speed as a function of the ratio of the local speed to the translation speed (V_L/V_T) for translation above and below the fixation point respectively. The lines in the legend show the model of Castet *et al.* (1993) fitted to the data with two free parameters α and β. Bars through the symbols show ± 1 SE. The speed of the standard was 2 deg./sec. The horizontal dashed and dotted line shows the 1:1 ratio of standard and comparison speed, indicating veridical perception of speed. Legends beside the graphs depict the stimulus conditions in each instance. Stimuli are described in detail in methods. Data points are the average of four observers, each observer's data point was the average of five speed estimates (n=4).

The data for translation above the fixation point, averaged over the four observers, is shown in Fig. 4.4 above. The data show the characteristic bias in perceived speed as the angle of inclination of lines approaches 90° (Castet *et al.* 1993; Scott-Brown & Heeley, 1995). The progressive misperception of speed towards horizontal lines concurs with the predictions made in the introduction as well as findings from previous work.

Although the data shows a reduced bias at zero degrees of eccentricity (square symbols) compared to all the other eccentricities, beyond zero degrees there is no systematic increase in misperception. As trajectories are moved to the periphery there is no appreciable increase in the bias in perceived speed. In addition, for each eccentricity, there is no qualitative change in the bias in perceived speed as the angle of tilt is increased.

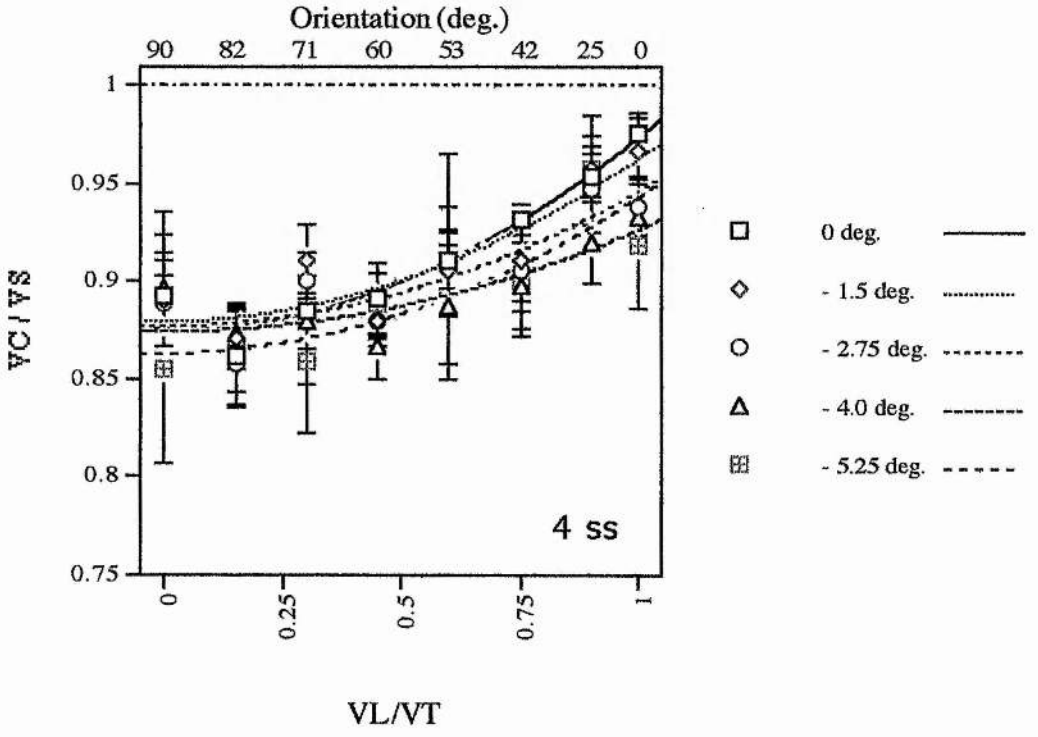

FIGURE 4.5

The data for translation *below* the fixation point (Fig. 4.5) is similar to that of previous results (chapter 2, experiments 2 and 3): there is a quantitatively similar progressive bias in perceived speed as a function of eccentricity for all eccentricities. This finding strongly suggests that the reduced bias for translation at the level of the fixation point (0 deg.) arose by chance - only two of the four observers displayed the effect.

The data for KSB (Fig. A.4 in Appendix 4.A) is consistent inasmuch as the data are grouped together in a similar fashion to the data for motion above the fixation point (Fig. 4.7). One slight exception is the data for - 5.25 degrees of eccentricity (crossed

squares) which does not follow the characteristic trend of a bias in perceived speed increasing with orientation, the reverse is in fact observed. The predictions of the experiment have been broadly supported with a small but ever-present bias in perceived speed observed at each eccentricity.

Observer EW (Fig. A.7 in Appendix 4.A) shows the characteristic trend of increasing speed misperception. There is however a difference between the data at zero eccentricity and peripheral data. This indicates that some caution should be exercised before extrapolating the results from chapters two and three. Thus the use of a control condition for the gap-size experiments in chapter three is justified. By using a line as long as the whole extent of the co-linear segment, it was possible to control for the possibility that the larger eccentricity of the co-linear stimuli influences the perceived speed of the stimulus. However, it is still possible that the terminators are less visible at higher eccentricities. This possibility is examined in experiment seven.

Table 4.1 and Fig. 4.6 show how the model parameters α and β (representing the contour and the terminators respectively) vary as a function of eccentricity. Analysis of covariance showed a main effect of eccentricity for α ($F(1,34) = 8.78$, $p < 0.01$) and β ($F(1,34) = 11.628$, $p < 0.01$).

ECCENTRICITY (deg.)	WEIGHT α	β
5.25	0.1211	0.879
4.0	0.161	0.806
2.75	0.123	0.792
1.5	0.142	0.818
0	0.0992	0.814
-1.5	0.083	0.877
-2.75	0.0687	0.874
-4.0	0.0521	0.863
-5.25	0.0797	0.874

TABLE 4.1. Weights attached to V_L and V_T as derived the model equation provided by Castet *et al.'s* (1993) model. The equation for the model is given in Chapter 2. The curve fitting procedure is also described therein. Data obtained from the average of four observers (n=4).

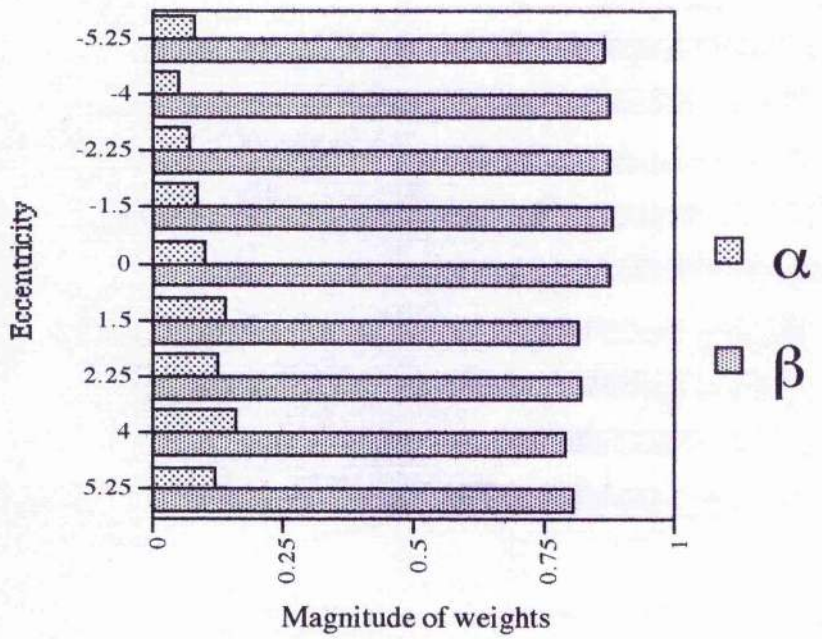

FIGURE 4.6 Magnitude of weights α and β for each eccentricity according to Castet et al's (1993) model (4 subjects). The equation for the model is given in Chapter 2. The curve fitting procedure is also described therein. Note that these data are not the average of the parameters from each subject

but are the parameters derived from the curve fitting procedure to the perceived speeds of the four subjects averaged (n=4).

From the bar chart in Fig. 4.6 it is clear that there is a slight difference in the magnitudes of the weights for trajectories above and below the fixation point. Below the fixation point α appears to be larger while the β component is smaller. The differences are small however, especially in the β parameters.

Fig. 4.7 compares the data from four subjects, for a given magnitude of eccentricity both above and below the fixation point. There is a stronger bias in perceived speed for the above fixation point trajectories.

The difference in the bias is reflected in the differences in the model weights as discussed above. The reason for this difference is unclear; perhaps it simply arose from the fact that most psychophysical and psychological experiments incorporate stimulus presentation above the fixation point. (All the observers were experienced psychophysical observers and had experience of psychological experiments using similar methodologies.)

Alternatively there may be some systematic pooling differences in the receptive fields of the upper and lower visual hemifields.

FIGURE 4.7 (Overleaf) Perceived speed as a function of the angle of inclination of the standard stimulus, expressed as the ratio of the translation signal and the component orthogonal to the contour. Eccentricity is shown in the legend (n=4).

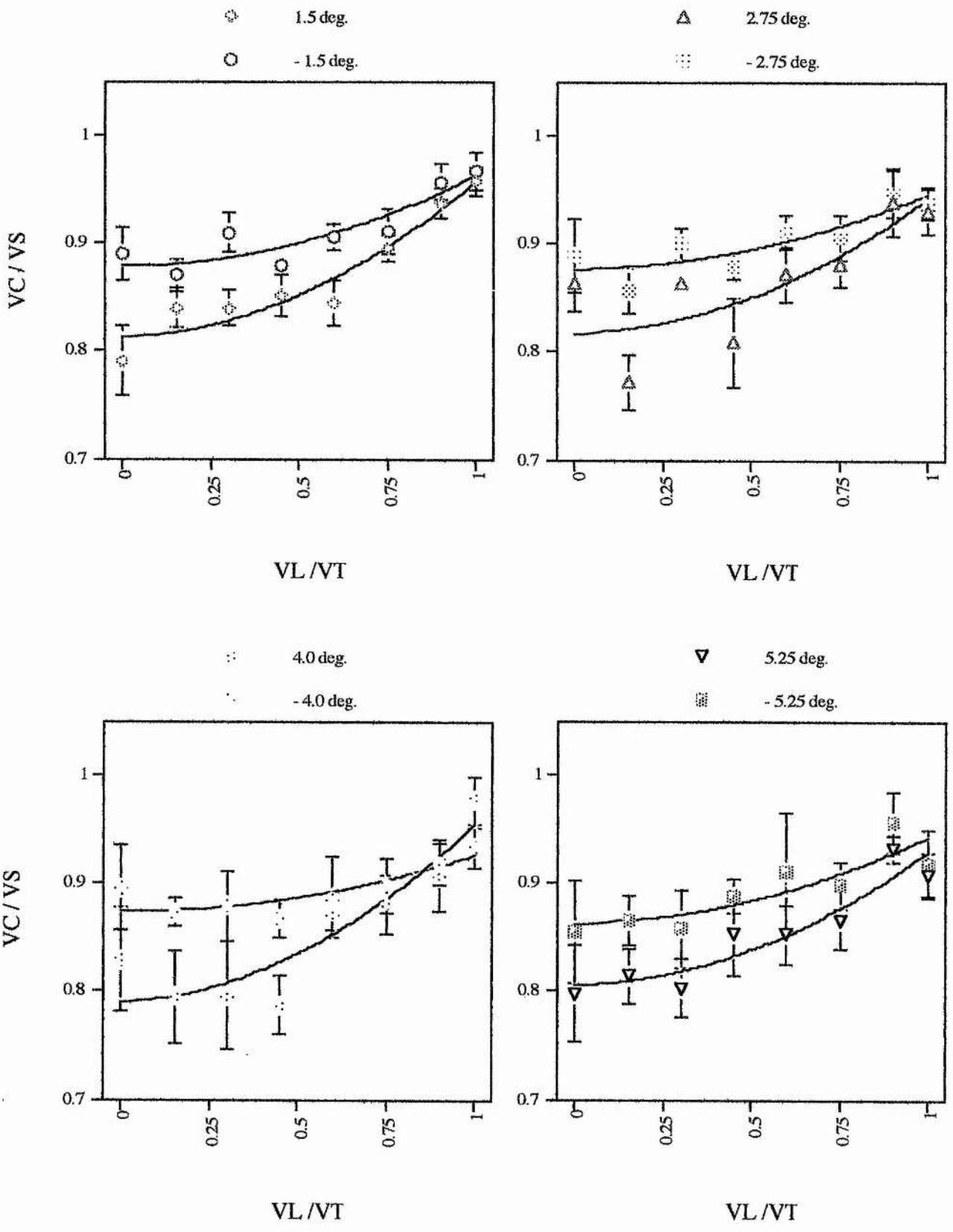
1.5 deg.
- 1.5 deg.
2.75 deg.
- 2.75 deg.
4.0 deg.
- 4.0 deg.
5.25 deg.
- 5.25 deg.
VC / VS
VL /VT
1
0.9
0.8
0.7
0
0.25
0.5
0.75

Experiment 7

This experiment increased the length of the line as the eccentricity increased to allow for the possibility that stimuli presented in the periphery are coded by larger receptive fields than stimuli in the foveal area (as discussed in the introduction). Fig. 4.8 shows the perceived speed at each eccentricity. The legend shows the length of each stimulus. Most of the error bars overlap indicating that the differences in perceived speed between eccentricities are small.

There is no substantial difference between the eccentricities and any effect is only apparent for stimuli travelling in the upper visual field (or the lower hemiretinae). This finding is consistent with the finding in experiment six which showed as stronger bias in perceived speed for stimuli in the upper visual field. The magnitude of the effect in this instance is much smaller; meaning that eccentricity per se cannot account for the bias in perceived speed of inclined lines observed in experiment six.

Perceived speed as a function of vertical eccentricity with Line Length as a parameter.

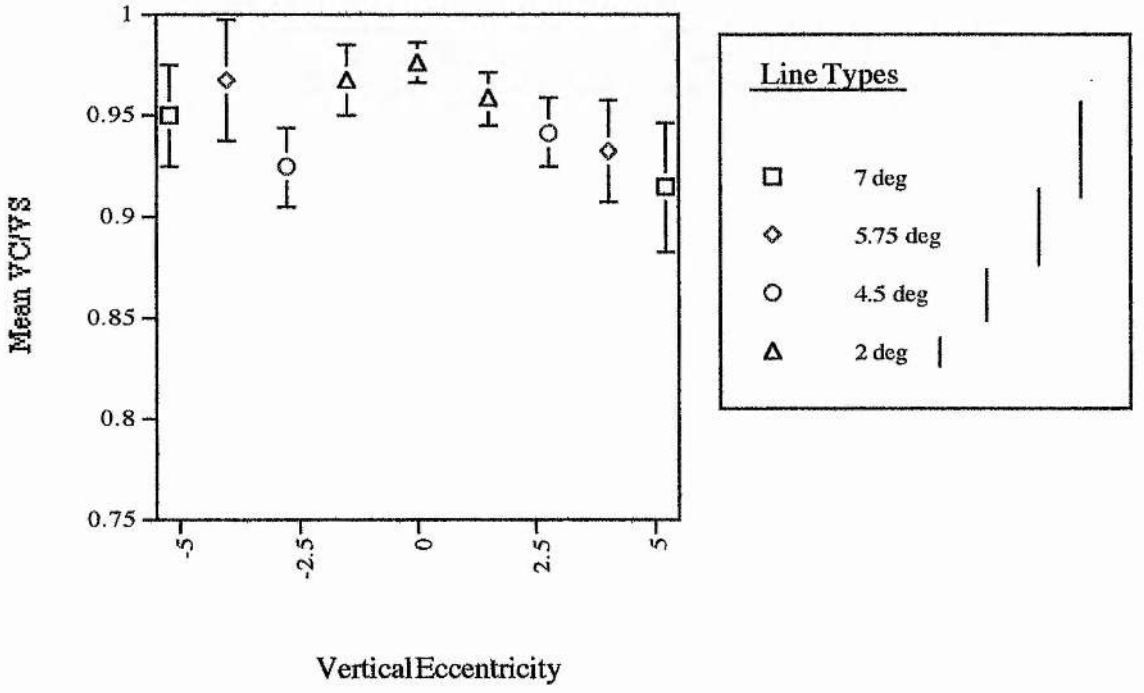

FIGURE 4.8 Relative perceived speed of the standard stimulus at each eccentricity. The standard and comparison stimuli were both vertical in this experiment. The line length of each stimulus is shown in the legend (drawings not to scale), (n=3).

DISCUSSION

Summary

The perceived speed of tilted lines in horizontal translation is biased towards the speed of orthogonal components. This phenomenon was replicated at each eccentricity of trajectory between zero to 5.25 degrees of visual angle.

Effect of eccentricity

The peripheral data for 1.5 to 5.25 degrees of vertical eccentricity are fairly well superimposed. This means that if there is an effect of eccentricity, it is not of a simple linear nature.

Effect of orientation

Perceived speed decreases as the angle between the translation signal V_T and the component signal V_L was increased.

Effect of stimulus configuration

Experiment seven has shown that increasing the line length has only a very small effect on the perceived speed of tilted lines at any of the eccentricities tested.

Previous Results

Lower apparent contrast of peripheral lines may affect their perceived speed (Thompson, 1982). As the eccentricity of the stimuli increases their perceived contrast may decrease and cause a lower perceived speed. If this explanation were to account for the data it would still have to justify different contrast perception in the upper and lower hemifields.

Differences in perceived velocity between upper and lower as well as left and right hemifields have been demonstrated in several subjects but not consistently across subjects (Smith & Hammond 1986). Seven out of ten subjects tested showed hemifield differences in favour of test gratings drifting in the lower hemifield. Subjects were required to adjust the speed of a drifting grating to match the speed of an adjacent drifting grating whilst fixating on a central point*. Some of the observed differences were non-significant but two observers showed particularly strong tendencies. Further speed matching experiments, involving a range of veridical velocities, were performed on these two observers confirming the initial findings with consistent errors at all velocities tested. The differences were not related to hand or eye-dominance. The authors concluded that the differences arose through individual differences rather than as a result of purposive hemispheric specialisation. Whilst the results were obtained

---

* Observers were prevented from matching pairs of line endings in the task: the upper and lower conditions featured horizontal test gratings drifting vertically while the left and right conditions comprised vertical gratings drifting on the horizontal axes.

using a different method from those in this chapter, the hemifield differences are of a similar nature and so the same explanation may apply here.

Motion detection thresholds in the four quadrants of visual space for random-dot kinematograms on a noisy background mimic the results reported in experiment 7 (Woods, unpublished results).

Applicability of the weighted average model of motion perception?

It has been shown that the model of Castet *et al.* (1993) does not provide a perfect account of the data because the weights for α have in some cases been below zero.

The experiment altered the spatial position of terminators relative to the fixation point, without affecting the perceived speed, as would be predicted by Castet *et al.* (1993).

CONCLUSION

The results were *qualitatively* similar to the conditions in the first experiment reported in chapter two; the pattern of results reported there holds for each of the four eccentricities examined. The progressive misperception of speed towards horizontal lines is supported by previous work (Lorenceau, Shiffrar, Wells, & Castet, 1993; Castet *et al.*, 1993) and conforms to the experimental hypotheses.

The implications of this finding are that the differences in perceived speed between the co-linear segments and the continuous line segments in previous experiments were *not* caused by the greater eccentricity of the co-linear segments.

Only two subjects exhibited a difference between central and peripheral translation suggesting that there is no major difference in the two types of horizontal translation.

Yo and Wilson (1992) found an average bias of 25 deg. in the perceived direction of type II plaid patterns at 15 deg. of eccentricity. The effect of bias in perceived direction was also contrast dependent, with 5% contrast eliciting a bias of 20 deg. This finding can be explained by the lack of influence of the veridical motion from terminators (the ends of the blobs) due to the combination of low contrast (rendering the terminators less salient) and the distance of the terminators from the fovea. It is worth noting that the Yo and Wilson (1992) experiment and the experiments of van de Grind, Koenderink and van Doorn (1986) used high levels of eccentricity, 25 and 48 deg. respectively. This is considerably more than was used in the experiments reported here. It is unlikely that the small changes in eccentricities used would drastically influence the results of the previous experiments (in chapter 2) involving co-linear segments.

However the results provide a note of caution sufficient to justify the use of the control condition in the co-linear experiments where the overall length of the co-linear segment stimuli (including the gaps) was matched by a single line as shown in Fig. 4.9.

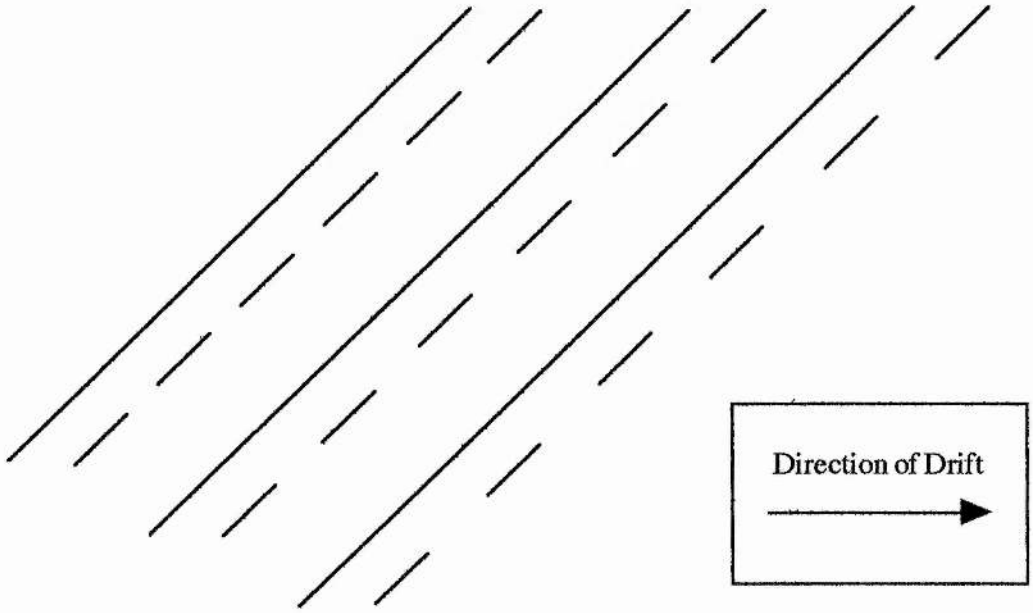

FIGURE 4.9 Reproduced from chapter 2.

Random perturbation of the length or the position of horizontally drifting tilted lines affects their perceived speed.

CHAPTER 5*

Terminator uncertainty affects perceived speed of inclined lines.

INTRODUCTION

To investigate the precise contribution of the features of tilted line stimuli on their perceived speed, the position of the line terminators was changed in two different ways. The first experiment comprised a random perturbation of the length of the lines over time, whilst the second experiment randomly changed the position of the lines over time.

A grating passing behind a jagged-edged aperture fails to elicit the usual barber-pole illusion (Kooi, 1993). The perceived direction of motion of gratings passing behind an aperture with straight edges and an aperture with indented edges was compared. Under straight-edged conditions subjects perceived the direction of motion to be along the long side of the aperture (in the direction of the ends of the lines of the grating). Under indented conditions the illusion was abolished and instead subjects perceived motion in the direction perpendicular to the bars. The illusion was abolished when indentation size was greater than or equal to one quarter of the grating period. This is shown graphically in Fig. 5.1. The explanation for this finding was that the veridical velocity signal from the terminators was abolished, leaving the local velocity vectors to provide the direction signal.

In fact the terminator signals were not abolished, merely changed, becoming the same as the local signals from the line. This is because the edges of the aperture became oriented on the oblique axes and thus the terminator motion also became oriented on the obliques.

---

* This data was first presented at the 1996 ARVO meeting, Fort Lauderdale, Florida. Scott-Brown, K. C. and Heeley, D. W. (1996) *Investigative Ophthalmology and Visual Science*, 37(3), 744.

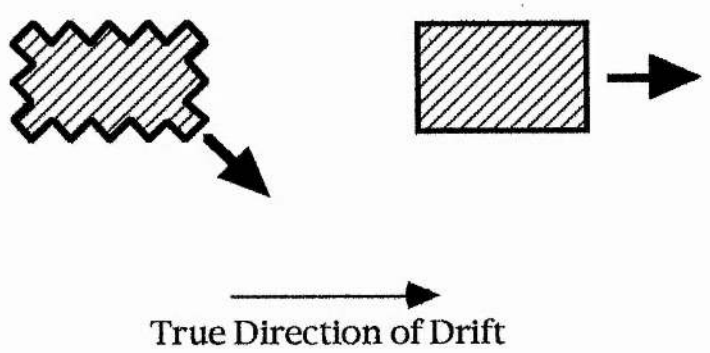

FIGURE 5.1 Perceived direction of gratings varies according to aperture construction. Gratings drifting behind jagged rectangular apertures appear to drift diagonally while gratings drifting behind straight-edged rectangular apertures are subject to the barber-pole illusion and appear to drift horizontally.

The classification of feature points as either intrinsic or extrinsic has a critical role in the determination of direction of motion. When parallel contours are presented to appear behind an aperture the motion of the terminators of the contour become classified as points of occlusion. The resultant perception of motion is unaffected by the terminators and so instead of the usual barber-pole illusion, observers perceive motion perpendicular to the contours. When parallel contours are presented to appear in front of an aperture the resultant percept is dictated by the motion of the terminators (Shimojo, Silverman & Nakayama, 1989).

Considering the above findings, the weighted average model (Castet *et al.*, 1993) predicts that the introduction of random perturbation of line length should further reduce the perceived speed of tilted lines in horizontal translation. In the same way, random perturbation of the vertical position of tilted lines during translation should further reduce apparent speed by removing the veridical velocity signals from the terminators. In the event the reverse occurred; random perturbation of line length and position abolished the speed reduction illusion.

METHODS

Apparatus and Procedure

The same apparatus and procedure as described in chapter two were used. In both experiments, the contrast was held constant at 0.05. The vertical eccentricity of the trajectory was 1.5 degrees of visual angle.

Observers

Five observers were used, of whom four were unaware of the purposes of the experiment. Observers were professionally refracted and had normal or corrected to normal vision with no astigmatism greater than 0.25 dioptres. Experiment 8 (a) used three subjects, experiment 8 (b) used five, experiment 9 (a) used two subjects and experiment 9 (b) used five.

Stimuli

Experiment 8 (a) & (b): Random perturbation of line length.

Line length variation was symmetrical about the centre. The length of the line was varied by 0, 10 or 25 %. The original length of the line was 2.0 deg. of visual angle. Fig 5.2 shows how length and spatial position changed over time. The length was randomly varied around the mid point of the line every 16 msec (milliseconds); the frame rate of the visual display was 66 Hz. The dotted line shows the mid-point of the line. The angular velocity of the line was held constant at two degrees per second.

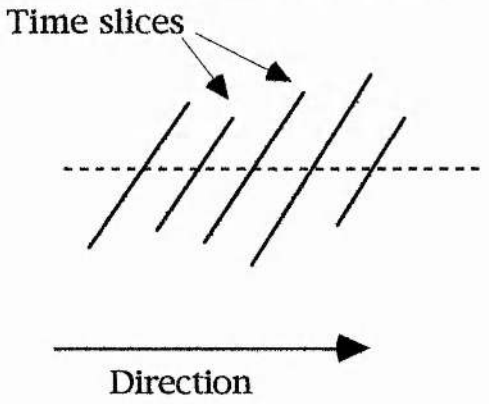

FIGURE 5.2 Diagram of stimulus arrangement.

Experiment 9 (a) & (b): Random perturbation of line position.

The vertical position of the line was varied about its horizontal trajectory by 0%, 10% or 25%. The length of the line was 2.0 deg. of visual angle. The tilted lines in Fig 5.3 show how the spatial position of the stimulus varied over time. The position was randomly varied around the mid point of the line every four frames. The average angular velocity of the line was two degrees per second. The experiment maintained constant line length for the stimulus, unlike experiment 8, but still provided uncertainty relating to the velocity of the terminators of the stimulus. The horizontal speed of the stimulus remains constant at 2 degrees per second over the duration of the stimulus interval.

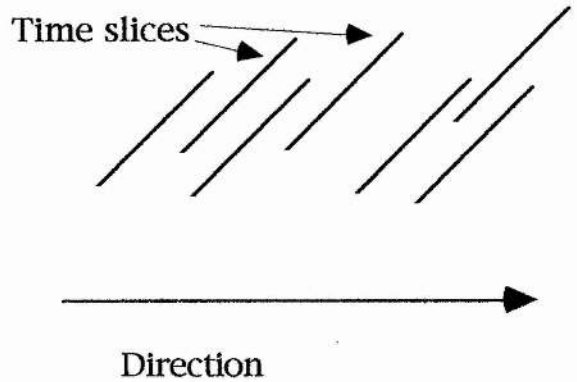

FIGURE 5.3 Stimulus arrangement for experiment 9.

RESULTS

Random perturbation of line length.

Experiment 8 (a)

Three subjects were used for an experiment to investigate the effects of random perturbation of line *length*. One orientation of standard stimulus was used: 72.54 degrees.

The results are shown below in Fig 5.4. The graph shows the average data from three observers. At 0% there is a significant bias in perceived speed but it can be seen that a variation of 10% is sufficient to abolish this misperception. Further levels of perturbation show a similar effect all the way up to 100% variation where the perceived speed of test and standard is still the same.

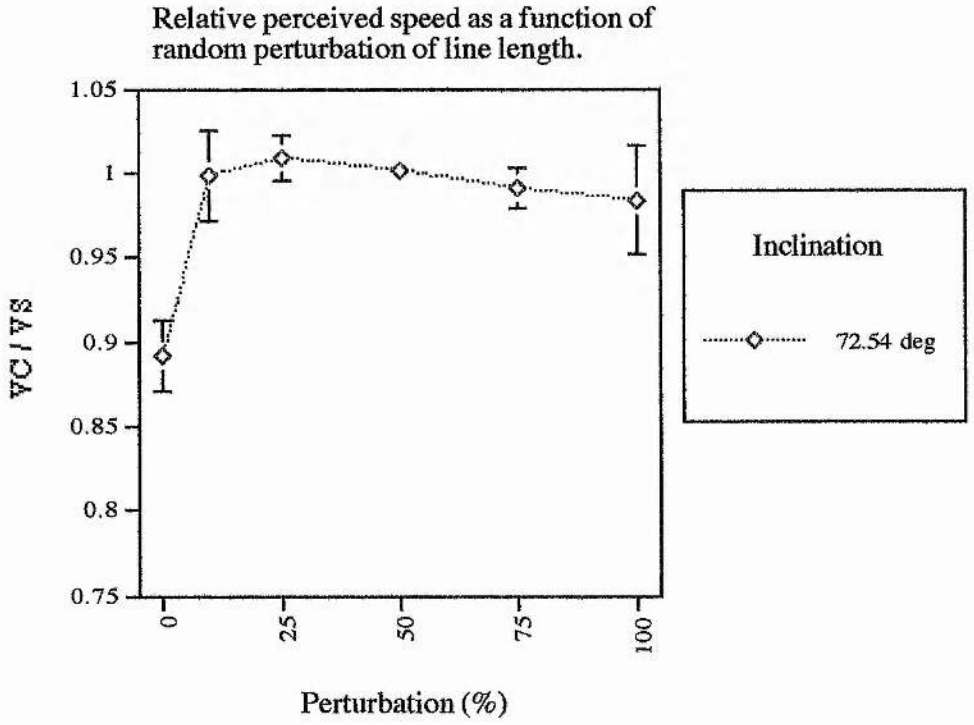

FIGURE 5.4 Relative perceived speed as a function of the level of perturbation of line position expressed as a percentage of the whole line length. Bars through the symbols show ± 1 SE. Speed of standard 2 deg./sec. The angle of inclination of the line stimuli was 72.54 degrees. Stimuli are described in detail in methods. Each data point is the average of five observations and three observers (n=3).

Experiment 8(b)

A more detailed investigation of the effects of random perturbation of length was performed using a reduced range of perturbations (0, 10, 25 and 50 %) and a range of angles of inclination (41, 73 and 90 degrees). Two experienced psychophysical observers and two relative novice observers participated in the experiment. All were

unaware of the purpose of the experiment. The data were qualitatively similar and so only the average data are presented here.

The characteristic curve for 0% perturbation is shown in Fig. 5.5. Relative perceived speed decreased from about 0.93 to 0.8 as the angle of inclination was increased. Lines that were subject to a random perturbation in length did not induce a significant bias in perceived speed, regardless of their angle of inclination. This is evident in the data for 10, 25 and 50 % perturbation. Relative perceived speed for each angle tested was around 1, indicating veridical perception of speed. The curves derived from the weighted average model of Castet *et al.* (1993) also reach a lower asymptote at 1 indicating that veridical perception is likely for all orientations.

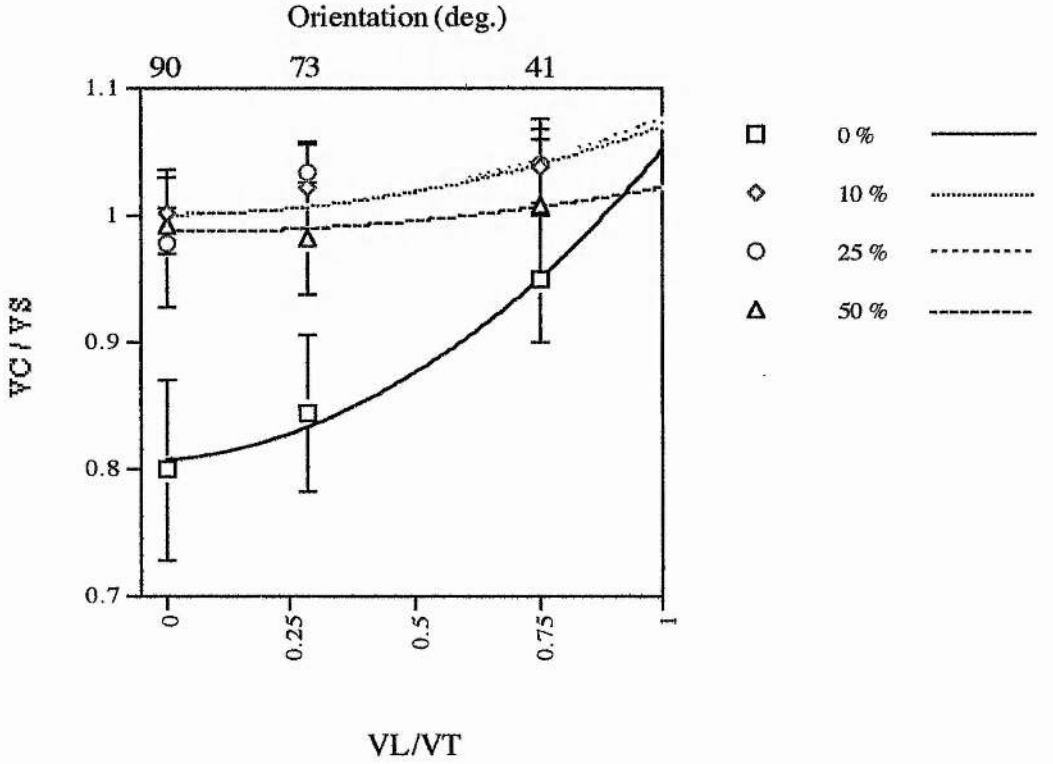

FIGURE 5.5 Relative perceived speed as a function of ratio of local speed to the translation speed with the level of perturbation of line position, expressed as a percentage, as a parameter. Bars through the symbols show ± 1 SE. The speed of the standard was 2 deg./sec. The legend depicts the level of perturbation in each instance, expressed as a percentage of the whole line length. Stimuli are described in detail in methods. Each data point is the average of five observations and five observers (n=5). As in previous chapters, the results are presented in the same manner as Castet *et al.* (1993). (V_C/V_S) is the ratio of the comparison speed to the standard speed. V_L/V_T, is the ratio of the speed of V_L (representing the orthogonal component) and V_T (representing the terminator speed).

The weighted-average model predicted that the parameter for the terminators V_T (β) should be lower when the line is subject to perturbation and so a greater bias towards the orthogonal components should be expected. Table 5.1 shows that the reverse occurred with increased weights for β under perturbation conditions. The original weight for β (shown in italics) was greater than one and so it was recalculated with constraints $0 < \beta < 1$ (as specified in the model of Castet *et al.*, 1993).

PERTURBATION (%)	WEIGHT α	β
0	0.240	0.809
10	0.069	1.000
25	0.076	1.000
50	0.035	0.986
10	*0.051*	*1.009*

TABLE 5.1. Weights attached to V_L and V_T as derived from the data according to Castet *et al.*'s (1993) model (n=5). (Figures rounded to three decimal places.)

Random perturbation of line position during horizontal translation.

Experiment 9(a)

Two subjects were used for an experiment to investigate the effects of random perturbation of line *position*. Two angles of inclination were used for the standard stimulus namely 72.54 and 90 degrees.

The results are shown below in Fig. 5.6. The graph shows the average data from two observers. At 0% there is a significant bias in perceived speed but it can be seen that a variation of 10% is sufficient to abolish this misperception. The veridical perception of speed for lines at both inclinations continues up to perturbation levels of 75 %.

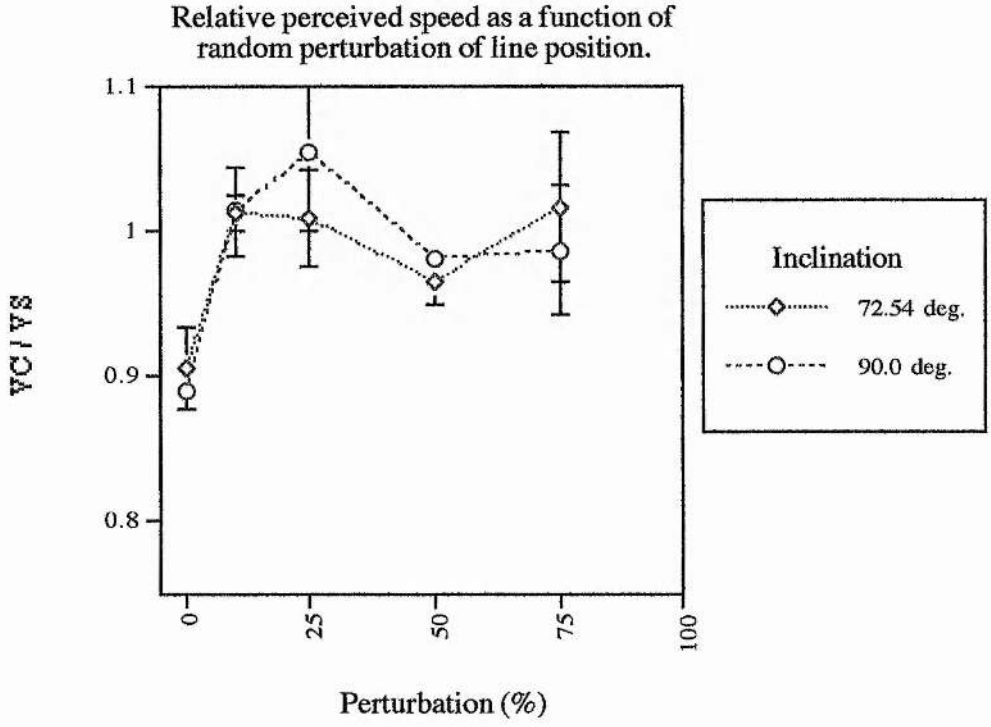

FIGURE. 5.6 Relative perceived speed as a function of the level of perturbation of line position expressed as a percentage. Bars through the symbols show ± 1 SE. The speed of the standard was 2 deg./sec. Legend depicts the angle of inclination in each instance. Stimuli are described in detail in methods. Each data point is the average of five observations and two observers (n=2).

Experiment 9(b)

To investigate the effect of random perturbation of line position in more detail a range of perturbations (0, 10, 25 and 50 %) and a range of angles of inclination (41, 73 and 90 degrees) was used. The author along with two experienced psychophysical observers and two relative novice observers participated in the experiment. Apart from

the author, all subjects were naive to the purpose of the experiment. The data were qualitatively similar for each subject and so only the average data are presented here.

Figure 5.7 shows the data for each level of perturbation of position, from 0 - 50 %. The characteristic pattern of data from experiment eight is repeated here. Perturbation of 0 % gives relative perceived speed variation from around 0.97 at 41 degrees of inclination (V_L/V_T = 0.75) down to 0.86 for horizontal lines. All other levels of perturbation yield an almost flat distribution of data (around 1) across orientations.

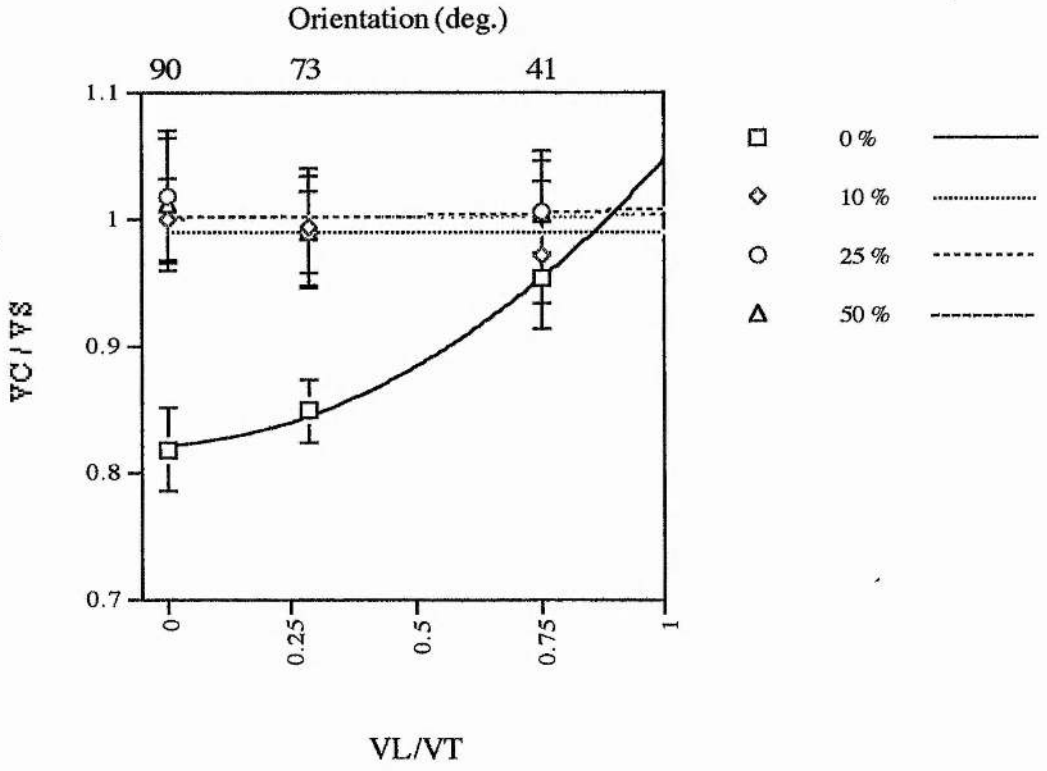

FIGURE 5.7 Relative perceived speed as a function of ratio of local speed to the translation speed with the level of perturbation of line position, expressed as a percentage, as a parameter. The data are presented in the same format as in experiment eight above, (n=5).

The weighted average model predicts that the weight for the terminators V_T (β) should be lower when the line position is subject to perturbation and so a greater bias towards the orthogonal components should be expected. Table 5.2 shows that, as in experiment eight, the reverse occurred; weights for β increased under perturbation conditions. The unconstrained weights derived from the model are shown in italics; at 10% perturbation the α weight was negative, and at 25 and 50 % perturbation the β weight was greater than one.

PERTURBATION (%)	WEIGHT α	β
0	0.179	0.864
10	4.708 E-10	0.988
25	0.008	1.000
50	0.007	1.000
10	*-0.048*	*0.998*
25	*-6E-05*	*1.004*
50	*0.001*	*1.001*

TABLE 5.2. Weights attached to V_L and V_T as derived from the data according to Castet *et al.'s* (1993) model (n=5). (Figures rounded to 3 decimal places.)

Framerate

Pilot experiments varied the duration of the interval between changes in *length* or *position* of the line from 8 msec up to 32 msec. These changes had no significant or systematic effect on the results reported above.

DISCUSSION

Summary

When the length or position of tilted lines in horizontal translation is varied, their perceived speed is *not* biased towards the speed of orthogonal components.

Effect of orientation

Perceived speed remained constant at the veridical value regardless of the angle between the translation signal V_T and the component signal V_L.

Effect of stimulus manipulations

In experiment 8, even a 10% variation of line length was sufficient to abolish the bias in perceived speed. Similarly experiment 9 has shown that a 10% variation of line position was sufficient to abolish the misperception of speed.

Applicability of the weighted averaging model of motion perception

It has been shown that the equation of Castet *et al.* (1993) provides a close fit to the data in both experiments. However the usual pattern of results expected from the weighted average hypothesis was not found. The model predicts that reduced veridical velocity signals from the terminators should result in a reduced weighting for β in the

weighted average calculation. In reality the reverse was observed with β approaching one.

Proposals for future research.

A further question is the precise role of terminators and local signals in determining perceived speed under a weighted-average rule. To test this the perceived speed of a standard line under perturbation conditions could be compared with a comparison line of fixed length. Since both stimuli would lie on the same angle of inclination, the difference between the two stimuli would be the motion of the terminators. The weighted average hypothesis predicts that the interval with perturbations of line length (or position) would be perceived to travel more slowly because its two terminators would not carry the veridical velocity signals of the non-perturbed line.

The properties of terminators and terminator uncertainty in perceived speed could be investigated in more detail. It would be possible to use three translating points in a similar fashion to the co-linear dot condition in chapter three. Instead of having four intermediate co-linear dots one middle dot could be moved sinusoidally about the centre line of the two peripheral dots. This is shown below in Fig. 5.8, the middle dot of the trio that form the stimulus oscillates horizontally relative to the translation of the two exterior dots. In this way the veridical motion of the ends of the line is preserved and the average horizontal speed of the stimulus will oscillate with the speed of the middle dot but at one third of its amplitude of oscillations.

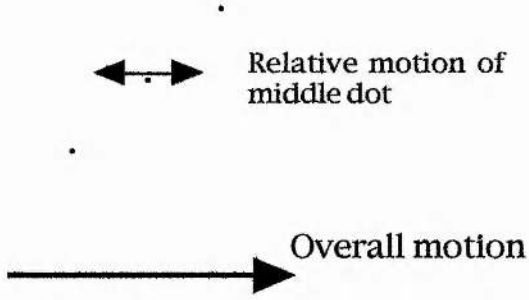

FIGURE 5.8 Proposal for variation of experiment one above. The middle dot of the trio that form the stimulus is moved forward and backwards horizontally relative to the translation of the two dots. In this way the veridical motion of the ends of the lines is preserved, the average motion of the stimulus is preserved but the motion of the "local" components is varied.

CONCLUSION

Variation of the spatial position of the terminators was sufficient to abolish the bias in perceived speed of horizontally drifting tilted lines. Shiffrar (personal communication)

suggests that, at the neuronal level, when line terminators are subject to perturbation of position, the "end stopped" cells in V2 are no longer receiving a meaningful signal. This could render MT unable to derive the usual velocity vector responsible for the bias in perceived speed. The problem with this interpretation is: without a veridical velocity vector from the terminators, the bias in perceived speed should increase not decrease.

The alternative combinatorial method is that a winner-take-all rule is applied rather than a weighted average rule (Salzman and Newsome, 1994). In this case it would still follow that a loss of veridical velocity vectors should result in an increase in bias in perceived speed. It could be argued that the bias should remain constant, but in no case should it be reduced.
In conclusion, variation of the spatial position of the terminators was sufficient to abolish the bias in perceived speed of horizontally drifting inclined lines (Castet *et al.*, 1993; Scott-Brown, & Heeley, 1995). Neither a "weighted-average" rule nor a "winner-take-all" rule is sufficient to account for the data.

A simulation of each type of combinatorial rule might reveal which method is used. Do either of the models reproduce the misperception observed experimentally and in addition do they abolish bias when perturbation is applied?
As the length of the contour changes the reliability of the terminator motion is reduced, and so it is possible that the visual system may reject local image interpretations based on terminator motion. A global interpretation may prove more effective. In chapter two, methods of investigating the relative importance of local and global properties of the stimulus were discussed.

Visual motion perception: the effect of terminators on perceived speed of inclined line segments in horizontal translation.

CHAPTER 6

Interim Discussion

SUMMARY

Observers have difficulty accurately perceiving the speed of an inclined line in horizontal translation, as originally reported by Castet *et al.* (1993). It was found that this misperception was not restricted to single continuous lines but was also evident in the perception of tilted co-linear segments. Further experiments measured the limits of this phenomenon by manipulating the number and size of the segments and the position of the terminators in the stimulus.

The data clearly show that the perceived velocity of line segments is not obtained by a simple averaging process of local velocity signals and veridical velocity signals of the line terminators as suggested by Castet et al. (1993).

Texture Boundaries and Feature Points

The mechanism by which Wilson *et al.* (1992) suggest that the visual system encodes the translation of a moving stimulus includes a texture boundary signal, obtained after squaring the signal and passing it through a filter (see review in Chapter One). Alternatively, the motion of feature points or "nodes" of stimuli such as plaids could provide the relevant translation signal (Castet *et al.*, 1993). Such feature points elicit motion consistent with known direction perception errors (Yo and Wilson, 1992; Castet *et al.* 1993). In addition this explanation is applicable across a wide range of psychophysical stimuli such as random dot stimuli, moving contours and plaids.

To test Wilson *et al's* (1992) model in more detail, the second order channel of the model can be examined using the stimuli shown in Fig. 6.1 below. If a speed bias was found for illusory contours (A), then that would suggest that the non-Fourier pathway also permitted a bias in perceived speed. This result would be consistent with the proposal that a cosine-weighted model combines Fourier and non-Fourier signals in a style analogous to the known behaviour of area MT. A further and related question would be whether the manipulation of the spatial arrangement of the components could be sufficient to affect the perceived speed of the stimulus. The arrangements shown in Fig. 6.1 (B, C & D) could distinguish whether the local or global orientation is the source of the misperception.

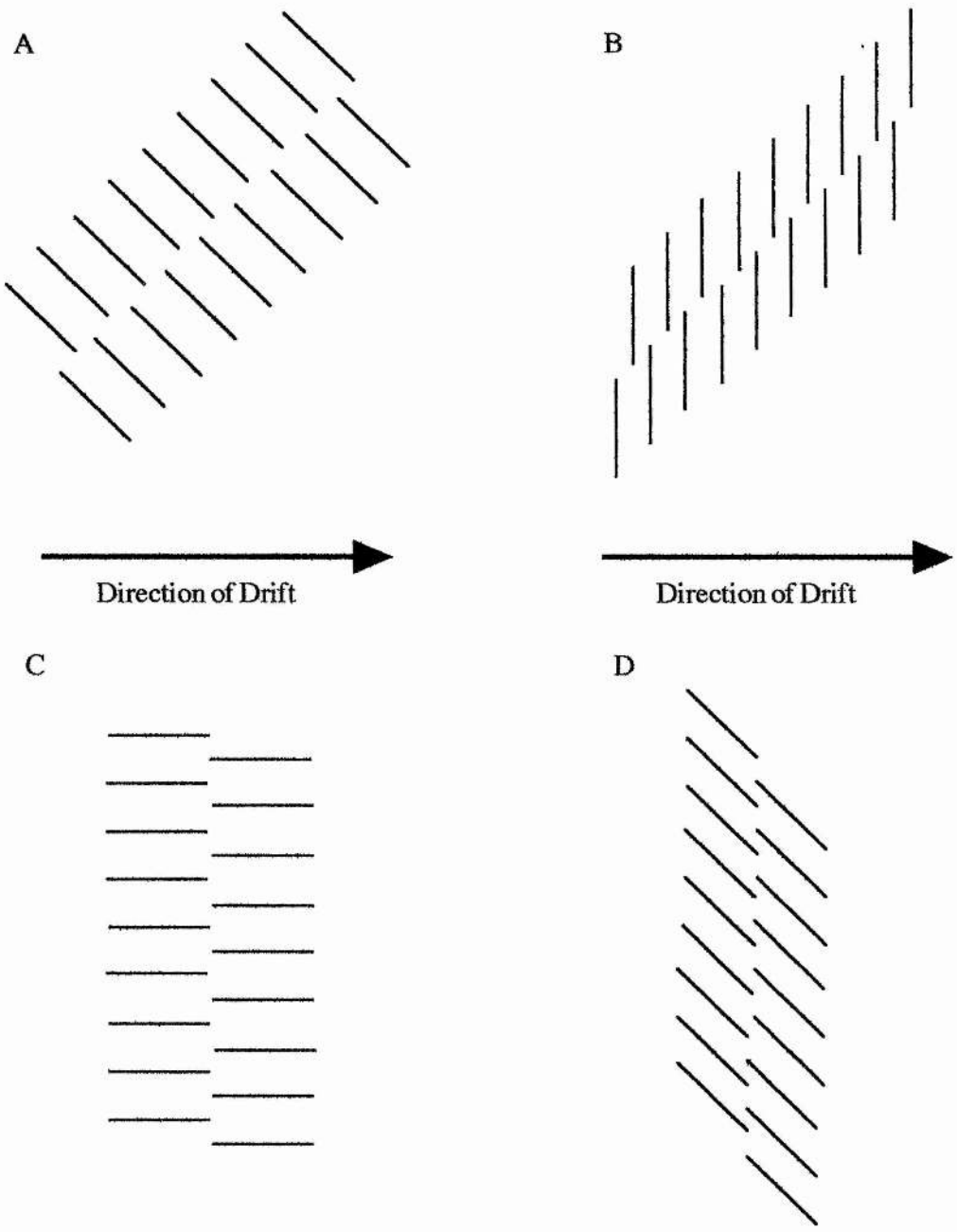

FIGURE 6.1 Stimulus conditions for a comparison of speed misperception for illusory contours and constituent line segments. A shows an oblique illusory contour with oblique constituent lines, whilst B shows an oblique illusory contour with vertical constituent lines. The vertical illusory contours in C and D compare the effect of local component orientation on speed perception whilst global orientation is held constant.

The psychophysical data from these chapters could be used in the design of neural networks to define the limits of performance. From such neural network studies, it is

possible to simulate the psychophysical data and then generate very precise, testable neurophysiological hypotheses. For example, in the field of learned birdsong, it is possible to build neural networks that can learn to sing in the same dialects as the mother (trainer). By observing the changes in time of the units of the network it is then possible to construct very specific hypotheses about the time varying properties of neurotransmitters (Sejnowski, personal communication).

Castet *et al.* (1993) tentatively propose that an average of the signals from end-stop cells and contour sensitive cells provides the motion signal in the visual system. The present results suggest that processing of a secondary or "higher" nature occurs before the final generation of a signal for velocity. There are two candidates for this process: one is further low level processing and the other is a higher-level process, where a speed judgement is made on a psychologically defined *object*. An experiment to test this proposition by disrupting the higher-level stimulus property of co-linearity using stereoscopic depth cues was discussed in chapter 2. Further possible investigations are outlined in chapter 9.

Attention has been shown to affect the perception of "short-range" motion such as that seen in random-dot displays. Sensitivity to motion was higher for motion in the expected as opposed to the unexpected direction (Sekuler & Ball, 1977). It would seem from the above that high level vision plays an active part in motion perception. This makes intuitive sense because it is likely that an observer would need image segmentation cues and recognition of parts before he/she can work out the speed of an object relative to its background.

Feature integration theory

The results may be interpreted in a high-level or psychological framework. The "feature integration" theory of attention (Treisman and Gelade, 1980) suggests that it is possible to sense higher order properties of stimuli such as symmetry and homogeneity. It is proposed that both focal attention (attention directed serially across space allowing features in the same "spotlight" to be integrated) and top-down processing (when brief exposure or overloading prevents focused attention) mediate our awareness of unitary objects. In most cases both operate transparently, however, one may be shown to operate independently of the other. Context allows for the prediction of familiar objects, then, matching of disjunctive features to the features in the display allows for verification. This obviates the need for checking the actual conjunctions between the features. This method is liable to error in the absence of context but within the highly context bound situations it is a good system. Tasks are performed less efficiently on occasions where there is low predictability or on tasks requiring specificity of conjunctions (eg. looking for a child in a school photograph). Focused attention must

be directed serially to each stimulus in the display because conjunctions of more than one separable feature are needed to characterise or distinguish the possible objects (child) presented. However, tasks such as psychophysical experiments and proof-reading of manuscripts rely heavily on focused attention.

Physiological and behavioural evidence suggests that we analyse things on functionally separable dimensions such as colour and orientation (Treisman and Gelade, 1980). It is possible that some relational aspects of a stimulus may be registered as basic features. Co-linearity, for example, may be one such feature. If so then this may go some way in explaining the results reported in the previous chapters.

GENERAL DISCUSSION

Although the Castet *et al.* (1993) model explains the bias in perceived speed for lines of increasing angles of inclination, increasing length and reduced contrast; it does not cope with co-linear segment stimuli. It is more parsimonious to have a mechanism that can account for both types of stimuli rather than have two mechanisms, exhibiting the same biases, for visual stimuli that are so similar.

It is possible that the β (terminator) parameter from the weighted-average model needs to be modified to allow different types of stimuli. Alternatively, the line may be subject to higher level recognition prior to the speed judgement. If this were the case, a further question is how far back down the system the signal could travel. Neurophysiological experiments may reveal the paths of such feedback connections.

The direction of drifting plaids I: physical rotation of patterns

CHAPTER 7

Direction discrimination thresholds for two-dimensional patterns drifting on the principal and oblique axes.

INTRODUCTION

Feature based processing versus two-stage processing of 2-D patterns.

Research by Stone, Watson and Mulligan (1990) and Stone and Thompson (1992) supports the hypothesis that the axis of drift is computed after initial component decomposition. By manipulating the apparent, as opposed to the true, velocity of the component gratings, it was shown that the axis of drift changed in ways compatible with the alteration of component speed within a modified IOC framework. The apparent speed was modified by changing the stimulus contrast - gratings of lower contrast appeared to move more slowly. Derrington and Suero (1991) also conclude the presence of a two-stage process on the basis of the finding that drift direction of a 2-D pattern is biased away from the axis predicted by a simple intersection of constraints (IOC) rule and in favour of an un-adapted grating. Adaptation in this experiment was conducted using a motion after effect.

van den Berg and van de Grind (1993) provide evidence in support of direct, single stage processing of the motion of the intersections of a plaid, based on local contrast. Contrast variations of the intersections induced by the addition of moving textures to the bars of one grating of a plaid were shown to disrupt the characteristic rigid appearance of symmetrical plaids. Disruption of rigidity involves the loss of perceptual coherence of a 2-D drifting object.

Plaids:

Ferrera and Wilson (1990) and Yo and Wilson (1992) have used comparisons of different classes of plaids to provide evidence against a strict interpretation of the IOC model.

There are three classes of coherent** plaid stimuli that may be generated with two gratings. The first picture in Fig. 7.1 is of a sine-wave grating. Two gratings such as these at different orientations may be superimposed to form a plaid pattern.

The first plaid pattern is called a "type I symmetrical plaid" (IS) because the vectors of the two component gratings are in antiomorphic form around the resultant perceived

---

** "Transparent" plaids are discussed in chapter one.

vector. This is shown graphically in the accompanying vector-space diagram. The two vectors are of equal length and are inclined at equal and opposite angles to the resultant vector - hence the term "symmetrical".

The "type I asymmetrical plaid" (IA) has two components arranged around the resultant; however the right hand component has a lower drift rate, as indicated by the shorter vector.

The "type II plaid" (II) pattern has component vectors of the same magnitude as the type IA plaid except that the longer vector is mirror reversed. Thus both components lie on one side of the resultant. The use of partner type IA and type II plaids allows the experimenter to match the speed of components across plaid types. Type IS stimuli may be generated with similar component vector lengths also. As the relative orientation of the components changes, the gratings overlap to differing degrees; in this way the length of the "blobs" increases as the bars overlap for more of their length.

FIGURE 7.1. (Overleaf) IOC diagrams in velocity-space for three types of plaid, type I symmetric (IS), type I asymmetric (IA) and type II. The thick arrows represent the perceived (resultant) velocity vector of the plaids. The thin arrows indicate the vectors for the component gratings of the plaids. Notice that so long as the vectors of the components lie on the circumference of the circle the angle between the component vector and the constraint line remains constant at 90 degrees; this allows the experimenter to calculate different component vectors from one resultant speed. The angle of inclination from resultant vector direction of component vectors (in degrees) is as follows: $\alpha = 48.2°$ $\beta = 70.5°$. Pictures of each type of plaid accompany the vector space diagrams. Type II patterns exhibit a "blob-like" appearance, indeed Ferrera and Wilson (1987) originally termed type II plaids "blobs".

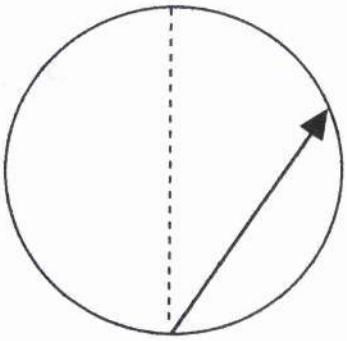

Single Grating:

Drift is perpendicular to the bars.

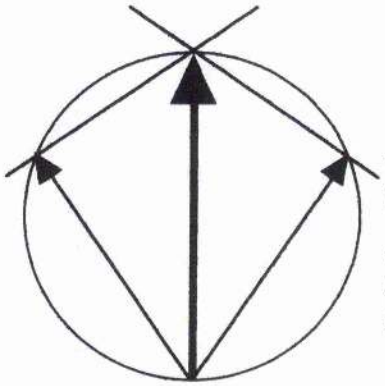

Type I Symmetrical Plaid:

One left and one right component combine to give vertical drift.

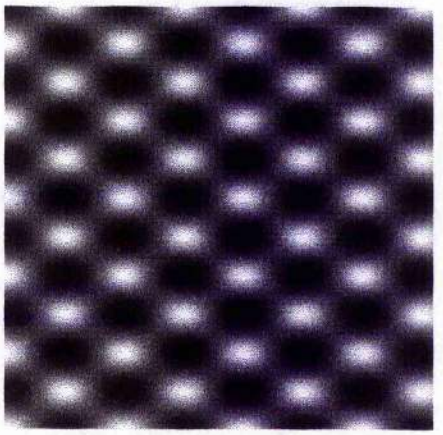

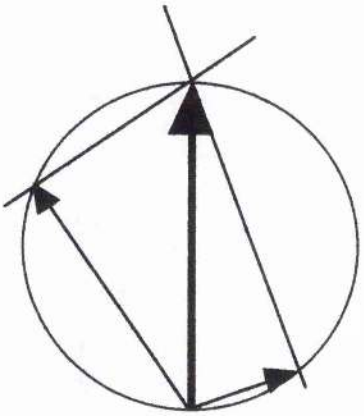

Type I Asymmetrical Plaid:

One left and one slower right component combine to give vertical drift.

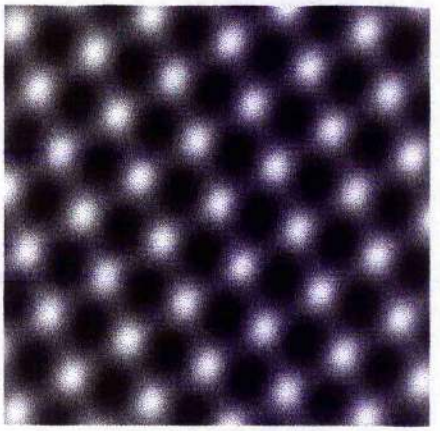

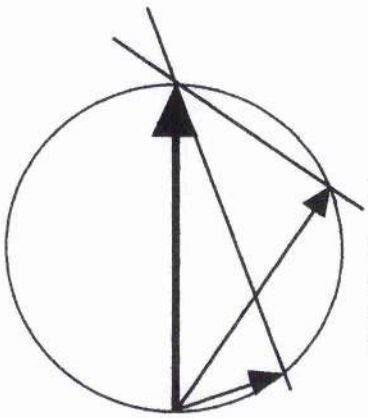

Type II Plaid:

Two right components, one fast and one slow combine to give vertical drift.

Direction discrimination thresholds have been found to be much higher for type II plaids (6.5°) compared with type I plaids (1°). Type II plaid patterns also showed a perceived bias towards the direction of the components (7.5°) [Ferrera and Wilson, 1990]. The proposed model used inhibition and perceptual broadening* to account for type II thresholds and biases. In addition extra parameters were fitted to predict the data. No independent evidence for the plausibility of these mechanisms was supplied. The model depicted in the paper features two alternative systems for 2-D motion processing, one for type I plaids and one for type II. As stated in chapter one, the most parsimonious model is one based on a single stage of processing eg. a feature based model such as that proposed by Gorea and Lorenceau (1991). Two-stage models must justify the use of two channels instead of one. In the Ferrera and Wilson (1990) model, the two systems operate in parallel. A more elaborate version by Wilson, Ferrera and Yo (1992) was discussed in chapter one.

Yo and Wilson (1992) found a strong bias of perceived motion of type II plaids in favour of the vector sum direction at short presentation durations. No such bias was found for type I plaids. The stimulus parameters of the duration experiment are important. Even the fastest resultant velocity of 16 degrees per second (dps) allows its pattern to traverse less than 1 degree at 60 milliseconds (msec). Case 2a (page 139, table 1) involves the slow component traversing approximately three foveal cones. The problem in comparing type I and type II at such low durations is that type II plaids are always going to have one component that is going much more slowly. With durations as low as this there is a possibility of low velocity sampling problems. At these very small velocities the grating only travels a quarter of a cycle. The nyquist limit is 2 samples per cycle so this means that the system will not be able to generate a reliable speed estimate at such short durations.

The Wilson et al. (1992) data do not clearly reveal what motion detection thresholds are like at very low stimulus durations - the only information available is the level of bias. A direction anisotropy was found for type II plaids moving away from the fovea. Biases were smeared much more broadly for oblique directions. Peripheral motion was analysed with a series of pairwise comparisons using one tailed t-tests. This runs the

---

* The relative angle between the directions of type II plaid components is relatively small. It is suggested that there may be some "cross-talk" between the units responding to the motion of the components. This would be because the units would be tuned to motion in similar directions. If this were the case then it would be reasonable to suppose that there was inhibition between such closely tuned units. Inhibition would cause the resultant signals to appear wider apart, if the combination rule is an average of the response of an array of units. Under IOC conditions, a broadening of the relative angle of the components would result in a direction bias consistent with psychophysical data for type II plaids (Ferrera and Wilson 1990).

risk of increasing the family-wise type I error to such an extent that the null hypothesis may be rejected incorrectly (Keppel, Sauffley & Tokunaga, 1992). The tests were performed in the absence of a main effect over subjects, but Yo and Wilson (1992) have then tried to generalise the combination of the positive results back to all the subjects. To make such comparisons in the absence of a main effect, the comparisons must be planned comparisons. The authors did not explicitly state that the comparisons performed were planned in advance of the experiments. The results for some of the subjects did mimic the oblique effect observed in the fovea.

Direction discrimination for type II plaids drifting on the principal and oblique axes.

The present study investigated direction discrimination thresholds for type II plaids in the fovea since this was not addressed in the Yo and Wilson (1992) study. Thresholds were recorded for plaids drifting vertically, horizontally and on the two oblique axes.

The experiment also set out to explore the meridional variation in direction discrimination thresholds for type IA and type IS plaids. The experiment exploited a useful facet of the plaids, namely their reversibility. Fig. 7.2 shows how, by mirror reversing the component vectors of IA and II plaids, it is possible to equalise the effect of different component directions across plaid types. The third row of the figure shows how the components of IS plaids can be arranged to copy either the long or the short component of the asymmetric plaid constructions.

Heeley and Buchanan-Smith (1992) report a pronounced oblique effect for the direction discrimination of moving type IS plaids. Thresholds were elevated when the perceived axis of drift was oblique rather than when the underlying components lay on the oblique axes. Performance for static plaids was reversed: with subjects showing raised thresholds for plaids with components oriented on the oblique axes as opposed to the principal axes. This implies that the perceived direction of drift of plaids is not dependent on the orientation of the underlying components. If it were then the oblique effect should be concentrated on the orientation of the components, rather than the overall orientation of the pattern direction.

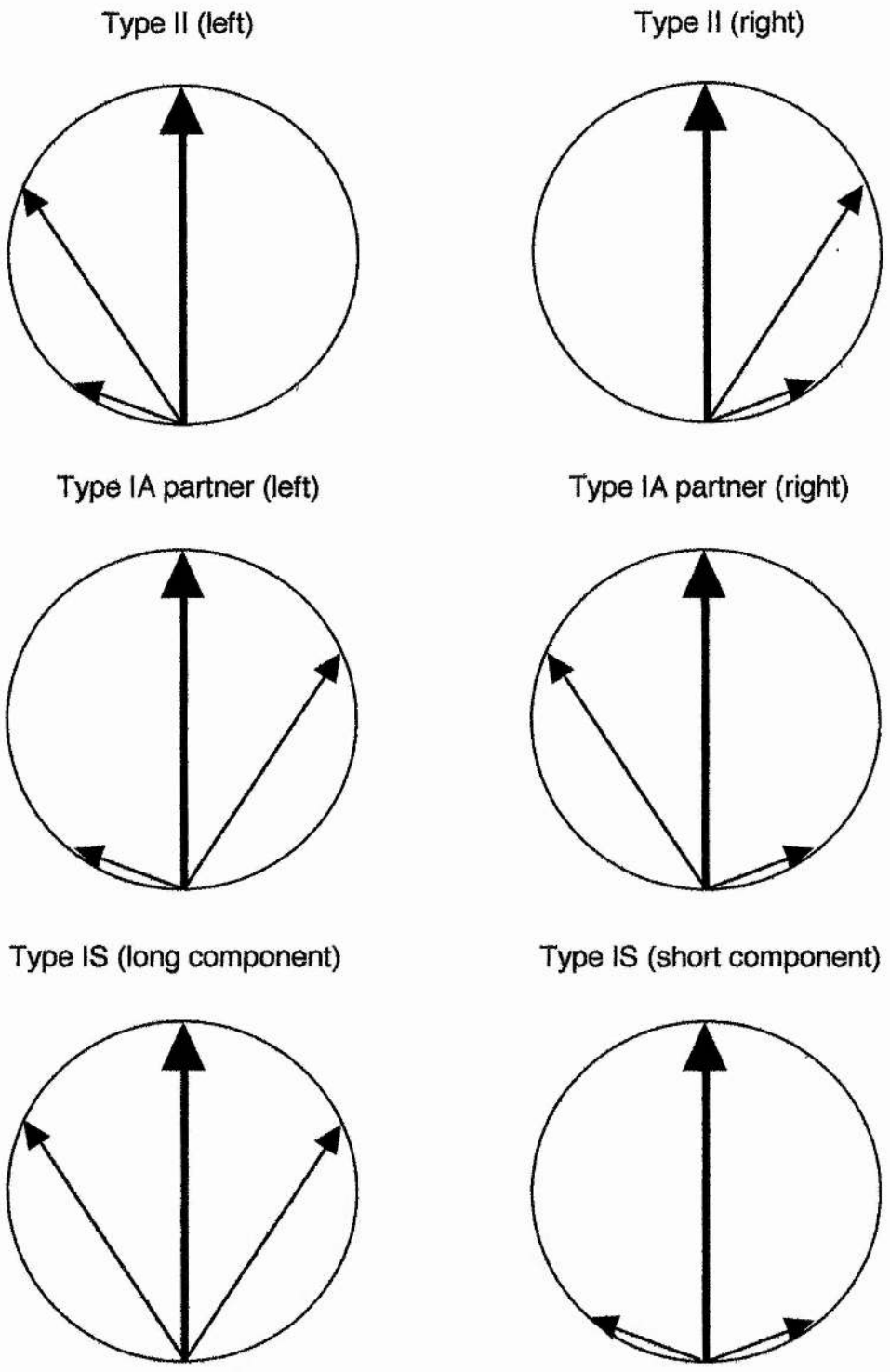

FIGURE 7.2. Type II plaids with "partner" IA plaids in velocity space. (Vertical vectors represent resultants.) Both the component vectors are the same magnitude; the only difference is that the orientation of the long component is mirror reversed. Also

shown are type IS plaids constructed from the long components (left hand plaid) and short components (right hand plaid).

The reason for using the three types of plaid is that the IOC rule predicts that the direction discrimination thresholds for type IA and type II plaids should be identical. The speed and direction of the two component vectors is matched across plaid type in this experiment.

The choice of plaids as stimuli is likely to yield results that are generalisable to other types of stimuli. Orientation discrimination thresholds for random dot kinematograms are of a similar order of magnitude to orientation discrimination thresholds for sine-wave gratings (Regan, 1989 and Heeley & Timney, 1988 respectively).

METHODS: EXPERIMENT 10

The experiment measured direction discrimination thresholds for *physical* rotation of drifting type II plaids, type I asymmetric (partner) plaids and type I symmetric plaids. Thresholds were estimated on four axes of drift: Vertical, Horizontal, Oblique 45 degrees and Oblique 135 degrees.

Apparatus and Stimuli

Gratings were generated by a "Picasso" image synthesiser and then displayed using a Tektronics 606A Monitor. The image synthesiser was linked up to a computer that could control the contrast, spatial frequency and orientation of the plaids' components independently. Prior to these experiments the luminance resolution of the apparatus was calibrated (Heeley & Buchanan-Smith, 1990; 1992; 1994). Stimuli could be presented with an orientation accuracy of 30 arc seconds. For completeness the full details of the calibration procedure are included in Appendix 7.A. Plaids were generated by interleaving two component gratings at a rate of 200 Hz; this yields a plaid percept. The progress of the experiment was controlled by the computer which also recorded the responses of the subject. The temporal envelope of contrast for the stimulus presentation interval was defined by a Gaussian with a spread coefficient of 250 msec truncated at +/- 750 msec. Each interval was preceded by a warning tone.

Procedure[*]

Estimates of direction discrimination threshold for stimulus drift direction were obtained using a modified method of constant stimulus differences, combined with a two-interval temporal forced choice. Pilot studies were used to determine the width of a set of six directions of drift, symmetrically arranged around a standard direction, to cover the range from the 5% to 95% frequency of seeing points. Of the two intervals in

[*] This section after Heeley and Buchanan-Smith (1990, 1992 & 1994).

any trial, one contained the standard stimulus and the other contained the test. The order of these was randomly varied. The "test" was selected randomly from the set of five possible tests. In each trial the observers' task was to indicate using the response box whether the second interval was drifting to the left or to the right of the first one. Each stimulus interval was preceded by a beep and the experiment was self paced.

The six possible pairings of test and standard were each repeated in random order, fifty times making a total of 300 observations for each condition. The order of presentation of the different types of stimuli was fully randomised for each subject. The data for each condition were collected in two 150 decision blocks on separate days. A cumulative Gaussian curve was fitted to the forced choice responses using the "maximum-likelihood method" described by Finney (1971) based on the method of Probits. This curve is termed a frequency-of-seeing curve. The calculation is based on an iterative process that stops when the slope parameter on a given calculation cycle differs from the value obtained on the previous cycle by less than 0.5%. The reciprocal of the slope of the regression of normalised probability against orientation of the test stimulus provides the threshold of orientation recognition (this is the same as the difference between 50% and 84% frequency-of-seeing points).

To minimise motion adaptation effects the direction of drift of a plaid on a given test axis was randomised. For example on vertical trials the direction of drift could be either upwards or downwards for a given pair of plaids. The drift direction on any particular trial was selected at random. The experimental computer calculated a single signed threshold. The thresholds were then averaged over left and right partners for each inter-element angle. This method prevents any differences in the perceptual properties of the four quadrants of visual space from confounding the data.

It is possible for observers to use stimulus recognition as opposed to orientation discrimination in these types of psychophysical tasks (Heeley & Buchanan-Smith, 1990). Random offset of both test and standard (in the same direction in a given trial) was introduced to prevent such inappropriate mediation of the task. The offset was drawn from a uniform probability density with a width of 5 degrees and was changed between each trial.

Observers

Four observers, two males and two females, aged between 21 and 26 were used. Three observers were naive to the purposes of the experiment; the fourth was the author. All observers were professionally refracted and showed no astigmatism greater than 0.25 dioptres.

Experimental Conditions

Type IA and type II plaids were presented in two ways (as shown in Fig 7.2), with the long component facing left and then right of the resultant. This ensured a balance for each of the asymmetric patterns when viewed. Table 7.1 shows the stimulus parameters of each plaid used in the experiment and Figs 7.3, 7.4 and 7.5 show the respective velocity space constructions. The two fold increase in inter-element-angle (IEA) provides a broad representation of each plaid type and increases the strength of the comparisons between each plaid type.

Plaid	*Spatial Freq.*	*C1*		*C2*		*P*	
		Direction	Speed	Direction	Speed	Direction	Speed
II A	2.5	*48.2*	**3.0**	*70.5*	**1.5**	0.0	**4.5**
II B	2.5	*33.6*	**3.7**	*70.5*	**1.5**	0.0	**4.5**
II C	2.5	*23.5*	**4.1**	*70.5*	**1.5**	0.0	**4.5**
IA A	2.5	*-48.2*	**3.0**	*70.5*	**1.5**	0.0	**4.5**
IA B	2.5	*-33.6*	**3.7**	*70.5*	**1.5**	0.0	**4.5**
IA C	2.5	*-23.5*	**4.1**	*70.5*	**1.5**	0.0	**4.5**
IS A	2.5	*-48.2*	**3.0**	*48.2*	**3.0**	0.0	**4.5**
IS B	2.5	*-33.6*	**3.7**	*33.6*	**3.7**	0.0	**4.5**
IS C	2.5	*-23.5*	**4.1**	*23.5*	**4.1**	0.0	**4.5**
IS D	2.5	*-70.5*	**1.5**	*70.5*	**1.5**	0.0	**4.5**

TABLE 7.1. Speed and direction values for component vectors (C1 & C2 - thin arrows in figures) and resultant vector (indicated by the thick arrows in figures) of components. These figures were calculated from the resultant motion of the symmetrical plaids in Heeley and Buchanan-Smith (1992). The use of these velocities allows comparisons to made with the data from that study. The angles were previously used by Ferrera and Wilson (1990). The units for each parameter were as follows: spatial frequency, (c/deg); direction of motion, (deg); and velocity, (deg/sec).

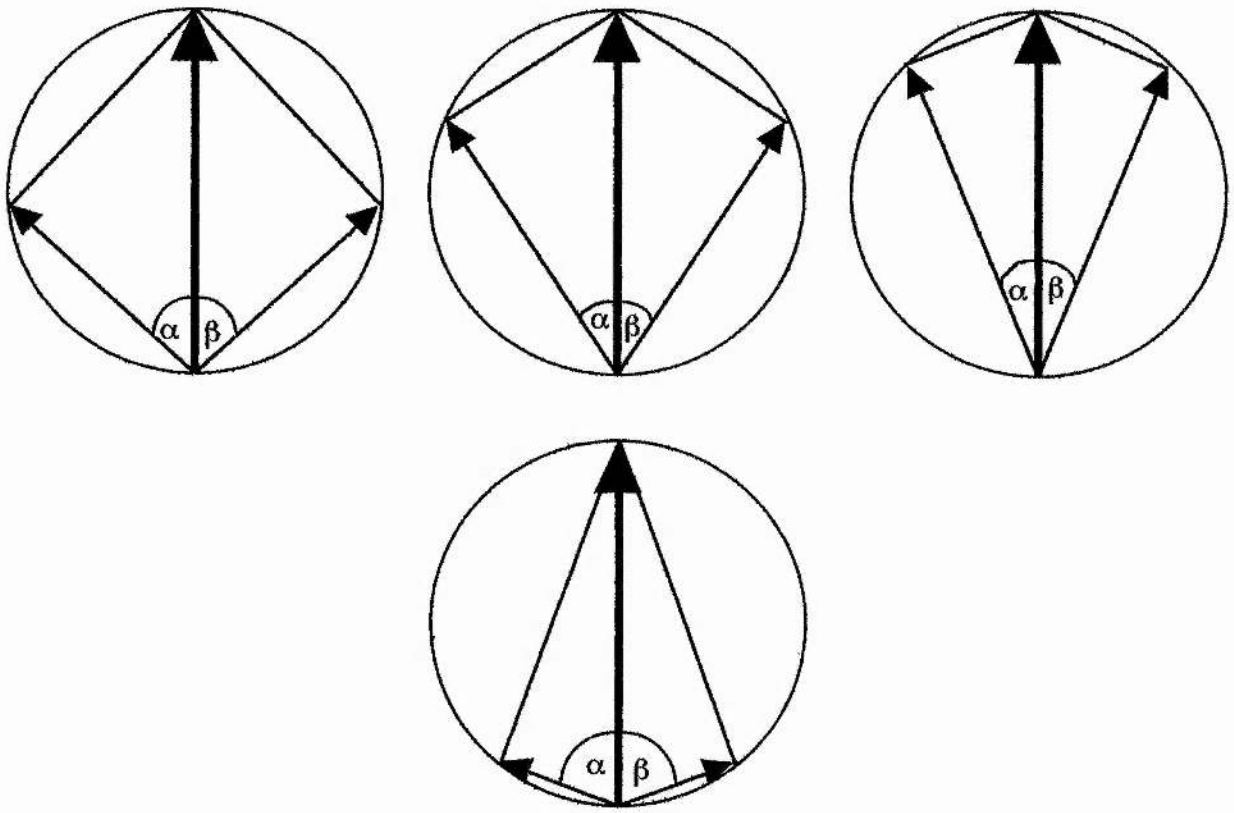

FIGURE 7.3. Velocity space diagrams for type IS plaids. All pictures depict vertical drifts.

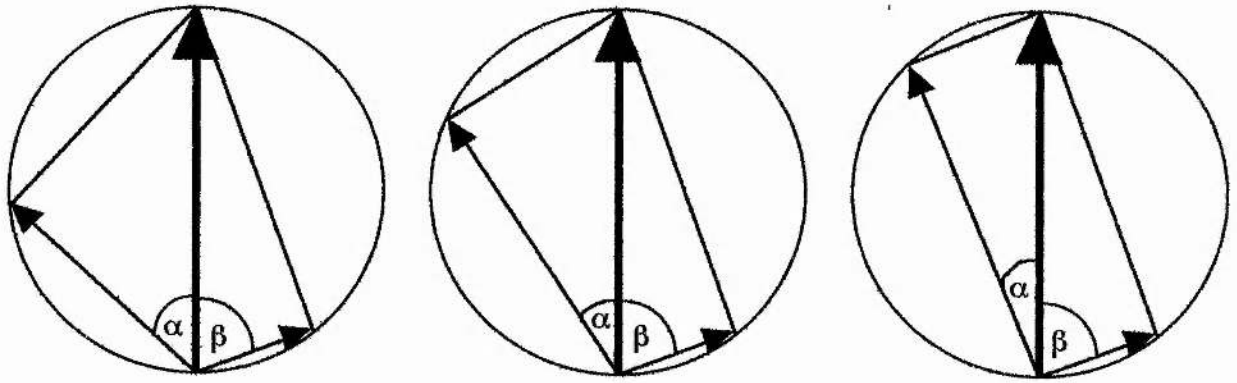

FIGURE 7.4. Velocity space diagrams for type IA plaids.

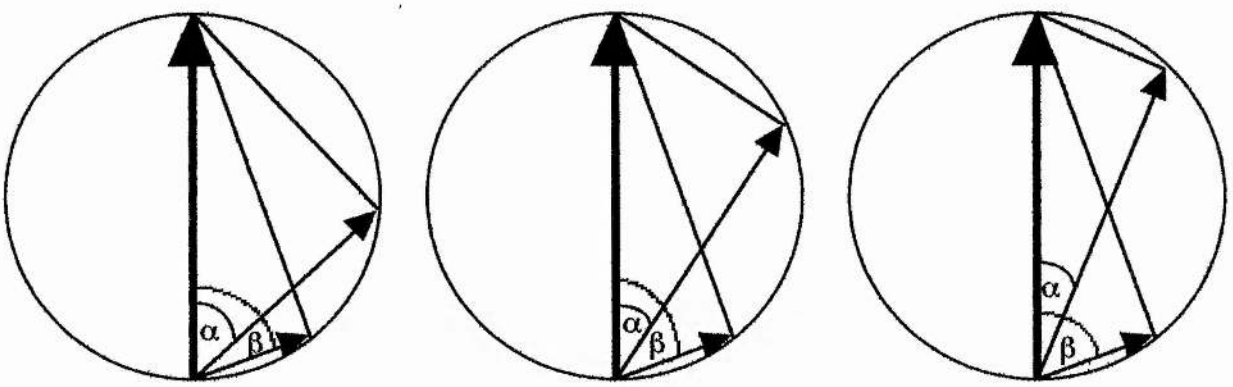

FIGURE 7.5. Velocity space diagrams for type II plaids.

RESULTS

Fig. 7.6 shows direction discrimination thresholds for type IS, IA and II plaids on separate graphs. The different styles of bar represent data from different subjects. The data are averaged over inter-element angles providing a single discrimination threshold for each plaid type. (The data showing thresholds for plaids at each inter-element-angle (IEA) is shown in Appendix 7 B, Fig. B1.) There were four inter-element-angles for type IS plaids and three for type IA and type II plaids as discussed in the methods section.

For type IS plaids averaged over the four inter-element angles, three out of the four subjects show an oblique effect. The effect was centred on the direction of drift rather than the orientation of the individual components. One subject, KSB, has uniformly low thresholds. This may be because he was a very experienced psychophysical observer with good visual acuity. Averaged over the four subjects, type IS thresholds differ by nearly a factor of two between principal and oblique directions of drift. This is the same pattern as Heeley and Buchanan-Smith (1992) found for type IS plaids with orthogonal component gratings.

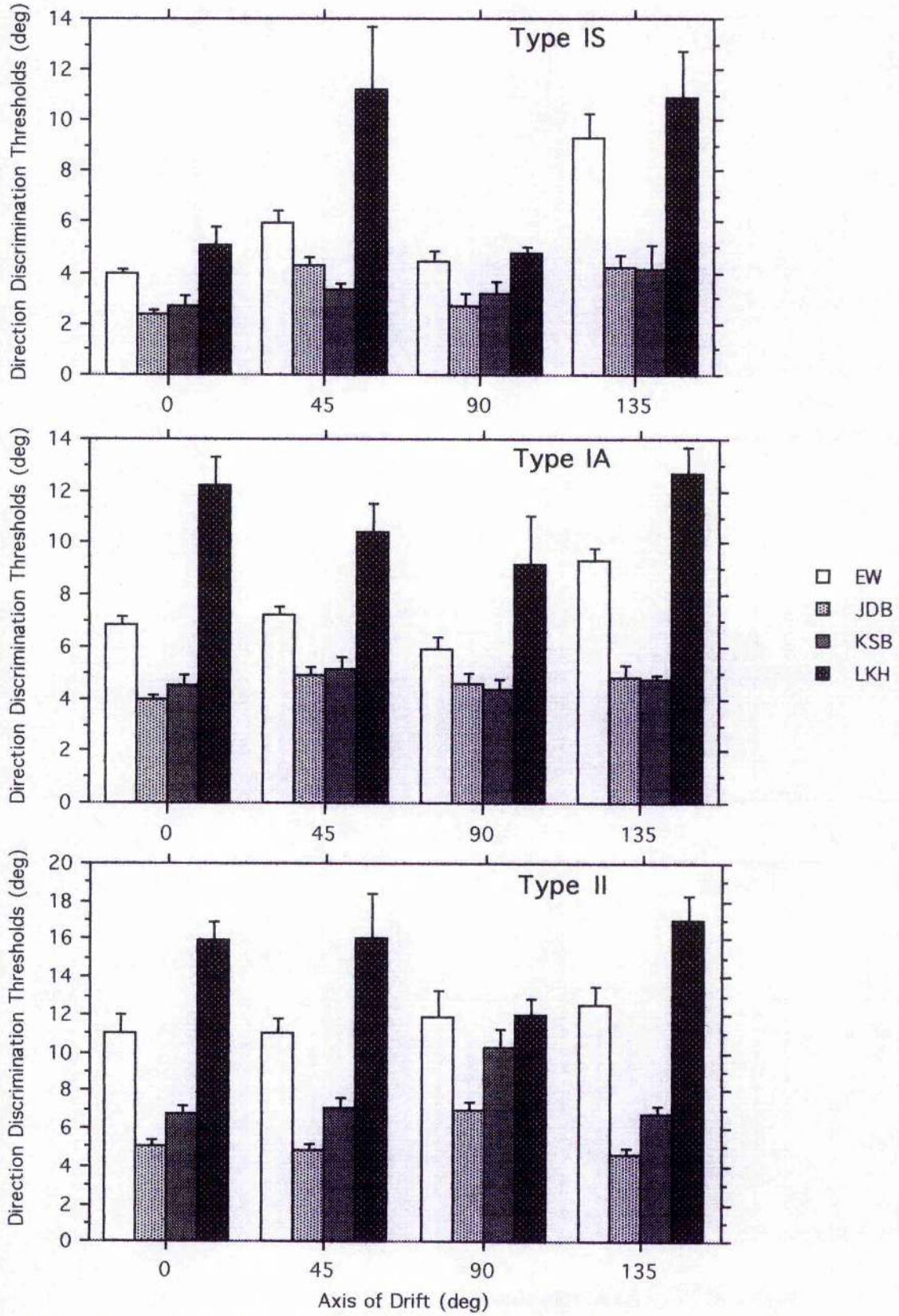

FIGURE 7.6 Direction discrimination thresholds for plaid types IS, IA and II as a function of axis of drift. Different styles of bar indicate threshold for the four observes as indicated in the legend. The thresholds are collapsed across the various inter element angles (IEAs) for each plaid described in the method section. The spatial frequency of the component gratings was 2.5 c/deg.

Type IA plaid direction discrimination thresholds for two subjects, JDB and KSB, follow the pattern of the oblique effect observed for type IS plaids. The other two subjects show horizontal thresholds consistent with an oblique effect but vertical thresholds equal to or in excess of oblique thresholds. The difference between thresholds for principal and oblique axes of drift is 12.9% compared to 44% for type IS plaids. Type II plaid thresholds for direction discrimination differ by only 0.09% between principal and oblique axes. This is shown graphically in Fig. 7.7 below.

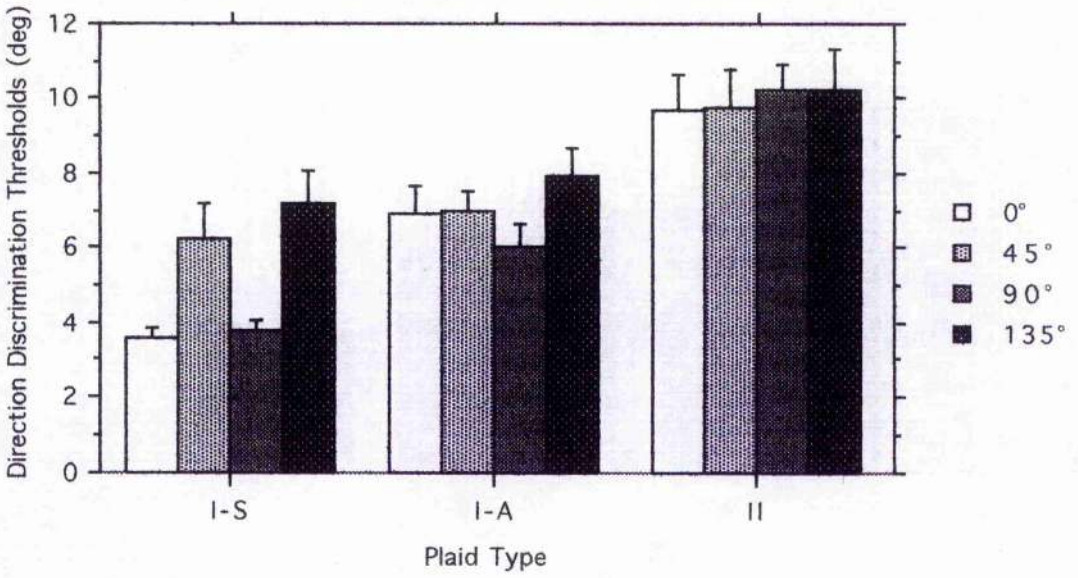

Figure 7.7. Direction discrimination thresholds for plaid types IS, IA and II. The different styles of bar indicate the four axes of drift for the stimuli. Thresholds are averaged over inter-element angle and subjects.

Mean thresholds for plaids drifting on the principal and the oblique axes are shown in Table 7.2.

Plaid Type	*Axis of Drift*	*Mean threshold (deg.)*	*Std. Dev.*	*Std. Error*
IS	Principal	3.668	1.227	.217
IS	Oblique	6.669	3.792	.670
IA	Principal	6.458	3.299	.476
IA	Oblique	7.422	3.211	.464
II	Principal	9.981	3.871	.559
II	Oblique	9.972	5.227	.754

TABLE 7.2. Means, standard deviations and standard errors for direction discrimination thresholds as a function of direction of drift. Data averaged over principal and oblique axes.

DISCUSSION

Summary

From the summary graph in Fig 7.7 (above), it is evident that there is an oblique effect for type I symmetrical plaids, but no obvious effect for type I and type II plaids.

Thresholds for type II plaids were higher than those for type IS and IA plaids for vertical drift directions. In addition thresholds for type II plaids drifting on the oblique axes were of a similar order of magnitude to those drifting on the principal axes. For drift on the principal and the oblique axes, type II thresholds were higher on average than those for type IA and type IS plaids.

Thresholds for type IA plaids drifting vertically were nearly a factor of two higher than thresholds for vertical type IS plaids. This finding is not anticipated by a strict interpretation of the IOC rule. However if the noise associated with the IOC decision arising from individual component uncertainty is taken into account then the data are consistent with an IOC model of integration.

There is a trend in favour of an oblique effect for IA plaids; thresholds are higher on the oblique axes than on the principal axes. Fig 7.7 shows, however, that this is concentrated on the 90 deg (horizontal) drift axis rather than on both of the vertical and horizontal axes. The inclusion of a type IS symmetrical plaid with two short component vectors ensures that the threshold elevation from types IS to type IA and II is not due to a difference in the threshold for rotation of the slow components. Thresholds for the short component symmetrical plaids are of the same order of magnitude as the thresholds for the long component symmetrical plaids (see Appendix 7.B, Fig B1).

Relation to Previous Research

The results replicated the findings of Yo and Wilson (1992): direction discrimination thresholds for type II plaids were elevated to around 6.5°. The oblique effect for type IS plaids follows the pattern of results observed by Heeley and Buchanan-Smith (1992) where thresholds also differed between principal and oblique directions of drift by a factor of nearly two. The oblique effect for plaids with a variety of IEAs confirms that the meridional variation in discrimination thresholds is centred on drift direction irrespective of the orientation of the individual components of the plaid. Heeley and Buchanan-Smith (1992) used plaids with a random variation of the orientation between the two elements and found similar results.

The results are explicable in terms of the uncertainty in the estimation of the speed and direction of each component grating (Ferrera & Wilson, 1990; Nakayama & Silverman, 1988). Fig. 7.8 shows how noise from the uncertainty associated with the speed and direction of the components of a plaid can affect the uncertainty surrounding the final estimate of the resultant velocity. There is an asymmetric region of uncertainty in the type II case with the error skewed in orientation space. This also highlights a factor relevant to induced rotation of type II plaids. A lengthening of the component vector (increase in speed) causes a greater change in the direction of the resultant than does a shortening of the component vector (decrease in speed).

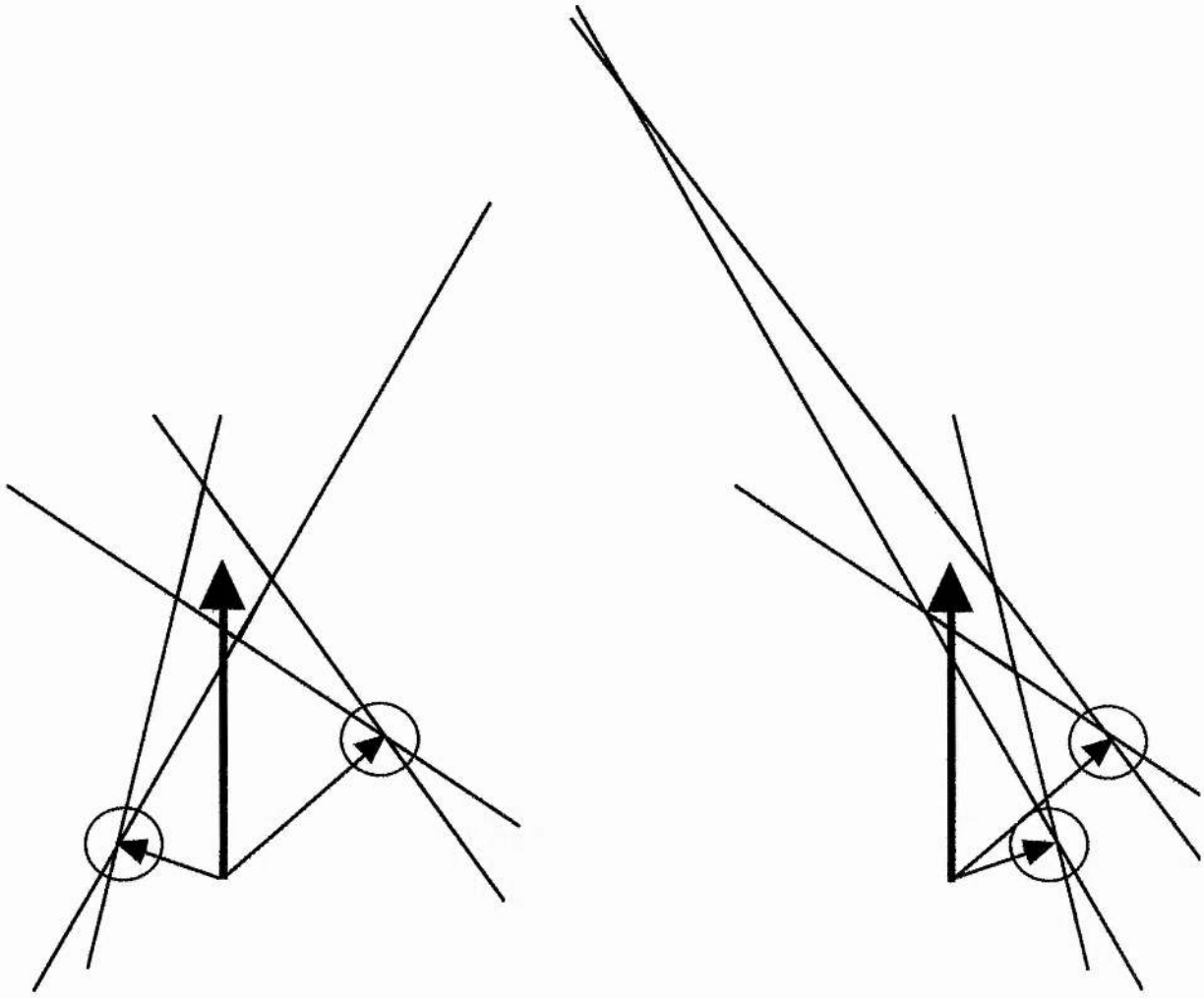

Fig 7.8. Component uncertainty affects the resultant direction of plaids under IOC rules. Thin arrows depict component vectors representing speed and direction of gratings. Surrounding, shaded circles indicate uncertainty associated with each component. Thick arrows show the resultant direction and speed of the plaids under IOC rules while the surrounding shaded areas depict the uncertainty resulting from component uncertainty. Adapted from Ferrera and Wilson (1990).

It is possible that the error associated with direction perception of type II plaids is multi-component. There could be error representing the component vectors, errors in the decision process. In addition, for the reasons discussed by Ferrera and Wilson (1990) one would expect greater error for type II plaids. Summation of variance over all the possible error in the decision process could be enough to swamp the pattern of oblique effect whether it lay on the principal or oblique axes.

Thus the IOC may well predict the results but because of the errors in detecting individual gratings and then combining their signals the judgement may be too noisy.

Alternatively the orientation of the blobs or the illusory contours could be dominating the perception of motion. Since the blobs are oriented on the vertical during the diagonal drift conditions they could account for the performance. Sejnowski (personal communication) notes that the attentional factors influencing plaids (and particularly transparency) are not clear. The role of eye movements in these studies needs to be established. Whether observers are tracking the blobs or are looking at the overall motion could have a critical effect on the perceived speed and direction of the overall pattern.

CONCLUSION

This chapter has cleared up the questions posed by Yo and Wilson (1992). The main experimental question was whether or not there is an oblique effect for the different patterns. Meridional variation in direction discrimination thresholds was observed for type IS plaids, slightly for type IA plaids but not for type II plaids.

The theoretical significance of the data is that it bears directly on the question of whether 2-D pattern perception is mediated by single-stage feature-based processing or by two-stage processing. It was found that direction discrimination thresholds for 2-D patterns (plaids) are *not* limited by the direction discrimination thresholds for their components. A strict IOC predicted identical thresholds for IS, type IA and type II plaids. However the results can still be consistent with the IOC rule if noise due to component uncertainty is taken into account. The presence of noise in the data suggests that the limiting factor in direction perception of 2-D patterns may not be at the level at which components are extracted but is at or beyond the level of pattern analysis [This agrees with the conclusions of Heeley and Buchanan-Smith (1994)].

The present results do not directly suggest the correct model for direction discrimination.

On the basis of the observed perceptual differences between the two types of stimuli, Ferrera and Wilson (1990), Yo and Wilson, (1992) and Wilson, Ferrera and Yo (1992) suggest that the neural circuitry underlying type I and II plaid perception is different. The second, non-Fourier, pathway of the model is proposed as the means by which type II plaids are signalled. This pathway is sensitive to the second order aspects of stimuli (eg. the illusory contours in type II plaids) and its processing is subject to a delay compared to the processing in the first channel. To test this model, Cropper, Badcock and Hayes (1994) measured perceived direction of "second-order" type I and type II plaids. Second order plaids are made up from individual components with non-Fourier energy properties, as opposed to the plaids used in this chapter which are made up of Fourier (first-order) components. The components of the plaids were dynamic random-dot fields subjected to sinusoidal contrast modulation. Since both type IA and type II plaids were defined by second-order components the Wilson, Ferrera and Yo

(1992) model predicted that they should not be subject to the bias in perceived direction at short durations (the bias is suggested to arise from the different processing speeds of the first and second-order channels). The perceived direction of the, "non-Fourier", type II plaids as a function of duration was very similar to the perceived direction of first-order type II plaids. This means that there must be another cause of the bias in perceived speed of first-order type II plaids as well as the cause proposed by Wilson, Ferrera and Yo (1992).

Fleet and Langley (1994)

Fourier analysis of visual stimuli assumes that a signal from a translation, when represented in the frequency domain, has all its non-zero power concentrated on a line through the origin (Adelson & Bergen, 1985). Several types of stimuli are inconsistent with Fourier analysis. These include sinusoidal beats (Derrington & Badcock, 1985); sampled motion (Nishida & Sato, 1992); drift balanced stimuli (Chubb & Sperling (1988) and theta motion (Zanker, 1993). No unified theory of the signalling mechanisms for "non-Fourier" motion in the visual system exists.

Fleet and Langley (1994) argue that non-Fourier stimuli may be characterised in a simple way in the frequency domain. This assertion is in contrast to the claim of Chubb and Sperling (1988, p. 1986) that "certain sorts of apparent motion cannot be directly understood in terms of their power spectra". As stated by Adelson and Bergen (1985) and Watson and Ahumada (1985), Fourier motion stimuli are characterised by the *location* of power in the frequency domain. (The slope of the line of power distribution through the origin determines velocity.) Fleet and Langley (1994) argue that non-Fourier stimuli may be understood in terms of the *orientation* of the local power distribution in the frequency domain. The proposed framework is used to describe non-Fourier motion contained in natural images. A computational basis for measurement of the location and orientation of spectral power also arises from the framework. This involves instantaneous phase and amplitude behaviour in the output of band pass filters. Representation of non-Fourier motion in a diffuse form in Fourier space could account for the elevated thresholds for type II plaids.

At the system level, the visual system seems to be treating the stimulus types differently: it is possible that a higher level feature of the type II stimulus is influencing the perceived direction of the stimulus. (Note that the blobs in type II plaids are not symmetrical.) An obvious candidate for this is the blobs of the type II plaid. The blobs resemble line segments inclined with respect to their direction of drift. Lorenceau, Shiffrar, Wells and Castet (1993) investigated the perceptual effects of the motion of a group of line segments tilted with respect to their direction of motion. The stimuli

behaved in very similar ways to the type II plaids reported here and by Yo and Wilson (1992). A vector average model was proposed as the method of integration of local motion signals. It was shown to model the psychophysical data. This has been discussed in detail in chapters 2 -5.

The direction of drifting plaids II: induced rotation of patterns

CHAPTER 8

Direction discrimination for rotation of drifting plaids induced by a change in speed of the underlying components[*]

INTRODUCTION

Welch (1989) suggests that the speed of each component grating of a coherent plaid is analysed separately and then combined. Speed discrimination thresholds reflected the speed of the constituent gratings of a plaid, as opposed to the speed of the plaid itself. This interpretation supports the assertion that while the only accessible velocity signal is generated by second stage pattern processing, plaid discrimination is limited by component processing. Heeley and Buchanan-Smith (1994) have highlighted an exception to this. By altering the length of the vectors (ie. the speed of a constituent grating), it is possible to cause a plaid to appear to rotate. The speed change in a component required to cause a perceived rotation was compared with the speed increment threshold for the same component presented in isolation. If the visual system is employing low level filtering and an IOC calculation, it should not be possible to see a plaid rotate when the local speed is changed by an amount that is less than its threshold. Perceptible rotations *can* be induced by speed changes that are undetectable when the components are presented in isolation. The conclusion drawn is that, in as far as direction is concerned, pattern perception is not determined by an intersection of constraints method - the visual system must be able to be calculate direction directly. A model was proposed that encodes motion by the successive displacements of the intersections of the gratings (Heeley & Buchanan-Smith, 1994).

Considering the research reported in the previous chapter a series of experiments was carried out to investigate the mechanisms underlying the perception of 2-D patterns. As described above, Heeley and Buchanan-Smith (1994) introduced changes to the spatio-temporal structure of the underlying components of plaids to induce liminal changes in drift direction. These changes to the components were undetectable when presented in isolation. A natural extension of these lines of enquiry is to apply these techniques to type II plaids.

---

[*] These data were first reported in:

Scott Brown, K. (1994) Exploring the limits of human visual performance. Runner up essay for the Gray Prize, University of St Andrews

As shown in the previous chapter, partner type II and type IA plaids can help to expose the contribution of component perception in 2-D pattern perception. Fig. 8.1 shows the pairs of mirror reversed type IA and type II plaids.

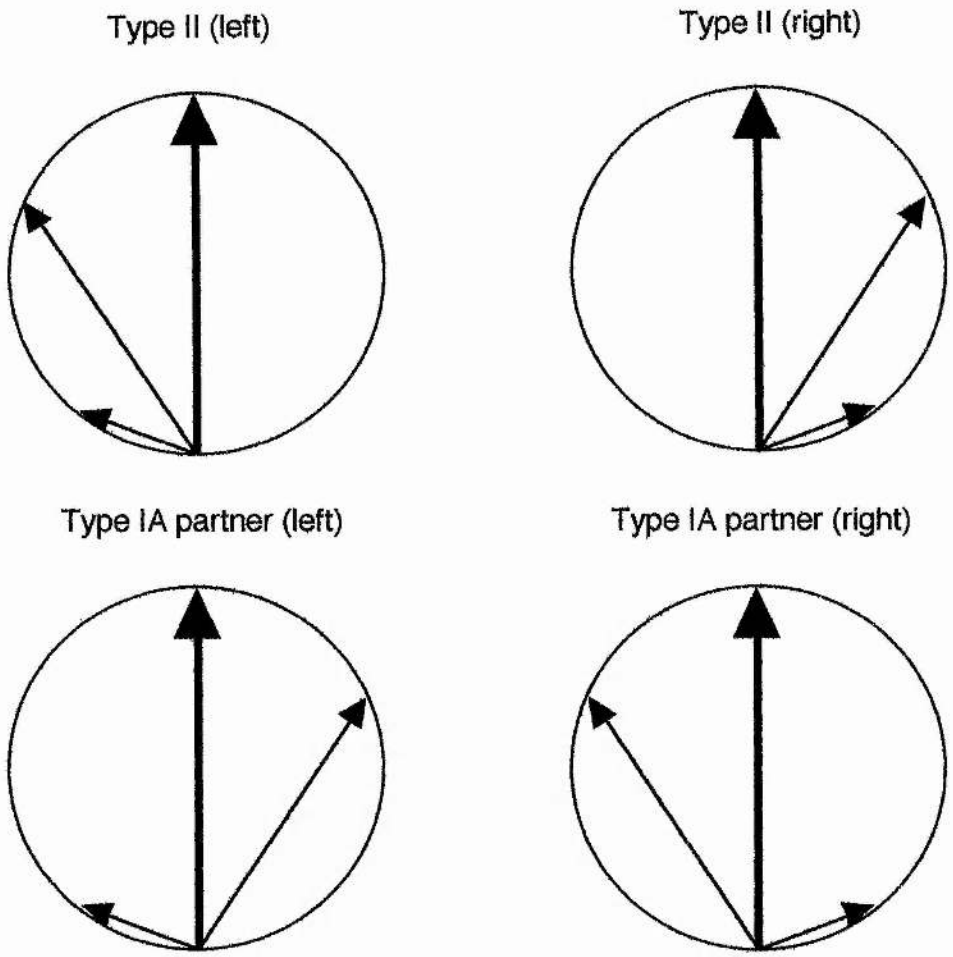

FIGURE 8.1. Type II plaids above their "partner" type IA plaids in velocity space. Both the component vectors are the same magnitude; the only difference is that orientation of the long component is mirror reversed. (Vertical vectors represent resultants.)

Estimates of threshold for apparent rotation of a plaid induced by a velocity asymmetry were performed using three types of plaid. In addition, velocity increment thresholds for components in isolation were estimated to allow comparison with the velocity increment thresholds for rotation. The experimental issue was to discover the velocity change sufficient to elicit a rotation of type II plaids. This can then be compared with velocity increment thresholds in isolation. Of particular interest is whether type II plaids and partner type IA plaids behave in the same way when subjected to induced rotation.

If the velocity of the components is analysed separately and then combined then one would expect that an identical change of speed in an underlying component would be sufficient to induce a perceptible rotation in each type of plaid. Under IOC rules the perception of rotation should be limited by the visual system's ability to discriminate a change in speed of an individual component. However the arrangement of the component in the type II construction means that a greater noise may be associated with the decision process. As discussed in chapter 7, under IOC rules, the type II construction of plaid is subject to greater directional error due to the effects of component uncertainty.

The predictions of the IOC model can be compared with the psychophysical performance of the observers from both this experiment and the experiment in the previous chapter. Large differences between the predicted performance and the actual performance would argue against the operation of an IOC rule in the processing of direction of motion of 2-D stimuli.

METHODS: EXPERIMENT 11

Observers

Three observers were used, two males and one female, aged between 18 and 25. Two of the three were naive to the purposes of the experiment; the third was the author. Full data sets were collected for two subjects and data for type II and type IS plaids were collected for the third subject. All subjects were professionally refracted and showed no astigmatism greater than 0.25 dioptres.

Apparatus

The experimental apparatus is described in chapter 7

Procedure

Part one: Gratings

Estimates of velocity discrimination thresholds for drifting gratings were obtained using a modified method of constant stimulus differences, combined with a two-interval temporal forced choice. Pilot studies were used to determine the width of a set of six drift velocities symmetrically arranged around a standard velocity, to cover the range from the 5% to 95% frequency of seeing points. Of the two intervals in any trial, one contained the standard stimulus and the other contained the test. The order of these was randomly varied. The "test" was selected randomly from the set of six possible tests.

In each trial the observer's task was to decide whether the second interval was moving faster or slower than the first. The responses were recorded by means of button presses on a response box (left button for second stimulus faster than first; right button for second stimulus slower than first; middle button for next trial). The experiment was self paced. The six possible pairings of test and standard were each repeated, in random order, fifty times, making a total of 300 observations for each condition. The data for each condition were collected in two 150 decision blocks in a random order. Table 8.1 shows the stimulus parameters used.

Components' Drift Direction (deg)	*Spatial Frequency (c/deg)*	*Speed (degrees per second)*
48.2	1.0	1.8
33.6	1.0	2.3
23.5	1.0	2.5
-48.2	1.0	1.8
-33.6	1.0	2.3
-23.5	1.0	2.5

TABLE 8.1. Table of velocities for gratings presented in isolation. These component speeds are consistent with a resultant plaid velocity of 2.7 degrees per second (as used previously in a study by Heeley and Buchanan-Smith (1992). The component drift directions were used by Ferrera and Wilson (1990).

Part two: Plaids

Directional acuity, for four human observers, for different types of moving two-dimensional pattern was estimated. Type IS, type I A and type II plaids were presented on the vertical, horizontal and both oblique axes using a two-alternative forced-choice (2AFC) paradigm. Rotation of the patterns was induced by changing the speed of one of the component gratings.

Measurements of the rotational threshold (directional acuity) for the perceived pattern as a function of the changing velocity of the long component were obtained using a modified method of constant stimulus differences combined with a two-interval temporal forced choice. This was achieved using the same method as in experiment 1. On this occasion however the result is expressed as a percentage and is defined as the velocity change required to induce a perceptible change in the direction of drift of the plaid.

Stimuli

Velocities of components are shown in Table 8.2. Thresholds were estimated for gratings with the same drift directions as the components of the type II plaids.

Plaid	*Spatial Freq.*	*C1*		*C2*		*P*	
		Direction	Speed	Direction	Speed	Direction	Speed
II A	1.0	*48.2*	**1.8**	*70.5*	**0.9**	0.0	**2.7**
II B	1.0	*33.6*	**2.3**	*70.5*	**0.9**	0.0	**2.7**
II C	1.0	*23.5*	**2.5**	*70.5*	**0.9**	0.0	**2.7**
IA A	1.0	*-48.2*	**1.8**	*70.5*	**0.9**	0.0	**2.7**
IA B	1.0	*-33.6*	**2.3**	*70.5*	**0.9**	0.0	**2.7**
IA C	1.0	*-23.5*	**2.5**	*70.5*	**0.9**	0.0	**2.7**
IS A	1.0	*48.2*	**1.8**	*48.2*	**1.8**	0.0	**2.7**
IS B	1.0	*33.6*	**2.3**	*33.6*	**2.3**	0.0	**2.7**
IS C	1.0	*23.5*	**2.5**	*23.5*	**2.5**	0.0	**2.7**

TABLE 8.2. Speed and direction values for component vectors (C1 & C2) and resultant vector (P) of components. These figures were calculated from the resultant motion of the symmetrical plaids in Heeley and Buchanan-Smith (1992). The use of these velocities allows comparisons to made with the data from that study. The angles were previously used by Ferrera and Wilson (1990). The units for each parameter were as follows: spatial frequency, (c/deg); direction of motion, (deg); and velocity, (deg/sec).

These velocities were the lower figures from a range used by Ferrera and Wilson (1990) and are centred on the point of maximum sensititvity to velocity as recorded by Welch (1989). Optimum velocity increment thresholds were found at these speeds. The use of these velocities allows comparisons to made with the data from that study.

The angles used were the same as in the preceding chapter and in the paper by Ferrera and Wilson (1990). The use of the same plaid stimuli allowed straightforward comparisons to be made between these results and those of Ferrera and Wilson, and Welch (1989).

Rotational thresholds for the three types of plaid stimuli were estimated for both left and right versions of the plaids partners as shown in Table 8.3. Figs. 8.2, 8.3 and 8.4 show the type IS plaids, the left type IA plaids and the right type II plaids.

Type II Plaids		*Type I Asymmetric Plaids*		*Type I Symmetric Plaids*
Left A	Right A	Left A	Right A	A
Left B	Right B	Left B	Right B	B
Left C	Right C	Left C	Right C	C

TABLE 8.3. Left and right versions of each type of plaid.

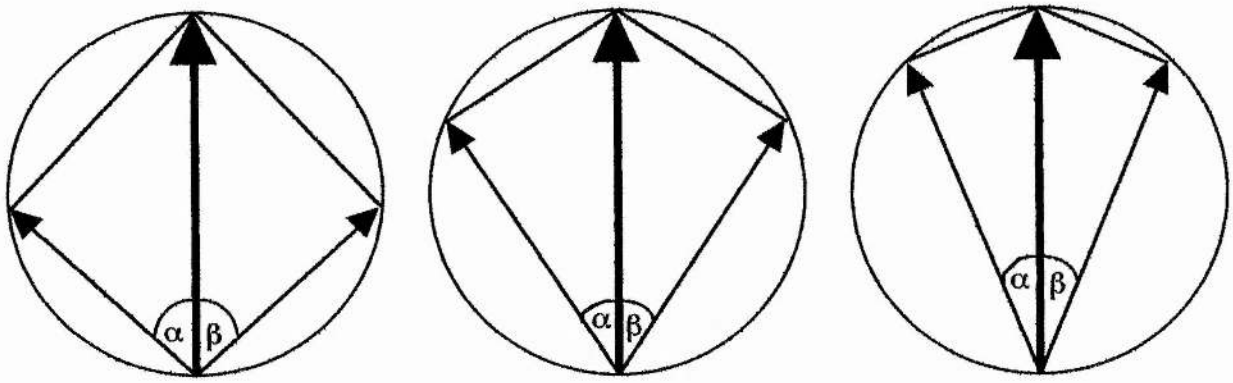

FIGURE 8.2 Velocity space diagrams for type IS plaids.

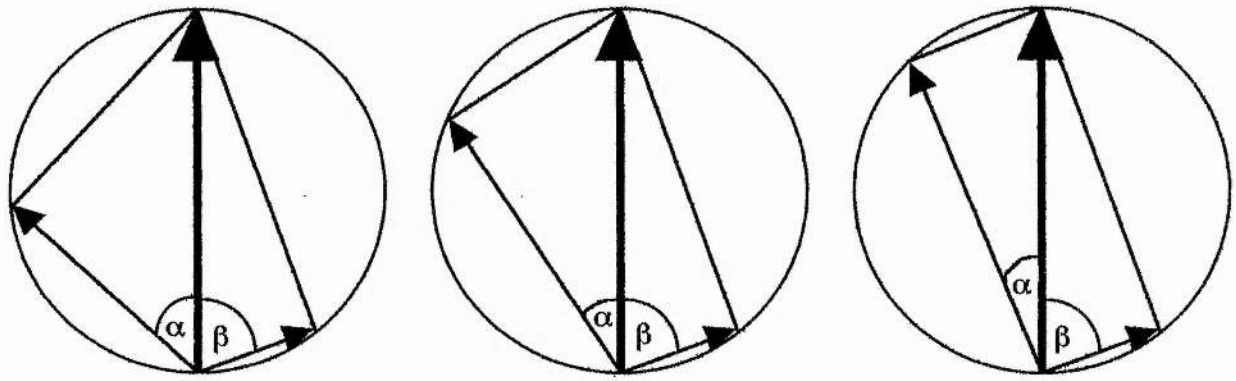

FIGURE 8.3. Velocity space diagrams for type IA plaids.

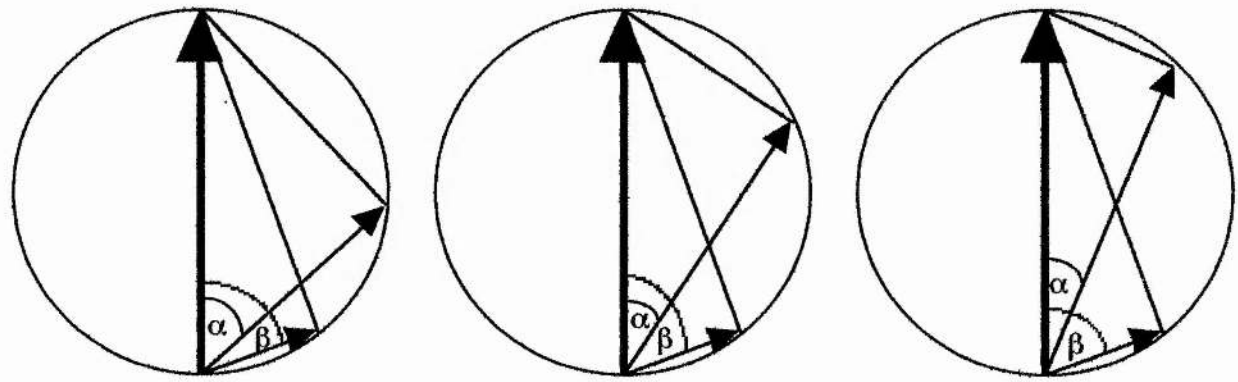

FIGURE 8.4 Velocity space diagrams for type II plaids.

RESULTS

Plaids and Gratings

The y-axis on Fig. 8.5 shows the velocity increment for inducing the rotation of a drifting plaid and the velocity increment threshold for a drifting grating in isolation. The different bars show data from different observers as indicated in the legend. Summary statistics are shown in Table 8.4.

Thresholds for type IA plaids were larger than those for type II plaids by 6.4% on average. No systematic pattern across subjects for type II and type IA plaid thresholds was found. From the figure it can be seen that one observer had higher thresholds for type II plaids, observer EW had nearly identical thresholds for type IA and type II plaids whilst KSB showed much reduced thresholds for type II plaids compared to type IA plaids. Thresholds for type IS plaids were much lower on average, however, differing from type II and IA plaids by 48% and 51% respectively. Thresholds were even lower for isolated gratings which differed from threshold for type IS plaids by 23% on average.

Note that a strict IOC interpretation predicts that threshold should be identical for all plaid types, if one assumes that the speed of the components limits the IOC decision. The greater uncertainty associated with the combination process for type II plaids could allow for higher thresholds for this stimulus type but in the event only one subject showed such thresholds. This argues against the IOC rule.

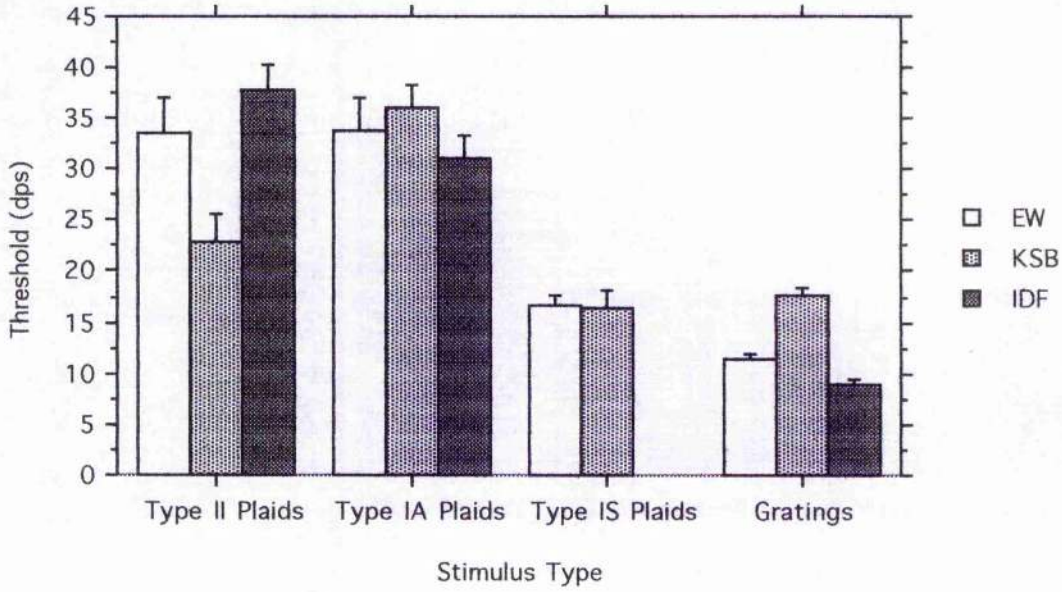

FIGURE 8.5 Velocity increment for inducing a pattern rotation of type IS, IA or type II plaids and the velocity increment threshold for single drifting sine-wave gratings at the same orientation as the long component gratings of the plaids. Thresholds are collapsed across the three long component angles (A = 48.2°, B = 33.6° and C = 23.5°). The different bars show data from different observers as indicated in the legend. The error bars indicate ± 1 S.E.

Stimulus Type	*Mean*	*Std. Dev.*	*Std. Error*
II Plaids	31.463	9.367	2.208
IA Plaids	33.601	6.535	1.540
IS Plaids	16.476	3.499	1.010
Gratings	12.639	3.946	0.930

TABLE 8.4. Means, standard deviations and standard errors for direction discrimination thresholds as a function of direction of drift. Data averaged over principal and oblique axes.

Fig. 8.6 shows thresholds averaged across the three observers for the three long component orientations of the plaids; also shown are the velocity increment thresholds for isolated drifting gratings. There was no apparent effect of component angle for type II plaids. Thresholds were lowest for type IS and type IA plaids with a long component oriented at 48.2°.

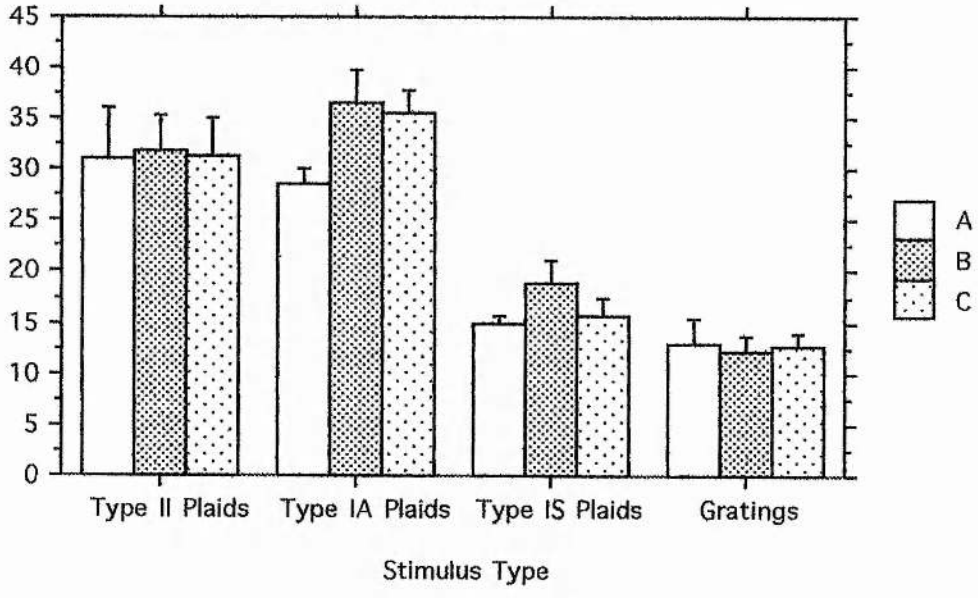

FIGURE 8.6. Velocity increment for inducing a pattern rotation of type IS, IA or type II plaids as well as the velocity increment threshold for single drifting sine-wave gratings at the same orientation as the long component gratings of the plaids. Thresholds are the average of three subjects for type II plaids, type IA plaids and gratings. Type IS thresholds are the average

of two subjects. The different bars show data from the three long component directions: A = 48.2°, B = 33.6° and C = 23.5° as indicated in the legend. The error bars indicate ± 1 S.E.

Individual observers' thresholds as a function of long component orientation for each stimulus type are shown in Appendix 8.B. For type IS plaids, thresholds were seen to peak at angle of 33.6° for both subjects. Type IA thresholds varied according to the subject: EW showed thresholds increasing for 33.6° and increasing further still for component angle 23.5°. KSB and IDF showed an initial increase from 48.2° to 33.6° followed by a decrease from 33.6° to 23.5°. The pattern of thresholds for type II plaids varied for each subject: an increase then a decrease for EW, a progressive increase for KSB and a progressive decrease for IDF.
Using the equations in Appendix 8.A, the data from chapter 7 for physical rotation of plaid patterns was used to calculate the velocity increment required to rotate the plaid by a perceptible angle under IOC rules. Fig 8.7 shows the calculated velocity increment threshold (δv) for each plaid type at each long component angle. Also shown are the velocity increment thresholds for each plaid type as well as the velocity increment thresholds for gratings in isolation (as reported in this chapter).

It can be seen from the graphs that the calculated (IOC) velocity increment thresholds for type II and type IA plaids are much higher than the observed velocity increment thresholds for both plaids and gratings, therefore the IOC is not supported. Instead this suggests that the perceived direction is calculated directly possibly from the motion of the intersections rather than from the speed of the underlying components.

FIGURE 8.7 (Overleaf) Velocity increment thresholds (δv) for each plaid type as a function of long component angle. Three velocity increment thresholds are shown: δv required to induce the rotation of a plaid, δv calculated from physical rotation data and δv for gratings in isolation. Plaid type is indicated in the top right corner of each graph.

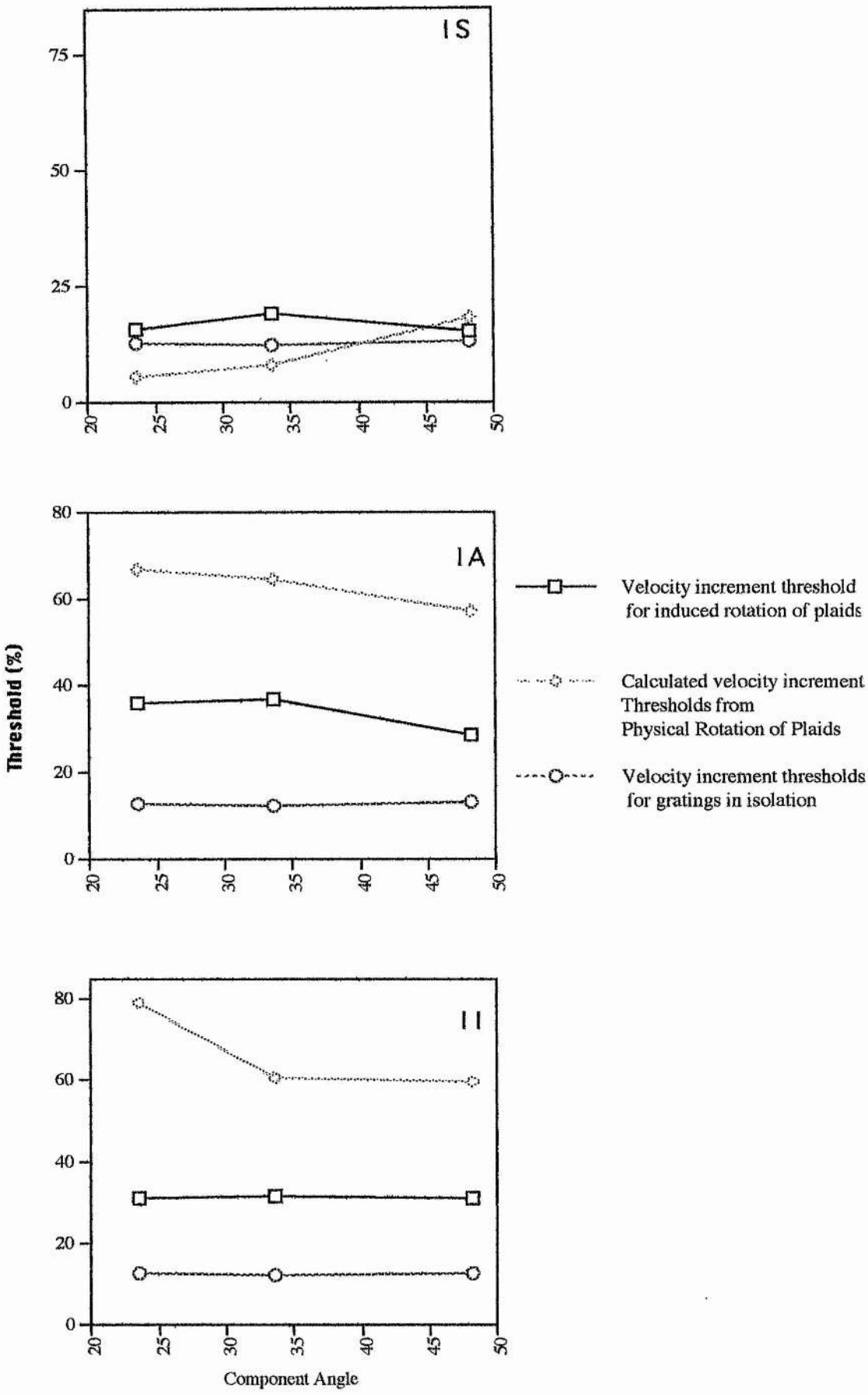
1S
1A
1I
75
50
25
0
80
60
40
20
0
20
25
30
35
40
45
50
Threshold (%)
Component Angle
Velocity increment threshold for induced rotation of plaids
Calculated velocity increment Thresholds from Physical Rotation of Plaids
Velocity increment thresholds for gratings in isolation

The equations were also used to calculate the effective rotation (under IOC rules) of the plaids from this chapter using the δv observed both for plaid rotation and for components in isolation. If the IOC is correct, then the orientation change (q) from the velocity increment thresholds for plaids and gratings should be the same. The results shown in Fig. 8.8 however show that the calculated q is much higher that the orientation thresholds for q from chapter 7. This again suggests that the orientation change is calculated directly rather than from the speed of the components.

FIGURE 8.8 (Overleaf) Orientation discrimination (θ) thresholds for each plaid type as a function of long component angle. Three orientation discrimination thresholds are shown: θ calculated from the δv required to induce the rotation of a plaid, θ calculated from the δv for gratings in isolation and θ observed from the physical rotation data in chapter 7. Plaid type is indicated in the top right corner of each graph.

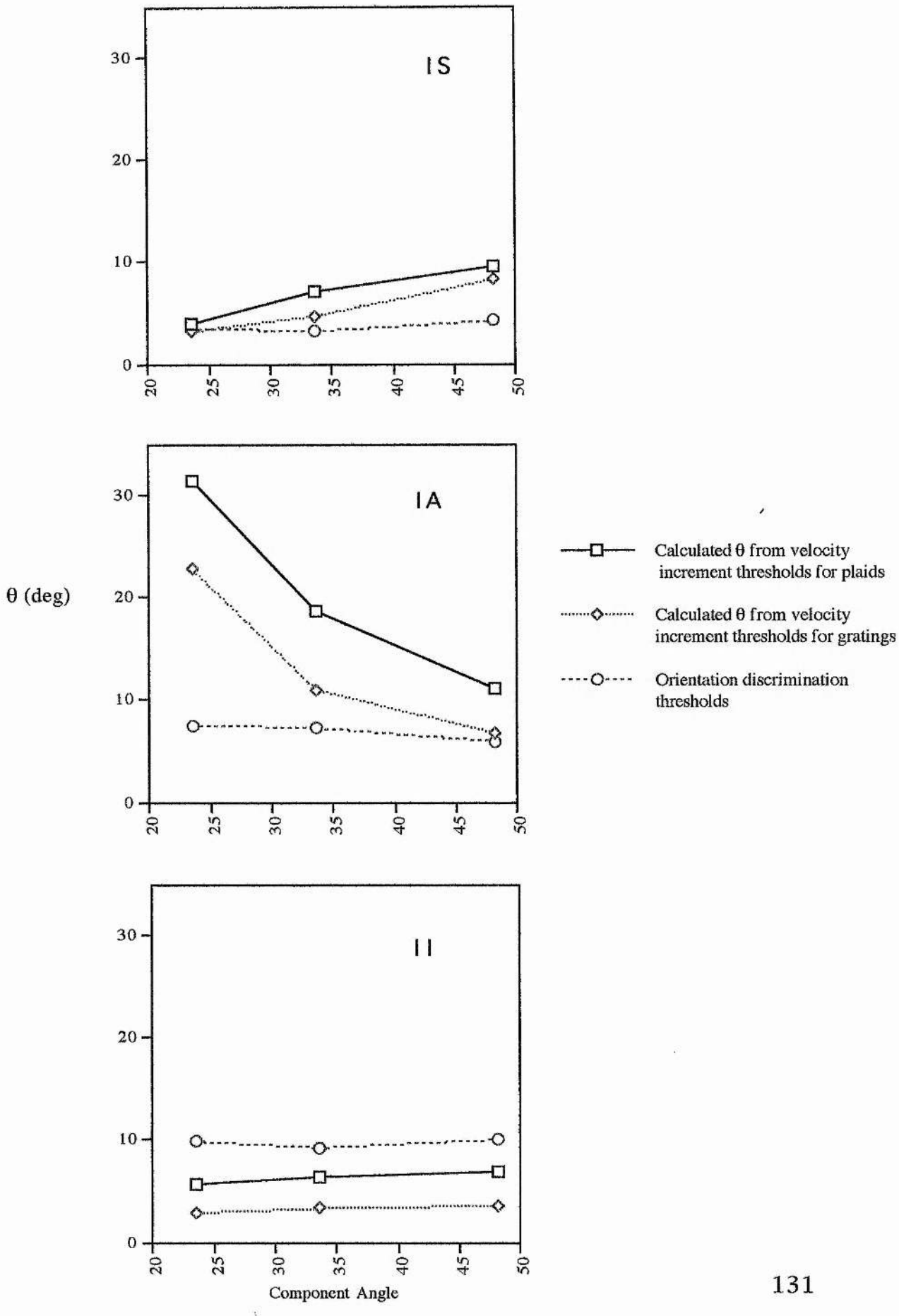
IS
IA
II
θ (deg)
30
20
10
0
20
25
30
35
40
45
50
Component Angle
Calculated θ from velocity increment thresholds for plaids
Calculated θ from velocity increment thresholds for gratings
Orientation discrimination thresholds

DISCUSSION

Thresholds for the velocity induced rotation of type IA and type II plaids were found to differ by as little as 6%. The IOC rule predicted that thresholds should be highest for type II plaids but in this case thresholds were, on average, highest for type IA plaids. Induced rotation thresholds for type IS plaids were nominally higher than the velocity increment thresholds for components in isolation. The finding that type IS plaids only rotate with component velocity changes at levels detectable in isolation is at odds with the results of Heeley and Buchanan-Smith (1994). A direct comparison of results is not possible since the inter element angles (IEAs) in the two experiments are different; IEAs in the present experiment were as small as 27°.

Component Angle

Heeley and Buchanan-Smith (1994) found a non-systematic change in velocity increment thresholds for rotation as a function of IEA. This resembles the present result for type IS plaids, with thresholds increasing from component angle 48.2° to 33.6° then decreasing from 33.6° to 23.5°. No consistent pattern of variation of thresholds between component angles for type IA and type II plaids was found. Velocity increment thresholds for individual gratings varied slightly with angle of drift of the component but this was almost certainly due to the reduced speed of gratings drifting at 70.5 degrees. According to Weber's law, lower drift rates should produce increased discrimination thresholds. The absolute values of velocity discrimination thresholds were of the same order of magnitude (12%) as those intimated by Nakayama (1985). Taking account of the variation in drift rates across orientations ensures that the results are broadly in line with previous findings that indicate that speed discrimination thresholds do not exhibit a meridional variation (Heeley & Buchanan-Smith, 1992).

CONCLUSIONS

The predictions of the IOC model were compared with the psychophysical performance of the observers. Large differences were found between the predicted performance and the actual performance. The results suggested that the change in orientation of 2-D stimuli is calculated directly from the motion of the pattern in question rather than from the motion of the constituent components.

The perceived rotation of 2-D plaid patterns is not governed by the velocity changes in the underlying components. Velocity increment thresholds for induced rotation of type IA and type II plaids were approximately double those for type IS plaids. The results argue against an IOC model since thresholds for type II and type IA plaids do not show

the differences such a model predicts. Type IA thresholds should be smaller than those for type II plaids.

Results indicate that the limiting factor in direction perception of 2-D patterns is not at the level at which components are extracted; it must be at or beyond the level of pattern analysis. This agrees with the conclusions of Heeley and Buchanan-Smith (1994) and Smith and Edgar (1991) that the IOC rule appears to be involved in perception of pattern *speed* but is not involved in the perception of direction.

Discussion: How are motion signals combined in the motion integration process?

CHAPTER 9

Summary and Conclusions

OVERVIEW OF THE SIGNIFICANT FINDINGS OF THE STUDY.

The perceived speed of an inclined line in horizontal translation was found to depend upon line length, line orientation and contrast. In addition it was found that topological arrangement of line segments affected their perceived speed. Co-linear segments showed a bias in perceived speed of a similar type to continuous lines. The magnitude of the misperception of speed was less for co-linear segments than for continuous lines. In all cases the bias in speed involved a decrease in perceived speed. Control experiments showed that the bias in speed was due to the co-linear arrangement of the stimuli rather than an artefact of eccentricity. The number of terminators was systematically varied and it was found that a proliferation of terminators in the co-linear segment condition was sufficient to compromise the original bias found with the stimulus configuration of six line segments. The size of the gaps between the segments did not affect the perceived speed of co-linear segments. However, when the segments consisted purely of dots, with no contours present, the bias in perceived speed was severely reduced. Experiments manipulating the length or position of translation lines showed that even a small perturbation of either stimulus parameter was sufficient to abolish the speed bias for inclined lines.

The results involving continuous inclined lines replicate the findings of Castet *et al.* (1993) and Lorenceau and Shiffrar (1992). However, the weighted-average model of Castet *et al.* has been shown to be unable to account for the perceived motion of more complicated inclined stimuli.

Experiments involving physical rotation of plaids and rotation induced by velocity changes in the underlying components of plaids showed that the IOC model of integration of motion measurements was unable to explain psychophysical performance. It is possible that multi-component noise could be masking the thresholds for type II plaids in physical rotation. However, the induced rotation data did not conform to the predictions of the IOC derived from real psychophysical data.

IMPLICATIONS OF THE STUDY FOR CURRENT THEORY

Intersection of constraints

The finding that type II plaids do not exhibit meridional anisotropy for direction discrimination thresholds on the oblique axes is consistent with the IOC hypothesis but it can still be accommodated by the feature-tracking hypothesis if one assumes that additive noise is present in the decision process. However the IOC does not predict the observed velocity increment thresholds for induced rotation of plaids.

Feature-tracking (Blob-tracking)

A feature-tracking solution provides a plausible account of the experimental data for plaid perception and is supported by experimental evidence from Gorea and Lorenceau (1992) and Burke and Wenderoth (1993). On this basis then, it seems that the same mechanism may in fact account for the perceptual properties of inclined line stimuli as well. Since plaids and tilted line stimuli behave in very similar ways creating similar biases in perceived speed and direction as a function of duration, it seems likely that that the mechanism that processes type II plaids is the same mechanism that processes tilted line segments. The alternative is the less parsimonious solution of a component based model for plaids but a different mechanism for line stimuli. The physical resemblance between the blobs of a type II plaid and tilted line stimuli lead intuitively to the common mechanism solution. To reinforce this interpretation, the stimuli themselves are subject to the same sort of perceptual errors as a function of duration and speed.

It is perhaps misleading to see the distinction between IOC and "blob-tracking" as an all or nothing issue. Gorea and Lorenceau (1991) suggest that motion perception may involve a parallel combination of both a blob-tracking and an IOC mechanism. The mechanism used depends on the particular stimulus situation.

Spatio-temporal integration

The model of Perrone (1990) can explain many of the features of integration measurements. However, the effect of contrast reported by Castet *et al.* (1993) cannot be explained by such a model. Alternative versions of such models may prove acceptable with the addition of averaging over spatial scales (Smith & Edgar, 1991). A class of model that accounts for more of the experimental data, which incorporates spatio-temporal integration mechanisms as part of a broader scheme and which receives more support in the literature is the cosine-weighted model (Wilson *et al.*, 1992; Smith, 1994c).

Integration schemes lacking cross-directional inter-connectivity

The cosine-weighted model of Wilson *et al.* (1992) provides a good account of the data for type II plaids. The physiological correlates of this system are easily identifiable, with V1, V2 and MT representing a possible cortical substrate for Fourier and non-Fourier motion processing. Whether the model could account for the data regarding tilted line segments in translation is a separate issue. As it stands it is not possible to test the predictions of this model with such data. Cropper (1994) has highlighted a limitation of the model however: "non-Fourier" plaids were shown to exhibit perceptual properties that, according to the model resulted from the interaction of the Fourier and non-Fourier pathways.

Current models underestimate the role that "higher-order" properties of stimuli have in the determination of speed and direction perception. The higher-order input is almost certainly multi-component: depth cues (Shimojo, Silverman & Nakayama, 1989), attention (Zeki *et al.* 1991) and feature-tracking (Gorea & Lorenceau, 1991) are all able to influence motion perception.

A model that takes account of attention has recently been published by Lu and Sperling (1995). It incorporates cognitive and attentional processes in the model and it accounts for the data in the paper. However, the motion stimuli are simple in nature and the model does not explicitly indicate the method of integration for motion signals; they simply give the label "further perceptual processes". To provide a general model of motion perception, the model must be able to account for more varied stimulus types and more complex viewing contexts. Wilson *et al.* (1992) do provide a method of combination but it is derived "post-hoc" from the data for plaid perception. Their model must also provide accounts for more varied stimulus types if it is to become a general model of vision. One obvious physiological finding that all models should be able to describe is the large number of back-projections in striate and extrastriate visual cortex (Felleman & van Essen, 1991). One possibility is that such connections convey "top-down" information which modifies initial motion analysis in the light of knowledge about the context of the object or the properties of the object itself.

Rigidity

An explanation of the results in chapter six is the "high-level" notion that the motion of the terminators in the perturbation conditions violates the assumption of *rigidity* (which is one of the implicit assumptions that we make about the visual world). The stimuli in chapter 5 experiment 1 are consistent with a variety of 3-D motions; the lines could be shrinking or could even be tumbling. The hypothesis is that if an object is assumed to be rigid a certain type of motion analysis is permitted. Non-rigid motion, however, means that fewer assumptions about an object's depth plane and speed can be made.

Thus the motion of a non-rigid object is less constrained and can be subject to different motion analysis from rigid motion. Since the system cannot assume constant depth, the possibility of shear, curl or deformation in the image means that a more conservative motion interpretation scheme must be employed.

Using stereo disparity or contrast cues (as discussed in chapter 2), the assumptions that the visual system makes on the terminators of the perturbation conditions could be manipulated. If the perceived speed of the stimuli varied as a function of depth then this would support the conjecture that implicit assumptions about the object motion affect speed perception.

Using the terminator motion from a tumbling object, de-coupled from the motion of the contours joining the object, it is possible to ascertain the constraints that knowledge of an object place on the perception of speed, direction and depth. An example of this is to compare the motion of a rotating wire-frame cube with the motion of the corners of the cube when the edges are not shown. Quite different percepts accrue once the true object identity is known to the observer. This indicates that the visual system has strong top-down capabilities. Knowledge of the stimulus conditions can strongly influence the interpretation of terminator motion.

Vector - averaging / Winner-take-all solutions

The results of the experiments involving random perturbation of line length and position have shown that the current explanations of integration of motion signals do not adequately describe what observers actually see. It appears that neither a vector-averaging nor a winner-take-all model sufficiently describes human psychophysical performance.

The relationship between "weighted average" and "winner-take-all" solutions needs to be specified more clearly. It is not sufficient to say that one works sometimes and the other works the rest of the time. If either is valid then an outline of how the two mechanisms switch between each other or combine to give a joint signal is needed.

It is possible that velocity computation (or speed computation or direction computation) may be reached as a result of mechanisms operating in parallel but that no single system gives accurate unambiguous velocity information in isolation. The information required from optic flow in a given circumstance may dictate the different combinations of motion computation process. If this is the case then human motion detection properties should vary according to the experimental conditions or features.

This is a feature of the Wilson *et al.* (1992) model, where the delay in processing of non-Fourier stimuli is used to account for the duration dependent bias in the perceived

direction of type II plaids. Initially type II plaids are subject to a strong bias, while the Fourier energy dominates. Over time however, following the rectifying non-linearity, the second-order elements of the signal come through the system and enter the equation. When this happens the bias in perceived direction is reduced in a manner consistent with the cosine weighted combination of the two-signals (Yo and Wilson, 1992).

A criticism of this type of model is that the motion system has to listen to more than one system posing the problem of knowing which system to listen to. In a cosine-weighted system, this is dealt with by the integration system. In general the parsimonious explanation (involving one system) is usually preferred in psychology. There is no reason in principle why this should dictate the choice of model, however. The brain can be seen as a hugely parallel network of distributed units. This means that it could use brute force to perform complex task relatively quickly thanks to the raw power built into the system. The multiple sub-systems approach is being adopted in the field of computer vision. Cues such as edge detection, texture, motion, stereopsis and colour give the observer independent cues to the distance, shape and material properties of 3-dimensional surfaces. The integration of such multiple cues by biological visual systems appears to make them particularly robust and reliable. The development of computational techniques on a parallel super computer (Poggio, Gamble and Little, 1988) has been aimed at simulating this method and proved that in principle it is feasible.

LIMITATIONS OF THE STUDY THAT MAY AFFECT THE VALIDITY OR GENERALISABLITY OF THE RESULTS

A recurrent problem in psychology is that the stimuli involved in a test devised to investigate a mechanism may not actually stimulate the mechanism in question. For example the co-linear segment stimuli may *in actuality* appear as a continuous line to the visual system if they are subject to certain spatial frequency filtering. The experiments manipulating the size of the gaps between segments and the experiments changing the number of terminators argue against this possibility. However, with the appropriate equipment an alternative way of ensuring the validity of the results could have been designed. Random gabor micro-patterns as used by Hess and Wilcox (1994) and Polat and Sagi (1994) could be used in co-linear arrangements to see if the same effects accrue for co-linear stimuli with a well defined spatial frequency content. A secondary feature of this stimulus type is that it would allow the investigation of the bias in perceived speed for inclined stimuli to encompass spatial frequency as well. Micro-patterns are useful because, besides varying the spatial frequency content of the stimulus, the local orientation of the components can be varied at the same time. Several possible arrangements are shown in Fig. 9.1.

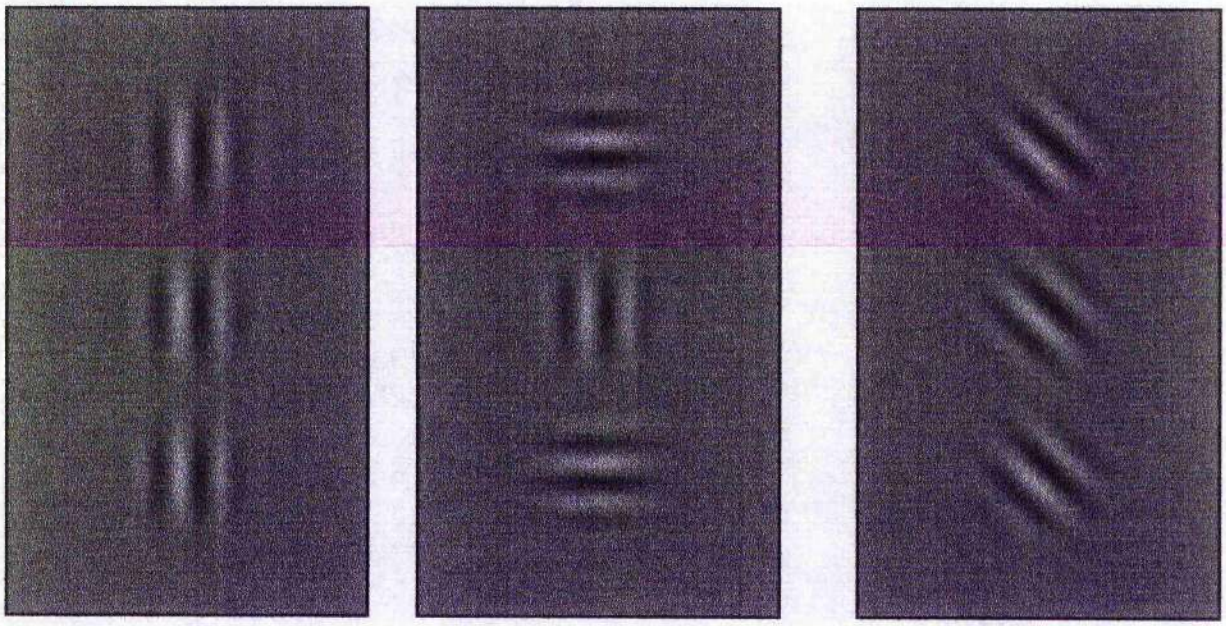

FIGURE 9.1 Stimulus arrangements for gabor micro-patterns.

One possible problem associated with induced rotation of plaids is that the change in speed of the underlying components may compromise the coherence of the plaid and cause a smearing of the pattern. This seems unlikely, however, because the rotation of plaids induced by velocity changes in the components has been shown to be indistinguishable from physical rotation of plaids over a range of component velocity asymmetries (Heeley and Buchanan-Smith, 1994).

RECOMMENDATIONS FOR FURTHER RESEARCH

There is considerable evidence for three parallel systems in motion perception (Lu and Sperling, 1995; Smith, 1994). The two low-level ones are a first-order luminance system and a second-order texture contrast system using independent motion-energy detectors (as reviewed in chapter one). The high-level one is the texture grabber (Lu & Sperling, 1995).

Research in this area can go in one of two ways: firstly one can examine each system on its own, and secondly one can use stimuli that trigger all three systems in psychophysics experiments. For example, a sine-wave stimulates all three systems. Depending on the duration of the stimulus, Fourier or long-range motion detectors can be stimulated; the sine-wave grating can also be used to trigger optokinetic nystagmus (OKN). In the real world, input to the visual system usually spans the three types of mechanism.

Experimental modulation of the relative input of each type of signal should help uncover how the systems interact. In addition the role of higher order processes on motion detection and discrimination should be explored in some detail. Future research should concentrate on providing a precise description of the limits of transparency and coherence of moving and stationary patterns with specific reference to depth, spatial frequency and speed. The most important variable however is stimulus duration, which is important since it may limit the misperception of speed. As Yo and Wilson (1993) indicate, the mechanisms responsible for 2-D motion perception may vary in their response latencies. At short stimulus durations, there may be insufficient time for the signals generated at higher levels to feedback down the system. By varying the high-level content of the stimulus while maintaining the second-order content of the stimulus it may be possible to dissociate the two processes. This is the challenge to investigators: to design experiments that clearly distinguish the mechanisms at work in a given situation.

Experiments of this nature can test the relative importance of top-down and bottom-up processing in the visual system. A key question in vision research is to what extent higher level processes can influence low-level vision. Using stimuli containing identical

amounts of local and terminator information (as described in chapter 2) but with different perceptual classifications regarding their object properties can allow us to distinguish the top-down influences on speed perception.

Three years down the line, the question is no longer "What is the integration mechanism?", instead it is "How do the three mechanisms interact to generate the motion signal and what accounts for the errors that sometimes occur?".

ACKNOWLEDGEMENTS

The empirical research reported in this thesis was funded by a SERC Studentship to the author and also by a SERC Grant to D. W. Heeley.

I am indebted to both my supervisor Dr. D. W Heeley and my second supervisor Dr D. P. Carey for all their help, advice and encouragement.

I would also like to thank my experimental subjects: Margaret Ramsay, Lisi Wacsmuth, Ian Du Feu, Lesley Harrison, Julie Brown, Abigail Fisher, Kevin Allan, Andrew Marr, Geoff Patching, Lindsey Murray and Michelle Busuttil for their patience and for so willingly giving of their time.

I am grateful to Maggie Shiffrar, Terri Lawton and Jane Raymond for their helpful comments at the 1995 ARVO meeting.

My thanks are also due to all the staff, postgraduates and students at the school of psychology who have contributed to such a rich environment for research and learning over the last three years.

REFERENCES

Adelson, E. H., & Bergen, J. R. (1985). Spatiotemporal energy models for the perception of motion. Journal of the Optical Society of America, A(2), 284-299.

Adelson, E. H., & Movshon, J. A. (1982). Phenomenal coherence of moving visual patterns. Nature, 300(5892), 523-525.

Alais, D., Wenderoth, P., & Burke, D. (1994). The contribution of one-dimensional motion mechanisms to the perceived direction of drifting plaids and their after effects. Vision Research, 34(14), 1823-1934.

Albright, T. D. (1984). Direction and orientation selectivity of neurons in the visual area MT of the macaque. Journal of Neuroscience, 52, 1106-1130.

Albright, T. D. (1992). Form cue invariant motion processing in primate visual cortex. Science, 255, 1141-1143.

Barlow, H., & Levick, R. W. (1965). The mechanism of directionally selective units in rabbit's retina. Journal of Physiology, 178, 477-504.

Blakemore, C., & Cooper, G. G. (1970). Development of the brain depends on the visual environment. Nature, 228, 477-8.

Braddick, O. J. (1974). A short-range process in apparent motion. Vision Reserach, 14, 519-527.

Braddick, O. J. (1980). Low-level and high-level processess in apparent motion. Philosophical Transactions of the Royal Society of London B, 290, 137-151.

Bulthoff, H., Little, J., & Poggio, T. (1989). A parallel algorithm for real-time computation of optical flow. Nature, 337(6207), 549-553.

Burbeck, C. A., & Yap, Y. L. (1990). Two mechanisms for localisation? Evidence for separation dependent and separation independent processing of position information. Vision Research, 30, 739-750.

Burke, D., Alais, D., & Wenderoth, P. (1994). A role for a low level mechanism in determining plaid coherence. Vision Research, 34(23), 3189-3196.

Burke, D., & Wenderoth, P. (1993). Determinants of two-dimensional aftereffects induced simultaneously- and alternately-presented plaid components. Vision Research, 33(3), 351-359.

Burton, G. J. (1973). Evidence for non-linear response processes in the human visual system from measuremens on the thresholds of spatial beat frequencies. Vision Research, 13, 1211-1225.

Castet, E., Lorenceau, J., Shiffrar, M., & Bonnet, C. (1993). Perceived Speed of Moving Lines Depends on Orientation, Length,Speed and Luminance. Vision Research, 33(14), 1921-1936.

Cavanagh, P. (1992). Attention-based motion perception. Science, 257, 1563-1565.

Cavanagh, P., & Anstis, S. (1991). The contribution of colour to motion in normal and color-deficient observers. Vision Research, 31(12), 2109-2148.

Cavanagh, P., & Mather, G. (1989). Motion: The long and the short of it. Spatial Vision, 4, 103-129.

Chubb, C., & Sperling, G. (1988). Drift-balanced random stimuli: A general basis for studying non-Fourier motion perception. Journal of the Optical Society of America, A, 5, 1986-2007.

Chubb, C., & Sperling, G. (1989a). Second-order motion perception: Space/time seperable mechanisms. Proceedings: IEEE Workshop on visual motion, 126-138.

Chubb, C., & Sperling, G. (1989b). Two motion perception mechanisms revealed through distance driven reversal of apparent motion. Proceedings of the National Academy of Science U.S.A., 86, 2985-2989.

Cornsweet, T. (1962). The staircase method in psychophysics. American Journal of Psychology, 75, 485-491.

Cropper, J., Badcock, D., & Hayes, A. (1994). On the role of Second-Order Signals in the Perceived Direction of Motion of Type II Plaid Patterns. Vision Research, 34(19), 2609-2612.

DeAngelis, G. C., Ohzhawa, I., & Freeman, R. D. (1995). Receptive-field dynamics in the central visual pathways. Trends in Neuroscience, 18(10), 451-458.

Derrington, A. M. (1987). Distortion products in geniculate X cells: A physiological basis for masking by spatially modulated gratings? Vision Research, 27, 1377-1386.

Derrington, A. M., & Badcock, D. R. (1985). Separate detectors for simple and complex patterns. Vision Research, 25, 1869-1878.

Derrington, A. M., & Badcock, D. R. (1992). Two-stage analysis of the motion of 2-dimensional patterns, what is the first stage? Vision Research, 32, 691-698.

Derrington, A. M., & Suero, M. (1991). Motion of complex patterns is computed from the perceived motions of their components. Vision Research, 31(1), 139-149.

Dobkins, K. R., & Albright, T. D. (1993). What happens if it changes color when it moves? Psychophysical experiments on the nature of chromatic input to motion detectors. Vision Research, 33(8), 1019-1036.

Dobkins, K. R., & Albright, T. D. (1994). What happens if it changes color when it moves? The nature of chromatic input to macaque visual area MT. Journal of Neuroscience, 14(8), 4854-4870.

Dubner, R., & Zeki, S. M. (1971). Response properties and receptive fields of cells in an anatomically defined area of the superior temoral sulcus. Brain Research, 35, 528-532.

Emerson, R. C., Bergen, J. R., & Adelson, E. H. (1992). Directionally selective complex cells and the computation of motion energy in visual cortex. Vision Research, 32, 203-218.

Felleman, D. J., & van Essen, D. C. (1991). Distributed heirarchical processing in the primate cerebral cortex. In A. Peters & E. G. Jones (Eds.), Cerebral Cortex, (Vol. 9, pp. 1-47). New York: Plenum.

Fennema, C. L., & Thompson, W. B. (1979). Velocity determination in scenes containing several moving objects. Computer Graphics and Image Processing, 9, 301-315.

Ferrera, V. P., & Wilson, H. R. (1987). Direction specific masking and the analysis of motion in two dimensions. Vision Research, 27(10), 1783-1796.

Ferrera, V. P., & Wilson, H. R. (1990). Perceived direction of moving two-dimensional patterns. Vision Research, 30, 273-287.

Ferrera, V. P., & Wilson, H. R. (1991). Perceived speed of moving two-dimensional patterns. Vision Research, 31, 877-894.

Finney, D. J. (1971). Probit Analysis. (3rd. ed.): Cambridge University Press U.K.

Fleet, D. J., & Langley, K. (1994). Computational analysis of non-Fourier motion. Vision Research, 34(22), 3057-3079.

Georgeson, M. A., & Harris, M. G. (1990). The temporal range of motion sensing and motion perception. Vision Research, 30(4), 615-619.

Gibson, J. J. (1950). The perception of the visual world. Boston: Houghton Mifflin.

Gorea, A., & Lorenceau, J. (1991). Directional performances with moving plaids: Component-related and plaid-related processing modes coexist. Spatial-Vision, 5(4), 231-252.

Grzywacz, N. M. (1992). One path model for contrast-independent perception of Fourier and non-Fourier motions. Investigative Ophthalmology and Visual Science (Suppl.), 33, 954.

Grzywacz, N. M., & Yuille, A. L. (1991). Theories for the visual perception of local velocity and coherent motion. In M. Landy & A. Movshon (Eds.), Computational models of visual processing, (pp. 119-133). Cambridge, Mass: MIT Press.

Harris, L. R., & Smith, A. T. (1992). Motion defined exclusively by second-order characteristics does not evoke optokinetic nystagmus. Visual Neuroscience, 9(6), 565-570.

Heeger, D. J. (1987). A model of the extraction of image flow. Journal of the Optical Society of America A, 4(1455-1471).

Heeley, D. W., & Buchanan-Smith. (1994). Changes in the perceived direction of drifting plaids induced by asymmetrical changes in the spatio-temporal structure of the underlying components. Vision Research, 34(6), 775-797.

Heeley, D. W., & Buchanan-Smith, H. M. (1990). Recognition of stimulus orientation. Vision Research, 30, 1429-1437.

Heeley, D. W., & Buchanan-Smith, H. M. (1992). Directional acuity for drifting plaids. Vision Research, 32, 97-104.

Heeley, D. W., & Timney, B. (1988). Meridional anisotropies of orientation discrimination for sine wave gratings. Vision Research, 28, 337-344.

Hess, R. F., & Wilcox, L. M. (1994). Linear and non-linear filtering in stereopsis. Vision Research, 34(18), 2431-2438.

Hess, R. H., Baker, C. L. J., & Zihl, J. (1989). The "motion-blind" patient: Low level spatial and temporal filters. Journal of Neuroscience, 9, 1628-1640.

Hildreth, E. (1984). The measurement of visual motion. Cambridge, Mass.: MIT Press.

Hildreth, E. C., & Koch, C. (1987). The analysis of visual motion: from computational theory to neuronal mechanisms. Annual Review of Neuroscience, 10, 477-533.

Horn, B. K. P., & Schunck, B. G. (1981). Determining Optic Flow. Artificial Intelligence, 17, 185-203.

Hubel, D., & Wiesel, T. (1968). Receptive fields and functional architecture of monkey striate cortex. Journal of Physiology, 195, 215-243.

Hubel, D. H. (1988). Eye, brain and vision. New York: Scientific American Library.

Johnston, A., McOwan, P. W., & Buxton, H. (1992). A computational model of the analysis of some first-order and second-order motion patterns by simple and complex cells. Proceedings of the Royal Society of London B, 250, 297-306.

Julesz, B., & Payne, R. A. (1968). Differences between monocular and binocular stroboscopic movement perception. Vision Research, 8, 433-444.

Keppel, G., Sauffley, W. H., & Tokunaga, H. (1992). Introduction to Design and Analysis. (2nd ed.): Freeman and Company.

Koenderink, J. J. (1986). Optic flow. Workshop on Systems Approach in Vision (1984, Amsterdam, Netherlands). Vision Research, 26(1), 161-179.

Koenderink, J. J., van Doorn, A. J., & van de Grind, W. A. (1985). Spatial and temporal parameters of motion detection in the peripheral visual field. Journal of the Optical Society of America A, 2, 252-259.

Kooi, F. (1993). Local direction of edge motion causes and abolishes the barber-pole illusion. Vision Research, 33(16), 2347-2351.

Kooi, F., De Valois, K. K., Switkes, E., & Grosof, D. H. (1992). Higher order factors influencing the perceived motion of plaids. Perception, 21, 583-598.

Ledgeway, T., & Smith, A. (1994). Evidence for separate motion-detecting mechanisms for first and second-order motion in human vision. Vision Research, 34(20), 2727-2740.

Lee, D. N. (1980). The optic flow field: The foundation of vision. Philosophical Transactions of the Royal Society of London B, 290, 169-179.

Limb, J. O., & Murphy, J. A. (1975). Estimating the velocity of moving images in television signals. Computer Graphics and Image Processing, 4, 311-327.

Livingstone, M., & Hubel, D. (1988). Segregation of form, color, movement, and depth: Anatomy, physiology, and perception. Science, 240(4853), 740-749.

Lorenceau, J., Shiffrar, M., Wells, N., & Castet, E. (1993). Different motion sensitive units are involved in recovering the direction of motion of moving lines. Vision Research, 33(9), 1207-1217.

Lu, Z.-L., & Sperling, G. (1995). The functional architecture of human visual motion perception. Vision Research, 35(19), 2697-2722.

Macleod, D. I. A., Williams, D. R., & Makous, W. (1992). A visual non-linearity fed by single cones. Vision Research, 32, 347-363.

Marr, D. (1982). Vision. San Francisco: Freeman.

Marr, D., & Ullman, S. (1981). Directional selectivity and its use in early visual processing. Proceedings of the Royal Society of London B, 211, 151-180.

Mather, G., & West, S. (1993). Evidence for second-order motion detectors. Vision Research, 33, 1109-1112.

Maunsell, J. H., & van Essen, D. C. (1983). Functional properties of neurons in middle temporal visual area of the macaque monkey: I. Selectivity for stimulus direction, speed, and orientation. Journal of Neurophysiology, 49(5), 1127-1147.

McKee, S. P. (1981). A local mechanism for differential velocity detection. Vision Research, 21(4), 491-500.

McKee, S. P., & Nakayama, K. (1984). The detection of motion in the peripheral visual field. Vision Research, 24, 25-32.

Mingolla, E., Todd, J. T., & Norman, J. F. (1992). The perception of globally coherent motion. Vision Research, 32(6), 1015-1031.

Morgan, M. J. (1992). Spatial filtering precedes motion detection. Nature (London), 365, 344-346.

Morgan, M. J., Findlay, J. M., & Watt, R. J. (1982). Aperture viewing: a review and a synthesis. Quarterly Journal of Experimental Psychology, 34A, 211-233.

Moulden, B. (1994). Collator units: second-stage orientational filters. In M. Morgan (Ed.), Higher-order processing in the visual system., (pp. 170-192). Chichester: Wiley.

Movshon, A. (1990). Visual processing of moving images. In H. Barlow, C. Blakemore, & M. Weston-Smith (Eds.), Images and Understanding, (pp. 122-139). Cambridge: Cambridge University Press.

Movshon, J. A., Adelson, E. H., Gizzi, M. S., & Newsome, W. (1985). The analysis of moving visual patterns. In C. Chagas, R. Gattas, & C. Gross (Eds.), Study

group on pattern recognition mechanisms, (pp. 117-151). Vatican City: Pontifica Academia Scientarum.

Murasugi, C. M., Salzman, C. D., & Newsome, W. T. (1993). Microstimulation in visual area MT: Effects of varying pulse amplitude and frequency. Journal of Neuroscience, 13(4), 1719-1729.

Nakayama, K. (1985). Biological image motion processing: A review. Vision Research, 25(625-660).

Nakayama, K., & Silverman, G. H. (1988). The aperture problem: II. Spatial integration of velocity information along contours. Vision Research, 28(6), 747-753.

Newsome, W. T., & Paré, E. (1988). A selective impairment of motion perception following lesions of the middle temporal visual area (MT). Journal of Neuroscience, 8(6), 2201-2211.

Nishida, S., & Sato, T. (1992). Positive motion after-effect induced by bandpass-filtered random dot kinematograms. Vision Research, 32(9), 1635-1646.

Noest, A. J., & van den Berg, A. V. (1993). The role of early mechanisms in motion transparency and coherence. Spatial Vision, 7(No 2), 125-147.

Perrone, J. A. (1990). Simple technique for optical flow estimation. Journal of the Optical Society of America A, 7, 264-278.

Polat, U., & Sagi, D. (1994). The architecture of perceptual spatial interactions. Vision Research, 34(1), 73-78.

Ramachandran, V. S. (1990). Visual perception in people and machines. In A. Blake & T. Troscianko (Eds.), AI and the Eye, (pp. 21-77). Chichester: Wiley.

Regan, D. (1989). Orientation discrimination for objects defined by relative motion and objects defined in luminance contrast. Vision Research, 29(10), 1398-1400.

Regan, D., Giaschi, D., Sharpe, J. A., & Hong, X. H. (1992). Visual processing of motion defined form: Selective failure in patients with parietotemporal lesions. Journal of Neuroscience, 12, 2198-2210.

Reichardt, W. (1961). Autocorrelation, a principle for the evaluation of sensory information by the nervous system. New York: Wiley.

Rodman, H. R., & Albright, T. D. (1987). Coding of visual stimulus velocity in area MT of the macaque. Vision Research, 27(12), 2035-2048.

Rovamo, J., & Virsu, V. (1979). An estimation and application of the human cortical magnification factor. Experimental Brain Research, 37, 495-510.

Salzman, C. D., Britten, K. H., & Newsome, W. T. (1990). Cortical microstimulation influences perceptual judgements of motion direction. Nature, 346(6280), 174-177.

Salzman, C. D., Murasugi, C. M., Britten, K. H., & Newsome, W. T. (1992). Microstimulation in visual area MT: effects on direction discrimination performance. Journal of Neuroscience, 12, 2331-2355.

Salzman, C. D., & Newsome, W. T. (1994). Neural mechanisms for forming a perceptual decision. Science, 264(5156), 231-237.

Schiller, P. H., Finlay, B. L., & Volman, S. F. (1976). Quantitative studies of single-cell properties in monkey striate cortex: I. Spatiotemporal organization of receptive fields. Journal of Neurophysiology, 39(6), 1288-1319.

Scott-Brown, K., & Heeley, D. W. (1995). Topological arrangement affects the perceived speed of tilted lines in horizontal translation. Investigative Ophthalmology and Visual Science, 36(4), 54.

Scott-Brown, K., & Heeley, D. W. (1996). Random perturbation of the length or position of tilted lines in horizontal translation affects their perceived speed. Investigative Ophthalmology and Visual Science, 37(3), 744.

Shimojo, S., Silverman, G. H., & Nakayama, K. (1989). Occlusion and the solution for the aperture problem for motion. Vision Research, 29(5), 619-626.

Smith, A. T. (1994a). Correspondence based and energy-based detection of second order motion in human vision. Journal of the Optical Society of America, 11(7), 1940-1948.

Smith, A. T. (1994b). The detection of second-order motion. In A. T. Smith & R. J. Snowden (Eds.), Visual Detection of Motion, (pp. 145-176): Academic Press Ltd.

Smith, A. T., & Edgar, G. K. (1991). Perceived speed and direction of complex gratings and plaids. Journal of the Optical Society of America, (A), 8, 1161-1171.

Smith, A. T., & Hammond, P. (1986). Hemifield differences in perceived velocity. Perception, 15(2), 111-117.

Smith, A. T., & Ledgeway, T. (1994). Adaptation to second-order motion. Paper presented at the Applied Vision Association, Annual Meeting, Bristol.

Smith, A. T., Snowden, R. J., & Milne, A. B. (1994). Is global motion really based on spatial integration of local motion signals? Vision Research, 34(18), 2425-2430.

Stone, L. S., & Thompson, P. (1992). Human speed perception is contrast dependent. Vision Research, 32, 1535-1549.

Stone, L. S., Watson, A. B., & Mulligan, J. B. (1990). Effect of contrast on the perceived direction of a moving plaid. Vision Research, 30, 1049-1067.

Stoner, G. R., Albright, T. D., & Ramachandran, V. S. (1990). Transparency and coherence in human motion perception. Nature, 344(153-155).

Thompson, P. (1982). Perceived rate of movement depends on contrast. Vision Research, 22, 377-380.

Treisman, A. M., & Gelade, G. (1980). A feature-integration theory of attention. Cognitive Psychology, 12(1), 97-136.

Trueswell, J. C., & Hayhoe, M. M. (1993). Surface segmentation mechanisms and motion perception. Vision Research, 33, 313-328.

Ullman, S. (1979). The interpretation of visual motion. Cambridge, Mass.: MIT.

Ungerleider, L. G., & Mishkin, M. (1979). The striate projection zone in the superior temporal sulcus of *Macaccamulatta:* Location and topographic organisation. Journal of Comparative Neurology, 188, 347-366.

Vallortigara, G., & Bressan, P. (1991). Occlusion and the perception of coherent motion. Vision Research, 31(11), 1967-1978.

van de Grind, W. A., Koenderink, J. J., & van Doorn, A. J. (1986). The distribution of human motion detector properties in the monocular visual field. Vision Research, 26(5), 797-810.

van de Grind, W. A., Koenderink, J. J., & van Doorn, A. J. (1992). Viewing-distance invariance of movement direction. Experimental Brain Research, 91, 135-150.

van den Berg, A. V., & van de Grind, W. A. (1993). Do component motions recombine into a moving plaid percept? Experimental Brain Research, (MS 264, accepted, in proof).

van Essen, D. C., Maunsell, J. H. R., & Bixby, J. L. (1981). The middle temporal visual area in the macaque: myleoarchitecture, connections, functional properties and topographic organisation. Journal of Comparative Neurology, 199, 293-326.

van Santen, J. P. H., & Sperling, G. (1985). Elaborated Reichardt detectors. Journal of the Optical Society of America A, 2, 330-321.

Wallach, H. (1976). On Perception. New York: Quadrangle.

Wallach, H., & O'Connell, D. N. (1953). The kinetic depth effect. Journal of Experimental Psychology, 45, 205-217.

Watson, A. B., & Ahumada, A. J. (1985). Model of human-visual motion sensing. Journal of the Optical Society of America A, 2, 322-342.

Watt, R. J., & Morgan, M. J. (1985). A theory of the primitive spatial code in human vision. Vision Research, 25, 1661-1674.

Welch, L. (1989). The perception of moving plaids reveals two motion-processing stages. Nature, 337, 734-736.

Werkhoven, P., Sperling, G., & Chubb, C. (1993). The dimensionality of texture-defined motion: A single channel theory. Vision Research, 33, 463-485.

Westheimer, G. (1982). The spatial grain of the perifoveal visual field. Vision Research, 22, 157-162.

Wetherill, G. B., & Levitt, H. (1965). Sequential estimation of points on a psychometric function. British Journal of Mathematical and Statistical Psychology, 18, 1-10.

Williams, D., & Phillips, G. (1987). Cooperative phenomena in the perception of motion direction. Journal of the Optical Society of America A, 4, 878-885.

Wilson, H. R., Ferrera, V. P., & Yo, C. (1992). A Psychophysically motivated model for two-dimensional motion perception. Visual Neuroscience, 9, 79-97.

Wilson, H. R., & Mast, R. (1993). Illusory motion of texture boundaries. Vision Research, 33, 1437-1446.

Wolfensohn, S., & Lloyd, M. (1994). Handbook of laboratory animal management and welfare. Oxford: Oxford University Press.

Wright, M. J. (1987). Spatiotemporal properties of grating motion detection in the center and the periphery of the visual field. Journal of the Optical Society of America A, 4(8), 1627-1633.

Yo, C., & Wilson, H. R. (1992). Perceived direction of moving two-dimensional patterns depends on duration, contrast and eccentricity. Vision Research, 32, 135-147.

Zanker, J. M. (1993). Theta motion: a paradoxical stimulus to explore higher order motion extraction. Vision Research, 33(4), 553-569.

Zeki, S. M. (1974). Functional organisation of a visual area in the posterior bank of the superior temporal sulcus of the rhesus monkey. Journal of Physiology, 236, 549-573.

Zeki, S. M., Watson, J. D. G., Lueck, C. J., Friston, K. J., Kennard, C., & Frackowiack, R. S. J. (1991). A direct demonstration of functional specialisation in human visual cortex. Journal of Neuroscience, 11, 641-649.

Appendices

CHAPTER 2

APPENDIX 2.A

Weighted average model

Vector calculus is used to obtain the magnitude of vector $\mathbf{Va_i}$ defined by equation (1) with angle θ between $\mathbf{V_L}$ and $\mathbf{V_T}$ (Fig 2.3). A Vectorial quantity is noted with bold characters whereas its magnitude is represented by normal ones.

$$\mathbf{Va_i} = \alpha * \mathbf{V_L} + \beta * \mathbf{V_T} \qquad (1)$$

with $\alpha + \beta = 1$.

By taking the square of both sides of the equation (1) we obtain:

$$(\mathbf{Va_i})^2 = \alpha^2 * \mathbf{Vl}^2 + \beta^2 * \mathbf{Vt}^2 + 2 * \alpha * \beta * \mathbf{V_L} * \mathbf{V_T} * \cos(\theta) \qquad (1')$$

substituting $\cos(\theta) = \mathbf{V_L} / \mathbf{V_T}$ onto (1'):

$$\mathbf{Va_i}^2 = \mathbf{Vt}^2 * (\beta^2 + (\alpha^2 + 2 * \alpha * \beta) * (\mathbf{V_L} / \mathbf{V_T})^2)$$

and finally

$$\mathbf{Va_i}^2 / \mathbf{V_T} = \sqrt{(\beta^2 + (\alpha^2 + 2 * \alpha * \beta)(\mathbf{V_L} / \mathbf{V_T})^2)} \qquad (2)$$

APPENDIX 2.B

FIGURES B1 -B4 overleaf: Data for individual observers.
FIGURES B5 -B7 overleaf: Data for four subjects at each contrast level.

(each page constitutes one figure)

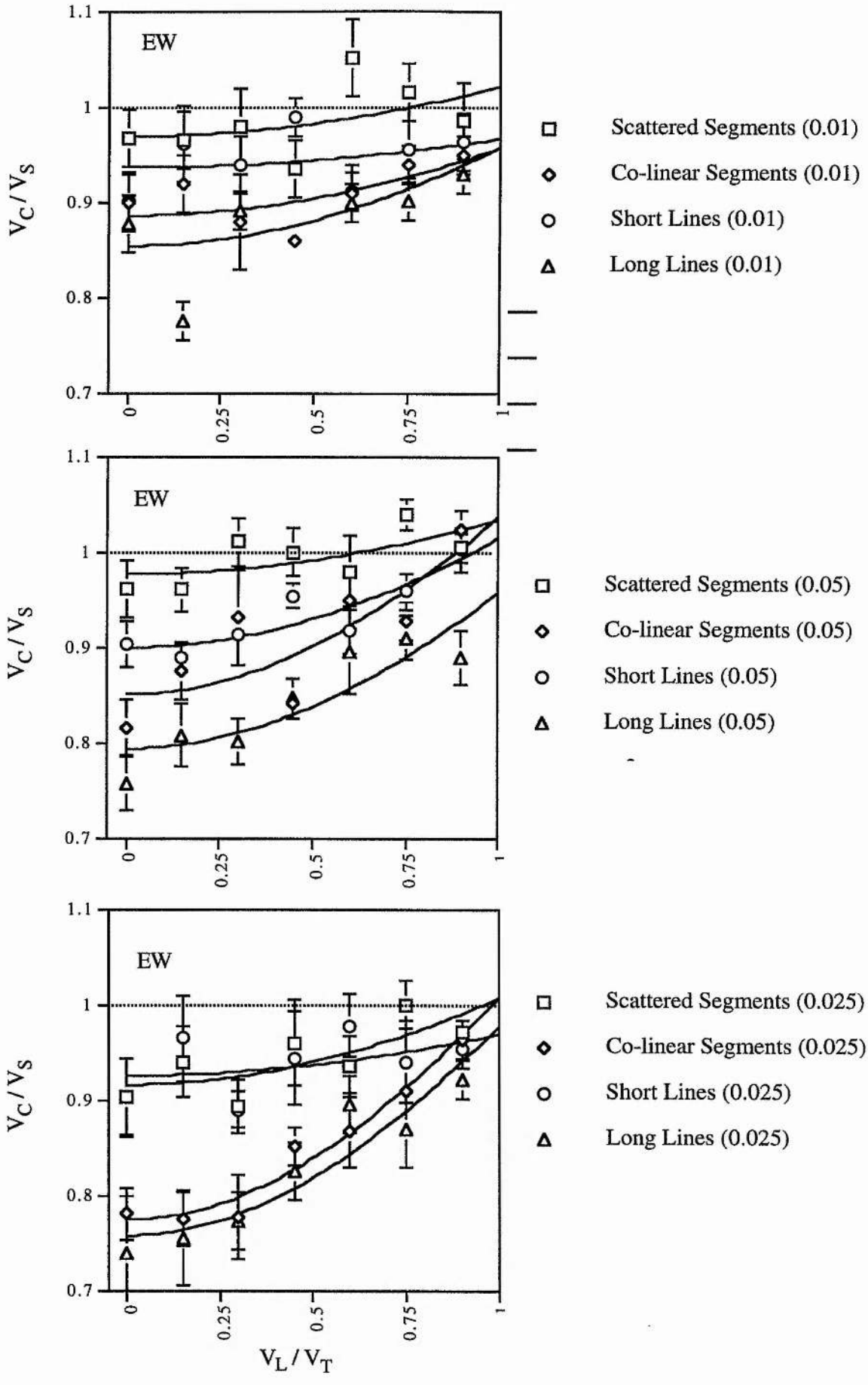
EW
V_C / V_S
1.1
1
0.9
0.8
0.7
0
0.25
0.5
0.75
1
Scattered Segments (0.01)
Co-linear Segments (0.01)
Short Lines (0.01)
Long Lines (0.01)
EW
V_C / V_S
Scattered Segments (0.05)
Co-linear Segments (0.05)
Short Lines (0.05)
Long Lines (0.05)
EW
V_C / V_S
Scattered Segments (0.025)
Co-linear Segments (0.025)
Short Lines (0.025)
Long Lines (0.025)
V_L / V_T

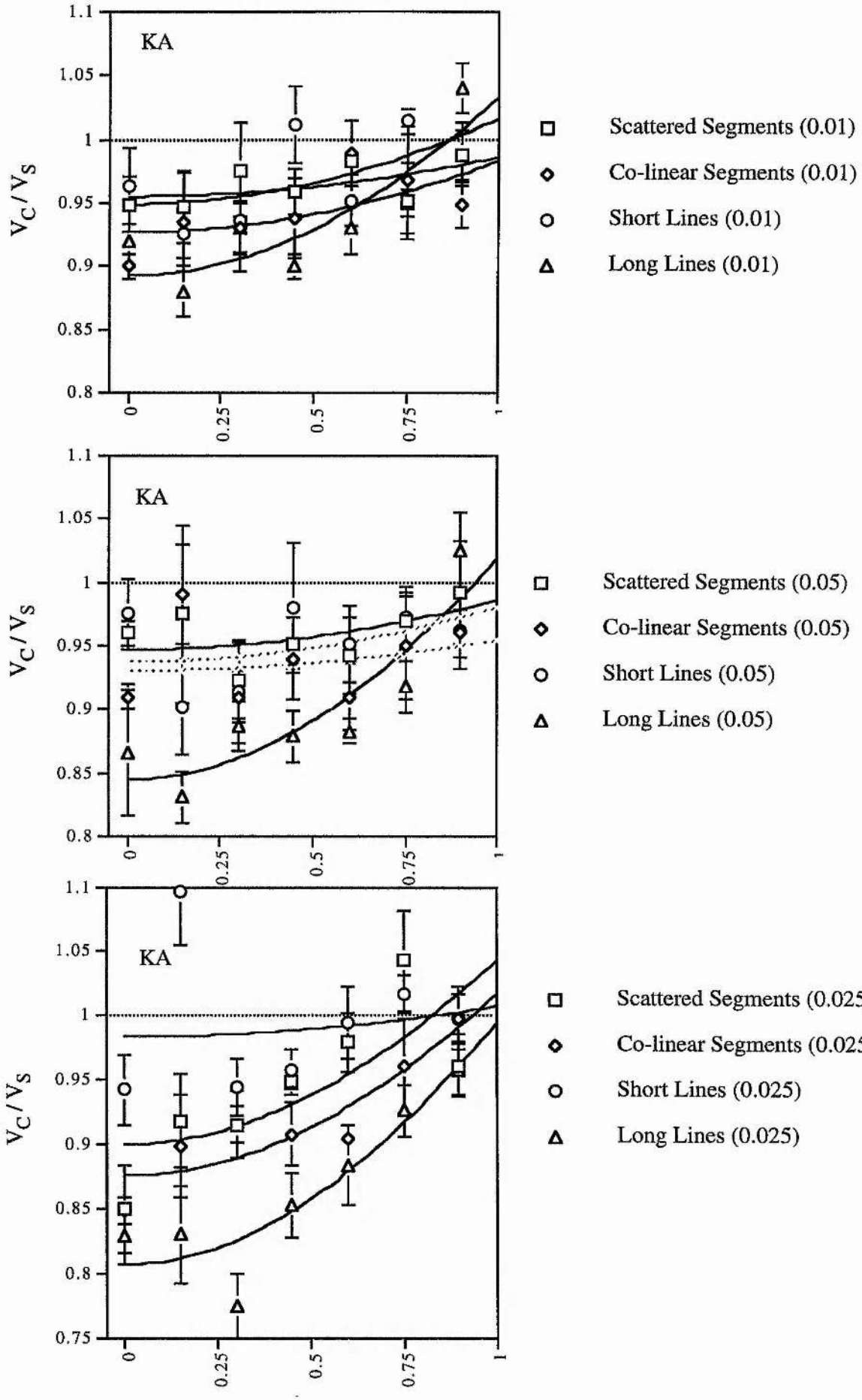
KA
V_C / V_S
1.1
1.05
1
0.95
0.9
0.85
0.8
0
0.25
0.5
0.75
1
Scattered Segments (0.01)
Co-linear Segments (0.01)
Short Lines (0.01)
Long Lines (0.01)
KA
V_C / V_S
Scattered Segments (0.05)
Co-linear Segments (0.05)
Short Lines (0.05)
Long Lines (0.05)
KA
V_C / V_S
0.75
Scattered Segments (0.025)
Co-linear Segments (0.025)
Short Lines (0.025)
Long Lines (0.025)

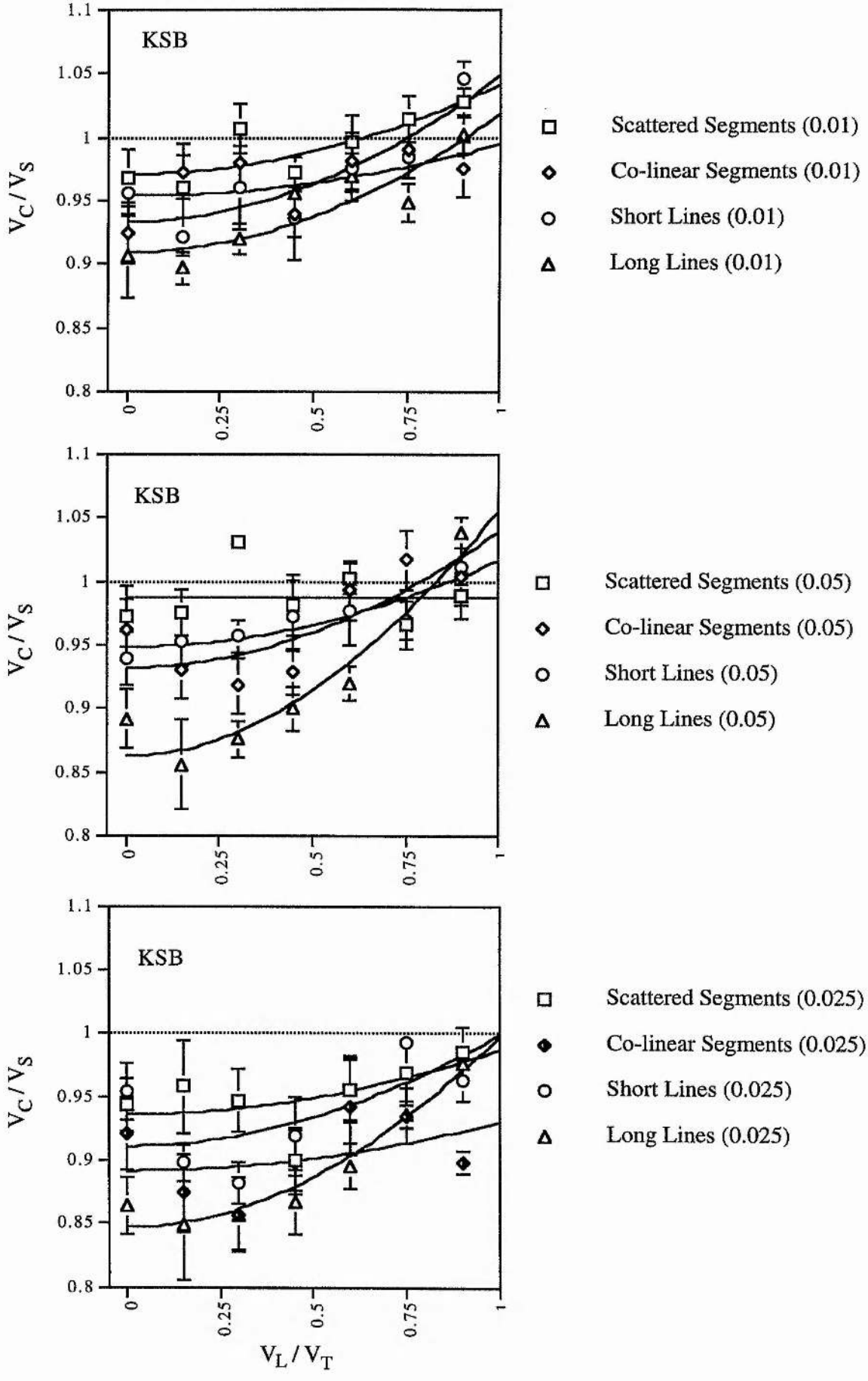
KSB
V_C / V_S
1.1
1.05
1
0.95
0.9
0.85
0.8
0
0.25
0.5
0.75
1
Scattered Segments (0.01)
Co-linear Segments (0.01)
Short Lines (0.01)
Long Lines (0.01)
KSB
V_C / V_S
Scattered Segments (0.05)
Co-linear Segments (0.05)
Short Lines (0.05)
Long Lines (0.05)
KSB
V_C / V_S
V_L / V_T
Scattered Segments (0.025)
Co-linear Segments (0.025)
Short Lines (0.025)
Long Lines (0.025)

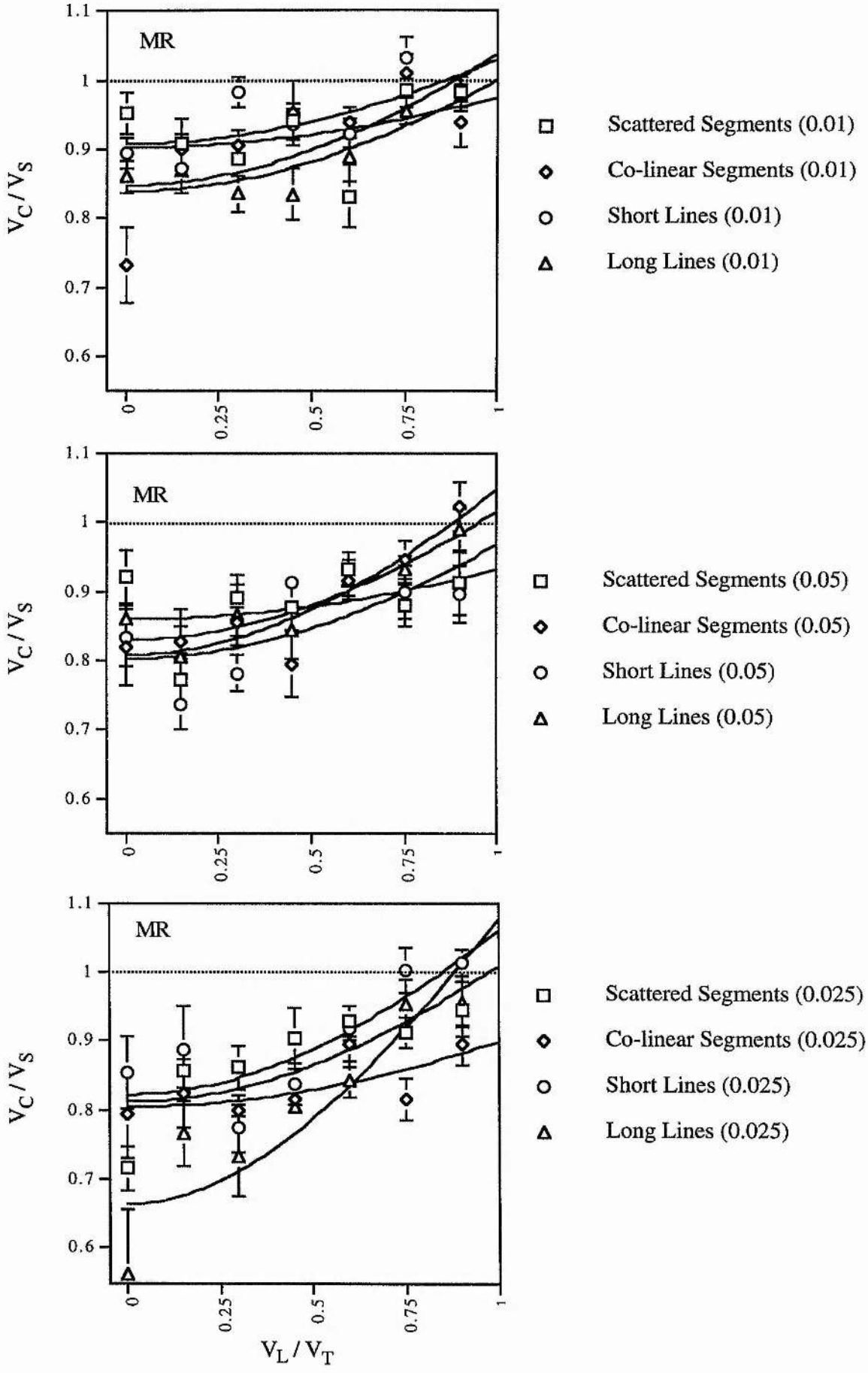
MR
V_C / V_S
1.1
1
0.9
0.8
0.7
0.6
0
0.25
0.5
0.75
1
Scattered Segments (0.01)
Co-linear Segments (0.01)
Short Lines (0.01)
Long Lines (0.01)
MR
V_C / V_S
Scattered Segments (0.05)
Co-linear Segments (0.05)
Short Lines (0.05)
Long Lines (0.05)
MR
V_C / V_S
Scattered Segments (0.025)
Co-linear Segments (0.025)
Short Lines (0.025)
Long Lines (0.025)
V_L / V_T

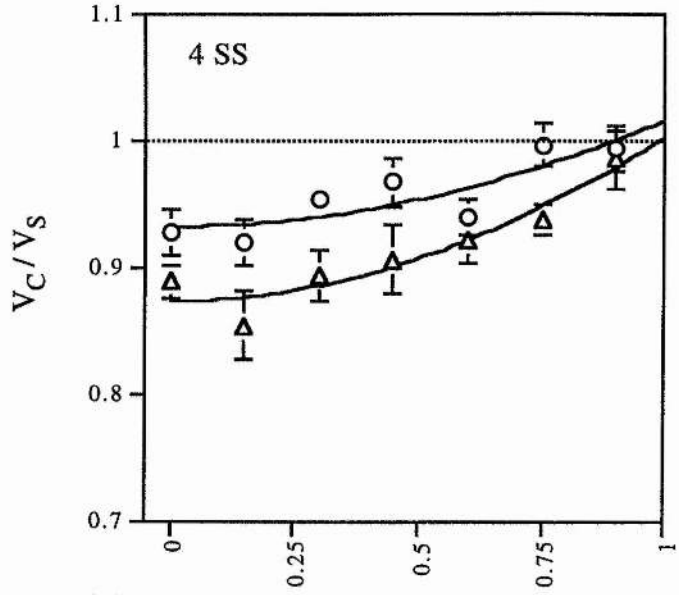

○ Short Lines (0.01)

△ Long Lines (0.01)

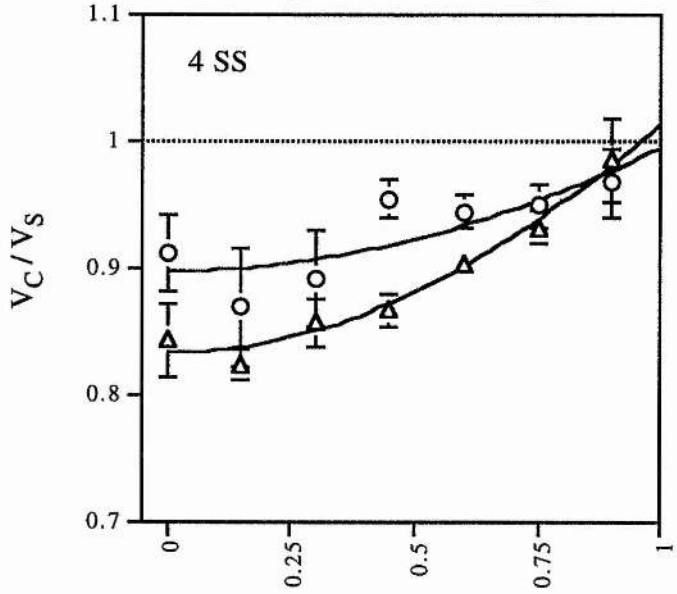

○ Short Lines (0.05)

△ Long Lines (0.05)

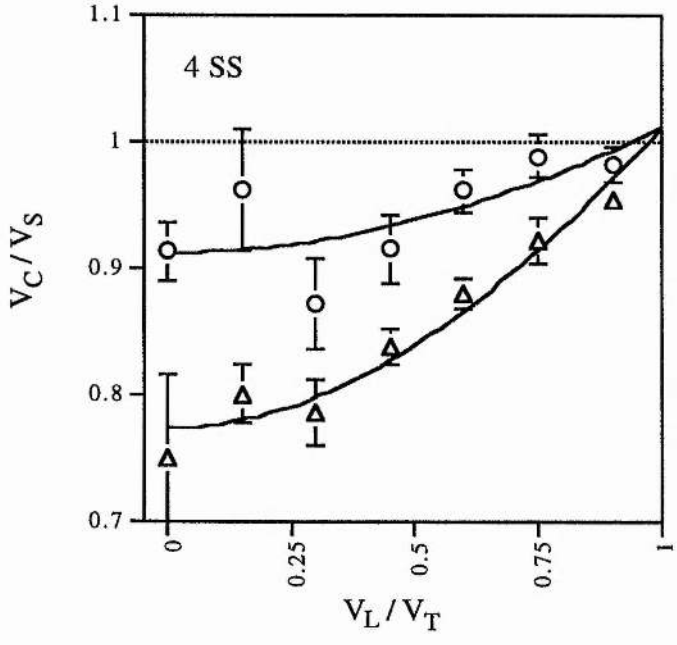

○ Short Lines (0.025)

△ Long Lines (0.025)

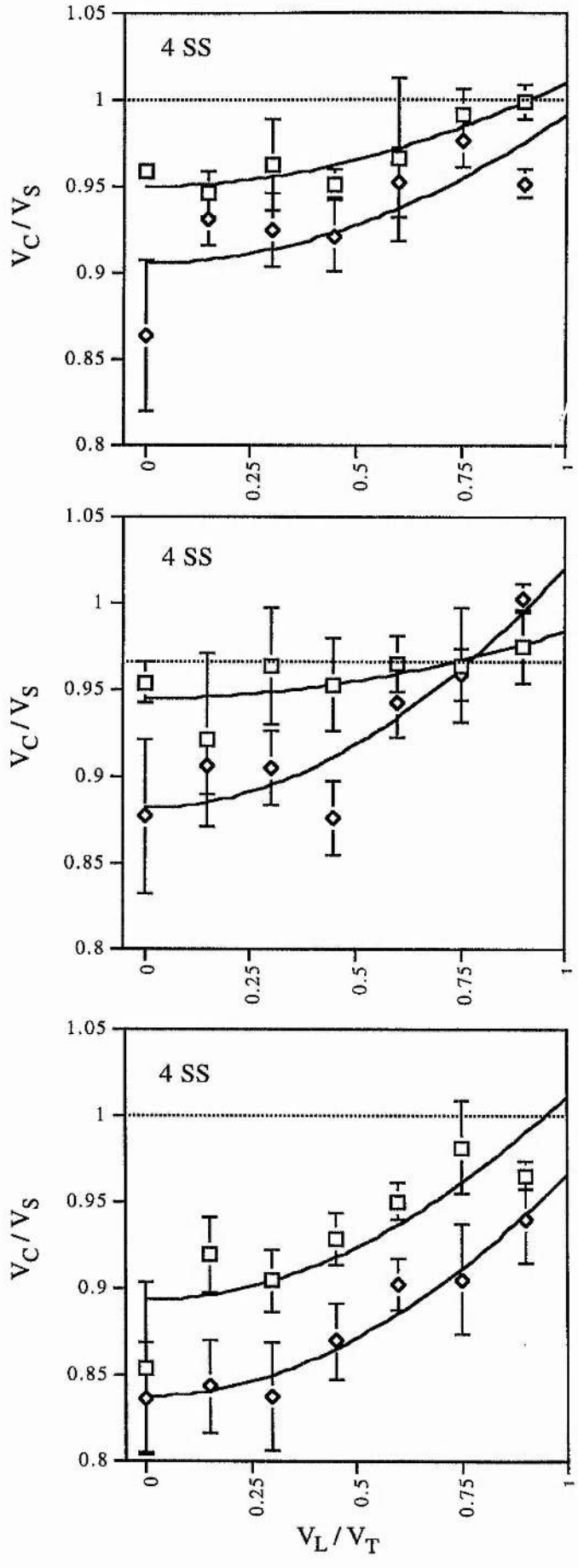

□ Scattered Segments (0.01)

◇ Co-linear Segments (0.01)

□ Scattered Segments (0.05)

◇ Co-linear Segments (0.05)

□ Scattered Segments (0.025)

◇ Co-linear Segments (0.025)

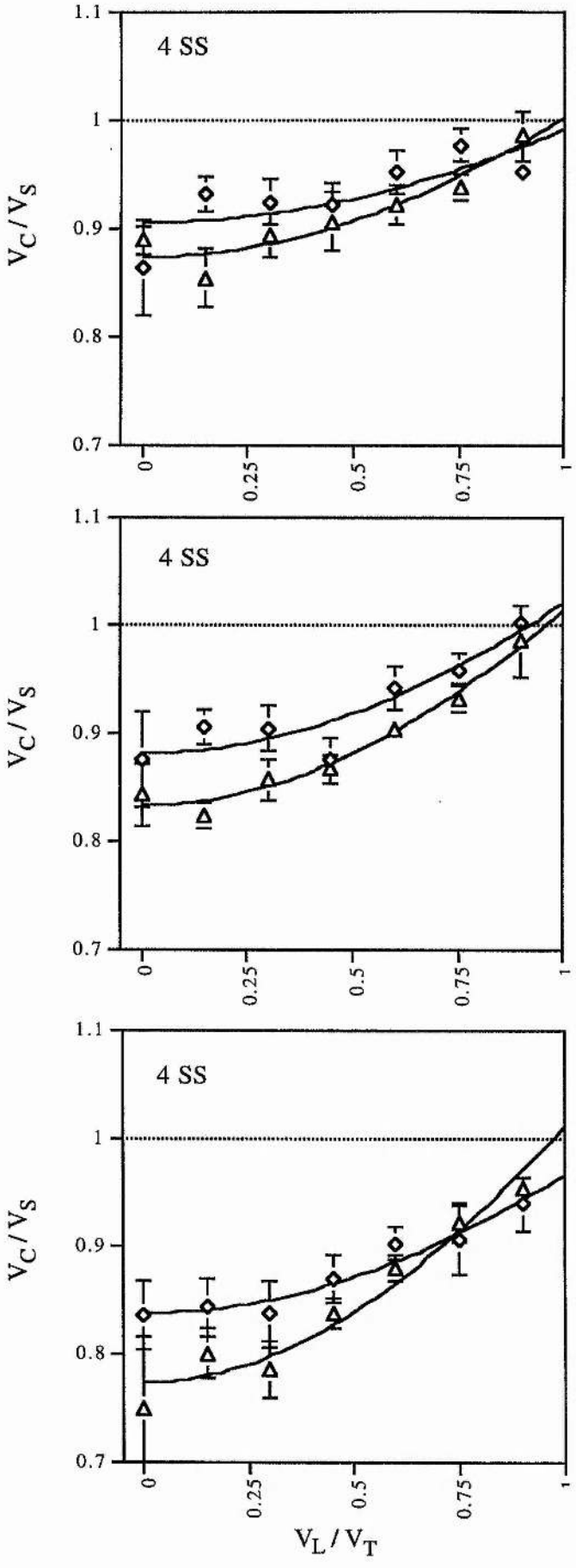
4 SS
V_C / V_S
1.1
1
0.9
0.8
0.7
0
0.25
0.5
0.75
1
Co-linear Segments (0.01)
Long Lines (0.01)
4 SS
V_C / V_S
Co-linear Segments (0.05)
Long Lines (0.05)
4 SS
V_C / V_S
Co-linear Segments (0.025)
Long Lines (0.025)
V_L / V_T

APPENDIX 4.A

Experiment 1

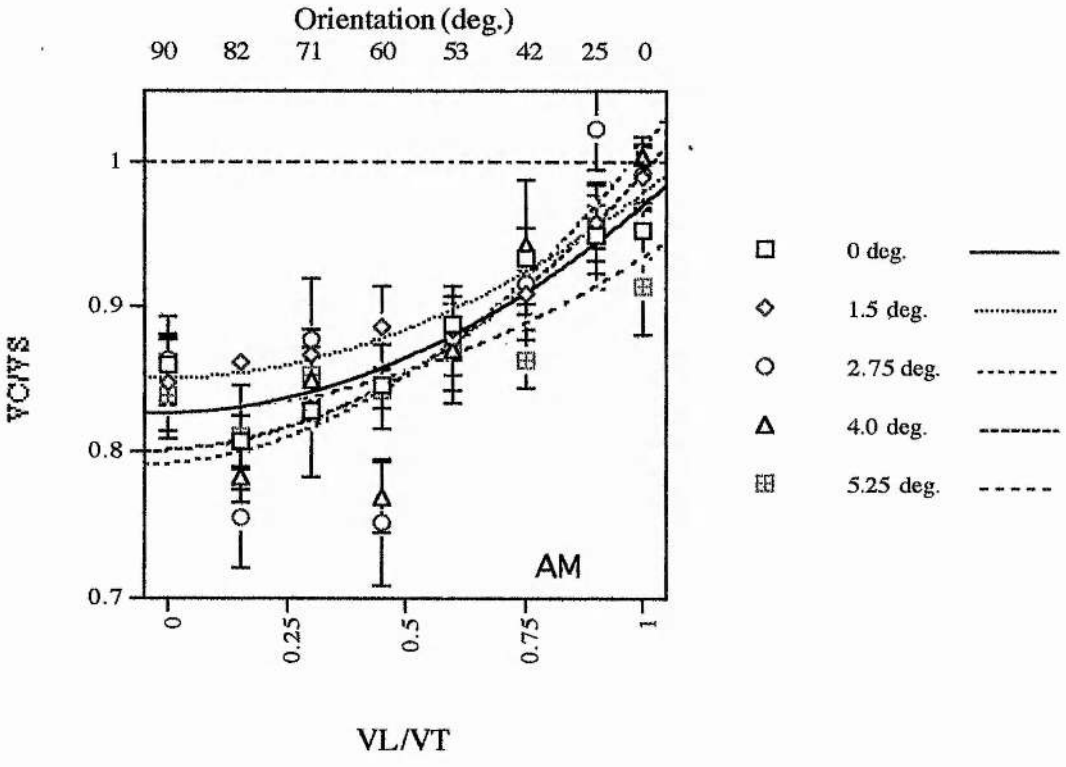

FIGURES. A.1- A.8 Relative perceived speed as a function of the ratio of the local speed to the translation speed (V_L/V_T). The lines in the legend show the model of Castet *et al.* (1993) fitted to the data with two free parameters α and β. Bars through the symbols show ± 1 SE. Speed of standard 2 deg./sec. The horizontal dashed and dotted line shows the 1:1 ratio of standard and comparison speed, indicating veridical perception of speed. Legends beside the graphs depict the stimulus conditions in each instance. Stimuli are described in detail in methods. Each data point is the average of five observations.

Fig A.1 shows the data from subject AM for standard lines travelling above the fixation point and comparison (vertical) lines travelling through the fixation point. The data show the characteristic bias in perceived speed as the angle of inclination of lines approaches 90° (Castet *et al.* 1993; Scott-Brown & Heeley, 1995). The progressive misperception of speed towards horizontal lines concurs with the predictions made in

the introduction as well as findings from previous work. The data for 2.75 degrees of eccentricity (circles) show two outlying data points, with particularly large biases in speed perception.

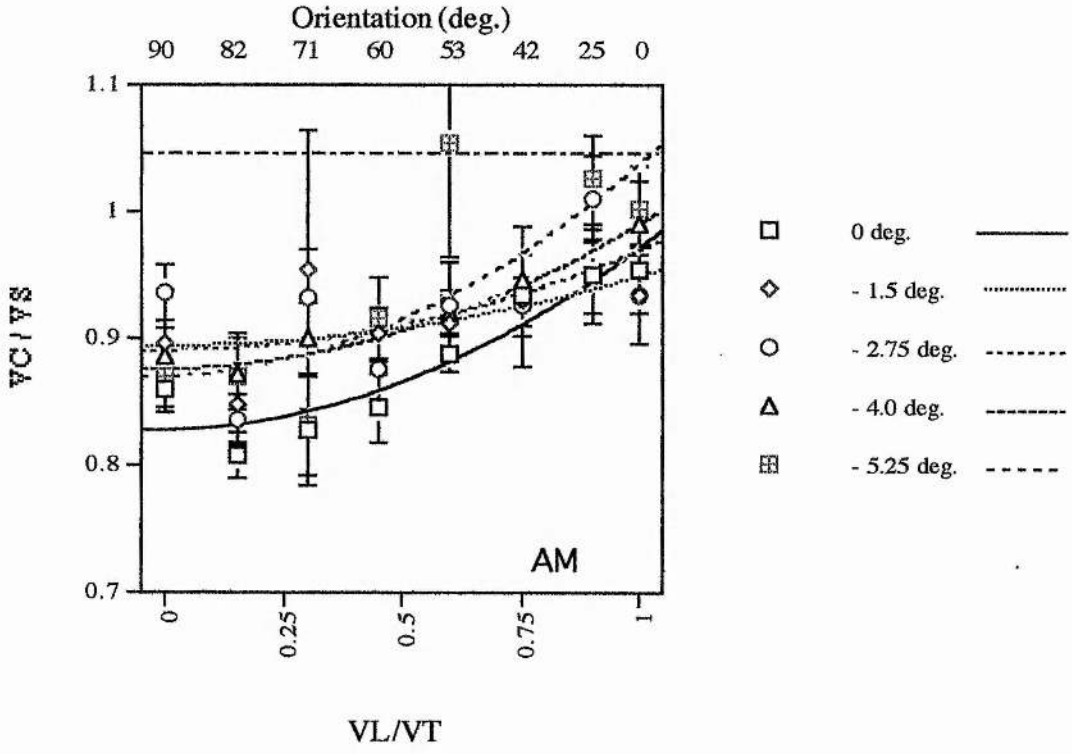

FIGURE A.2

The pattern is repeated with AM for standard lines travelling underneath the fixation point. On this occasion the outlier is the 53 deg. point on the - 5.25 degrees of eccentricity data set. The 71 deg point at -1.5 deg. of eccentricity has a particularly large error bar; this is due to an especially large value of one of the speed estimates that make up the average perceived speed, namely 2.763 dps. This value differs by 64% from the average of the four other points, which was 1.7 dps.

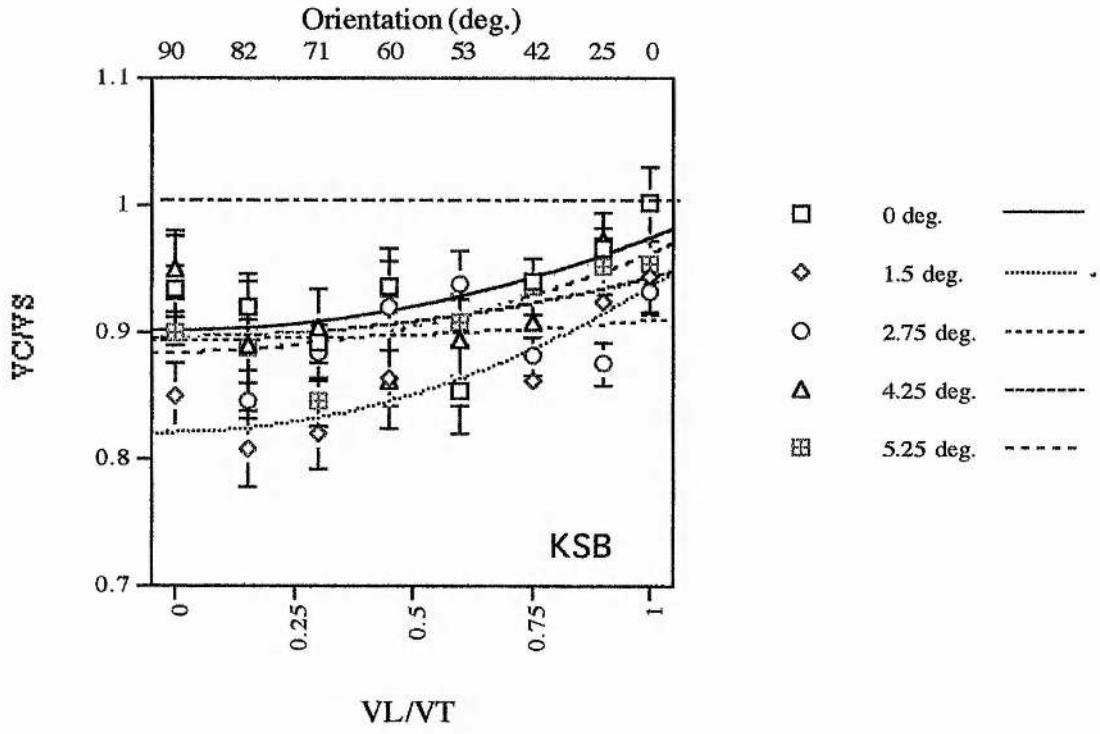

FIGURE A.3

The data for observer KSB (Fig. A.3) shows the familiar trend of a progressive bias in perceived speed as a function of the inclination of the line. The bias is not as large as with some observers but, as the curves of the model fitted to the data show, the usual trend is still apparent. The curves virtually superimpose on each other at the larger angles of inclination, apart from the 1.5 deg. data (diamonds) which shows a greater bias than the rest. For all eccentricities, however, there is a small but consistent bias in perceived speed.

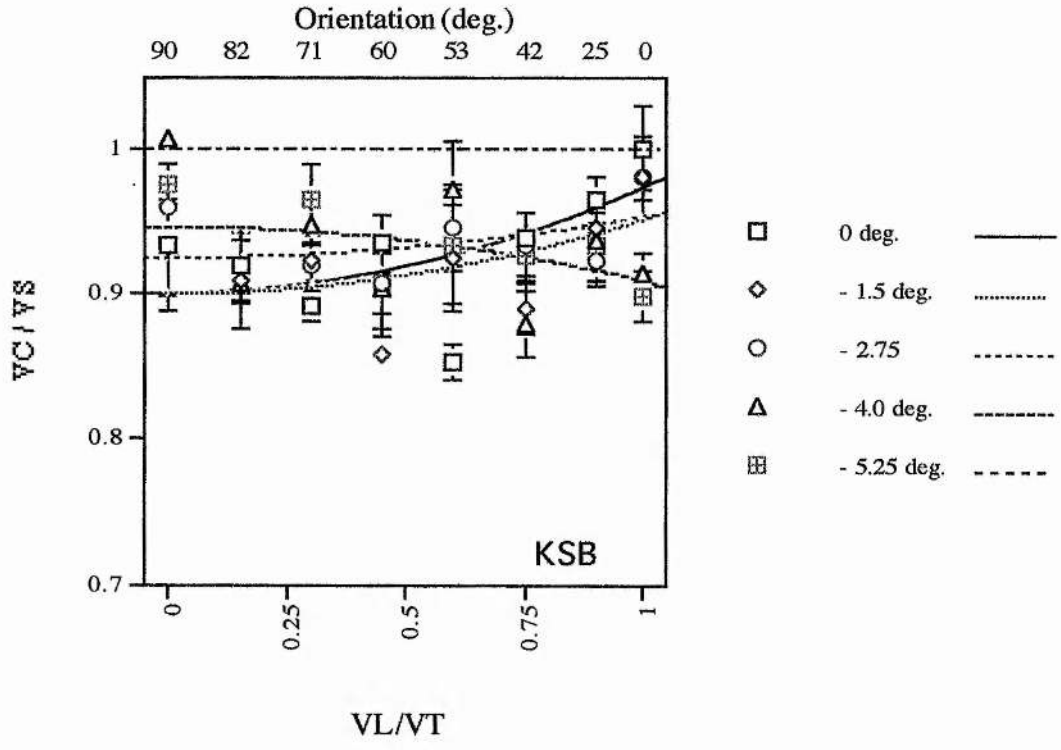

FIGURE A.4

The data for KSB (Fig A.4) is consistent in as much as the data are grouped together in a similar fashion to the data for motion above the fixation point. One slight exception is the data for - 5.25 degrees of eccentricity (crossed squares) which does not follow the characteristic trend of a bias in perceived speed increasing with orientation, the reverse is in fact observed. The predictions of the experiment have been broadly supported with a small but ever-present bias in perceived speed observed at each eccentricity.

The curve derived from the model describes the data for translation of -5.25 degrees of eccentricity quite accurately. However the pattern of results does not conform to the pattern described by Castet *et al.* (1993) in that as can be seen from Table A.1 below the α parameters for -4.0 and -5.25 deg. of eccentricity are negative.

ECCENTRICITY (deg.)	WEIGHT α	β
-5.25	-0.0383	0.946
-4.0	-0.0370	0.946
-2.75	0.0286	0.925
-1.5	0.0517	0.810
0	0.0727	0.901
1.5	0.114	0.821
2.75	0.0153	0.893
4.0	0.046	0.896
5.25	0.0775	0.884

TABLE A.1. Weights attached to V_L and V_T as derived from the data according to Castet *et al.*'s (1993) model. The equation for the model is given in Chapter 2. The curve fitting procedure is also described therein.

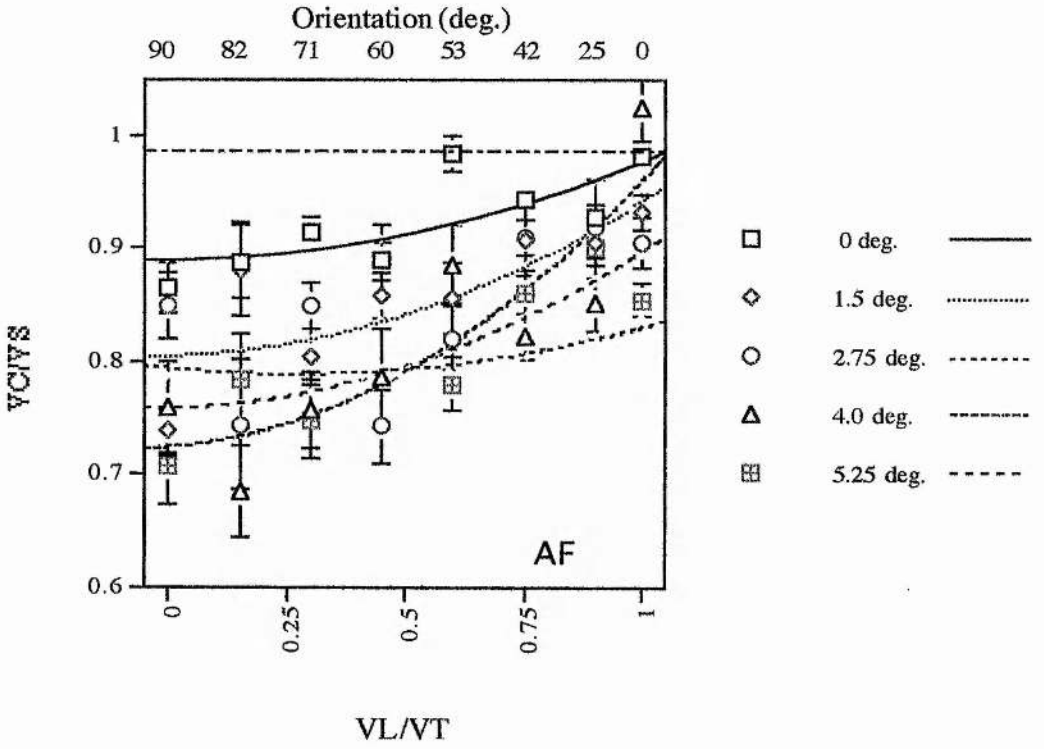

FIGURE A.5

In contrast to the data for the first two subjects the data for subject AF (Fig. A.5) is considerably more spread out. The bias in perceived speed remains present at all eccentricities. On this occasion the bias appears to increase as the eccentricity of the standard line increases.

This finding supports the use of a control condition for the gap-size experiments in chapter two. By using a continuous line, the length of the whole extent of the co-linear segment, it is possible to control for the possibility that the larger eccentricity of the co-linear stimuli could be influencing the perceived speed of the stimulus. However it is possible that the the terminators are less visible at higher eccentricities.

Another deviation from the expected results is the slightly u-shaped curve for the model fitted to the data for 2.75 degrees of eccentricity (circles). Inspection of the data shows that this may simply be a result of the rather variable nature of the results rather than a specific trend. The curve is a poor description of the data in as far as the data points are not particularly close to the curve.

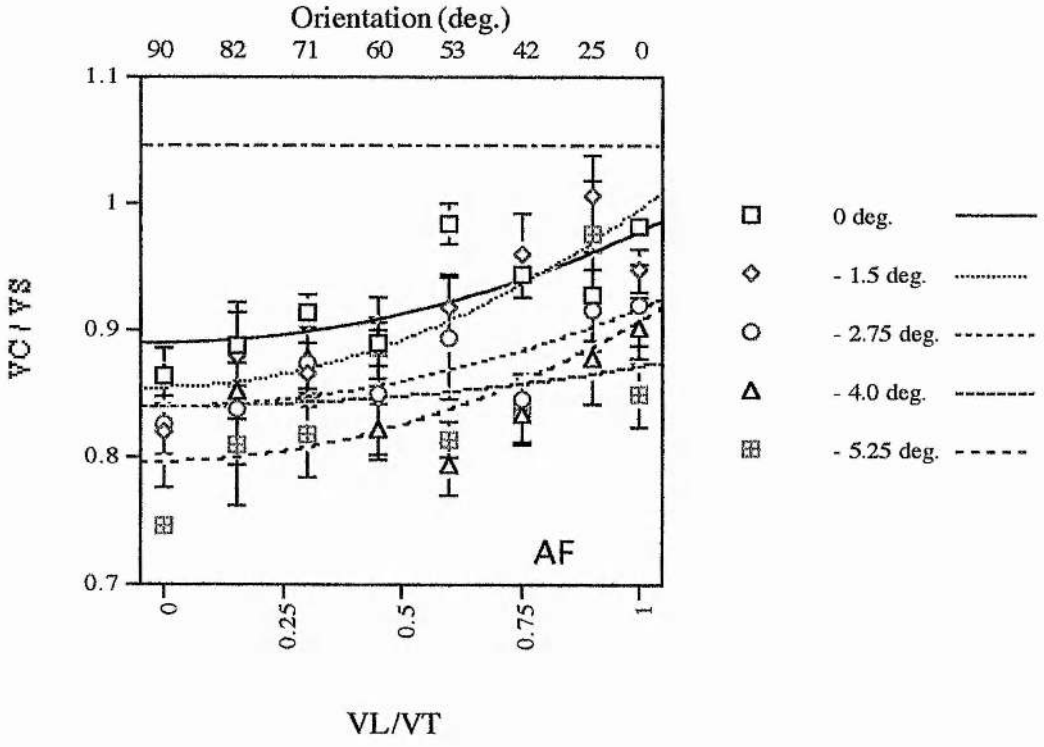

FIGURE A.6

The data for the standard lines traversing below the fixation point (Fig. A.6) is very similar to the corresponding data above the fixation point. There is slightly less evidence of spread in the data. Again the trend of increasing bias in perceived speed as a function of increasing line orientation is replicated. The greatest variability in data points on this occasion appears for - 4.0 degrees of eccentricity (triangles), where a reversal of the progressive trend is evident.

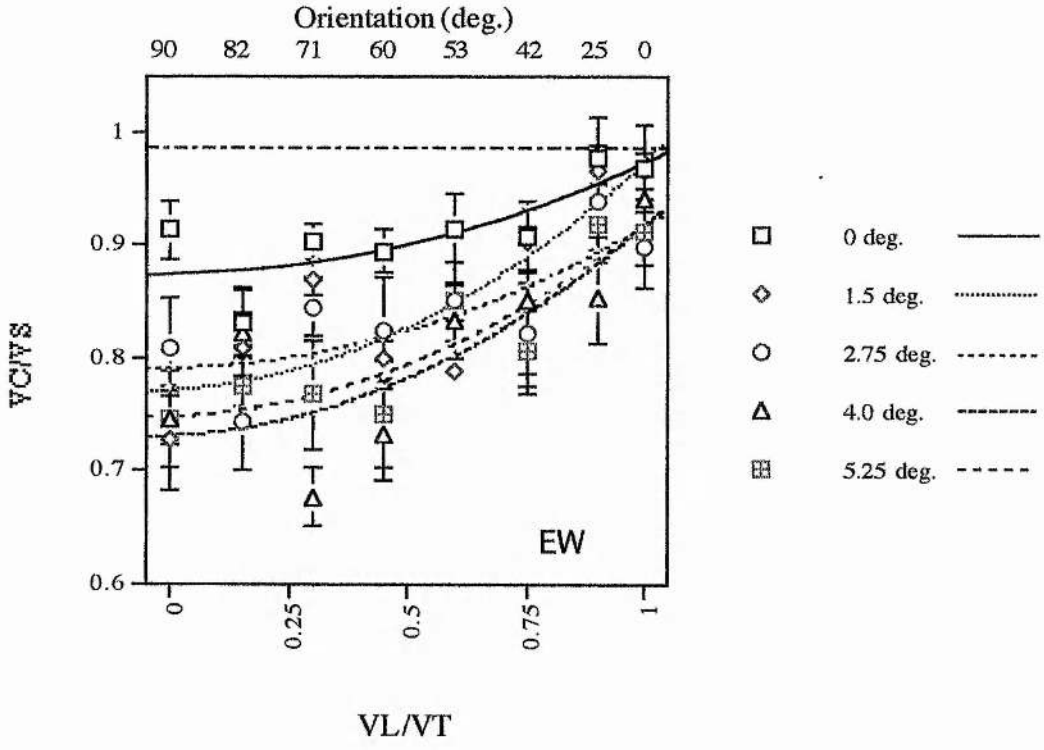

FIGURE A.7

Observer EW (Fig. A.7) shows the characteristic trend of increasing speed misperception. Apart from the two outliers at 4.0 degrees of eccentricity (triangles), the data are nicely grouped. There is however a difference between the data at zero eccentricity and peripheral data. This indicates that some caution should be exercised before extrapolating the results from chapters three and four.

The peripheral data for 1.5 to 5.25 degrees of vertical eccentricity are fairly well superimposed which implies that if there is an effect of eccentricity, it is not of a simple linear nature.

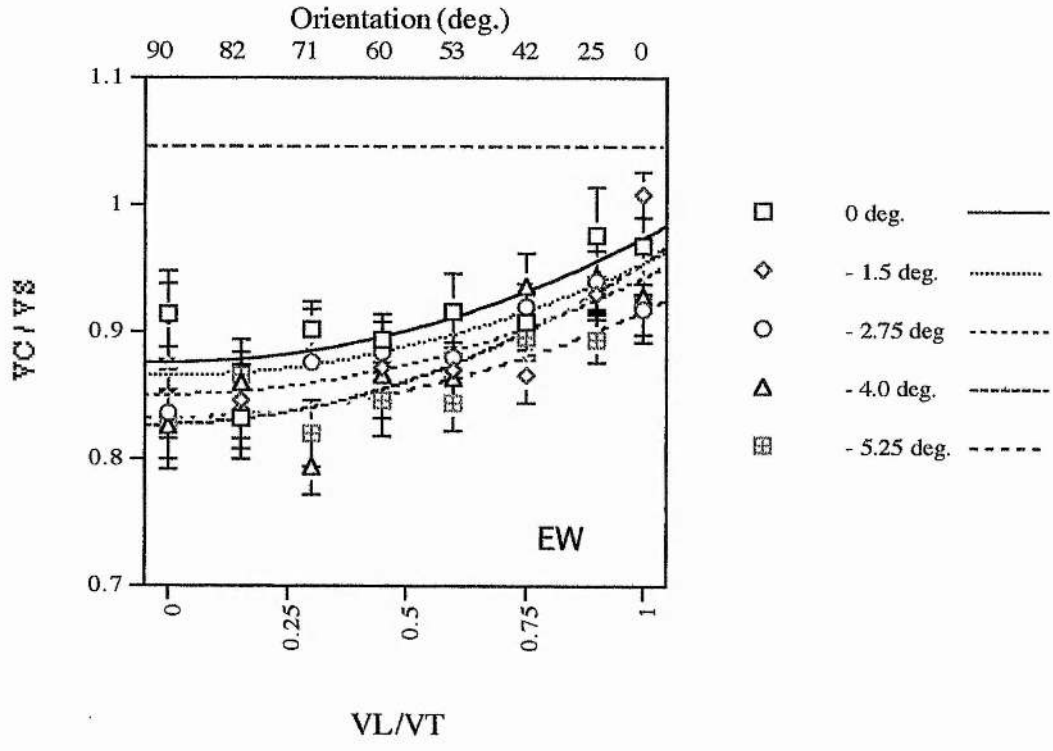

FIGURE A.8

Fig. A.8 shows data for lines translating below the fixation point. EW shows a close grouping of the curves, in line with the predictions. There is no appreciable effect of eccentricity; the data follows the same trend at each eccentricity.

APPENDIX 7.A

Calibration details from Heeley and Buchanan-Smith (1994).

The stimuli were plaids that had been formed by superimposing two independent drifting sine-wave gratings of different orientation. They were synthesised by an Innisfree "Picasso" image generator and displayed on the face of a Tektronix 606A monitor. The image generator was connected to a set of specially constructed computer interfaces that permitted independent control of all of the spatio-temporal parameters of the two sine-wave gratings. The monitor had a P31 yellowish-green phosphor at a mean luminance of 31cd/m^2.

The display luminance was calibrated with a Tektronix J16 digital photometer. Stimulus orientation was calibrated with a travelling microscope that had been fitted with a spectrometer slit in the image plane. The spectrometer slit carried a ring bezel that had been accurately engraved in 5 deg steps over a range of 360 deg. A vertical thin line stimulus was imaged onto the slit. Internal adjustments were made to the monitor until the thin line remained aligned with the slit over the full vertical traverse of the microscope. This procedure was then repeated with a similar horizontal line. After these calibrations had been conducted, intermediate orientations were calibrated by rotating the slit by the required amount, and checking that a thin line of the required orientation was imaged parallel to the slit jaws. Modification of the internal circuits of the Tektronix monitor enabled the computer to set the orientation of the stimulus with a resolution of 30 sec arc. Stimulus contrast was calibrated by replacing the microscope eye-piece with a linear photo diode and imaging alternating light and dark bars of square-wave gratings of different contrast onto the active surface. Contrast was found to be linear within 2% by this technique up to the maximum of 0.7 that the monitor could display.

The apparatus was under the control of a laboratory computer that was used to define the progress of the experiment, accumulate the responses of the observer and analyse the results. An opaque card screen that contained a circular aperture was fitted to the face of the monitor. The aperture defined a free viewing area that subtended 6 deg at the viewing distance of 114 cm. A small opaque circular spot was placed in the centre of the viewing area as an aid to fixation and accommodation. The display was viewed binocularly through natural pupils in a darkened experimental chamber. Mild head restraint was employed in the form of a chin rest, temple pads and forehead bar.

APPENDIX 7.B

FIGURE. 7.B 1 Overleaf

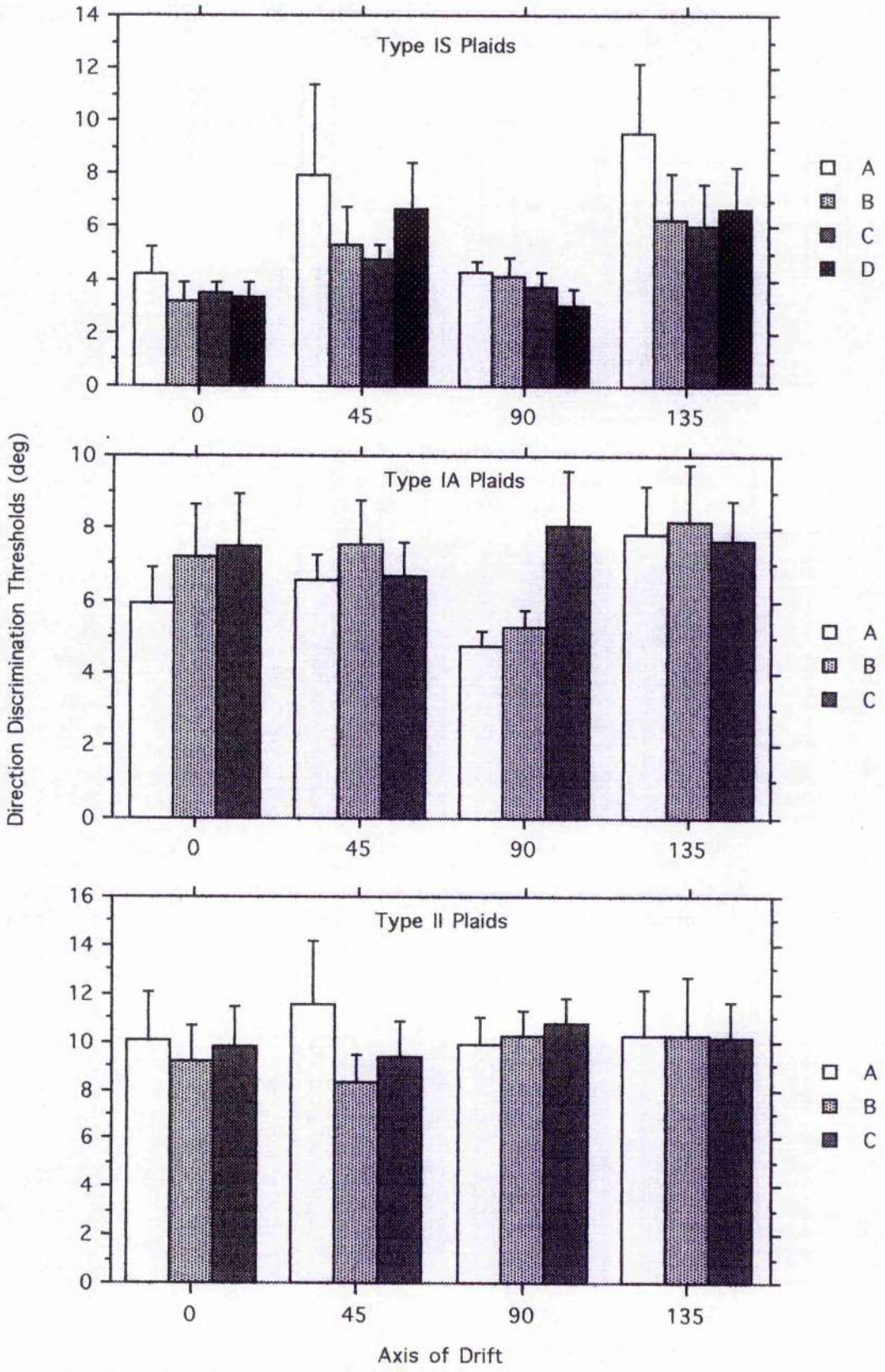

FIGURE 7.B1. Direction discrimination for type IS type IA and type II plaids respectively. Long component angle is shown in the legend: A = 48.2, B = 33.6, C = 23.5 deg. Thresholds are averaged across 4 subjects.

CHAPTER 8

APPENDIX 8 A

Type IA plaids:

$$\tan\gamma = \frac{a\,.\,\cos\theta_2 - (b + \delta b)\cos\theta_1}{a\,.\,\sin\theta_2 - (b + \delta b)\sin\theta_1} \qquad [A1]$$

Type II plaids:

$$\tan\gamma = \frac{a\,.\,\cos\theta_2 - (b + \delta b)\cos\theta_1}{a\,.\,\sin\theta_1 - (b + \delta b)\sin\theta_2} \qquad [A2]$$

APPENDIX 8 B

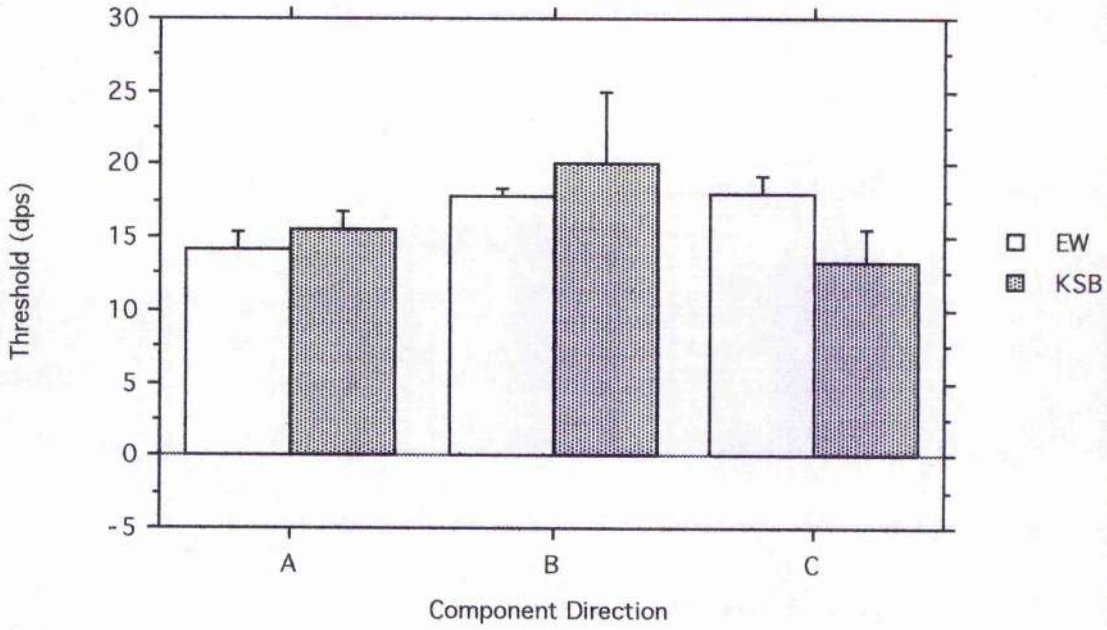

FIGURE 8 B1. Velocity increment threshold for inducing a pattern rotation of type IS plaids. The x axis shows the three long component directions: A = 48.2°, B = 33.6° and C = 23.5°. The different bars show data from different observers as indicated in the legend. The error bars indicate ± 1 S.E.

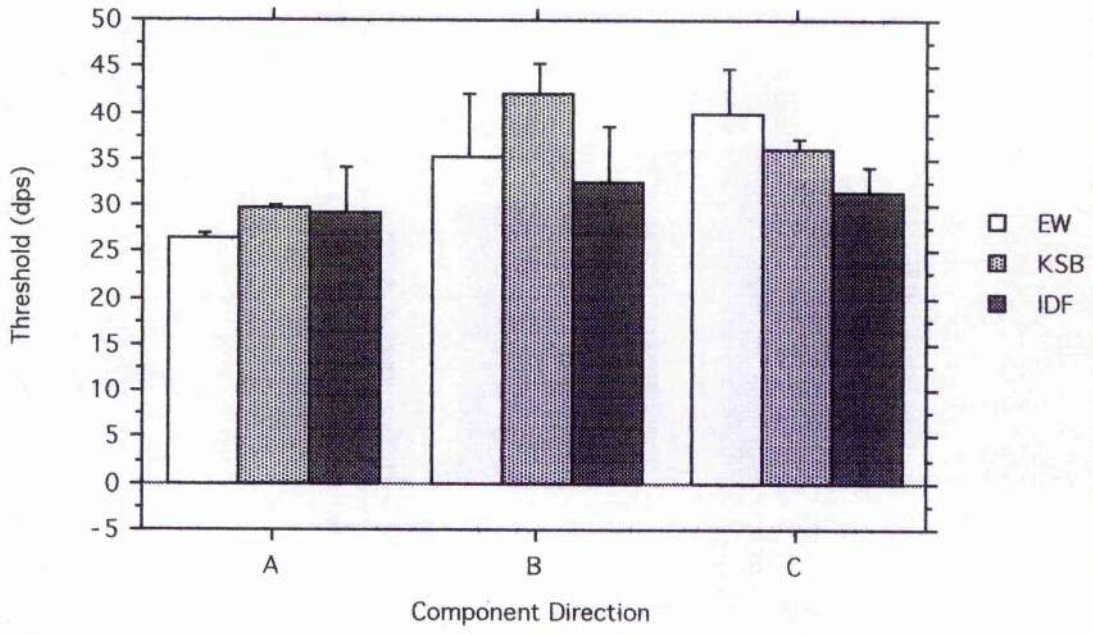

FIGURE 8 B2. Velocity increment threshold for inducing a pattern rotation of type IA plaids. The x axis shows the three long component directions: A = 48.2°, B = 33.6° and C = 23.5°. The different bars show data from different observers as indicated in the legend. The error bars indicate ± 1 S.E.

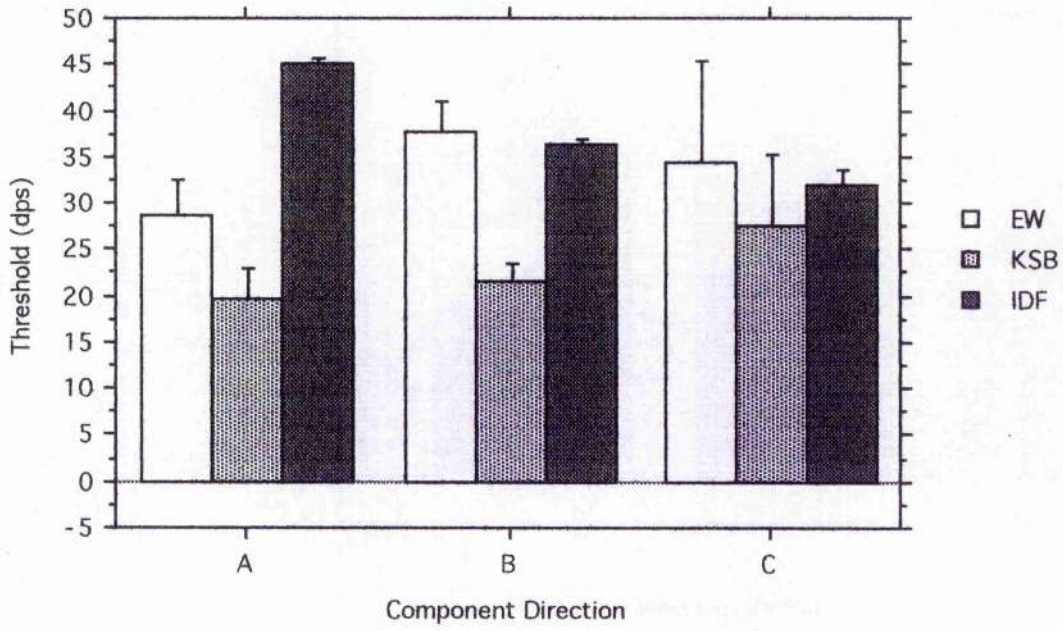

FIGURE 8 B3. Velocity increment threshold for inducing a pattern rotation of type II plaids. The x axis shows the three long component directions: A = 48.2°, B = 33.6° and C = 23.5°. The different bars show data from different observers as indicated in the legend. The error bars indicate ± 1 S.E.

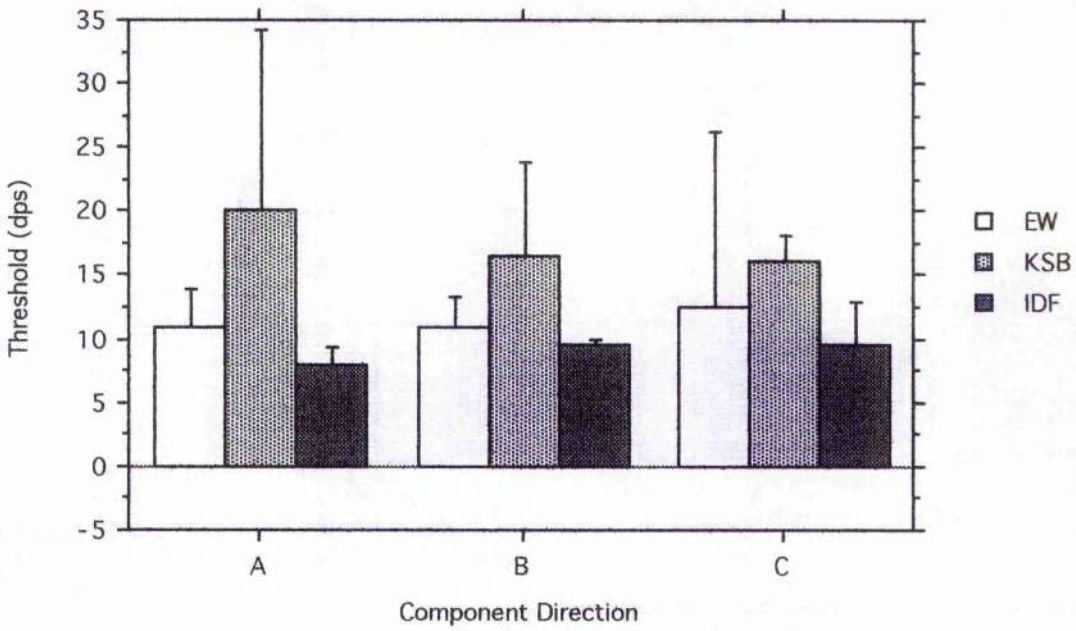

FIGURE 8 B4. Velocity increment threshold for single drifting sine-wave gratings at the same orientation as the long component gratings of the plaids used in the experiment. The x axis shows the three long component directions: A = 48.2°, B = 33.6° and C = 23.5°. The different bars show data from different observers as indicated in the legend. The error bars indicate ± 1 S.E.